1994

Assessment and prediction of the behavior of dent-damaged and internally grout repaired tubular steel bracings using moment curvature- based integration methods

Chih-Ping Fan
Lehigh University

AUTHOR:

Fan, Chih-Ping

TITLE:

Assessment and Prediction of the Behavior of Dent-Damaged and Internally Grout Repaired Tubular Steel Bracings Using Moment...

DATE: May 29, 1994

Assessment and Prediction of the Behavior of Dent-Damaged and Internally Grout Repaired Tubular Steel Bracings Using Moment Curvature-Based Integration Methods

by

Chih-Ping Fan

A Thesis

Presented to the Graduate and Research Committee

of Lehigh University

in Candidacy for the Degree of

Master of Science

in

Civil Engineering

Lehigh University

May, 1994

This thesis is accepted and approved in partial fulfillment of the requirements for the Master of Science

May 17, 1994
Date

Dr. James Ricles
Thesis Advisor

Dr. Le. W Lu
Chairperson of Department

Acknowledgements

I would like to express my sincere gratitude to Professor James Ricles for his continuous and generous guidance, as well as his valuable advice during this study. Special thanks are also due to Dr. Took Kowng Sooi and Mr. William M. Bruin for kindly providing the experimental data required in preparation of this thesis.

I am grateful to my parents for their encouragement and generous support through the course of this work. This work is dedicated to them.

TABLE OF CONTENTS

LIST OF TABLES :

LIST OF FIGURES :

(F'g=5 ksi and Fy=34.8 ksi)

Figure 5-42 : Limit State Equation for KL/r=60, D/t=64

(F'g=5 ksi and Fy=34.8 ksi)

ABSTRACT

Two computer programs were developed to predict the force-deformation behavior of dent-damaged and internally grout repaired tubular steel members, respectively, subjected to axial compression, end moment and lateral loading. Each program utilizes a numerical integration approach in combination with moment curvature expressions. The moment curvature expressions for the dent-damaged, unrepaired members are based on the regression analysis of experimental data, while the moment curvature relationships for the internally grout repaired members are derived from a fiber analysis of the cross section. The programs generate the axial load-shortening and axial load-lateral displacement relationships for members with one or more arbitrary located dents.

The programs were verified by comparing the predicted strength of 113 test specimens with their experimental results. Comparisons were also made between the moment curvature approach and other existing prediction methods (Parsanejad's equation, the so-called modified AISC method and the simplified AISC method) for the internally grout repaired specimens. The moment curvature approach is shown to be more reliable and accurate than these other existing strength prediction methods.

An extensive parametric study was performed using the computer programs to investigate the influences of the geometric parameters of dent depth, member diameter-to-thickness ratio and out-of-straightness, in addition to material properties of steel yield

strength, grout strength and modular ratio on the dent-damaged and internally grout repaired member's strength under compressive axial load. A set of design-oriented curves were developed from these results.

In addition, the domain with respect to dent depth and out-of-straightness, in which a repaired member will have a strength equal to or greater than its undamaged strength, has been evaluated. It was found that members with minimal out-of-straightness and a slenderness ratio of KL/r=60 can be successfully repaired by internal grouting when their dent depth-to-diameter (d_d/D) ratio is less than 0.34, 0.37 and 0.40, respectively, for member diameter-to-thickness (D/t) ratio of 34, 46 and 64. For a member with out-of-straightness, such as that suffered due to a collision causing denting and overall bending, the d_d/D ratio is smaller.

1. INTRODUCTION

1.1 Background

There are presently over 6000 fixed offshore platforms throughout the world. These structures have a typical construction consisting of a steel jacket made of tubulars welded together, see Fig 1. In the marine environment offshore structures such as these are highly susceptible to member damage resulting from the accidental impact with a vessel or a falling object, which affects the structural integrity of the platform. It has been reported that collision of vessels or dropped objects with offshore platforms accounts for over 29% of offshore accidents where 14% of these accidents result in severe damage or total loss of structure [Ellinas and Ualsgard, 1985]. Damage of the platform due to collision usually takes one of the following forms : (1) local denting of the tube wall without the overall bending of the member; (2) overall bending without denting of the tube wall; and (3) combined overall bending and denting. A large number of offshore platform structures are known to have suffered some form of damage. Because of the need to requalify and recertify platforms, it is critical that one can analytically assess the effects of damage from collisions on the ultimate load-carrying capacity of its members.

In the offshore field, grout has been historically used in the connections of fixed bottom structures by grouting the annulus between a platform's legs and piles . Design guidance can be found in the API RP-2A [1984, 1993] as well as other design manuals. Grout can also be used to improve strength of undamaged members as well as dent-

damaged members by internal grouting. While some closed form solutions based on a beam-column formulation have been developed [Parsanejad, 1987a], no guidance exist in offshore codes for assessing the strength feasibility of internally grout repaired tubular bracing.

The ability to reliably predict the strength of internally grout repaired dent-damaged members is essential, since their strength and effect on the behavior of the platform must be known in order to requalify the platform.

1.2 Previous Experimental Work

1.2.1 Dent-Damaged Members

The ultimate strength and behavior of dented tubular members has been previously studied both experimentally and analytically. Smith, Kirkwood and Swan (1979) performed small-scale axial compression tests with dent depths ranging from 0.011D to 0.0082D. Full-scale tests were later conducted by Smith, Somerville and Swan (1981). A series of small-scale tests had been undertaken by Taby (1986) to develop a database for member strength. Ricles, Gillum and Lamport (1987) conducted 6 large-scale experimental tests with member diameter-thickness ratios (D/t), respectively of 34, 46 and 64, end eccentricities ranging from 0.0D to 0.2D and dent depth equal to 0.1D. Landet and Lotsberg (1992) performed 35 small scale tests on dented tubes subjected to axial load, pure bending and combined loading with dent depths, respectively, of 0.0D, 0.1D and 0.2D, obtaining experimental moment-thrust-curvature relationships. All of the above

tests indicated that dent damage reduces the axial compression strength of the member, and that it is a function of dent depth. None of these tests considered combined local dent-damage and out-of-straightness from bending.

1.2.2 Dent-Damaged, Internally Grout Repaired Members

The results from tests on 8 undamaged internally grout filled specimens were published in 1984 and 1986 by Wimpy JIRRP. The test results indicated that the ultimate strength of specimens with internal grouting were 1.7 and 1.2 times as much as that without internal grouting for specimens with a D/t ratio of 72 and 32, respectively. Parsanejad (1987) performed 10 small-scale tests on internally grout repaired specimens with dent depths ranging from 0.0D to 0.15D. Boswell and D'Mello (1988) conducted both small-scale and a few large-scale internally grout repaired specimens with dent depths ranging from 0.0D to 0.16D. Ricles, Gillum and Lamport (1992) also conducted 3 large-scale tests involving internally grout repaired specimens with a dent depth equal to 0.1D and D/t equal to 34, 46, and 64. In addition, they also performed a grouted clamp repair involving a dent depth of 0.1D and D/t equal to 64. The tests showed that for members with small dent damage (dent depth=0.1D) that the internally grout repair successfully reinstated their strength to at least that of an equivalent undamaged member.

1.3 Previous Analytical Studies

There have been several analytical studies conducted on both dent-damaged and

internally grout repaired dent-damaged tubular members. These existing prediction approaches can be generally classified into three groups, namely : unity check, or beam-column equation; integration methods, and the finite element method. A unit check or beam-column equation is based on moment-axial load interaction and some assumptions. Numerical integration procedures involve the use of moment-curvature relationships or moment-rotation relationships. Finite element analysis usually involve accounting for nonlinear material and geometric effects by proper constitutive relationships and kinematics. It is the most expensive and difficult to use of all the methods.

1.3.1 Dent-Damaged Members

Smith et al. (1979), and Smith et al. (1981) used a elasto-plastic beam-column analysis to determine the residual strength of damaged non-repaired members. Ellinas (1983) developed a simple design-oriented close-form expression (i.e. beam-column equation) based on a member with a dented midspan section and first yield defined as the ultimate strength condition. Ricles et al. (1992b) modified the Ellinas' equation by taking the end eccentricity into account. Taby (1988) developed a semi-empirical model and incorporated it into the computer program DENTA-II to predict the load deformation behavior of dented tubular bracing subjected to combined axial loading and bending.

Padula, and Ostapenko (1991) proposed an analytical approach to consider the nonlinear behavior of a dent-damaged member by a regression model to predict the load-

axial shortening relationships for damaged, pin-ended tubular columns. Kim, and Ostapenko (1992) later proposed a step-by-step integration procedure to predict the residual strength, axial compression-shortening and axial compression-lateral deflection responses based on moment-thrust-rotation and moment-thrust-axial strain relationships (M-P-θ and M-P-ε). Recently, Duan et al. (1993) developed a computer program (BCDENT) to analyze the behavior and the ultimate strength of dented non-repaired members, using Newmark's integration procedure in conjunction with M-P-Φ and M-P-ε empirical relationships. These empirical relationships were based on the results of numerous tests and analysis of non-repaired dented tubulars.

The nonlinear finite element method were successfully used to assess the residual strength of dent-damaged tubular members by MacIntyre and Birkmoe (1991), and Salman, Birkmoe, and Ricles, (1993).

1.3.2 Internally Grout Repaired Members

Parsanejad (1987) developed a simple explicit quadratic expression to estimate the ultimate strength of internally grout repaired tubular members. The analysis is based on the solution to a beam-column equilibrium condition with first yield collapse criteria.

Loh (1991) proposed a modified AISC-LRFD approach for assessing the strength of grout filled dented tubulars. The two modifications are the buckling curve and the interaction equation. A simplified approach was also presented (Loh, 1991). The

difference between these two approaches is that in the simplified approach neglects the grout's contribution to the Euler buckling load. The simplified approach therefore has the advantage of not requiring the knowledge of the value of the grout's elastic modulus of the grout. The above 3 prediction methods will be discussed in detail in Section 4.3.1.

1.4 Objectives

While the problem of residual strength and grout repaired strength has been studied previously, there is a need to develop and assess more robust methods of analysis which are reliable, economical and enable one to account for out-of-straightness, transverse loading, multiple dents and produce load-deflection curves for the member. To fulfill this need, this study was pursued, having as its objective to develop and assess the use of M-P-Φ based methods in predicting the general behavior of dent-damaged, nonrepaired and internally grout repaired, dent-damaged tubular steel bracing.

1.5 Scope

Presented herein is a comprehensive study involving an investigation of the behavior and the prediction of the ultimate strength of non-repaired dent-damaged and internally grout repaired dent-damaged tubular members using a numerical integration procedure in conjunction with M-P-Φ and M-P-ε relationships. Chapter 2 presents the M-P-Φ and M-P-ε relationships for non-repaired dent-damaged and internally grout repaired dent-damaged tubular members.

The general numerical integration algorithm for obtaining a member's force-deformation response using the M-P-Φ and M-P-ε relationships and the development of the computer programs is discussed in Chapter 3. The validation of the computer programs through a comparison of experimental test results with predictions by the programs is provided in Chapter 4.

Chapter 5 presents the results of a parametric study, performed using the computer programs to investigate member geometric and material parameters. A set of design-oriented charts and feasibility functions for internal grout repair based on this study are also presented for practical engineering purposes.

2. MOMENT-THRUST-CURVATURE RELATIONSHIPS

2.1 General

This chapter describes the moment-thrust-curvature (M-P-Φ) and moment-thrust-axial strain (M-P-ε) relationships. The derivation of exact M-P-Φ and M-P-ε relationships for undented, non-grout filled sections will be illustrated in Section 2.2; approximate M-P-Φ and M-P-ε expressions for both undamaged and dent-damaged non-grout filled sections in Section 2.3; and the derivation of exact M-P-Φ and M-P-ε relationships for internally grout repaired sections in Section 2.4.

2.2 Derivation of Exact Moment-Thrust-Curvature Relationships

An undamaged tubular section subjected to combined axial compression and bending moment can have one of the three following stress conditions, namely : (1) an elastic stress state throughout its cross-section; (2) yielding in the compression zone (primary plastic); (3) yielding in both the compression and tension zones (secondary plastic). These stress states are depicted in Fig. 2-1. The moment-axial force interaction surfaces corresponding to each of these stress conditions, in terms of normalized axial load $p=P/P_y$ and moment $m = M/M_p$ is shown in Fig. 2-2. The relationship for each of three stress conditions is : (Ellis, 1958)

(1) elastic state stress condition (Fig. 2-1(a))

$$p=\bar{\varepsilon}_0 \tag{2.1}$$

$$\bar{m}=\frac{\pi\phi}{4} \tag{2.2}$$

(2) yielding in the compression zone (Fig. 2-1(b))

$$p=1-\frac{\phi}{\pi}\left[\left(\frac{\pi}{2}+\psi_1\right)\sin\psi_1+\cos\psi_1\right] \tag{2.3}$$

$$\bar{m}=\phi\left(\frac{\pi}{8}-\frac{\psi_1}{4}+\frac{\sin\psi_1\cos\psi_1}{4}\right) \tag{2.4}$$

$$\psi_1=\sin^{-1}\left(\frac{1-\bar{\varepsilon}_0}{\phi}\right) \tag{2.5}$$

where ψ_1 is shown in Fig. 2-1(b)

(3) yielding in both compression and tension zones (Fig. 2-1(c))

$$p=\frac{2\psi_2}{\pi}-\frac{\phi}{\pi}\left[\left(\psi_1+\psi_2\right)\sin\psi_1+\left(\cos\psi_1-\cos\psi_2\right)\right] \tag{2.6}$$

$$\bar{m}=\frac{\phi}{4}\left(\psi_1+\psi_2+\sin\psi_1\cos\psi_1+\sin\psi_2\cos\psi_2\right) \tag{2.7}$$

where $\psi_1 \neq \psi_2$

$$\psi_1 = \sin^{-1}\left(\frac{1-\bar{\varepsilon}_0}{\phi}\right) \tag{2.8}$$

$$\psi_2 = \sin^{-1}\left(\frac{1+\bar{\varepsilon}_0}{\phi}\right) \tag{2.9}$$

and

ϕ is the cross section normalized curvature, where $\phi=\Phi/\Phi_y$

ψ_1 , ψ_2 are shown in Fig. 2-1(c)

In the above equations the normalized axial load p, moment m, and strain ε_0 are defined as

$$p=\frac{P}{P_y}=\frac{P}{A\sigma_y} \tag{2.10}$$

$$\bar{m}=\frac{M}{M_p} \tag{2.11}$$

$$\bar{\varepsilon}_0=\frac{\varepsilon_0}{\varepsilon_y} \tag{2.12}$$

where P, P_y, M, M_y , respectively, are the applied axial load, yield load, applied moment, yield moment; and A, σ_y, ε_0, ε_y , respectively, are equal to cross sectional area, yield stress, axial strain at the cross-section's geometric centroid, and yield strain.

When a tubular section is subjected to a constant axial load with an incrementally increasing bending moment and develops no local buckling, the cross section will experience the elastic state, yielding in the compression zone, followed by yielding in both the tension and compression zones as the curvature in the member increases. Fig. 2-3 shows an idealized M-P-Φ curve with these stress conditions as the moment approaches its capacity m_{pc}. The corresponding boundaries to define these three stress states are given below for a tubular undented section of radius R :

(1) primary yielding (m1, ϕ1)

$$\Phi_1 = \frac{\varepsilon_y - \varepsilon_0}{R} \qquad (2.13)$$

and normalizing Eq. (2.13) by introducing

$$\phi_1 = \frac{\Phi_1}{\Phi_y} \qquad (2.14a)$$

where Φ_y is the curvature corresponding to initial yielding in compression of the top fiber

for a tubular without axial load :

$$\Phi_y = \frac{\varepsilon_y}{R} \qquad \textbf{(2-14b)}$$

The result for ϕ_1 is obtained by substituting Eq. (2.12) into Eq. (2.13) and normalizing where

$$\phi_1 = 1 - \bar{\varepsilon}_0 \qquad \textbf{(2.15)}$$

The moment in the elastic region is equal to

$$m = \frac{4\bar{m}}{\pi} \qquad \textbf{(2.16)}$$

Where $m=M/M_y$. By substituting Eq. (2.1) and Eq. (2.2) into Eq. (2.15) and Eq. (2.16), the values for m_1 and ϕ_1 are obtained, where

$$m_1 = 1 - p \qquad \textbf{(2.17)}$$

$$\phi_1 = 1 - p \qquad \textbf{(2.18)}$$

(2) secondary yielding (m2,ϕ2)

Defining

$$\Phi_2 = \frac{\varepsilon_y + \varepsilon_0}{R} \tag{2.19}$$

and normalizing the axial strain at the geometric center

$$\bar{\varepsilon}_0 = \frac{\varepsilon_0}{\varepsilon_y} = \phi_2 - 1 \tag{2.20}$$

and

$$\sin\psi_2 = \frac{2}{\phi_2} - 1 \tag{2.21}$$

From Eq. (2.3), Eq. (2.4) and Eq. (2.5), we can obtain

$$p = \frac{\phi_2}{2} + \frac{\psi_2}{\pi}(\phi_2 - 2) - \frac{\phi_2}{\pi}\cos\psi_1 \tag{2.22}$$

$$m2 = \phi_2\left(\frac{1}{2} + \frac{\psi_2}{\pi} + \frac{1}{\pi}\sin\psi_1\cos\psi_2\right) \tag{2.23}$$

Moment-thrust-curvature relationship can be generated for a specified load p by going through a trial and error iteration algorithm to solve for ϕ_2 and Ψ_1 from Eq. (2.21) and Eq. (2.22) and then substituting ϕ_2 into Eq. (2.23) to obtain m_2.

(3) fully plastic moment (m_{pc})

The fully plastic state is achieved when Φ approaches a value of infinity. The fully plastic moment, m_{pc} can be derived considering the stress state shown in Fig. 2-4 corresponding to the applied moment M_{pc} and axial load P. The result of integrating the stresses over the cross section leads to

$$M_{pc}=4R^2t\sigma_y\sin\alpha \qquad (2.24)$$

and

$$P=2Rt(\pi-2\alpha)\sigma_y \qquad (2.25)$$

where α is defined in Fig. 2-4, and is equal to

$$\alpha=\frac{\pi}{2}(1-p) \qquad (2.26)$$

For a thin wall tubular section the yield load P_y and moment M_y can be written in terms of the member's radius R and thickness t, where

$$P_y=2\pi Rt\sigma_y \qquad (2.27)$$

and

$$M_y = \pi t R^2 \sigma_y \qquad (2.28)$$

Combining Eq. (2.24) to Eq. (2.28), M_{pc} is obtained in terms of the axial load p

$$m_{pc} = \frac{M_{pc}}{M_y} = \frac{4}{\pi} \sin\left(\frac{\pi (1-p)}{2}\right) \qquad (2.29)$$

2.3 Approximate Moment-Thrust-Curvature Relationships

As described in Section 2.2, a trial and error iteration must be performed to obtain the exact moment curvature relationship. The stability analysis of the steel tubular members would be greatly simplified if an M-P-Φ relationship can be found to avoid the iteration to accurately approximate the exact moment-thrust-curvature relationship. Using a curve fitting method Chen and Atsuta [1976] generated an empirical expression for the exact moment-thrust-curvature relationship that avoids iteration. The relationship involves dividing the M-Φ curve for a constant axial load into the same three regions corresponding to the three stress conditions discussed previously (see Fig. 2-1 and Fig. 2-2). The M-Φ expression for each stress condition corresponding to the normalized curvature Φ are :

(1) elastic region

$$m = a\phi \tag{2.30}$$

where

$$a = \frac{m_1}{\phi_1} \tag{2.31}$$

(2) primary plastic region

$$m = b - \frac{c}{\sqrt{\phi}} \tag{2.32}$$

where

$$b = \frac{m_2\sqrt{\phi_2} - m_1\sqrt{\phi_1}}{\sqrt{\phi_2} - \sqrt{\phi_1}} \tag{2.33}$$

and

$$c = \frac{m_2 - m_1}{\frac{1}{\sqrt{\phi_1}} - \frac{1}{\sqrt{\phi_2}}} \tag{2.34}$$

(3) secondary plastic region

$$m = m_{pc} - \frac{f}{\phi_2^2} \tag{2.35}$$

$$f = (m_{pc} - m_2)\,\phi_2^2 \tag{2.36}$$

The normalized moments m_1, m_2, and m_{pc}, as well as normalized curvature $\phi 1$ and $\phi 2$ of Eq. (2.30) through Eq. (2.36) are functions of normalized thrust p, which can be determined by either a regression analysis of experimental data or numerical computations for a specific cross section under a constant axial thrust p. The moment curvature relationship based on Eq. (2.30) through (2.36) is shown schematically in Fig. 2-5(a), where also the approximate moment curvature relationship for a constant axial load with local buckling effect is shown. Expressions for the variables and parameters for both the cases of with and without local buckling are given in Appendix A.

Duan et al. [1993] developed a set of closed-form M-P-Φ and M-P-ε expressions for dented tubular sections under combined multidirectional bending and axial compression as well, based on the regression analysis of data from 151 experimental tests. These M-P-Φ and M-P-ε expressions describe the effects of local buckling and distorted cross section (ovalization) during loading. It was found that the effects of local buckling on the behavior and strength of tubular bracings becomes more significant with an increase in diameter-to-thickness ratio, and a decrease in slenderness ratio. The applicable range

of D/t ratio in their expressions is between 20 and 130, which covers the typical range for most offshore tubulars of D/t =30 to 90. The applicable range of dent depth-to-diameter ratio (d_d /D) is 0 to 0.3. The accuracy of the expressions outside of the applicable ranges is questionable, and needs to be further verified in the future. The moment-thrust-curvature relationship for a dented tubular includes both a ascending branch and descending branch, as shown in Fig. 2-5(b). The corresponding parameters and equations are listed in Appendix A. The moment curvature relationships generated using Duan et al. expressions for a tubular with D/t=34, KL/r=60, and Fy=35.1 ksi are shown in Fig. 2-6(a), (b) and (c). The comparison of M-P-Φ and M-P-ε_0 relationships between theory and empirical analysis for a non-dented tubular is shown in Fig. 2-7.

2.4 Derivation of Moment-Thrust-Curvature Relationships for Internally Grouted Sections

For internally grout filled sections, unlike unrepaired sections, the ovalization effect is not significant and can be neglected. With this simplification the moment-thrust-curvature relationships for grout filled tubulars can be more easily developed.

The approach used to develop the moment-thrust-curvature relationships (M-P-Φ and ε-P-Φ curves) is based on the so called "Fiber Model" or "Laminar Model". The fiber model idealizes the internally grout section, either undented or dented, by dividing it into

an appropriate number of discrete layers (see Fig. 2-8). To preserve the area of the steel tube in the dented section, which has the same radius of R, the width of the steel layer is extended in the dent saddle as shown in Fig. 2-8. The uniaxial stress-strain history of each of these layers are then used in the computations along with kinematic and equilibrium requirements to generate the M-P-Φ and ε-P-Φ relationships (see Fig. 2-9).

2.4.1 Material Property Idealization for Steel Tube

Fig. 2-10 shows 2 types of stress-strain relationships for the steel tubular. Type 1 stress-strain curve is an elastic-perfectly plastic stress-strain relationship. The type 2 stress-strain curve takes the local buckling effect into account with a descending branch in the compression region. An empirical expression for the descending branch of the steel stress-strain relationship was proposed by Sato and Suzuki (1992) as follows :

$$\sigma = \sigma_{cr} \left(\frac{\epsilon}{\epsilon_{cr}} \right)^{n} \qquad (2\text{-}37)$$

where

σ_{cr} : the critical stress when local buckling occurs ($=\alpha\sigma_y$)

ε_{cr} : the critical strain when local buckling occurs ($=\gamma\varepsilon_y$)

n : empirical parameter ($\approx$ -0.2)

α and γ : empirical parameters

σ_y : yield stress

ε_y : yield strain

2.4.2 Material Property Idealization for Grout

Since the grout is surrounded by the steel tubular column in an internally grout-filled repaired member, the grout is likely to be at least partially confined until local buckling of the tube's wall occurs. The strength and ductility of well-confined grout is significantly greater than that of unconfined grout. Kent and Park (1971) proposed the compressive stress-strain relationships shown in Fig. 2-11 for unconfined and confined concrete. In the region between a strain ε of zero to ε_0 the compressive stress-strain (fc-ε)relationship is represented by the following second order expression :

$$f_c = f_c' \left[\frac{2\varepsilon}{\varepsilon_0} - \left(\frac{\varepsilon}{\varepsilon_0} \right)^2 \right] \qquad (2.38)$$

and the elastic modulus of concrete is defined as :

$$Ec = \frac{2 f_c'}{\varepsilon_0} \qquad (2.39)$$

where f'c and ε_0 are the concrete maximum compressive stress and the corresponding strain.

Chen and Atsuta (1976) proposed the three types of stress-strain relationships for

concrete shown in Fig. 2-11(b). Type 1 defines an unconfined concrete material in which the maximum compressive stress of 0.85 f'c is reached, after which the stress decreases with strain beyond ε_0. Type 2 defines a concrete having an increase in ductility due to the confinement of the steel, but no increase in stress. Type 3 accounts for the triaxial state of stress in concrete due to the confinement of steel. The confinement of the grout is assumed to increase both its ductility and compressive strength. Grout inside a tube will not develop full confinement because of the Poisson effect causing the steel to radially expand outward more than the grout, as well as the local buckling in the tube. Consequently, the model for the grout's compressive stress-strain relationship for the confined grout proposed in the study consists of Kent and Park's parabola equation for the ascending curve with either a sustained strength (grout stress-strain curve Type 1), or a sustained strength followed by a decrease in stress at a rate of β Eg beyond the strain ε_{bu} (grout stress-strain curve Type 2). Fig. 2-12 shows the Type 1 and Type 2 stress-strain curves, where ε_{bu} corresponds to the local buckling of the steel tube adjacent to the grout. The quantities β and Eg respectively, represent an empirical factor and the grout's initial modulus, where

$$E_g = \frac{2f'_g}{\varepsilon_0} \qquad \textbf{(2-40)}$$

The strain ε_{bu} is calculated by the following

$$\varepsilon_{bu} = \phi_{cr}(y_{N.A.} - y_{grout}) \qquad \textbf{(2-41a)}$$

where

$$\phi_{cr} = \frac{\varepsilon_{cr}}{y_{N.A.}} \qquad \textbf{(2-41b)}$$

in which

y_{grout} = distance from top of tube to grout top fiber

$y_{N.A.}$ = distance from the top fiber to neutral axis

ε_{cr} = steel critical strain when local buckling occurs

ϕ_{cr} = curvature associated with local buckling in steel

For completely unconfined grout (e.g. a grout tube) ε_{bu} corresponds to ε_0

The comparisons of the stress-strain curves between experimental data and the proposed grout equation are plotted in Fig. 2-13, Fig 2-14 and Fig 2-15. In the model, it is assumed that the grout has no strength in tension.

2.4.3 Assumptions of the Fiber Model Analysis

In the development of moment-thrust-curvature relationships for a grout filled tube the following assumptions were made :

(1) Plane sections remain plane during bending.

(2) Shear deformations and their effects are neglected.

(3) Poisson effects are neglected.

(4) The residual stress of the steel tube is neglected.

(5) The ovalization of the cross section is neglected.

2.4.4 Computational Procedures

Because of the nonlinear stress-strain relationships of the materials, an iterative computational procedure is employed to generate the M-P-Φ and ε-P-Φ curves. The steps for generating the M-P-Φ and ε-P-Φ curves for a specified axial compression load P_{spec} are outlined below :

Step 1 : Assume an initial curvature (Φ).

Step 2 : Specify a neutral axis position.

Step 3 : Calculate the corresponding axial strain of each layer, (positive for compression, negative for tension), where for layer i

$$\epsilon_i = \phi \ (y_{N.A.} - y_i)$$

where

y_i = distance form top fiber tubular section to each layer i

$y_{N.A.}$ = distance form top fiber tubular section to neutral axis

Step 4 : Calculate the corresponding axial forces

$$P_{cal} = \int_A \sigma(y)\, dA = \sum_1^N \sigma_i dA_i$$

where σ_i corresponds to the strain ε_i for the layer i from its stress-strain curve; and dA_i is the area of layer i.

Step 5 : Compare P_{cal} with P_{spec}

If the difference is greater than a specified tolerance (say : P_{spec} /1000)

then go to Step 2 (If it does not converge after a specified number of cycles then go to Step 1).

Step 6 : Calculate the contribution of each layer and sum the moments with respect to the centroid axis.

$$M = \int_A y\sigma(y)\, dA = \sum_1^N y_i \sigma_i dA_i$$

where y is referenced from the centroid of the undented section.

Step 7 : Calculate the axial strain at the centroid.

$$\varepsilon_{axial} = \phi\ (y_{N.A.} - R + d_d - e_s)$$

where $y_{N.A.}$ is referenced from the centroid of the undented section, e_s is the distance between the centroids of the undented and dented sections, and d_d is equal to the dent depth. Note that for an undented section, d_d and e_s are both equal to zero. The effect of including the term e_s in the above equation was found to be minimal, and is excluded

from the computer program.

Step 8 : Record the values of P, Φ, M and ε.

Step 9 : Increment the curvature by an amount of $\Delta\Phi$: $\Phi = \Phi + \Delta\Phi$,

and go to step 2

The above nine steps provide the M-P-Φ and ε-P-Φ relationships corresponding to a specified axial load P for a desired range of curvature. Fig. 2-16 and Fig. 2-17 show the M-P-Φ and ε-P-Φ curves for a undented, internally grout filled section for various axial loads calculated using the above procedure. The M-P-Φ and ε-P-Φ curves for a dented, internally grout filled section for various axial loads based on the above procedure are shown in Fig. 2-18 and Fig. 2-19. The moment curvature relationships obtained from the fiber analysis are represented by a set of data points instead of a continuous function. The moment curvature relationships between two data points is obtained through interpolation.

3. M-P-Φ NUMERICAL INTEGRATION COMPUTER PROGRAM

3.1 General

The M-P-Φ and ε-P-Φ relationships presented in Sections 2.3 and 2.4 were implemented into the Fortran computer programs in order to predict the behavior and strength of dent-damaged and internally grout repaired tubular members. In the numerical integration procedure, the member is first divided into a specified number of segments. Through the numerical integration procedure of incremental load control the axial compression-shortening response as well as axial compression-lateral deflection response are then obtained. This chapter describes the computational details of the numerical integration procedure.

3.2 Numerical Integration Procedure

The integration procedure is based on the assumption that the behavior of a segment is described by curvatures and forces at the stations at its ends. The numerical integration procedures for the dent-dented and internally grout repaired members are basically the same. The only difference is that the moment curvature relationships for the non-damaged and nonrepaired, dent-damaged members used in the computer program are adopted from Sohal and Chen [1987,1988] and Duan et al. [1993], while the moment curvature relationships for the internally grout repaired members is derived through the fiber model as described in Chapter 2. The basic steps involved in the numerical integration procedure to obtain the member load-displacement response are as follows :

Step 1 : Divide the tubular into a specified number of n segments. (see Fig. 3-1)

Step 2 : Set P=0.0

Step 3 : Assign an initial value of load P and a load increment ΔP

Step 4 : P = P + ΔP

Step 5 : Assume the initial deflections at all stations ($Yassume_i$).

Step 6 : Calculate the moments at all stations considering the second order effect (P-δ) by using the following equations. For undented segments (see Fig. 3-2) :

$$M_i = P(Yassume_i) + M_L - Reaction_L(x_i) - \int_0^{x_i} (x_i - x)\, w(x)\, dx \qquad (3\text{-}1)$$

For dented, unrepaired segments (see Fig. 3-3) :

$$M_i = P(Yassume_i + e_s) + M_L + Reaction_L(x_i) + \int_0^{x_i} (x_i - x)\, w(x)\, dx \qquad (3\text{-}2)$$

where

$$e_s = \frac{D}{2\pi}(\sin\alpha - \alpha\cos\alpha) \qquad (3\text{-}3)$$

and

$$\alpha = \cos^{-1}\left(1 - \frac{2d_d}{D}\right) \qquad (3\text{-}4)$$

in which :

e_s = geometry centroid change due to the dent damage

D = outer diameter of the tubular member

d_d = dent depth

α = angle shown in Fig. 3-3

For the internally grout repaired segments, both undamaged and damaged, use Eq. 3-1, since the moment curvature relationships for the internally grout repaired members are derived about the geometric centroid of an undamaged segment.

Step 7 : For the calculated moment at each segment obtain the corresponding curvature from the moment curvature relationships.

Step 8 : Compute the corresponding curvature Φ_i for each segment, accounting for local buckling, by going through the following process :

For undamaged and nonrepaired, dent-damaged tubular members :

Compare M_i with M_{max} for undamaged segments, and M_i with M_{pud} for dent-damaged segments (see Fig. 2.5(a), (b), and Appendix A). If M_i is smaller than M_{max} for an undamaged segment, or M_i is smaller than M_{pud} for a dent-damaged segment, then the corresponding curvature is on the ascending branch of the M-P-Φ relationship. If M_i is larger than M_{max} for an undamaged segment, or M_i is larger than M_{pud} for an dent-damaged segment, then the corresponding curvature should be on the descending branch. Once M_i exceeds M_{max} for an undamaged segment, or M_{pud} for a dent-damaged segment, the axial force P must start to unload. Record the controlling station number. For the remaining part of the computation the curvatures of all the stations except the controlling

station must always lie on the ascending branch. The curvature of the controlling station will always lie on the descending branch. The load increment ΔP should be given a negative specified value, and proceed to Step 4 in order to force M_i to become less than M_{max} or M_{pud}.

For internally grout repaired segments :

Compare M_i with M_{peak} , where M_{peak} is the flexural capacity for the section for the specified axial load. If M_i is smaller M_{peak}, then interpolate the curvature from the moment curvature relationships. If M_i is larger than M_{peak}, then the corresponding curvature is on the descending branch. Once M_i exceeds M_{peak} , the axial force P must start to unload. Record the controlling station number. For the remaining part of the computation the curvatures of all the stations except the controlling station must always lie on the ascending branch. The curvature of the controlling station will always lie on the descending branch. The load increment ΔP should be given a negative specified value, and proceed to Step 4 in order to force M_i to become less than M_{peak}.

Step 9 : Calculate the deflection ($Ycal_i$) for each station (see Fig. 3-4), where $\Theta_0 = y_0 = 0$, and

$$\theta_i = \theta_{i-1} - \left(\frac{\Phi_{i-1} + \Phi_i}{2}\right) \Delta x_i \qquad (3\text{-}5)$$

$$Ycal_i = Ycal_{i-1} + \theta_{i-1} \Delta x_i - \int_{i-1}^{i} x\Phi(x)\, dx \qquad (3\text{-}6)$$

Assuming a linear variation in curvature between station i and i-1, Eq. (3-6) can be

simplified as shown below

$$Ycal_i = Ycal_{i-1} + \theta_{i-1}\Delta x_i - (2\Phi_{i-1} + \Phi_i)\frac{(\Delta x_i)^2}{6} \qquad (3\text{-}7)$$

where :

Δx_i = segment length

Step 10 : Apply a linear correction to satisfy the end condition, $Y_n = 0$ (see Fig. 3-5) to compute the newly calculated member displacement y_{ic} at each station, where at station i :

$$Y_{ic} = Y_i - \left(\frac{i}{n}\right) Y_n \qquad (3\text{-}8)$$

Step 11 : Compare Y_{ic} with $Yassume_i$ for each station. If the difference between Y_{ic} and $Yassume_i$ is greater than the tolerance (say Y_{ic} / 1000), then set $Yassume_i = Y_{ic}$ and go back to Step 6. Otherwise go to next Step 12.

Step 12 : Compute the axial shortening response. (Details will be discussed in Section 3.3)

Step 13 : Repeat Steps 4 through Step 12 until the axial load decreases, after reaching the capacity of the member, to a specified percentage of P_y.

3.3 Axial Load-Shortening Relationships

The axial shortening Δ of a beam-column results from two parts. The first is from the

axial shortening Δ_s due to the axial strain of the material, the other is the geometric shortening Δ_g due to the lateral deflection.

$$\Delta = \Delta_s + \Delta_g \qquad (3\text{-}9)$$

3.3.1 Axial Shortening due to Axial Strain

Duan et al. (1993) proposed a set of M-P-ε_0 curves for both undamaged and dent-damaged segments. For the internally grout repaired segments, as noted in Step 7 in Section 2.4.4, the ε-P-Φ relationships are derived about the centroid axis of an undamaged section for the given load and moment. The axial shortening due to axial strain can be obtained from following equations.

For the dent-damaged members :

$$\Delta_s = \sum_{i=1}^{i=n} (\Delta x_i)(\varepsilon_{0i}) \qquad (3\text{-}10)$$

For the internally grout repaired members :

$$\Delta_s = \sum_{i=1}^{i=n} (\Delta x_i)(\varepsilon_i) \qquad (3\text{-}11)$$

where :

n = total number of segments

Δx_i = length of segment i

ε_{0i} = axial strain of segment i determined from M-P-ε_0 curve

ε_i = axial strain of segment i interpolated from ε-P-Φ expressions.

3.3.2 Axial Shortening due to Geometric Change

The axial shortening due to the geometric change is obtained from the calculated lateral deflections of all stations, where

$$\Delta_g = \sum_{i=2}^{i=n-1} [\Delta x_i - \sqrt{(\Delta x_i)^2 - (Y_i - Y_{i-1})^2}] \qquad (3\text{-}12)$$

where :

Y_{i-1} = the deflection at the left end of segment i, where $y_1 = 0$

Y_i = the deflection at the right end of segment i, where $y_{n+1} = 0$

3.4 Modelling Aspects and Guidance

The previous section illustrated the algorithm of the numerical integration procedure. This section will discuss the influence of some modelling techniques on the results of the computed behavior.

3.4.1 Dent-damaged and Internally Grout Repaired Members

(a). Increment of load steps : The numerical integration procedure in the computer program is using moment curvature relationships in combination with a load control algorithm. The program allows the user to discretize the history of loading to a finite number of increments. In order to minimize overshooting problems at peak load, a value

of $\Delta P = 0.005$ Py is recommended. However it really depends on the accuracy the user tries to achieve.

(b). Length of dented segment : The length of a dented segment is correlated with the dent depth, diameter and thickness of a tubular member. The longitudinal profile of the dent and the length of the dented segment recommended here are adopted from the relationships analytically derived by Wierzbicki and Suh (1986). The model of the dented segment is based on the assumption of a knife edge load imposing the dent (see Fig. 3-6). The dent length can be expressed as

$$l_d = D\sqrt{\frac{\pi\, d_d}{4\, t}} \qquad (3\text{-}13)$$

where :

D = outer diameter of the undented segment

t = thickness of the undented segment

d_d = dent depth

The length of dented segment was taken to be $L_d = 2.0\, l_d$. This assumption was proven to be appropriate when comparisons of member response correlated well with the experimental results.

(c). Number of segments : Theoretically the larger the number of segments is, the more accurate the result will be. It should be emphasized that when the difference between the

length of a dented and undented segment becomes larger, there is a greater tendency not to achieve convergence during the iteration process. This situation is especially dominant when the iteration goes to the descending branch of the moment curvature relationships.

(d). Out-of-Straightness : The maximum value of out-of-straightness usually occurs at the dented section. It should be measured after, instead of before, the dent-damage occurs. The out-of-straightness of the dent-damaged member is modelled as a half-sine wave distribution along the member and has a maximum value at the dented section.

(e). Long dents : The longest dent-damaged tube was tested by Smith (1983). Its ultimate strength was found to be similar to a tubular having a knife-edge dent profile. Equation (3-13) assumes a knife edge denting device, hence for long dents one should be more cautious in assuring that the dented segment's length is compatible with the actual length of the dent. The experimental data used for comparison of the analytical results is from specimens with knife-edge dent profiles.

(f). Convergence factor : The convergence in the computer programs is based on a tolerance that is specified by the user as a convergence factor. Convergence is achieved when the difference between the new and old value for displacement is within the reciprocal of the convergence factor times the new value for all stations, e.g.

for all i :

$$\frac{yassume_i - y_{ic}}{y_{ic}} \leq \frac{1}{\text{Convergence Factor}}$$

It is worth mentioning that setting a larger convergence tolerance does not result in a significant time saving because of the iteration procedure's convergence characteristics. In general, setting the convergence factor equal to a value of 1000 is recommended.

(g). Consideration of local buckling : For an undamaged member with a D/t ratio greater than 36 the local buckling affects not only the ultimate strength but also the moment curvature relationships. For damaged members, however, the effects of local buckling are not as pronounced as in undamaged members, especially for members with dent depth-to-diameter ratios greater than 0.05 [Smith et al., 1979]. This is because the ultimate strength of a dent-damaged member is controlled mainly by the plastification of its dent segment rather than local buckling. When the dent segment is not located at midspan, or the member is subjected to large end moment producing double curvature, the collapse can possibly be initiated by local buckling in the undented portion of the member. It is therefore recommended that local buckling always be considered in the analysis, as assumed by the computer programs. For the internally grout filled members, as mentioned previously local buckling was accounted for by the use of the stress-strain relationship of Eq. (2-37) for the steel tubular member, and the effects on the internal grout accounted for in its stress-strain curve (see Fig. 2.12 and Eq. (2-41)).

3.4.2 Internally Grout Repaired Members

(a). Section geometry idealization : The computer program is designed to let the user specify the numbers of layers in 3 groups (see Fig. 2-8), where the programs then will automatically generate the area of each layer. The method used in the program to generate the area of each layer is described below (see Fig 3-7).

For an undamaged section :

$$d1 = \frac{t}{N1} \tag{3-14}$$

$$d2 = \frac{(D-2t)}{N2} \tag{3-15}$$

$$d3 = \frac{t}{N3} \tag{3-16}$$

For the dent-damaged section :

$$d1 = \frac{t}{N1} \tag{3-17}$$

$$d2 = \frac{(D-2t-d_1)}{N2} \tag{3-18}$$

$$d3=\frac{t}{N3} \qquad \textbf{(3-19)}$$

where :

N1, N2, N3 = number of specimen layers in groups 1,2, and 3

d1 = the depth of each layer in the group #1

d2 = the depth of each layer in the group #2

d3 = the depth of each layer in the grout #3

D = the outer diameter of the tube

t = thickness of tubular

d_d = dent depth

The area of each layer i for both undamaged and dent-damaged sections is then obtained as follows. For the undamaged section :

Group 1

$$As1_i=2d1\sqrt{(\frac{D}{2})^2-(\frac{D}{2}-id1+\frac{d1}{2})^2} \qquad \textbf{(3-20)}$$

$$Ag1_i=0.0 \qquad \textbf{(3-21)}$$

Group 2

$$As2_i + Ag2_i = 2d2\sqrt{\left(\frac{D}{2}\right)^2 - \left(\frac{D}{2} - N1d1 - id2 + \frac{d2}{2}\right)^2} \qquad \textbf{(3-22)}$$

$$Ag2_i = 2d2\sqrt{\left(\frac{D}{2} - t\right)^2 - \left(\frac{D}{2} - N1d1 - id2 + \frac{d2}{2}\right)^2} \qquad \textbf{(3-23)}$$

$$As2_i = (Eq.3\text{-}22) - (Eq.3\text{-}23) \qquad \textbf{(3-24)}$$

Group 3

$$As3_i = 2d3\sqrt{\left(\frac{D}{2}\right)^2 - \left(\frac{D}{2} - N1d1 - N2d2 - id3 + \frac{d3}{2}\right)^2} \qquad \textbf{(3-25)}$$

$$Ag3_i = 0.0 \qquad \textbf{(3-26)}$$

For the dent-damaged section, including a correction factor ϕ to preserve the steel cross-section area :

Group 1

$$As1_i = \phi\ 2d1\sqrt{\left(\frac{D}{2}\right)^2 - \left(\frac{D}{2} - d_d - id1 + \frac{d1}{2}\right)^2} \qquad \textbf{(3-27a)}$$

$$\phi = \frac{\pi\, Dt - \Sigma As2_i - \Sigma As3_i}{\Sigma As1_i} \qquad \textbf{(3-27b)}$$

$$Ag1_i = 0.0 \qquad \textbf{(3-28)}$$

Group 2

$$As2_i + Ag2_i = 2d2\sqrt{\left(\frac{D}{2}\right)^2 - \left(\frac{D}{2} - d_d - N1d1 - id2 + \frac{d2}{2}\right)^2} \qquad \textbf{(3-29)}$$

$$Ag2_i = 2d2\sqrt{\left(\frac{D}{2} - t\right)^2 - \left(\frac{D}{2} - d_d - N1d1 - id2 + \frac{d2}{2}\right)^2} \qquad \textbf{(3-30)}$$

$$As2_i = (Eq.2\text{-}29) - (Eq.2\text{-}30) \qquad \textbf{(3-31)}$$

Group 3

$$As3_i = 2d3\sqrt{\left(\frac{D}{2}\right)^2 - \left(\frac{D}{2} - d_d - N1d1 - N2d2 - id3 + \frac{d3}{2}\right)^2} \qquad \textbf{(3-32)}$$

$$Ag3_i = 0.0 \qquad (3\text{-}33)$$

where :

$As1_i$ = the steel area of layer i in group #1

$Ag1_i$ = the grout area of layer i in group #1

$As2_i$ = the steel area of layer i in group #2

$Ag2_i$ = the grout area of layer i in group #2

$As3_i$ = the steel area of layer i in group #3

$Ag3_i$ = the grout area of layer i in group #3

The accuracy of a given analysis is related to the number of layers used in the discretization of the cross-section. It is advisable to concentrate a sufficient number of layers near the ends (group #1 and group #3) in order to capture the spread of plasticity in the steel tube as well as local buckling.

(b). Influence of steel model : The stress-strain relationship model for the steel used in the analysis was shown previously in Fig. 2-10. Type 1 steel stress-strain curve is assumed to be elastic perfectly plastic. The use of this stress-strain curve is reasonable to predict the member's capacity, for in most cases the ultimate strength will be reached before local buckling occurs. However, in order to obtain both the ascending and descending branch of the load-deflection response curves the Type 2 steel stress-strain curve must to be used.

(c). Influence of grout model : The Type 1 stress-strain relationship for the grout is assumed to be a parabola up to the grout strength (f'g), and sustaining a stress of f'g for continued strain. This assumption is based on complete interaction taking place between the steel and the grout and the triaxial state of stress increasing the grout's ductility. In reality, the Type 2 grout stress-strain relationship is more appropriate for it accounts for the partial confinement and the effect of local buckling in the steel tubular.

(d). Stress-Strain history : The computer program was designed to allow the user to trace the stress-strain history in a maximum of 3 specified fibers (either steel or grout) during the integration process up to when the ultimate load is reached. The stress-strain history can be used to compare with the experimental behavior. The user specifies the desired fibers by their identification numbers.

3.5 Analysis Examples

A user's guide and examples of input and output files for the dent-damaged, unrepaired members are listed in Appendix C. A user's guide and examples of input and output files for internally grout repaired specimens are given in Appendix D.

4. CORRELATION STUDY

4.1 General

In this chapter the verification of the two computer programs for non-repaired, dented and grout repaired analysis is presented by comparing the predicted response with experimental behavior. A set of comparisons between the accuracy of several other existing prediction methods and the moment curvature approach for the internally grout repaired specimen are also presented.

4.2 Dent-Damaged Specimens

The results from 28 test specimens were used to verify the moment curvature computer program, and are summarized in Table 1(a) (Ricles and Gillum, 1992), Table 2(a) (Ostapenko et al., 1993), Table 3(a) (Landet and Lotsberg, 1992), Table 4(a) (Smith et al, 1979) and Table 5(a) (Taby, 1986a, 1986b). 28 specimens are included in these tables, namely : diameter-to-thickness (D/t) ratio from 25 to 90; a dent depth-to-diameter (dd/D) ratio from 0.0 (undamaged) to 0.2; a dent depth-to-thickness (dd/t) ratio from 0.0 to 9.5; and an out-of-straightness-to-length (δ/L) ratio from 0.0001 to 0.0112. The dent location of all specimens was at their midspan. The corresponding residual strength-to - yield load (Pu,mc/Pu,exp) ratios for each specimen are given in Table 1(b), Table 2(b), Table 3(b), Table 4(b), and Table 5(b). Included in these tables are a comparison with the predicted capacity Pu,mc using the moment curvature approach. The histogram of predicted-to-measured ultimate strength (Pu,mc/Pu,exp) ratio for the 28 specimens is

plotted in Fig. 4-1, which has a mean equal to 0.98 and coefficient of variation equal to 0.096.

Comparisons of axial compression-shortening and axial compression-lateral deflection responses for Specimen A1 [Ricles and Gillum, 1992b], having a dent depth ratio (d_d/D) of 0.1 and diameter-to-thickness ratio (D/t) of 34, are shown in Fig. 4-2 and Fig. 4-3. The solid line represents the prediction by the moment curvature numerical integration approach, while the triangular data points correspond to test results. Comparisons of axial-shortening and axial compression-lateral deflection response for Specimen A2 [Ricles and Gillum, 1992b] with d_d/D=0.1, D/t=34, and end eccentricity e equal to 0.2D are shown in Figs.4-4 and 4-5. Figs. 4-6 and 4-7 show the comparisons of axial compression-shortening and axial compression-lateral deflection response for Specimen B1 [Ricles and Gillum, 1992b] having d_d/D=0.1 and D/t=46. Figs. 4-8 and 4-9 illustrate the comparisons of axial compression-shortening and axial compression-lateral response for Specimen C2 [Ricles and Gillum, 1992b] having d_d/D=0.1 and D/t=64. The moment curvature approach is shown to predict accurately the behavior of dent-damaged tubular members on the ascending branch. For the post-ultimate load range the experimental data has a higher strength than theoretical predictions. Due to the complexity of the post-ultimate range the predictions are considered to be reasonable. In all of these analysis the number of segments was 21, with a length of 2 l_d (see Eq. 3-13) for the dented segment. The sensitivity of the result to this will be discussed later.

4.3 Internally Grouted Specimens

4.3.1 Previous Prediction Methods

In this section the moment curvature integration approach along with several other existing prediction methods for estimating the repaired strength of dent-damaged tubular members with internally grout repair are compared with experimental data. These existing prediction methods include : API RP-2A [1984, 1986]; BS 5400 [1984]; Modified BS 5400 [Loh, 1991]; the AISC-LRFD [1986] approach; a modified AISC-LRFD approach [Loh, 1991]; a simplified AISC-LRFD approach [Loh, 1991]; and Parsanejad's Equation [1987]. The API RP-2A and AISC-LRFD methods are those commonly used in practice, where the former neglects the contribution of the grout and the latter ignores dent damage and considers the grout to act as concrete. The BS 5400 and the modified BS 5400 approaches are described in Appendix B. The remaining methods are described below.

4.3.1.1 Parsanejad's Approach

Parsanejad's approach [1987] is based on the simplifying assumptions that : (1) Full interaction exists between the grout and the damaged tube; and (2) grout provides sufficient support to the tube wall in the damaged region to inhibit local buckling. The load-carrying capacity is based on using transformed section properties in a beam-column analysis in conjunction with the first yield collapse criteria. First yield collapse criteria assumes that the ultimate capacity of the member is reached when yielding first occurs in the saddle of the dent. The equation for estimating the ultimate strength of internally

grout repaired members is based on the equilibrium of the member in its deformed position corresponding to ultimate load, where

$$\sigma_u \left(\frac{A^*_{tr}}{A_{tr}}\right) + \frac{1}{Z_{tr}} \left(\sigma_u A^*_{tr} \frac{e_t}{1 - \frac{\sigma_u}{\sigma_e}}\right) = \sigma_y \qquad (4\text{-}1)$$

where :

σ_y = yield stress of steel tubular

σ_u = ultimate axial stress

A_{tr} = transformed cross sectional area at the dent

A_{tr}^* = transformed cross sectional area of the undamaged section

z_{tr} = elastic section modulus of the transformed section at the dent with respect to the dented saddle

σ_e = Euler buckling strength

e_t = e (end eccentricity) + δ (eccentricity caused by the overall bending damage) + e_{tr} (distance between the centroids of dented and undented transformed cross section)

4.3.1.2 Modified AISC-LRFD and Simplified Approaches

If it is assumed that the full length of an internally grout filled member is a prismatic member with the cross section at the dent, then the equations recommended in AISC-LRFD [1986] can be used. The modified AISC-LRFD approach is the same as the simplified approach except that in the former 80 percent of the grout stiffness ($E_g I_g$) is

assumed to contribute to the composite member's Euler buckling load. These two approaches have been proposed by Loh, J. T (1991) and are outlined as below :

(a). Modified AISC-LRFD approach : The approach consists of a unity check equation for combined axial load and bending moment :

$$U.C. = \frac{P}{P_{cr}} + \left[\frac{C_m M}{(1-\frac{P}{P_E})M_u}\right] \leq 1.0 \qquad \textbf{(4.2)}$$

Where

the axial compression capacity is defined as

$$P_{cr} = F(\lambda)\, P_u \qquad \textbf{(4-3)}$$

and the squash load as

$$P_u = F_y A_s + 0.67 A_g f'_g \qquad \textbf{(4-4)}$$

The Euler buckling load for the composite section is determined from Eq. (4-5) :

$$P_E = \frac{\pi^2}{(KL)^2}(E_s I_s + 0.8 E_g I_g) \qquad \textbf{(4-5)}$$

where

$$\lambda = \sqrt{\frac{P_u}{P_E}} \qquad \textbf{(4-6)}$$

and, for $\lambda \leq \sqrt{2}$

$$F(\lambda) = 1 - \frac{1}{4}\lambda^2 \qquad \textbf{(4-7)}$$

or for $\lambda > \sqrt{2}$

$$F(\lambda) = \frac{1}{\lambda^2} \qquad \textbf{(4-8)}$$

The bending moment capacity M_u is defined by

$$M_u = M_p(1 + 0.01m) \qquad \textbf{(4-9)}$$

where :

$$M_p = (D-t)^2 t F_y \qquad \textbf{(4-10)}$$

and

$$m = 5.5\left[\left(\frac{0.6F'_g}{F_y}\right)\left(\frac{D}{t}\right)\right]^{0.66} \qquad \textbf{(4-11)}$$

(b). **Simplified Method :** The simplified method is basically the same as the modified AISC-LRFD approach, except Eq. (4-5) is replaced with the Eq. (4-12) in order to reflect

the fact that the Euler buckling load is based on only the stiffness (E_sI_s) of the steel section.

$$P_E = \frac{\pi^2 E_s I_s}{(KL)^2} \qquad \textbf{(4-12)}$$

4.3.2 Comparisons with the Experimental Results

Verification of the moment curvature numerical integration approach for grout-filled tubular response prediction was performed through a comparison with 12 undamaged, internal grouted tubes and 55 damaged internally grout repaired tests. The experimental data of the undamaged specimens corresponded to tests by Tebbett and Forsyth (1987) and Wimpy (1986). The repaired specimen experimental data corresponded to tests by Ricles and Gillum (1992b) ,Parsanejad (1986, 1987), and Boswell and D'Mello (1990). The material properties and member dimensions are listed in Table 6(a), 7(a), 8(a) and 9(a) for these specimens.

4.3.2.1 Undamaged, Internally Grout Filled Specimens

Table 6(b) shows the ultimate strength prediction results for the 12 undamaged specimens tested by Wimpy Lab. [1986] and Tebbett and Forsyth [1984] using 7 different approaches, namely : API RP-2A, BS 5400, modified BS 5400, AISC-LRFD, modified AISC-LRFD, simplified AISC-LRFD method, and moment curvature approach. The mean value and coefficient of variation of the predicted-to-measured ultimate strength ratio for these methods corresponding to the 12 tests are summarized in Table 10. It can be seen

that the moment curvature approach provides a reliable estimate of member strength, having for the predicted-to-experimental capacity ratio a mean value equal to 0.98 and coefficient of variation equal to 0.15. The others have a mean value ranging from 0.88 to 1.05, with the coefficient of variation ranging from 0.20 and 0.28. These coefficient of variations are larger than the 0.15 value from the moment curvature approach.

4.3.2.2 Dent-Damaged, Internally Grout Repaired Specimens

The test data for the 55 dent-damaged, internally grout specimens were compared with the strength prediction results of 4 different approaches, which included : Parsanejad's equation; modified AISC-LRFD method; simplified AISC-LRFD method; and the moment curvature numerical integration approach. It is worth noting that all of the Boswell's specimens had a reported modular ratio (Es/Eg) equal to 18.24. These modular ratios appear to be much larger than typical values for a grout strength which is in the range of 6 to 10.5 ksi. Typical values of modular ratios versus grout strength from grout material tests are plotted in Fig. 4-10, which confirms that a value of 18.24 is too large. Due to the questionable data reported for the modular ratio from Boswell and D'Mello's tests, three stages of verification were conducted as follows :

Stage 1 : 27 test results (include only first 9 of Boswell and D' Mello's tests in Table 9(a))

Stage 2 : 55 test results (include all of Boswell and D' Mello's tests)

Stage 3 : 55 test results (include all of Boswell and D' Mello's tests with a modified modular ratio value of 10.0 only in the moment curvature approach)

The predicted-to-measured ultimate strength (Pu,mc/Pu,exp) ratios of the stage 1 verifications including 27 tests are listed in Tables 7(b), 8(b), and first 9 specimens of Table 9(b) The histograms of the predicted-to-measured ratios of 27 tests in term of the 4 different approaches are plotted in Figs. 4-11 to 4-14. The comparisons of accuracy of these 4 prediction methods are listed in Table 11(a). The predicted-to-measured ultimate strength ratio of stage 2, as well as stage 3, verifications are listed in Tables 7(b), 8(b), 9(b) and 9(c). The corresponding histograms of predicted-to-measured ultimate strength ratio by the 4 prediction methods are plotted in Figs. 4-15 to 4-19, and the comparisons of accuracy of these prediction methods are listed in Table 11(b).

An examination of the results from the first stage of verifications indicates that the moment curvature approach is the overall best method of analysis, having for the predicted-to-measured strength ratio a mean equal to 0.96 and coefficient of variation of 0.14. The other approaches had a mean value of 0.93, 0.92, and 0.80, with corresponding coefficient of variations of 0.14, 0.18, and 0.22 as shown in Table 11(a). The second and third stage of verifications resulted in the moment curvature approach having a mean value of 0.86 and 0.92 and a coefficient of variation of 0.18 and 0.14 (see Table 11(b)). The mean value of 0.86 in the second stage seems to be low due to the 28 questionable data values of Boswell and D' Mello. After the modifications in Stage 3, the mean value of 0.92 and the coefficient of variation of 0.14 for the moment curvature approach represented a closer lower bound solution. Other approaches with the modified modular ratio assumption have the mean values ranging from 0.80 to 0.90 and coefficient of

variations ranging from 0.16 to 0.19 as also shown in Table 11(b). Overall, the verifications indicate that the moment curvature approach is the most accurate and consistent among the prediction methods. The results also indicate the need for accurate material property data.

4.4 Comparisons of Predicted Axial Compression-Shortening and Axial Compression-Lateral Deflection Response with Experimental Results

Figs. 4-20 through 4-22 show the comparisons of axial compression-shortening and axial compression-lateral deflection responses generated from the moment curvature integration method (solid line) and experimental data (data symbol) for Ricles and Gillum's [1992b] Specimens A3, B3, and C3. The specimen properties are noted in these figures. Comparisons were also made with Ricles et al. [1994] Specimens A7, A9, and B7 and are shown in Figs. 4-23 through 4-25, where the specimen properties are also noted. Member properties and comparison of predicted strength with experimental results are shown in Table 12. It can been seen that the prediction of member behavior by the moment curvature approach agrees reasonably well with that of the test specimens.

4.5 Behavior of Internally Grout Filled Specimens

In order to further investigate the behavior (up to when the ultimate strength is reached) of selected internally grouted members, the strains at three different locations of the midspan segment at the top extreme fiber of the steel tube; the top extreme fiber of grout; and the bottom extreme fiber of steel, were investigated. For the undamaged,

internally grout filled members (Specimens 1, 3, and 5 of Tebbett and Forsyth [1984]), the axial compression versus strain diagrams are shown in Figs. 4-26 through 4-28. Furthermore the corresponding strains on the stress-strain diagrams at the peak loads are shown in Fig. 4-32. For selected damaged, internally grout repaired members (Ricles and Gillum's [1992b] Specimens A3, B3, and C3) , the axial compression versus strain diagrams are plotted in Figs. 4-29 through Fig. 4-31. The corresponding strains on the stress-strain diagrams at the peak loads are shown in Fig 4-33.

As it can be shown in Fig. 4-32 for the relatively short member (Spec. #1, KL/r=29), yielding occurred in the steel at the top and bottom fibers and the grout crushed when the member ultimate strength was reached. For the relatively longer members (Spec. #3, KL/r=58 and Spec. #5, KL/r=87), only the top fiber of the steel tube reached yielding when the member ultimate strength was obtained, with the grout nearing its crushing strain. This result is associated with the excessive deflection due to the second order effect (P-δ) which caused an instability once the top steel fibers yielded. Fig. 4-33 shows that for the repaired tubular with a constant KL/r of 60 that the smaller D/t ratio members (Spec. #A3, D/t=35) had the steel yield at the top and bottom fibers and the grout crush, whereas the relatively larger D/t ratio member (spec. #C3, D/t=64) had only the top and bottom steel fibers reach yielding.

4.6 Biases of Moment Curvature Approach

4.6.1 Dent-Damaged, Unrepaired Members

The biases of the moment curvature approach with respect to the geometrical parameters (δ/L, D/t, d_d/D and d_d/t) of unrepaired, dent-damaged tubulars was

investigated. By the observation of Figs. 4-34 through 4-37, it can be concluded that there is no perceptible variation in bias for predicted member strength with respect to δ/L, D/t, d_d/D and d_d/t for the moment curvature approach.

4.6.2 Internally Grout Repaired Members

The biases of the moment curvature approach with respect to the geometrical parameters (δ/L, D/t, and d_d/D) and material parameters (F'g and modular ratio) were investigated for internally grout repaired tubulars. As illustrated in Figs. 4-38 through 4-42, there is no significant variation in prediction bias with respect to these parameters.

4.7 Effect of Dented Segment Length

For non-repaired members the dented segment length used in the model plays an important role in the post-ultimate load range during the numerical integration procedures as illustrated in Figs. 4-43 and 4-44. Fig. 4-43 shows the variation in a member's ultimate strength predicted by the moment curvature approach using different dented segment lengths. Only a negligible change of the ultimate strength occurs when the dented segment length varies from 0.5D to L_d . However, as seen in Fig. 4-44, the axial compression-shortening response in the post-ultimate range will be influenced by the model's dented segment length. This is due to the empirical nature of moment curvature expressions. For internally grout repaired members a similar effect was observed.

4.7 Effect of Local Buckling Material Parameters

The sensitivity of the material parameters Γ, n and β were explored, with selected results, plotted in Figs. 4-45 to 4-47. It is apparent in Fig. 4-45 that as Γ increased the ultimate load is unaffected while the post-ultimate load response has a slower descent. Based on the experimental data [Ricles and Gillum, 1992b, Ricles et al. 1994] it was found that Γ varied from a value of 2.0 (for D/t=64) to 6.0 (for D/t=34). For smaller values of the exponent n similar trends were found (see Fig. 4-46). The value of n=-0.3 was determined to fit experimental data analyzed by Sato and Suzuki [1992] for concrete filled tubulars, and also worked well for the moment curvature analysis of the grouted tubular presented herein. Figure 4-47 shows that a large variation in the value of β results in some difference in the response. Grout cube tests show β ranging from 290 ksi to 340 ksi (see Figs. 2-13 through 2-15). It was determined that the value for γ dominated the response, and that this response was not too sensitive to changes in β once the parametric value for γ was selected.

5. PARAMETRIC STUDY

5.1 General

Extensive parametric studies were performed to investigate the effects of various factors which may affect the residual and repaired strengths of tubular members. This parametric study involved using the moment curvature computer programs for the analysis of both dent-damaged and internally grout repaired members, and considered the variation of the following parameters : dent depth-to-diameter (d_d/D) ratio, member diameter-to-thickness (D/t) ratio, out-of-straightness-to-length (δ/L) ratio, steel yield stress Fy, and grout strength F'g. All the results presented are based on a member diameter of 8.625 inches and unless noted, the following material properties :

(1). Yield stress (Fy) = 34.8 ksi

(2). Young's modulus (Es) = 29071 ksi

(3). Grout strength (F'g) = 5.0 ksi

(4). Elastic modulus of grout (Eg) = 2907.1 ksi

(5). KL/r = 60.

5.2 Dent-Damaged, Unrepaired Members

5.2.1 Effect of Dent Depth

The effects of dent depth on the residual strength of unrepaired members with different D/t (34, 46 and 64) ratios having δ/L=0.0001 are shown in Fig. 5-1. Similarly Figs. 5-2 through 5-7 show the effects of dent depth on the residual strength of unrepaired members

with different D/t ratios and δ/L=0.0005, 0.001, 0.002, 0.005, 0.01 and 0.02. Fig 5-8 (based on nonlinear finite element analysis [Ricles et al. 1994]) also shows the effects of dent depth on the residual strength of D/t=34 and 64 members with the δ/L=0.0005. The finite element analysis results are shown to agree reasonably well with the moment curvature approach. By observing Fig. 5-1 through 5-8 the effects of dent depth on an unrepaired member's residual strength is shown to be significantly more critical for deeper dents. For δ/L equal to 0.0001, a small d_d/D ratio of 0.1 has a 37% reduction of member strength for D/t ratio equal to 34, a 44% reduction of member strength for D/t equal to 46, and a 52% reduction of member strength for D/t ratio equal to 64.

5.2.2 Effect of Member Diameter-to-Thickness Ratio

The effects of D/t ratio of 34, 46 and 64 were investigated. The D/t ratios in this range are usually used in fixed offshore structures. It can be seen from Fig. 5-1 to Fig. 5-8 that the effects of D/t ratio on the Pu/Py ratio are proportional to the d_d/D ratio as well as δ/L ratio, where members of higher D/t ratio with specified values for the d_d/D ratio and δ/L ratio have a lower residual strength. When d_d/D and δ/L become large the ultimate strength of the member is controlled by the excessive deflection due to the second order effects (P-δ) instead of the plastification of the section. It can also be seen in Fig. 5-1 that the Pu/Py ratios for members of D/t=34, 46, and 64 are all equal to 0.99 for d_d/D=0 and δ/L=0.0001, which corresponds to a straight member without any dent damage.

5.2.3 Effect of Out-Of-Straightness

The residual strength as a function of the δ/L ratio are plotted in Figs. 5-9 through 5-11 for the six different d_d/D ratios and D/t ratios equal to 34, 46 and 64. As seen in these figures, the effects of out-of-straightness on reducing residual strength becomes larger for members with a smaller d_d/D ratio, This is attributed to the mode of failure becoming more dominated by overall buckling due to the p-δ effects when d_d/D is small.

5.3 Internally Grout Repaired Members

5.3.1 Effect of Dent Depth

The effects of dent depth on the ultimate strength of repaired members with different D/t (34, 46, and 64) ratios and δ/L=0.0001 are shown in Fig. 5-12. Similarly, Figs. 5-13 through 5-18 show the effects of dent depth on the ultimate strength of repaired members with different D/t ratio and δ/L=0.0005, 0.001, 0.002, 0.005, 0.01 and 0.02.

It can be seen that the ultimate strength of an internally grout repaired member deteriorates less compared to the dent-damaged, unrepaired member as the d_d/D ratio increases. This is because of the fact that the internal grout arrests the growth of the dent during the loading history, resulting in the member developing a greater resistance.

5.3.2 Effect of Member Diameter-to-Thickness Ratio

The three curves (D/t=34, 46, 64) plotted in Figs. 5-12 through 5-18 for the internally grout repaired members have an opposite ordering in terms of the D/t ratios for a

specified residual strength compared to Figs. 5-1 through 5-7 for unrepaired members. In other words, the internally grout repaired members with the highest D/t ratio have larger ultimate strength; whereas among the unrepaired members the highest D/t ratio have lower residual strength.

5.3.3 Effect of Out-Of-Straightness

The repaired strength as a function of the δ/L ratio are plotted in Figs. 5-19 to 5-21 for six different d_d/D ratios and D/t ratios equal to 34, 46, and 64. As seen in these figures, the effects of out-of-straightness on repaired strength become larger for members with a smaller d_d/D ratio. This is attributed to the influence the d_d/D ratio has on the residual strength.

5.3.4 Effect of Steel Yield Stress

The effects of yield stress (Fy) in the range between 25 ksi and 80 ksi were investigated. The results are shown in Figs. 5-22 and 5-23 and based on the following material properties : in Fig 5-22 - D/t=34, KL/r=60, F'g=6.9 ksi, δ/L=0.0006; and in Fig 5-23 - D/t=64, KL/r=60, F'g=6.9 ksi, δ/L=0.0006

As seen in these figures the repaired strength is somewhat sensitive to Fy. For both D/t=34 and D/t=64, a member's repaired strength will increase by approximately 5 to 8 % as the yield stress increases by 5 ksi.

5.3.5 Effect of Grout Strength

The effect of grout strength (F'g) in the range between 4 ksi and 12 ksi with the modular ratio between 4 and 12 was analyzed. The results are shown in the Figs. 5-24 through 5-26, and were based on the following material properties : Fig. 5-24 - Fy=39.4 ksi, KL/r=60, D/t=34, d_d/D=0.1, δ/L=0.0006; Fig. 5-25 - Fy=39.4 ksi, KL/r=60, D/t=64, d_d/D=0.1, δ/L=0.0006; and Fig. 5-26 - Fy=39.4 ksi, KL/r=60, D/t=64, d_d/D=0.2, δ/L=0.0006. There are five sets of data in each figure, where each represents a specific modular ratio. As was shown in the Fig. 4-10, the modular ratio will decrease when the grout strength increases. In selecting a typical grout strength and the corresponding modular ratio from Fig 4-10, and referring to Figs. 5-24 through 5-26, it is estimated that an increase in F'g of 2 ksi will result in an increase in the member's repaired strength by approximately 10 to 15 %.

This appreciable increase is attributed to the confined effect of a higher grout strength increasing the member's capacity and the lower modular ratio resulting in a stiffer member that is less susceptible to P-δ effects.

5.4 Combined Effects for Dent-Damaged and Internally Grout Repaired Members

A set of seven figures have been plotted to evaluate the effectiveness of an internal grout repair. Figs. 5-27 through 5-33 are a combination of Figs. 5-1 through 5-7 and Figs. 5-12 through 5-18. The data from these figures was also plotted for each D/t ratio, with dent depth (d_d/D) and out-of-straightness (δ/L) as independent variables, in order to

generate surfaces for the member's repaired strength (see Figs. 5-34 through 5-36). It is apparent that the internal grout repair is significantly affected by out-of-straightness and dent depth, particularly their combined effect, with the repair being less effective as these quantities become larger. The internally grout repaired strength surfaces in these three figures were each compared with the strength of an undamaged member (d_d=0) having the maximum API RP-2A out-of-straightness of δ_p/L=0.001, see Figs. 5-37 through 5-39. Figs. 5-37, 5-38, and 5-39 are a useful design aid for repair strategy, for they provide information to enable one to determine which of the following three situations exists for a given damage scenario involving specified d_d/D and δ/L ratios :

1. Dent-damage has a small influence on the ultimate capacity of the tubular bracing member. Internally grout repair is not necessary if the residual strength exceeds the required strength to resist the applied loads.
2. Dent-damage results in a significant loss in ultimate capacity of the tubular bracing. Internally grout repair can reinstate the ultimate capacity of the tubular bracing.
3. Dent-damage results in a significant loss in ultimate capacity of the tubular bracing. Internally grout repair cannot reinstate the ultimate capacity of the tubular bracing.

To qualitatively evaluate the effect of dent depth and out-of-straightness damage on the internally grout repair, the curve associated with the intersection of the internally grout repaired and undamaged surfaces for D/t=34, 46, and 64, respectively, were fitted, as shown in Figs. 5-40 to 5-42, using regression analysis.

The result was as follows :

for D/t=34

$$f\left(\frac{\delta}{L}, \frac{d_d}{D}\right) = -\left(\frac{\delta}{L}\right) + 0.0099 - 0.008\left(\frac{d_d}{D}\right) - 0.00639\left(\frac{d_d}{D}\right)^2 \qquad \textbf{(A)}$$

for D/t=46

$$f\left(\frac{\delta}{L}, \frac{d_d}{D}\right) = -\left(\frac{\delta}{L}\right) + 0.00132 - 0.0128\left(\frac{d_d}{D}\right) - 0.0634\left(\frac{d_d}{D}\right)^2 \qquad \textbf{(B)}$$

and for D/t=64

$$f\left(\frac{\delta}{L}, \frac{d_d}{D}\right) = -\left(\frac{\delta}{L}\right) + 0.0171 - 0.0225\left(\frac{d_d}{D}\right) - 0.0501\left(\frac{d_d}{D}\right)^2 \qquad \textbf{(C)}$$

where

δ / L = normalized out-of-straightness

d_d / D = normalized dent depth

These equations can be used to evaluate the effectiveness of internally grout repair, for a given δ/L, d_d/D and D/t.

If

$$f\left(\frac{\delta}{L}, \frac{d_d}{D}\right) < 0.0$$

then the internally grout repair will not be fully effective in reinstating the member's strength to its undamaged strength.

If

$$f\left(\frac{\delta}{L}, \frac{d_d}{D}\right) \geq 0.0$$

then the internally grout repair will be fully effective in reinstating the member's strength to its undamaged strength. Note that Figs. 5-40 through 5-42 indicate that dent depth-to-diameter (d_d/D) ratios greater than 0.34, 0.37, and 0.41, respectively, for members with D/t=34, 46, and 64 will not have their damaged strength reinstated to their non-damaged strength by internal grouting with a grout strength of 5 ksi and steel yield stress of 34.8 ksi.

6. SUMMARY, CONCLUSIONS, AND RECOMMENDATIONS

6.1 Summary

In this thesis, computer programs for analyzing the behavior and ultimate strength of dent-damaged and internally grout repaired tubular steel members was developed. The theoretical background and derivations of the numerical procedures based on the moment curvature relationships that formed the basis for the analysis method programmed into the computer were described. A series of correlation studies were performed to verify the accuracy and reliability of the computer programs, including the results from 28 dent-damaged test specimens and 55 internally grout repaired dent-damaged test specimens and 12 internally grout filled undamaged test specimens. The ratio of predicted-to-experimental capacity using the moment curvature approach had a mean value of 0.98 and coefficient of variation of 0.096 for dent-damaged, unrepaired specimens and a mean value of 0.92 and coefficient of variation of 0.14 for the internally grout repaired specimens. The comparisons of axial compression-shortening and axial compression-lateral deflection responses with the test results were also illustrated. The comparisons show the predicted behavior to be in good agreement with the experimental results.

Comparisons for strength prediction by the moment curvature approach and other existing analytical methods were then made for the internally grout filled members. It was found that the predictions by the moment curvature approach have better and more consistent correlation with the experimental results than these other methods.

After the verification study, an extensive parametric study was performed by using the moment curvature computer programs to investigate the effects of d_d/D, D/t, δ/L for dent-damaged members and d_d/D, D/t, δ/L, F'g and Fy for internally grout repaired members on strength. The results were used to developed a set of design-oriented charts. From these charts the loss of ultimate strength due to dent-damage and the evaluation of the effectiveness of internal grout repair can be estimated precisely.

6.2 Conclusions

The numerical integration procedures based on moment curvature relationships can accurately predict the behavior and ultimate strength of both dent-damaged and internally grout repaired members, and are more reliable and consistent than other existing prediction approaches. Various parameters were found to affect the residual and internally grout repaired member strength. It was determined that the combined effects of dent depth and out-of-straightness due to overall bending from a collision can be significant on capacity and must be considered in member residual strength determination and grout repair assessment.

6.3 Recommendations

(1) The moment curvature expressions for the internally grout sections were generated as a set of data points. Future work should consider developing an approximation to this set of data points by a regression analysis to develop a continuous function. The use of this function would save a significant amount of computational effort during the

numerical integration process.

(2) The moment-curvature numerical integration computer programs were verified to have good agreement with a total of 113 tests. Further confirmation should be made for deeper dent depths, as the test data becomes available.

(3) The effects of lateral loading should be investigated for the members subjected to wave loading.

REFERENCES :

[1] Boswell, L. F., and D'Mello, C. A., "Residual and Fatigue Strength of Grout-Filled Damaged Tubular Members," OTH 89 314, Offshore Technology Report, U.K. DEn., 1988.

[2] Chen, W. F., and Atsuta, T., Theory of Beam-Columns, Vol. 1 - In-Plane Behavior and Design, McGraw-Hill, New York. 1976.

[3] Chen, W. F., and Atsuta, T ., Theory of Beam-Columns, Vol. 2 - Space Behavior and Design, McGraw-Hill, New York. 1976.

[4] Chen, W. F., and Han, D. J., Tubular Members in Offshore Structures, PITMAN, London, England. 1985.

[5] Chen, W. F., and Lui, E. M., Structural Stability - Theory and Implementation, ELSEVIER, New York. 1988

[6] Duan, L., Loh, J. T., and Chen, W. F., "Moment Curvature Relationships for Dented Tubular Sections," Journal of Structural Division, ASCE, 119(3), 1993. pp. 809-830

[7] Ellinas, C. P. "Ultimate Strength of Damaged Tubular Bracing Members," Journal of Structural Division, ASCE, Vol. 110, No. 2, February 1984, pp. 245-259

[8] Ellis, J. S. (1958), "Plastic Behavior of Compression Members," Transactions, Engineering Institute of Canada, 2(2), 49-60

[9] Gillum, T.E., "Residual Strength and Grout Repair of Damaged Offshore Structural Steel Tubular Bracing" (supervised by J. M. Ricles), M. S. Thesis,

University of California, San Diego, September 1992.

[10] Kaba, S. A., and Mahin, S. A., "Interactive Computer Analysis Methods for Predicting the Inelastic Cyclic Behaviour of Structural Sections," Report No. UCB/EERC-83/18, Earthquake Engineering Research Center, College of Engineering, University of California, Berkeley, California, July 1983.

[11] Kent, D. C., and Park, R., "Flexural Members with Confined Concrete," Journal of Structural Division, ASCE, Vol. 97, No, ST7, July 1971, pp. 1969-1990

[12] Kim, W. B., "Ultimate Strength and Behavior of Damaged Tubular Columns with End Restraints" (supervised by A. Ostapenko), Ph.D. Dissertation, Lehigh University, September 1992.

[13] Landet, E., and Lotsberg, I., "Laboratory Testing of Ultimate Capacity of Dented Tubular Members," Journal of Structural Engineering, ASCE, Volume 118, No. 4, April 1992, pp. 1071-1089

[14] Loh, J. T., "Grout-Filled Undamaged and Dented Tubular Steel Members," Offshore Division Report, Exxon Production Research Company, Houston, Texas, May 1991.

[15] Loh, J. T., Kahlich, J. L., and Broekers, D. L., " Dented Tubular Steel Members," Offshore Division Report, Exxon Production Research Company, Houston, Texas, March 1992.

[16] Padula, J. A., and Ostapenko, A., "Load-Shortening Behavior of Damaged Tubular Columns," Proceedings of the Offshore Technology Conference, OTC Paper 6382, Houston, Texas, May 1990.

[17] Parsanejad, S., "Preliminary Tests on Grout-Filled Damaged Tubular Members," Procs. of the Workshop on National Needs, Capabilities and Resources for offshore Engineering, Monash University, Melbourne, 1986a, pp. 97-104

[18] Parsanejad, S., "Tests on Grout-Filled Damaged Tubular Members," Research Report No. 016.09.86, Department of Civil Engineering & Surveying, University of Newcastle, N.S.W., Australia, 1986b.

[19] Parsanejad, S., "Strength of Grout-Filled Damaged Tubular Members," Journal of Structural Division, ASCE, 113(3), March 1987a, pp. 590-603

[20] Parsanejad, S., Tyter, S., and Chin, K. Y., "Experimental Investigation of Grout-Filled Damaged Tubular Members," Procs. Int'l Conf. on Steel and Aluminum Structures, University College, Cardiff, United Kingdom, pp. 251-259, July, 1987b.

[21] Ostapenko, A., Word, B., Chowdhury, A., and Hebor, M. (1993), "Residual Strength of Damaged and Deteriorated Tubular Members in Offshore Structures," ATLSS Report No. 93-03, Lehigh University, Bethlehem, PA

[22] "Recommended Practice for Planning, Design and Construction Fixed Offshore Platforms," (1984), RP 2A, 13th Edition, American Petroleum

[23] "Recommended Practice for Planning, Design and Construction Fixed Offshore Platforms," (1993), RP 2A, 20th Edition, American Petroleum

[24] Ricles, J. M., Lamport, W. B., and Gillum, T. E., "Residual Strength of Damaged Offshore Steel Tubular Bracing ," Proceedings of the Offshore Technology Conference, OTC Paper 6938, Houston, Texas, May 1992a.

[25] Ricles, J. M., Lamport, W. B., and Gillum, T. E., "Residual Strength and Grout Repair of Dented Offshore Tubular Bracing," ATLSS Research Center Report, No. 92-14, Lehigh University, Bethlehem, Pennsylvania, October 1992b.

[26] Ricles, J. M., Sooi, T. K., and Bruin, W. M., "Residual Strength and Repair of Dent-Damaged Tubular and Implication on Offshore Platform Reassessment and Requalification," 13th International Symposium on Offshore Mechanics and Arctic Engineering, Paper 1269, Houston, Texas, 1994.

[27] Sato, T and Suzuki, K (1992), "Proposal on Story Drift Limit Based on Axial Behavior of Column under Seismic Loads", Composite Construction in Steel and Concrete II, ASCE

[28] Smith, C. S., Kirkwood, W., and Swan , J. W., "Buckling Strength and Post-Collapse Behavior of Tubular Bracing Members Including Damage Effects," BOSS '79, Imperial College, London, England, 1979.

[29] Smith, C. S., Somerville, J. W., and Swan, J. W., "Residual Strength and Stiffness of Damaged Steel Bracing Members," Proceedings of the Offshore Technology Conference, OTC Paper 3981, Houston, Texas, 1981.

[30] Smith, C. S., "Assessment of Damage in Offshore Steel Platforms," Procs. Int. Conf. on Offshore and Marine Safety Glasgow, pp 279-307, September 1983

[31] Sohal, I. S., and Chen, W. F., "Moment Curvature Expressions for Fabricated Tubes," Journal of the Structural Division, ASCE, 110(11), 1984. pp. 2738-2757.

[32] Sohal, I. S., and Chen, W. F., "Local Buckling and Sectional Behavior of Fabricated Tubes," Journal of Structural Division, ASCE, 113(3), 1987. pp. 519-

533

[33] Sohal, I. S., and Chen, W. F., "Local and Post-Buckling Behavior of Tubular Beam-Columns," Journal of Structural Division, ASCE, 114(5), 1988. pp. 1073-1090

[34] Sugimoto, T., and Chen, W. F., "Inelastic Post-Buckling Behavior of Tubular Members," Journal of Structural Division, ASCE, 111(9), 1985, pp. 1965-1978

[35] Taby, J., "Experiments with Damaged Tubulars," NTNF Programme for Marine Structures, SINTEF Report No. 6.07, Trondheim, October 1986a.

[36] Taby, J., " Residual Strength of Damaged Tubulars. Final Report," NTNF Programme for Marine Structures, SINTEF Report No. 6.10, Trondheim, October 1986b.

[37] Tebbett, I. E. and Forsyth, P., "New Test Data on the Capacity of Cement Filled Steel Tubulars," OTC 5484, April, 1984

[38] Ueda, Y., and Rashed, S.M.H., "Behaviour of Damaged Tubular Structural Members," 4th International Symposium on Offshore Mechanics and Arctic Engineering , Dallas, Texas, February 1985.

[39] Wierzbicki, T. and Suh, M. S. (1986), "Denting Analysis of Tubes Under Combined Loading," Tech. Report MITSG 86-5, MIT Sea Grant College Program, Massachusetts Institute of Technology, March, NA84AA-D-0046 R/0-19

[40] Wimpy Offshore, "Static Testing of Grout-Filled Joints and Members," Doc. No. wol 2/86A, Report to EPR Co, Southwest Research Institute, December 1986

Table 1(a) : Geometric and Material Properties of Gillum and Ricles' Specimens (1992)

Specimen No.	Outer Diameter (in)	Thickness (in)	Length (in)	Yield Stress (ksi)	Dent Depth (in)	Deltap/L	Young's Modulus (ksi)
A1	8.626	0.247	178.8	34.8	0.868	0.0007	29071
A2	8.624	0.246	178.8	34.8	0.861	0.0006	29071
A5	8.636	0.248	178.8	50.9	0.000	0.0002	29071
B1	8.631	0.186	178.9	33.4	0.862	0.0009	30714
B2	8.636	0.186	178.9	33.4	0.861	0.0026	30714
B5	8.642	0.186	178.9	48.6	0.000	0.0001	30714
C1	8.642	0.134	180.1	39.4	0.861	0.0012	30800
C2	8.643	0.136	180.1	39.4	0.861	0.0007	30800
C5	8.643	0.136	180.1	40.2	0.000	0.0009	30800

Deltap = Out-Of-Straightness after Denting

Table 1(b) : Comparison between Experimental Results and Moment Curvature Predictions (Gillum and Ricles' Specimens, 1992)

Specimen No.	D/t	dd/D	dd/t	Pu,exp/Py	Pu,mc/Py	Pu,mc/Pu,exp
A1	34.92	0.10	3.51	0.611	0.605	0.99
A2	35.06	0.10	3.50	0.397	0.400	1.01
A5	34.82	0.00	0.00	0.459	0.450	0.98
B1	46.40	0.10	4.63	0.588	0.530	0.90
B2	46.43	0.10	4.63	0.311	0.340	1.09
B5	46.46	0.00	0.00	0.449	0.470	1.05
C1	64.49	0.10	6.43	0.437	0.435	1.00
C2	63.55	0.10	6.33	0.325	0.300	0.92
C5	63.55	0.00	0.00	0.428	0.475	1.11

Table 2(a) : Geometric and Material Properties of Lehigh Tests (Ostapenko et al,1993)

Specimen No.	Outer Diameter (in)	Thickness (in)	Length (in)	Yield Stress (ksi)	Dent Depth (in)	Deltap/L
FF1	15.00	0.260	424.2	42.66	0.7500	0.00070
FF2	17.03	0.375	418.2	57.25	2.3842	0.00160
FF3	24.50	0.321	412.2	59.23	1.2250	0.00005
FS1	10.36	0.360	294.0	54.18	1.7612	0.00270
FS2	10.38	0.375	294.0	53.30	1.5570	0.00340
FS3	13.55	0.444	336.0	43.95	2.3035	0.00077
FS4	13.59	0.439	336.0	40.50	2.0385	0.00176

Deltap = Out-Of-Straightness after Denting

Table 2(b) : Comparison between Experimental Results and Moment Curvature Predictions (Lehigh Tests, Ostapenko et al, 1993)

Specimen No.	D/t	dd/D	dd/t	Pu,exp/Py	Pu,mc/Py	Pu,mc/Pu,exp
FF1	57.69	0.05	2.88	0.638	0.62	0.97
FF2	45.41	0.14	6.36	0.46	0.385	0.84
FF3	76.32	0.05	3.82	0.658	0.65	0.99
FS1	28.78	0.17	4.89	0.31	0.365	1.18
FS2	27.68	0.15	4.15	0.381	0.38	1.00
FS3	30.52	0.17	5.19	0.552	0.455	0.82
FS4	30.96	0.15	4.64	0.458	0.47	1.03

Table 3(a) : Geometric and Material Properties of Landet and Lotsberg's Specimens (1992)

Specimen NO.	Outer Diameter (in)	Thickness (in)	Length (in)	Yield Stress (ksi)	Dent Depth (in)	Deltap/L
D1-32	5.51	0.178	105.39	50.76	0.551	0.0042
D1-33	5.51	0.178	105.39	49.31	1.102	0.0112
D1-35	5.51	0.119	105.39	53.37	0.551	0.0041
D1-36	5.51	0.119	105.39	58.02	1.102	0.0090

Deltap = Out-Of-Straightness after Denting

Table 3(b) : Comparison between Experimental Results and Moment Curvature Predictions (Landet and Lotsberg's Specimens, 1992)

Specimen No.	D/t	dd/D	dd/t	Pu,exp/Py	Pu,mc/Py	Pu,mc/Pu,exp
D1-32	31.04	0.10	3.10	0.551	0.555	1.01
D1-33	30.91	0.20	6.18	0.382	0.315	0.82
D1-35	46.20	0.10	4.62	0.524	0.490	0.94
D1-36	46.36	0.20	9.27	0.287	0.255	0.89

Table 4(a) : Geometric and Material Properties of Smith et al Specimens (1979)

Specimen No.	Outer Diameter (in)	Thickness (in)	Length (in)	Yield Stress (ksi)	Dent Depth (in)	Deltap/L
F2	15.59	0.39	305.28	42.50	1.99	0.0018
F2s	2.56	0.06	52.17	39.74	0.33	0.0050

Deltap = Out-Of-Straightness after Denting

Table 4(b) : Comparison between Experimental Results and Moment Curvature Predictions (Smith et al. Specimens, 1979)

Specimen No.	D/t	dd/D	dd/t	Pu,exp/Py	Pu,mc/Py	Pu,mc/Pu,exp
F2	40.00	0.13	5.10	0.560	0.540	0.96
F2s	40.94	0.13	5.22	0.480	0.475	0.99

Table 5(a) : Geometric and Material Properties of Taby's Specimens (1986a, 1986b)

Specimen No.	Outer Diameter (in)	Thickness (in)	Length (in)	Yield Stress (ksi)	Dent Depth (in)	Deltap/L
A3	2.42	0.083	84.6	32.8	0.114	0.0055
B3	3.06	0.067	84.6	28.8	0.248	0.005
B4	3.06	0.067	84.6	28.8	0.034	0.005
C3	3.94	0.067	84.6	33.9	0.134	0.004
C4	3.94	0.067	84.6	36.6	0.063	0.005
D3	3.5	0.041	84.6	68.2	0.130	0.003

Deltap = Out-Of-Straightness after Denting

Table 5(b) : Comparisons between Experimental Results and Moment Curvature Predictions (Taby's Specimens, 1986a, 1986b)

Specimen No.	D/t	dd/D	dd/t	Pu,exp/Py	Pu,mc/Py	Pu,mc/Pu,exp
A3	29.16	0.047	1.37	0.48	0.4	0.83
B3	45.67	0.081	3.70	0.52	0.45	0.87
B4	45.67	0.011	0.50	0.61	0.56	0.92
C3	58.81	0.034	2.00	0.76	0.78	1.03
C4	58.81	0.016	0.94	0.84	0.86	1.02
D3	85.37	0.037	3.16	0.53	0.6	1.13

Table 6(a) : Geometric and Material Properties of Undamaged, Internally Grout Filled Specimens (Wimpy, 1986)

Spec #	D_outer(in)	t(in)	L(in)	Fy(ksi)	Es(ksi)	F'g(ksi)	Eg(ksi)	Ecc(in)
1	8.504	0.118	85	60.6	29000	10.15	4570	2.098
2	8.504	0.118	85	60.6	29000	8.09	3640	10.484
3	6.626	0.177	132.3	58.6	29000	8.45	3800	1.614
4	6.626	0.177	132.3	58.6	29000	8.16	3670	16.122
5	6.094	0.374	175.6	70.9	29000	9.29	4180	1.429
6	6.094	0.374	175.6	70.9	29000	9.1	4100	14.303
7	6.016	0.188	240	36.5	29000	12.2	5490	0
8	6.016	0.188	240	37.4	29000	11.5	5180	0
a1	1.754	0.055	49.4	84.5	29000	4.63	2390	0
c1	2.752	0.055	73.2	73.1	29000	4.63	2390	0
c3	3.002	0.104	61.4	72.9	29000	10.73	1590	0.034
p1	3.002	0.104	61.4	72.9	29000	10.73	1590	0

D_outer = outer diameter
t = thickness
L = length
Fy = steel yield stress
Es = Young's modulus
F'g = grout strength
Eg = elastic modulus of grout
Ecc = end eccentricity

Table 6(b) : Comparison between Experimental Results and Various Analytical Methods, Internally Grout Repaired Wimpy's Specimens (1986)

Spec #	Eg / Eg	dd / D	D / t	Pu,exp (kips)	Pu,1 / Pu,exp	Pu,2 / Pu,exp	Pu,3 / Pu,exp	Pu,4 / Pu,exp	Pu,5 / Pu,exp	Pu,6 / Pu,exp	Pu,7 (kips)	Pu,7 / Pu,exp
1	6.346	0	72.07	303.5	0.32	0.94	0.89	0.61	0.58	0.53	302.50	1.00
2	7.967	0	72.07	75.1	0.49	0.84	0.82	0.69	0.65	0.64	58.49	0.78
3	7.632	0	37.44	149.5	0.61	1.01	1.00	0.84	0.83	0.74	147.25	0.98
4	7.902	0	37.44	32.4	0.67	0.84	0.84	0.82	0.79	0.76	25.13	0.78
5	6.938	0	16.29	130.9	1.03	1.45	1.45	1.15	1.16	1.05	167.69	1.28
6	7.073	0	16.29	40.5	1.04	1.28	1.28	1.20	1.14	1.09	42.50	1.05
3.1	5.282	0	32	180.3	0.60	1.30	1.30	1.20	1.37	1.12	204.10	1.13
3.2	5.598	0	32	157.8	0.66	1.28	1.28	1.20	1.39	1.09	180.61	1.14
a1	12.13	0	31.89	16.04	0.78	0.87	0.87	0.83	0.94	0.78	14.29	0.89
c1	12.13	0	50.04	28.9	0.65	0.93	0.93	0.81	0.88	0.92	26.75	0.93
c3	18.24	0	28.87	86.33	0.62	0.81	0.81	0.75	0.88	0.82	70.78	0.82
p1	18.24	0	28.87	69.69	0.76	1.01	1.01	0.93	1.09	1.01	70.78	1.02

Pu,exp = Experimental Results
Pu,1 = API RP 2A Equation for Steel Members
Pu,2 = BS 5400
Pu,3 = Modified BS 5400
Pu,4 = AISC-LRFD Approach
Pu,5 = Modified AISC-LRFD
Pu,6 = Simplified Method
Pu,7 = Moment Curvature Approach (Proposed)

Table 7(a) : Geometric and Material Properties of Gillum and Ricles' Internally Grout Repaired Specimens (1992)

Spec. #	D_outer(in)	t(in)	L(in)	dd(in)	Fy(ksi)	Es(ksi)	F'g(ksi)	Eg(ksi)	Ecc(in)	deltap/L
A3	8.625	0.247	178.8	0.857	34.8	29071	4.375	2907	1.725	0.0006
B3	8.634	0.187	178.9	0.863	33.4	30714	3.885	2559	1.7268	0.0011
C3	8.643	0.135	180.1	0.86	39.4	30800	6.894	2566	1.7286	0.0009

D_outer = outer diameter
t = thickness
L = length
dd = dent depth
Fy = steel yield stress
Es = Young's modulus
F'g = grout strength
Eg = elastic modulus of grout
Ecc = end eccentricity
deltap = out-of-straightness after denting

Table 7(b) : Comparison between Experimental Results and Various Analytical Methods, Internally Grout Repaired Gillum and Ricles' Specimens (1992)

Spec. #	Es / Eg	dd / D	D / t	Pu,exp (kips)	Pu,1 (kips)	Pu,1 / Pu,exp	Pu,2 (kips)	Pu,2 / Pu,exp	Pu,3 (kips)	Pu,3 / Pu,exp	Pu,4 (kips)	Pu,4 / Pu,exp
A3	10	0.1	35.1	191.00	228.054	1.19	170.800	0.75	160.500	0.70	175.700	0.92
B3	12	0.1	46.5	117.00	126.828	1.08	139.800	1.10	129.130	1.02	128.010	1.09
C3	12	0.1	63.9	122.00	123.220	1.01	141.200	1.15	119.689	0.97	130.440	1.06

Pu,exp = experimental results
Pu,1 = Parsanejad's Equation
Pu,2 = Modified AISC-LRFFD Approach
Pu,3 = Simplified Method
Pu,4 = Moment Curvature Approach

Table 8(a) : Geometric and Material Properties of Parsanejad's Internally Grout Repaired Specimens (1987a, 1987b)

Spec. #	D_outer(in)	t(in)	L(in)	dd(in)	Fy(ksi)	Es(ksi)	F'g(ksi)	Eg(ksi)	Ecc(in)	deltap/L
A1	1.754	0.055	49.4	0.000	84.5	28800	4.63	2390	0.0000	0.0001
A2	1.754	0.054	49.4	0.127	85.1	28600	4.63	2390	0.0117	0.0000
B1	1.756	0.055	49.4	0.246	81.7	28600	4.63	2390	0.0238	-0.0003
B2	1.756	0.055	49.4	0.223	83.6	28500	4.63	2390	0.0885	0.0045
C1	2.752	0.055	73.2	0.000	73.1	28600	4.63	2390	0.0337	0.0002
C2	2.751	0.056	73.2	0.207	77.6	28500	4.63	2390	0.0372	-0.0001
D1	2.751	0.055	73.2	0.398	71.5	28800	4.63	2390	0.0388	0.0004
D2	2.75	0.055	73.2	0.411	75.1	28900	4.63	2390	0.0809	0.0042
E1	1.751	0.058	49.4	0.192	53.4	27800	4.28	2270	0.0191	0.0052
E2	1.751	0.058	49.4	0.270	50.9	26500	4.28	2270	0.0085	0.0002
F1	1.749	0.028	52.6	0.248	26.0	29000	2.28	2160	0.0040	0.0017
G1	2.753	0.055	75	0.193	31.8	29000	2.28	2160	0.0030	0.0001
G2	2.75	0.055	75	0.396	33.6	29000	2.28	2160	0.0080	0.0006
G3	2.75	0.055	75	0.346	33.5	29000	2.28	2160	0.0100	0.0043
H1	3.496	0.061	75	0.500	32.4	29000	2.28	2160	0.0090	0.0022

D_outer = outer diameter
t = thickness
L = length
dd = dent depth
Fy = steel yield stress
Es = Young's modulus
F'g = grout strength
Eg = elastic modulus of grout
Ecc = end eccentricity
deltap = out-of-straightness after denting

Table 8(b) : Comparison between Experimental Results and Various Analytical Methods, Parsanejad's Internally Grout Repaired Specimens (1987a, 1987b)

Spec #	Es / Eg	dd / D	D / t	Pu,exp (kips)	Pu,1 (kips)	Pu,1 / Pu,exp	Pu,2 (kips)	Pu,2 / Pu,exp	Pu,3 (kips)	Pu,3 / Pu,exp	Pu,4 (kips)	Pu,4 / Pu,exp
A1	12.1	0	31.9	14.00	13.725	0.98	13.208	0.94	10.853	0.78	14.290	1.02
A2	12.0	0.072	32.5	15.58	13.431	0.86	12.268	0.79	10.183	0.65	13.330	0.86
B1	12.0	0.14	31.9	13.84	11.533	0.83	10.406	0.75	8.759	0.63	12.700	0.92
B2	11.9	0.12	31.9	10.65	8.950	0.84	7.553	0.71	6.574	0.62	8.180	0.77
C1	12.0	0	50	28.90	30.421	1.05	25.575	0.88	19.396	0.67	26.752	0.93
C2	11.9	0.075	49.1	27.87	27.594	0.99	23.821	0.85	18.097	0.65	26.400	0.95
D1	12.1	0.145	50	23.31	21.385	0.92	20.095	0.86	15.540	0.67	23.470	1.01
D2	12.1	0.149	50	19.71	16.991	0.86	14.387	0.73	11.526	0.58	17.340	0.88
E1	12.2	0.11	30.2	8.78	7.982	0.91	7.378	0.84	6.552	0.75	8.270	0.94
E2	11.7	0.154	30.2	12.12	10.100	0.83	10.632	0.88	9.182	0.76	11.420	0.94
F1	13.4	0.142	62.5	5.44	3.831	0.70	4.090	0.75	3.400	0.63	4.308	0.79
G1	13.4	0.07	50.1	20.50	20.918	1.02	17.672	0.86	16.016	0.78	17.425	0.85
G2	13.4	0.14	50	19.48	15.460	0.79	16.508	0.85	14.537	0.75	16.173	0.83
G3	13.4	0.126	50	14.19	11.537	0.81	10.750	0.76	9.523	0.67	12.636	0.89
H1	13.4	0.143	57.3	28.78	23.210	0.81	23.210	0.81	21.162	0.74	25.028	0.87

Pu,exp = experimental results
Pu,1 = Parsanejad's Equation
Pu,2 = Modified AISC-LRFFD Approach
Pu,3 = Simplified Method
Pu,4 = Moment Curvature Approach

Table 9(a) : Geometric and Material Properties of Boswell and D' Mello's Internally Grout Repaired Specimens (1988)

Spec. #	D_outer[in]	t[in]	L[in]	dd[in]	Fy[ksi]	Es[ksi]	F'g[ksi]	Eg[ksi]	Ecc[in]	deltap/t
A1	1.750	0.050	35.4	0.179	75.2	29000	6.23	1590	0	0.00131
A2	1.750	0.049	35.4	0.18179	75.2	29000	10.73	1590	0	0.00103
A3	1.750	0.049	35.4	0.221	75.2	29000	6.23	1590	0	0.00198
A4	1.750	0.048	35.4	0.242	75.2	29000	10.73	1590	0	0.00203
A5	1.750	0.049	35.4	0.181	75.2	29000	10.73	1590	0	0.00176
B1	1.750	0.063	35.4	0.185	75.0	29000	6.23	1590	0	0.00142
B2	1.750	0.063	35.4	0.185	75.0	29000	10.73	1590	0	0.0012
B3	1.750	0.063	35.4	0.232	75.0	29000	6.23	1590	0	0.00248
B4	1.750	0.062	35.4	0.251	75.0	29000	10.73	1590	0	0.00211
C1	3.002	0.104	61.4	0.131	72.9	29000	10.73	1590	0	0.00035
C2	3.002	0.104	61.4	0.131	72.9	29000	10.73	1590	0	0.00018
C3	3.002	0.104	61.4	0	72.9	29000	10.73	1590	0	0
D1	3.002	0.104	61.4	0.468	73.3	29000	10.73	1590	0	0.00301
D2	3.002	0.104	61.4	0.472	73.3	29000	10.73	1590	0	0.00279
F1	3.002	0.126	71.3	0.292	67.3	29000	10.73	1590	0	0.0012
F2	3.002	0.126	71.3	0.289	67.3	29000	10.73	1590	0	0.00124
G1	3.002	0.130	61.0	0.28	70.5	29000	10.73	1590	0	0.00071
G2	3.002	0.130	61.0	0.288	70.5	29000	10.73	1590	0	0.00113
H1	3.002	0.128	50.8	0.293	68.4	29000	10.73	1590	0	0.00105
H2	3.002	0.128	50.8	0.287	68.4	29000	10.73	1590	0	0.0013
J1	3.002	0.063	72.8	0.307	74.0	29000	10.73	1590	0	0.001
J2	3.002	0.063	72.8	0.299	74.0	29000	10.73	1590	0	0.00177
K1	3.002	0.063	62.2	0.288	72.4	29000	10.73	1590	0	0.00149
K2	3.002	0.063	62.2	0.297	72.4	29000	10.73	1590	0	0.00076
L1	3.002	0.063	52.0	0.301	72.7	29000	10.73	1590	0	0.00106
L2	3.002	0.063	52.0	0.297	72.7	29000	10.73	1590	0	0.00085
M1	3.002	0.107	71.7	0.288	71.9	29000	10.73	1590	0	0.00096
M2	3.002	0.107	71.7	0.293	71.9	29000	10.73	1590	0	0.00088
N1	3.002	0.104	61.4	0.3	70.8	29000	10.73	1590	0	0.00176
N2	3.002	0.104	61.4	0.304	70.8	29000	10.73	1590	0	0.0013
O1	3.002	0.106	51.2	0.309	69.8	29000	10.73	1590	0	0.00214
O2	3.002	0.106	51.2	0.3	69.8	29000	10.73	1590	0	0.00092
P1	3.002	0.104	61.4	0	72.9	29000	10.73	1590	0	0
Q1	8.642	0.315	193.3	1.164	46.3	29000	10.73	1590	0	0.00155
Q2	8.642	0.319	193.3	1.138	46.3	29000	10.73	1590	0	0.0027
Q3	8.642	0.319	193.3	0.809	46.3	29000	10.73	1590	0	0.00139
Q4	8.642	0.321	193.3	0.818	46.3	29000	10.73	1590	0	0.00114

D_outer = outer diameter
t = thickness
L = length
dd = dent depth
Fy = steel yield stress
Es = Young's modulus
F'g = grout strength
Eg = elastic modulus of grout
Ecc = end eccentricity
deltap = out-of-straightness after denting

Table 9(b) : Comparison between Experimental Results and Various Analytical Methods, Boswell and D' Mello's Internally Grout Repaired Specimens (reported data, 1988)

Spec. #	Ec / Eg	dd / D	D / t	Pu,exp (kips)	Pu,1 (kips)	Pu,1 / Pu,exp	Pu,2 (kips)	Pu,2 / Pu,exp	Pu,3 (kips)	Pu,3 / Pu,exp	Pu,4 (kips)	Pu,4 / Pu,exp
A1	18.2	0.102	36	12.70	16.08	1.27	17.64	1.39	16.08	1.27	16.70	1.31
A2	18.2	0.104	35.8	19.15	16.23	0.85	20.16	1.05	17.90	0.93	17.08	0.89
A3	18.2	0.126	35.8	14.37	14.09	0.98	14.97	1.04	13.69	0.95	15.28	1.06
A4	18.2	0.138	36.1	16.19	13.61	0.84	15.27	0.94	13.61	0.84	15.35	0.95
A5	18.2	0.103	35.8	21.70	15.28	0.70	16.95	0.78	15.07	0.69	16.01	0.74
B1	18.2	0.106	28	18.71	18.52	0.99	20.12	1.08	18.90	1.01	19.45	1.04
B2	18.2	0.106	28	20.59	18.89	0.92	22.38	1.09	20.59	1.00	20.09	0.98
B3	18.2	0.133	27.8	14.79	16.08	1.09	17.00	1.15	15.90	1.08	18.02	1.22
B4	18.2	0.143	28.1	15.94	15.94	1.00	17.91	1.12	16.60	1.04	18.19	1.14
C1	18.2	0.044	28.9	84.31	69.11	0.82	73.96	0.88	68.54	0.81	60.67	0.72
C2	18.2	0.044	28.9	93.53	71.40	0.76	73.65	0.79	68.77	0.74	60.67	0.65
C3	18.2	0	28.9	86.33	88.09	1.02	75.73	0.88	70.76	0.82	60.67	0.70
D1	18.2	0.156	29	50.43	41.00	0.81	45.03	0.89	41.68	0.83	47.32	0.94
D2	18.2	0.157	29	57.71	41.52	0.72	45.80	0.79	42.12	0.73	49.01	0.85
F1	18.2	0.097	23.8	83.41	50.25	0.60	57.13	0.68	52.46	0.63	54.39	0.65
F2	18.2	0.096	23.8	74.42	50.28	0.68	56.38	0.76	52.04	0.70	54.39	0.73
G1	18.2	0.093	23.2	82.06	66.72	0.81	80.45	0.98	76.69	0.93	65.72	0.80
G2	18.2	0.095	23.2	87.23	63.67	0.73	75.85	0.87	72.09	0.83	63.90	0.73
H1	18.2	0.097	23.5	85.66	71.96	0.84	90.17	1.05	87.41	1.02	71.30	0.83
H2	18.2	0.096	23.5	86.11	70.58	0.82	86.11	1.00	82.80	0.96	69.52	0.81
J1	18.2	0.102	47.7	44.29	30.76	0.69	36.30	0.82	29.72	0.67	33.83	0.76
J2	18.2	0.1	47.7	42.72	29.26	0.68	29.26	0.68	24.55	0.57	31.01	0.73
K1	18.2	0.096	48	53.84	36.38	0.68	41.10	0.76	34.51	0.64	39.14	0.73
K2	18.2	0.099	48	51.48	39.00	0.76	48.57	0.94	40.86	0.79	40.53	0.79
L1	18.2	0.1	48	59.13	44.80	0.76	58.55	0.99	52.33	0.88	46.20	0.78
L2	18.2	0.099	48	59.58	45.83	0.77	60.18	1.01	54.16	0.91	46.20	0.78
M1	18.2	0.096	28	56.23	46.58	0.80	56.53	0.97	50.20	0.86	50.80	0.87
M3	18.2	0.096	28	89.25	46.73	0.52	56.13	0.63	50.14	0.56	50.80	0.57
N1	18.2	0.1	29	63.40	50.32	0.79	56.61	0.89	51.97	0.82	53.13	0.84
N2	18.2	0.101	29	71.27	52.40	0.74	61.44	0.86	56.12	0.79	54.79	0.77
O1	18.2	0.103	28.2	79.36	57.51	0.72	67.83	0.85	64.00	0.81	59.81	0.75
O2	18.2	0.1	28.2	76.44	64.24	0.84	81.32	1.06	78.00	1.02	63.13	0.83
P1	18.2	0	28.9	69.69	88.22	1.27	75.75	1.09	70.39	1.01	60.67	0.87
Q1	18.2	0.135	27.4	442.18	269.01	0.65	381.19	0.86	353.74	0.80	311.34	0.70
Q2	18.2	0.132	27.1	476.19	267.52	0.56	326.16	0.68	305.25	0.64	300.98	0.63
Q3	18.2	0.094	27.1	430.28	325.97	0.76	421.84	0.98	394.75	0.92	335.70	0.78
Q4	18.2	0.095	26.9	544.22	336.94	0.62	453.52	0.83	425.17	0.78	336.35	0.62

Pu,exp = experimental results
Pu,1 = Parsaneyad's Equation
Pu,2 = Modified AISC-LRFD Approach
Pu,3 = Simplified Method
Pu,4 = Moment Curvature Approach

Table 9(c) : Comparison between Experimental Results and Various Analytical Methods, Boswell and D' Mello's Internally Grout Repaired Specimens (modified grout modulus)

Spec. #	Eg / Ep	dg / d	d / t	Pu,exp (kips)	Pu,1 (kips)	Pu,1 / Pu,exp	Pu,2 (kips)	Pu,2 / Pu,exp	Pu,3 (kips)	Pu,3 / Pu,exp	Pu,4 (kips)	Pu,4 / Pu,exp
A1	18.2	0.102	35	12.70	16.08	1.27	17.64	1.39	16.08	1.27	16.70	1.31
A2	18.2	0.104	35.8	19.15	16.23	0.85	20.16	1.05	17.90	0.93	17.08	0.89
A3	18.2	0.126	35.8	14.37	14.09	0.98	14.97	1.04	13.69	0.95	15.28	1.06
A4	18.2	0.138	36.1	16.19	13.61	0.84	15.27	0.94	13.61	0.84	15.35	0.95
A5	18.2	0.103	35.8	21.70	15.28	0.70	16.95	0.78	15.07	0.69	16.01	0.74
B1	18.2	0.106	28	18.71	18.52	0.99	20.12	1.08	18.90	1.01	19.45	1.04
B2	18.2	0.106	28	20.59	18.89	0.92	22.38	1.09	20.59	1.00	20.09	0.98
B3	18.2	0.133	27.8	14.79	16.08	1.09	17.00	1.15	15.90	1.08	18.02	1.22
B4	18.2	0.143	28.1	15.94	15.94	1.00	17.91	1.12	16.60	1.04	18.19	1.14
C1	10.0	0.044	28.9	84.31	69.11	0.82	73.96	0.88	68.54	0.81	69.09	0.82
C2	10.0	0.044	28.9	93.53	71.40	0.76	73.65	0.79	68.77	0.74	69.09	0.74
C3	10.0	0	28.9	86.33	88.09	1.02	75.73	0.88	70.76	0.82	70.78	0.82
D1	10.0	0.156	29	50.43	41.00	0.81	45.03	0.89	41.68	0.83	54.06	1.07
D2	10.0	0.157	29	57.71	41.52	0.72	45.80	0.79	42.12	0.73	55.77	0.97
F1	10.0	0.097	23.8	83.41	50.25	0.60	57.13	0.68	52.46	0.63	59.65	0.72
F2	10.0	0.096	23.8	74.42	50.28	0.68	56.38	0.76	52.04	0.70	59.65	0.80
G1	10.0	0.093	23.2	82.06	66.72	0.81	80.45	0.98	76.69	0.93	74.85	0.91
G2	10.0	0.096	23.2	87.23	63.67	0.73	75.85	0.87	72.09	0.83	73.03	0.84
H1	10.0	0.097	23.5	85.86	71.98	0.84	90.17	1.05	87.41	1.02	80.21	0.94
H2	10.0	0.095	23.5	86.11	70.58	0.82	86.11	1.00	82.80	0.96	80.21	0.93
J1	10.0	0.102	47.7	44.29	30.76	0.69	36.30	0.82	29.72	0.67	39.46	0.89
J2	10.0	0.1	47.7	42.72	29.26	0.68	29.26	0.68	24.55	0.57	36.64	0.86
K1	10.0	0.096	48	53.84	36.38	0.68	41.10	0.76	34.51	0.64	46.13	0.86
K2	10.0	0.099	48	51.48	39.00	0.76	48.57	0.94	40.86	0.79	48.92	0.95
L1	10.0	0.1	48	59.13	44.80	0.76	58.55	0.99	52.33	0.88	57.40	0.97
L2	10.0	0.099	48	59.58	45.83	0.77	60.18	1.01	54.16	0.91	57.40	0.96
M1	10.0	0.096	28	58.23	46.58	0.80	56.53	0.97	50.20	0.86	55.88	0.96
M2	10.0	0.098	28	89.25	46.73	0.52	56.13	0.63	50.14	0.56	57.58	0.65
N1	10.0	0.1	29	63.40	50.32	0.79	56.61	0.89	51.97	0.82	61.43	0.97
N2	10.0	0.101	29	71.27	52.40	0.74	61.44	0.86	56.12	0.79	63.09	0.89
O1	10.0	0.103	28.2	79.36	57.51	0.72	67.83	0.85	64.00	0.81	69.78	0.88
O2	10.0	0.1	28.2	76.44	64.24	0.84	81.32	1.06	78.00	1.02	73.10	0.96
P1	10.0	0	28.9	69.69	88.22	1.27	75.75	1.09	70.39	1.01	70.78	1.02
Q1	10.0	0.135	27.4	442.18	289.01	0.65	381.19	0.86	353.74	0.80	369.00	0.83
Q2	10.0	0.132	27.1	476.19	267.52	0.56	326.16	0.68	305.25	0.64	347.30	0.73
Q3	10.0	0.094	27.1	430.26	325.97	0.76	421.84	0.98	394.75	0.92	393.58	0.91
Q4	10.0	0.095	26.9	544.22	335.94	0.62	453.52	0.83	425.17	0.78	394.34	0.72

Pu exp = experimental results
Pu 1 = Parsanejad's Equation
Pu 2 = Modified AISC-LRFD Approach
Pu 3 = Simplified Method
Pu 4 = Moment Curvature Approach

Table 10 : Assessment of Various Analytical Methods for 12 Undamaged, Internally Grout Filled Specimens (Wimpy, 1986)

	Pu,prediction/Pu,exp		
Approach	mean	S.D.	C.O.V.
API RP 2A Equation for Steel Members	0.69	0.19	0.28
BS 5400	1.05	0.21	0.20
Modified BS 5400	1.04	0.22	0.21
AISC-LRFD Approach	0.92	0.21	0.22
Modified AISC-LRFD Approach	0.98	0.25	0.25
Simplified Method	0.88	0.19	0.21
Moment Curvature Approach	0.98	0.16	0.15

Table 11(a) : Assessment of Various Analytical Methods for 27 Dent-Damaged, Internally Grout Repaired Specimens (excluding Boswell and D' Mello's latter 28 Specimens)

	Pu,prediction/Pu,exp		
Approach	mean	S.D.	C.O.V.
Parsanejad's Equation	0.93	0.13	0.14
Modified AISC-LRFD	0.92	0.17	0.18
Simplified Method	0.80	0.17	0.22
Moment Curvature - Stage 1	0.96	0.14	0.14

Table 11(b) : Assessment of Various Analytical Methods for 55 Dent-Damaged, Internally Grout Repaired Specimens (including all of Boswell and D' Mello's Specimens)

	Pu,prediction/Pu,exp		
Approach	mean	S.D.	C.O.V.
Parsanejad's Equation	0.84	0.16	0.19
Modified AISC-LRFD	0.90	0.15	0.16
Simplified Method	0.80	0.15	0.19
Moment Curvature - Stage 2	0.86	0.15	0.18
Moment Curvature - Stage 3	0.92	0.13	0.14

Table 12(a) : Geometric and Material Properties of Bruin's Specimens (1994)

Spec. #	D_outer	t	L	dd	Fy	Es	F'g	Eg	Ecc	deltap/L
A7	8.6445	0.25	180.1	1.304	35	29000	4.5	2416.7	0	0.002
A9	8.6328	0.2533	180.1	2.563	36	29000	4.5	2416.7	0	0.01
B7	8.625	0.1895	180.1	1.285	38	29000	4.5	2416.7	0	0.002

D_outer = outer diameter
t = thickness
L = length
dd = dent depth
Fy = steel yield stress
Es = Young's modulus
F'g = grout strength
Eg = elastic modulus of grout
Ecc = end eccentricity
deltap = out-of-straightness after denting

Table 12(b) : Comparison between Experimental Results and Moment Curvature Integration Method, Bruin's Internally Grout Repaired Specimens (1994)

Spec. #	Es/Eg	dd/D	D/t	Pu,exp(kips)	Pu,mc(kips)	Pu,mc/Pu,exp
A7	12	0.15	34	243	250.0	0.97
A9	12	0.3	34	138	130.2	1.06
B7	12	0.15	46	211	226.0	0.93

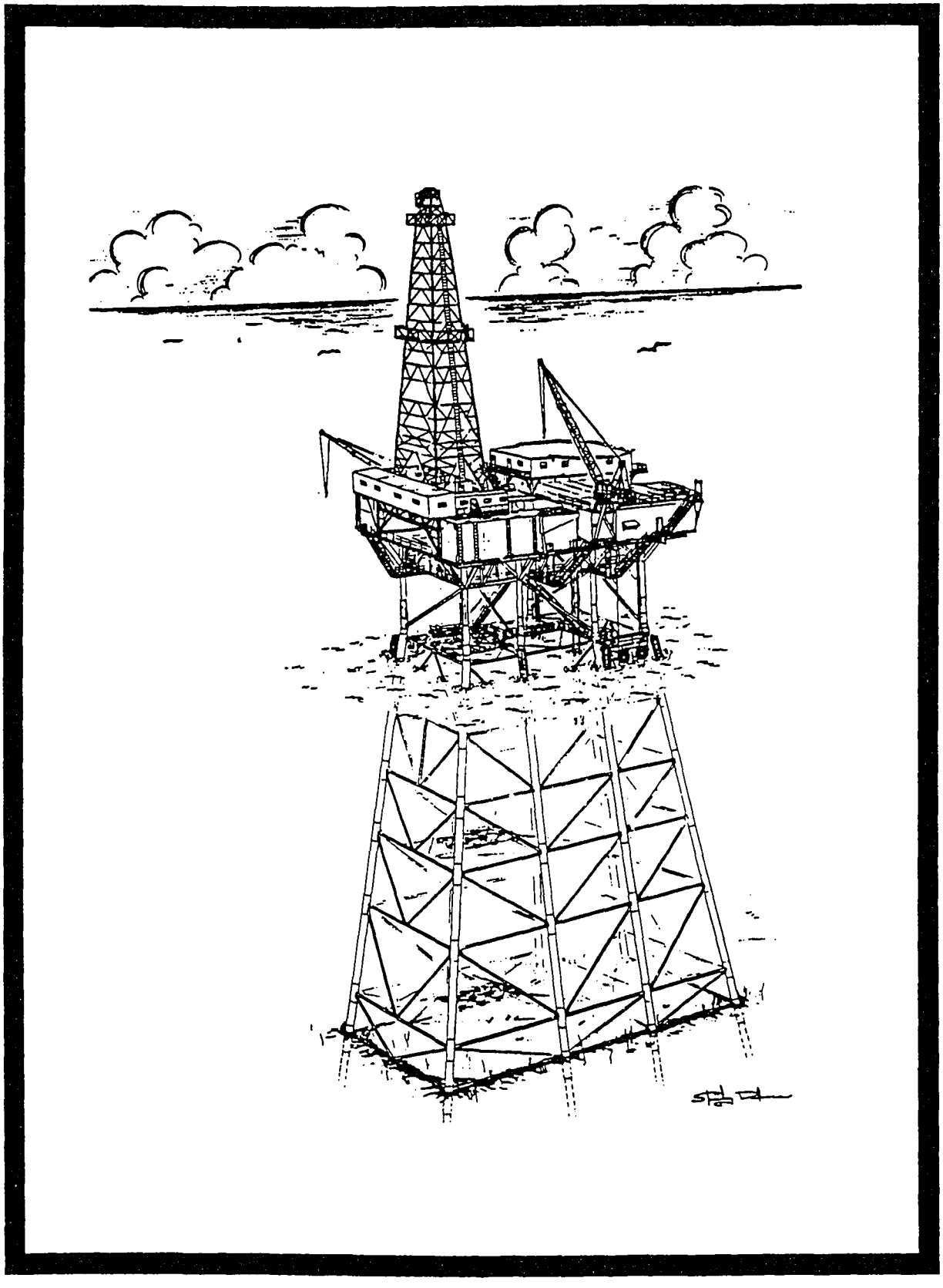

Figure 1 : Typical Offshore Structure

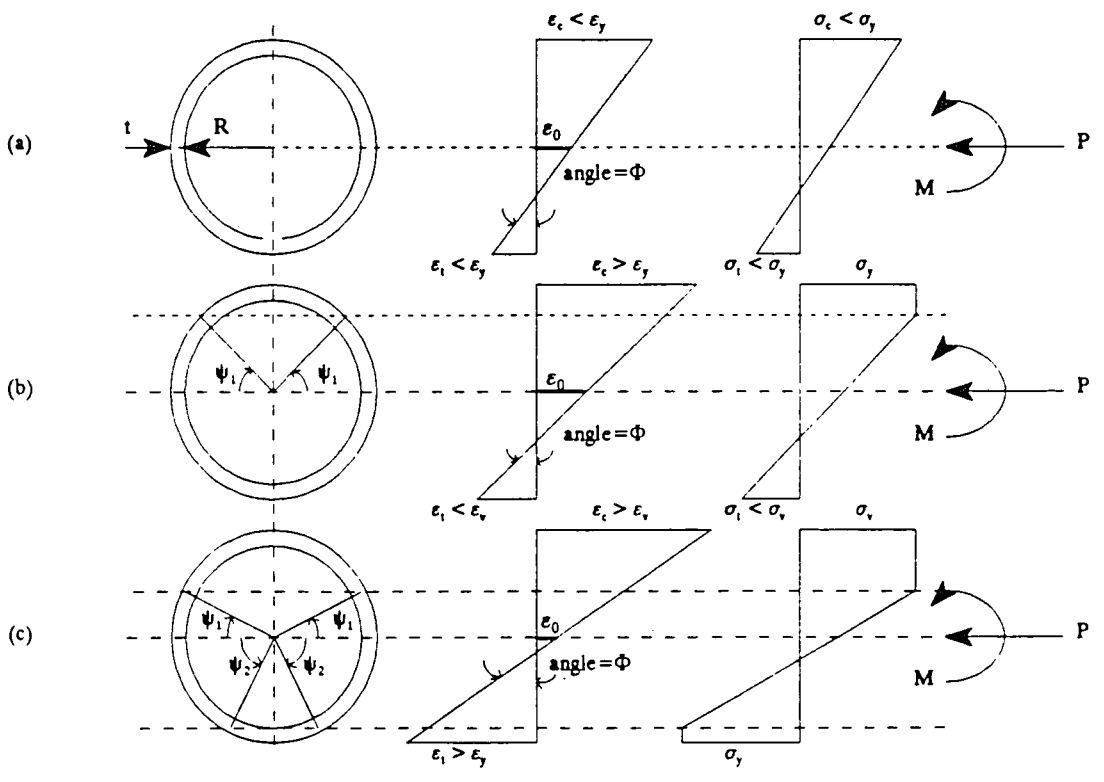

Figure 2-1 : Stress States of a Tubular Section Subjected to Axial Load :

(a) Elastic State; (b) Yielding in Compression Zone; (c) Yielding in Tension and Compression Zones

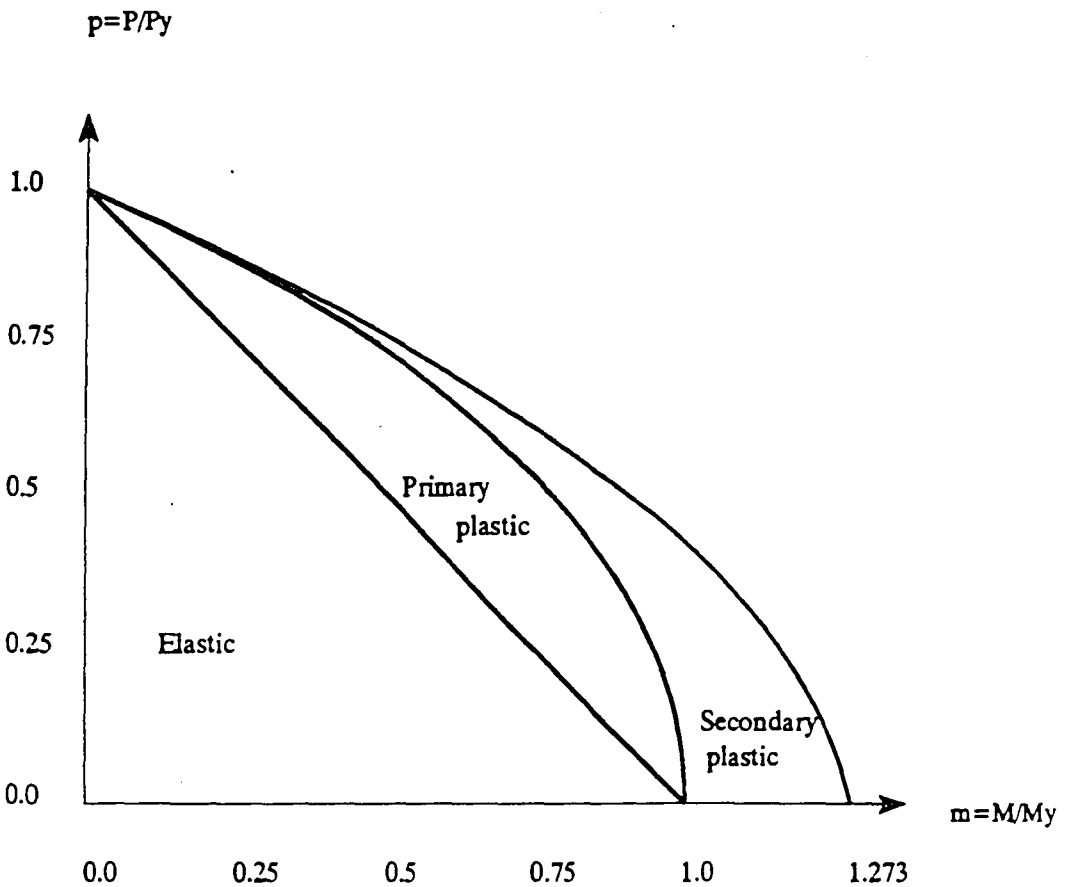

Figure 2-2 : Interaction Curves for Tubular Sections

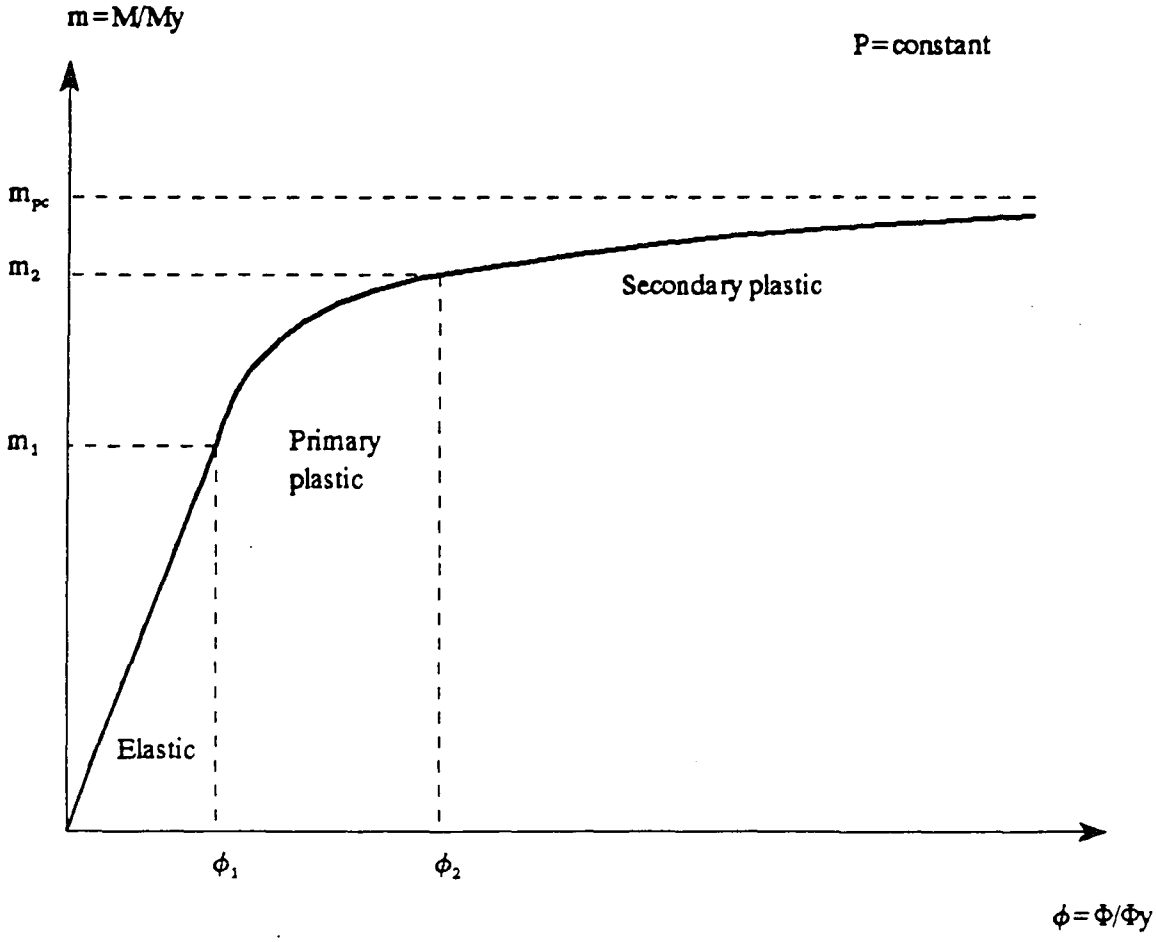

Figure 2-3 : Moment-Thrust-Curvature Relationships for a Tubular Section (without Local Buckling and Damage)

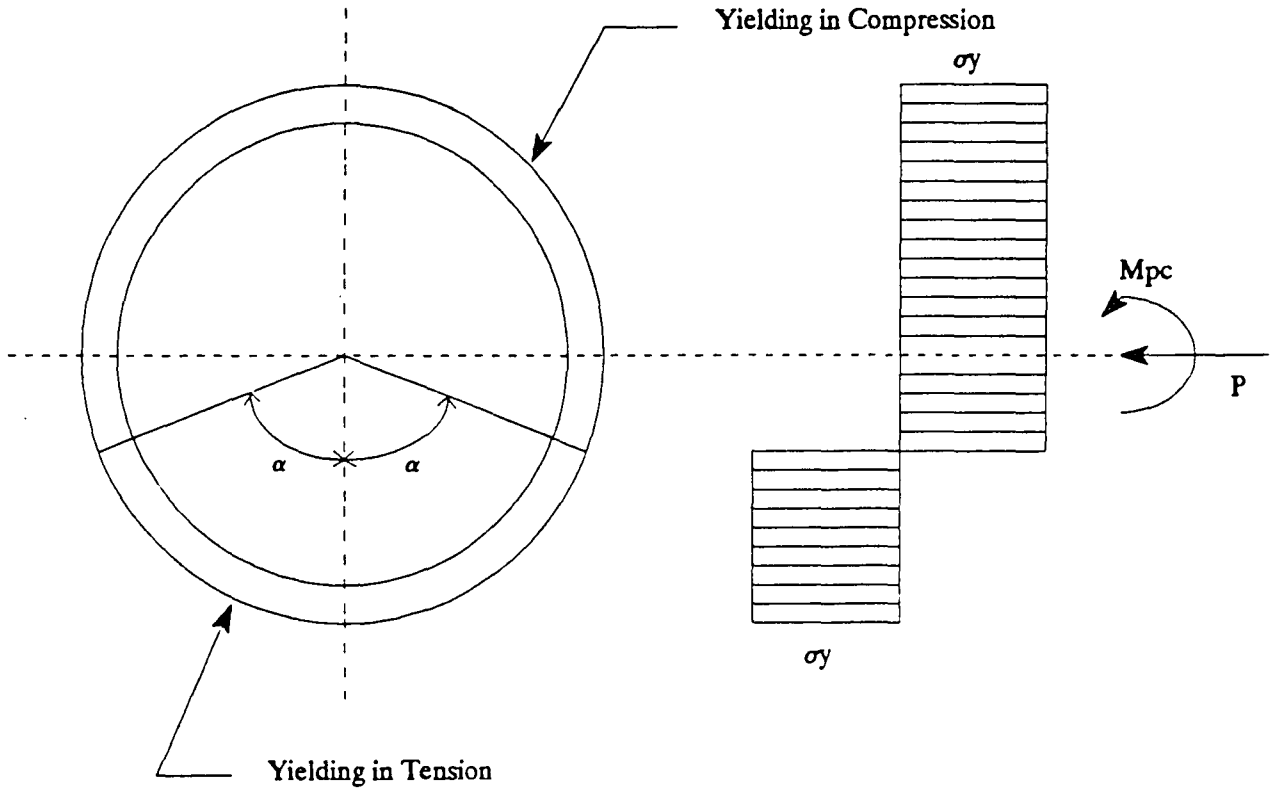

Figure 2-4 : Fully Plastic Section

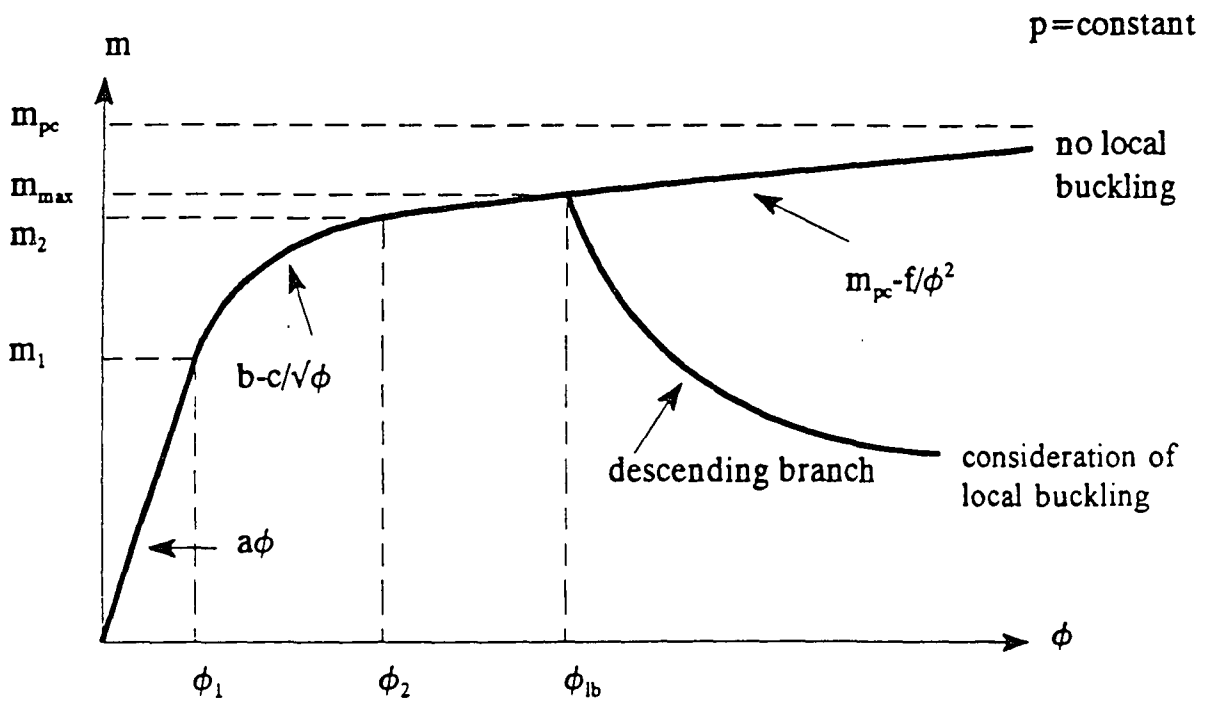

Figure 2-5(a) : Empirical Moment Curvature Relationships for Undented Tubular Sections (Duan et al, 1993)

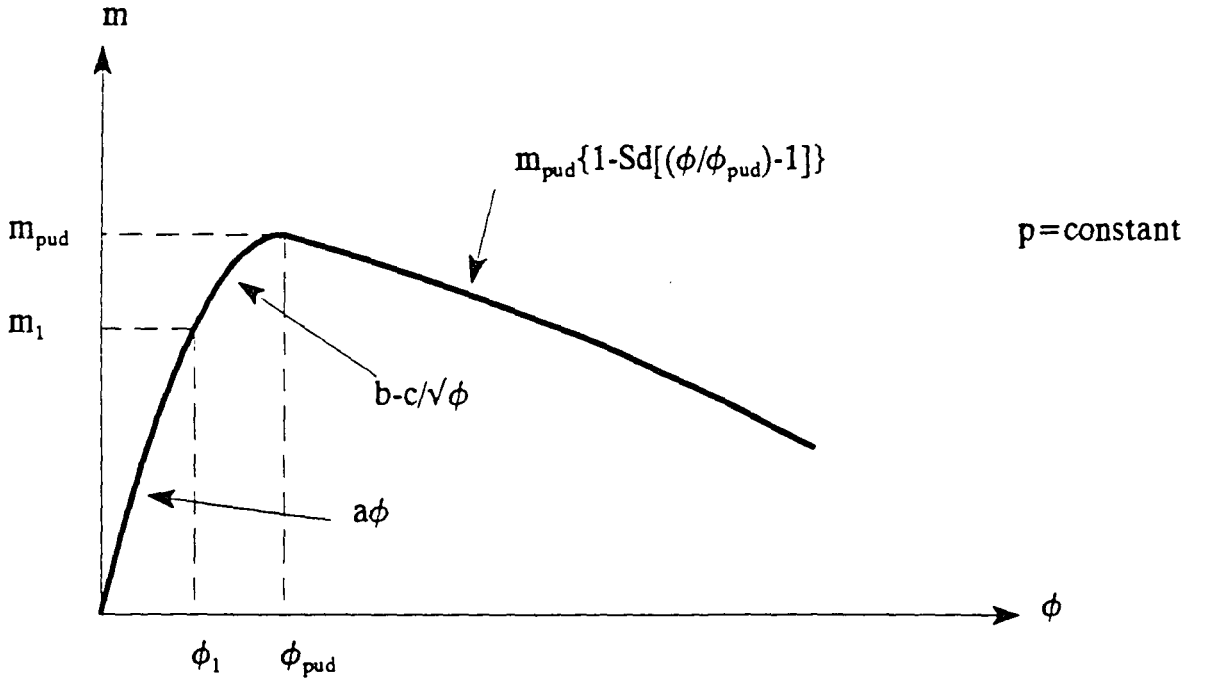

Figure 2-5(b) : Empirical Moment Curvature Relationships for Dent-Damaged Tubular Sections (Duan et al, 1993)

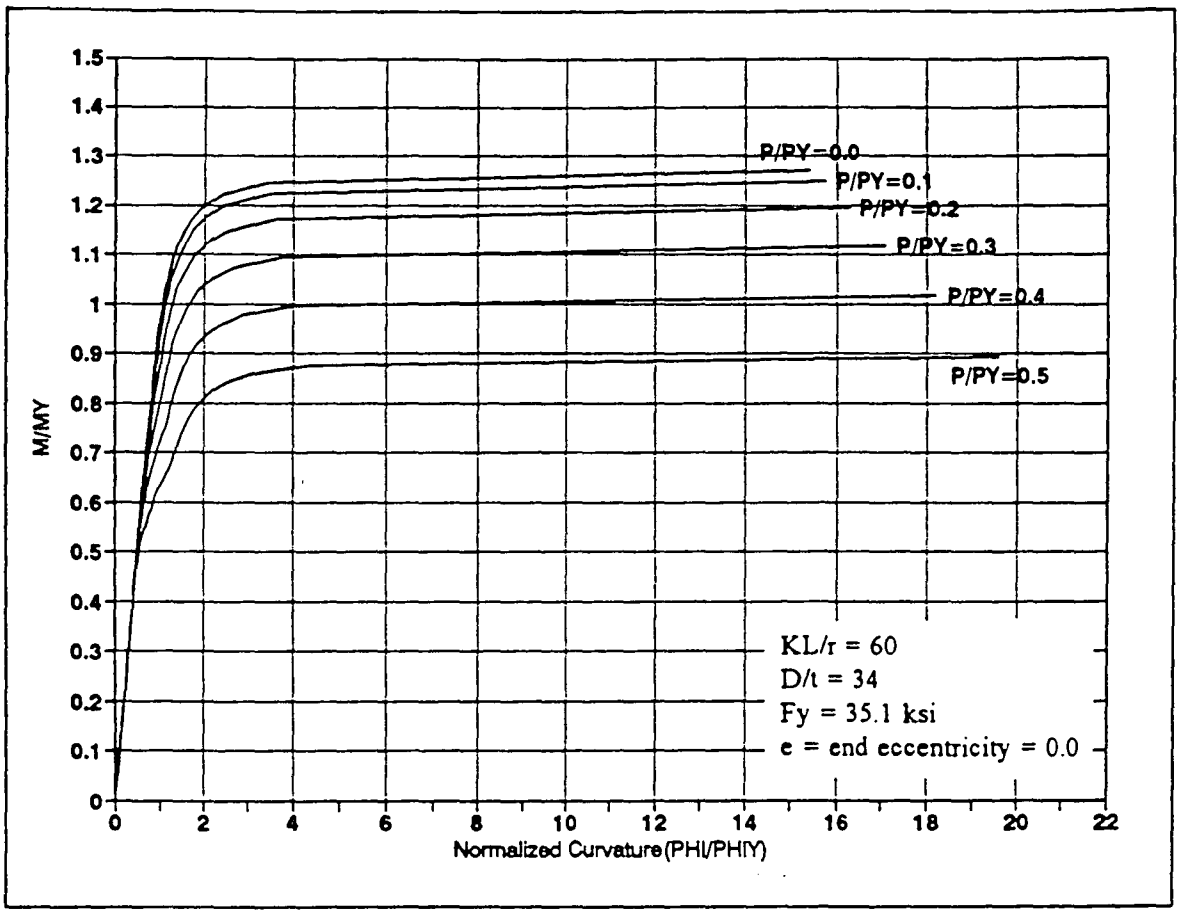

Figure 2-6(a) : Moment Curvature Relationships for Undented Tubular Sections without Local Buckling

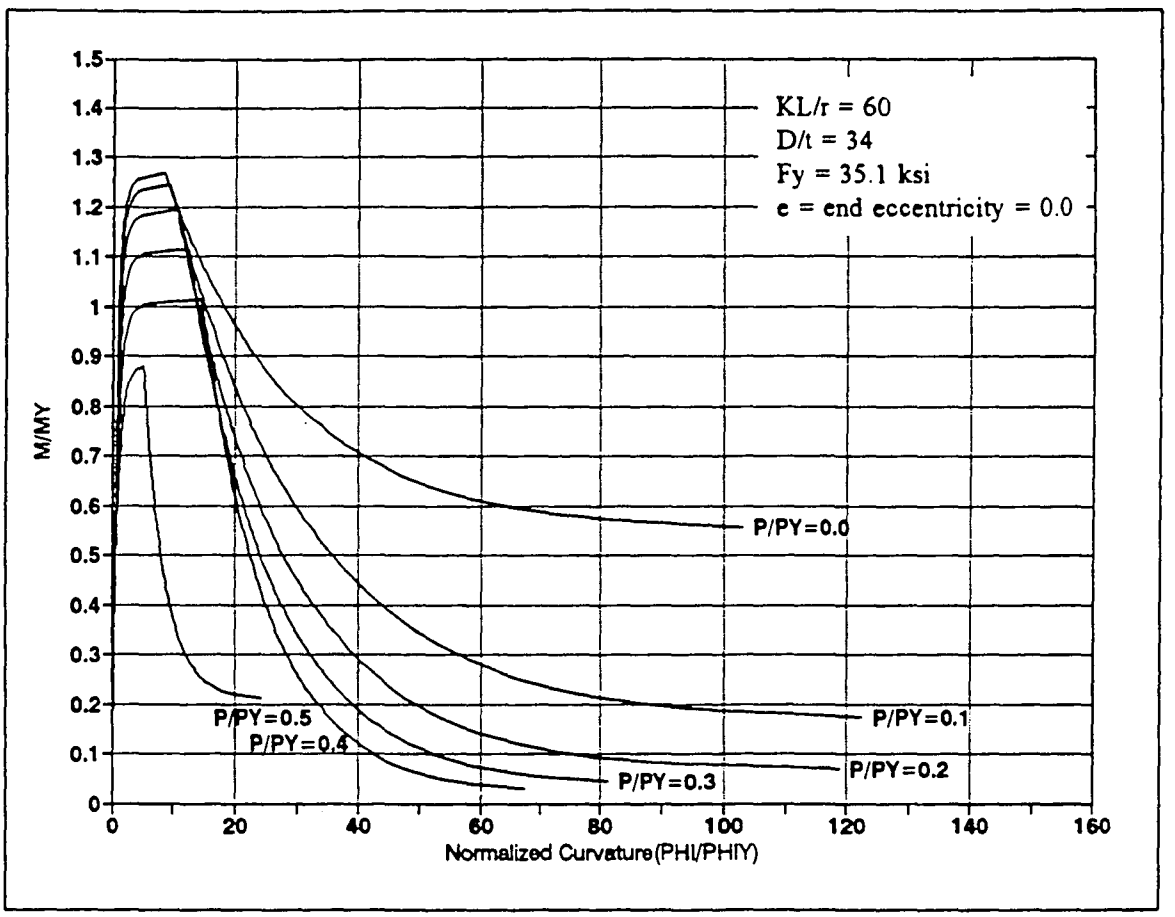

Figure 2-6(b) : Moment Curvature Relationships for Undented Tubular Sections with Local Buckling

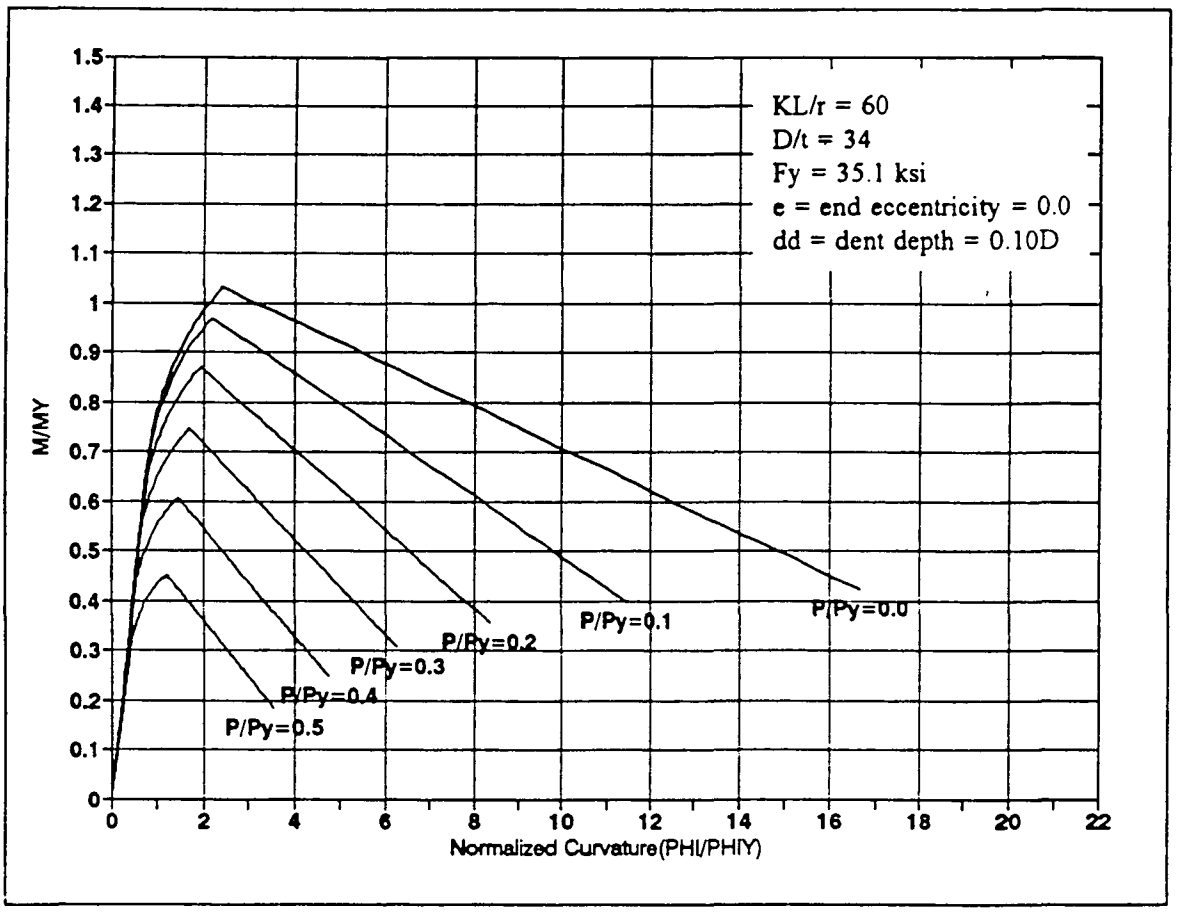

Figure 2-6(c) : Moment Curvature Relationships for Dent-Damaged Tubular Sections

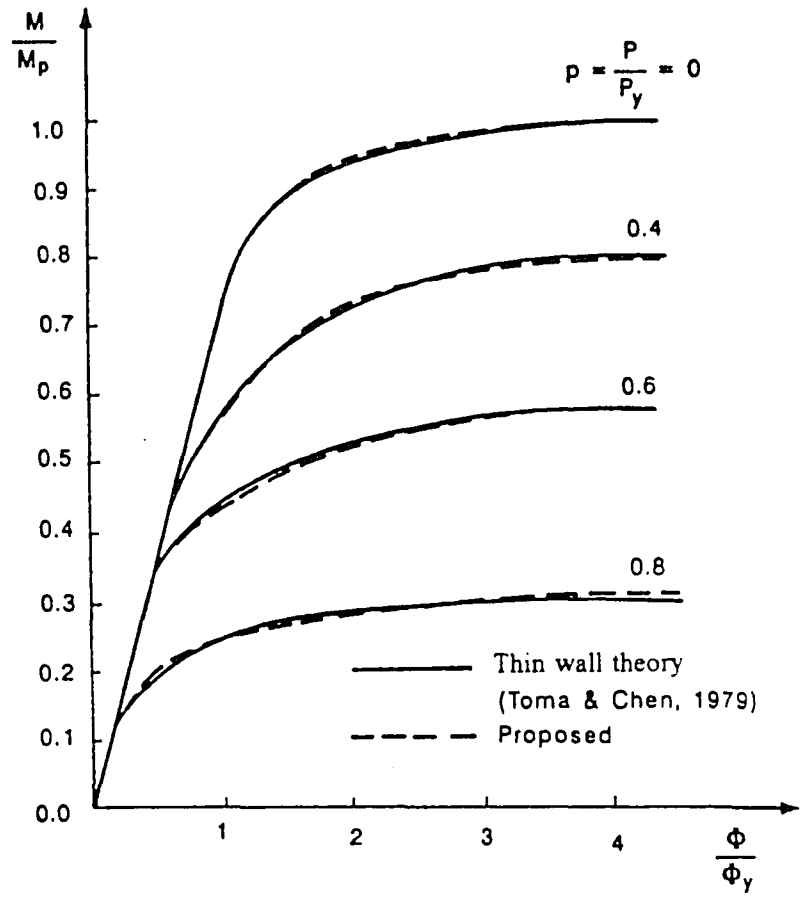

Figure 2-7(a) : Comparison of Moment-Thrust-Curvature Relationships between Exact Theory and Empirical Expressions by Duan et al., 1993, Undented Tubular

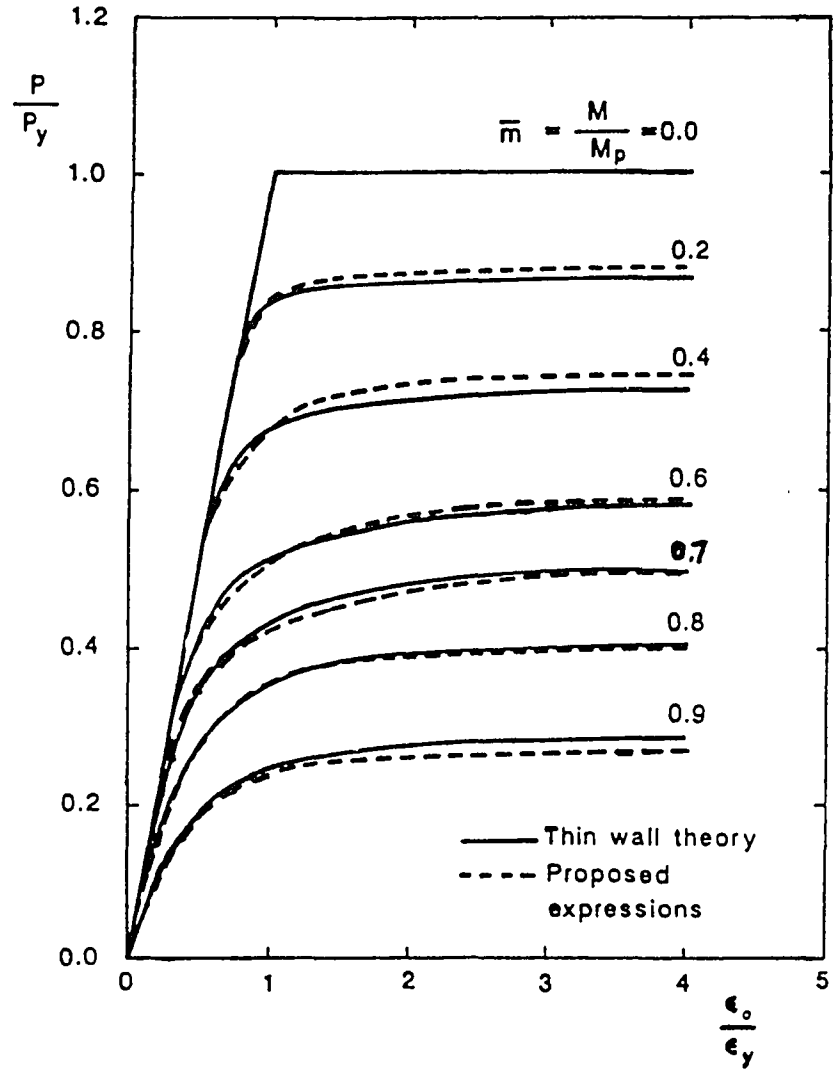

Figure 2-7(b) : Comparison of Moment-Thrust-Strain Relationships between Exact Theory and Empirical Expressions by Duan et al., 1993, Undented Tubular

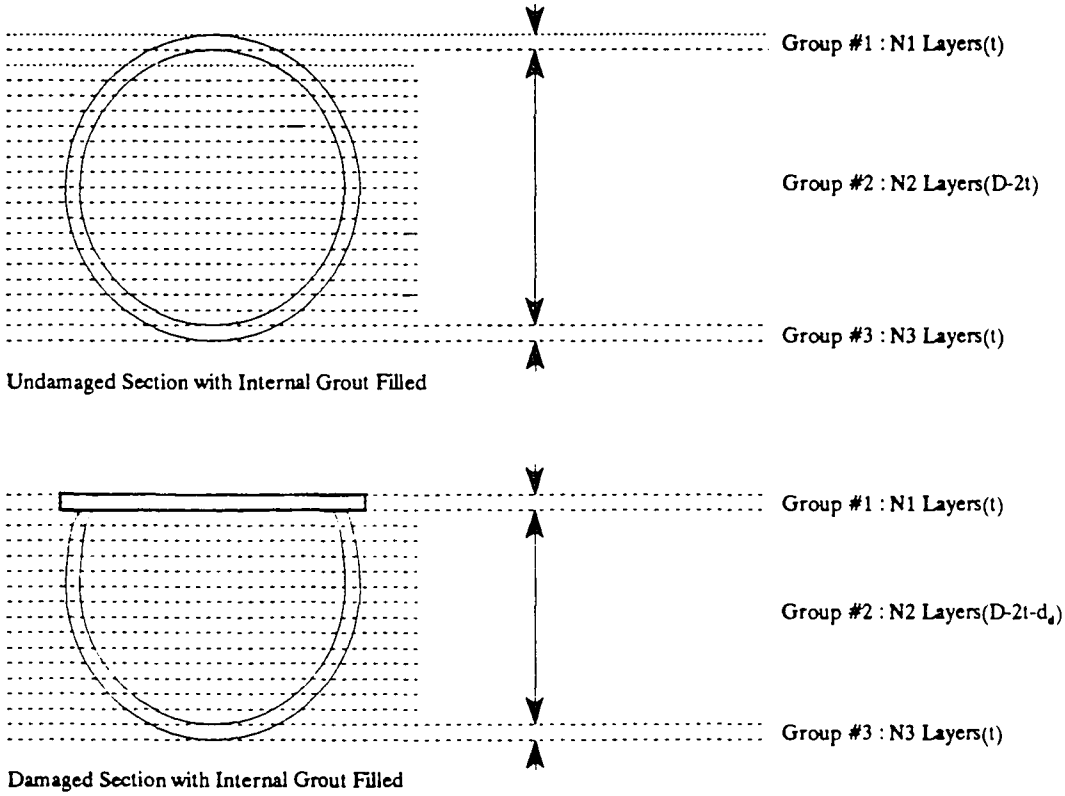

Figure 2-8 : Discretization of Internally Grout Filled Tubular Cross-Section into Layers

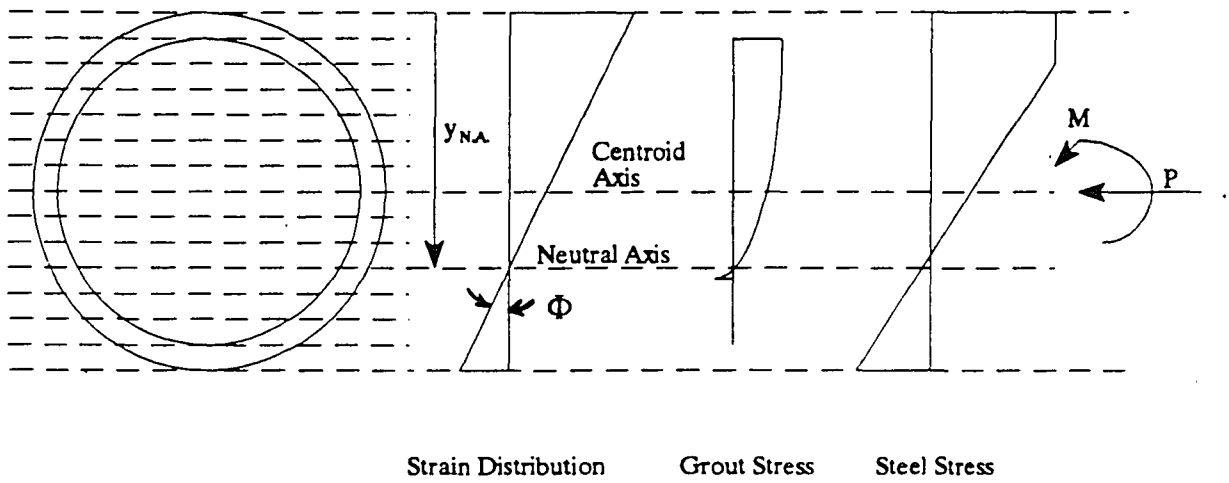

Figure 2-9 : Fiber Model Used to Generate the Moment Curvature Relationships

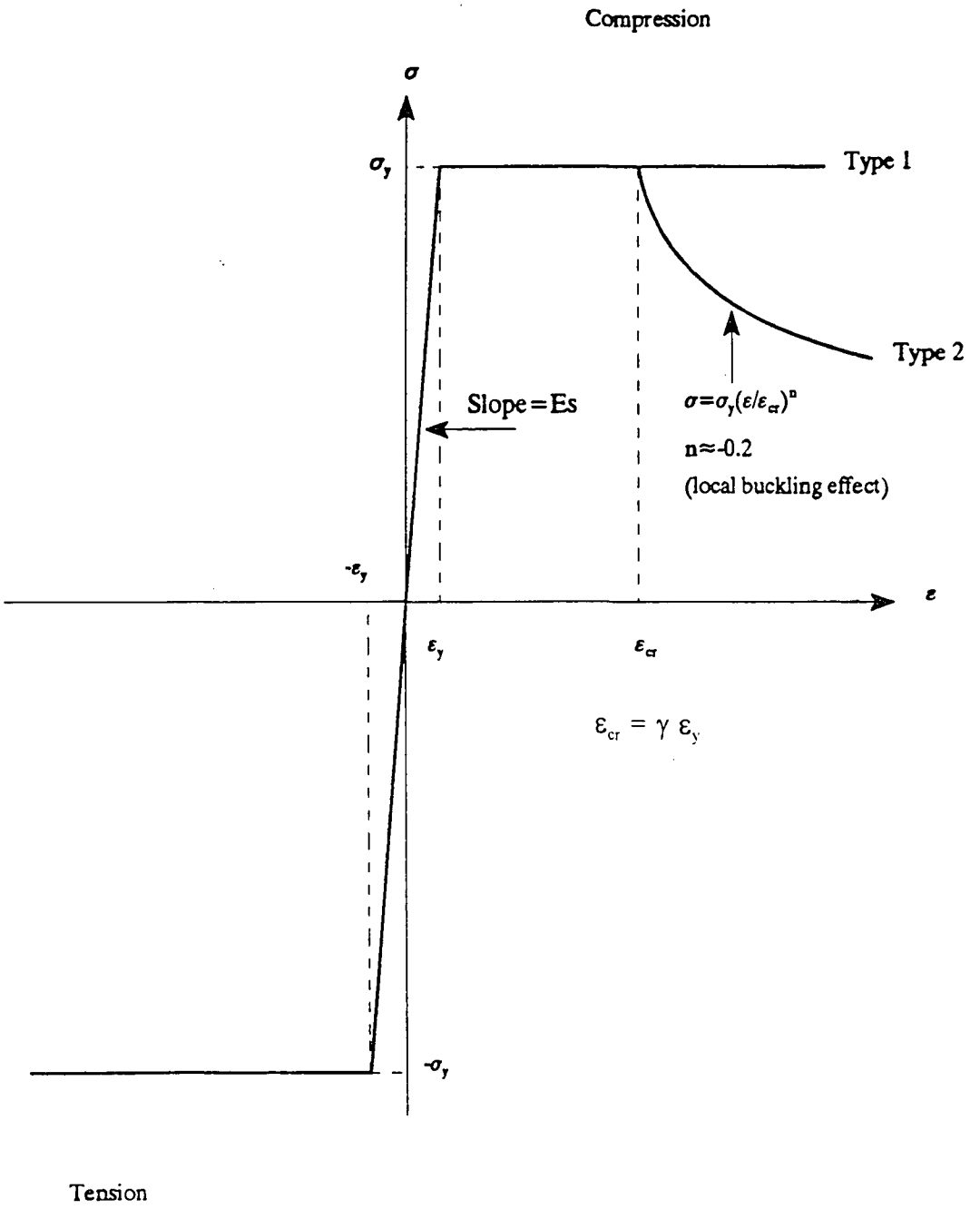

Figure 2-10 : Stress-Strain Relationship of Steel

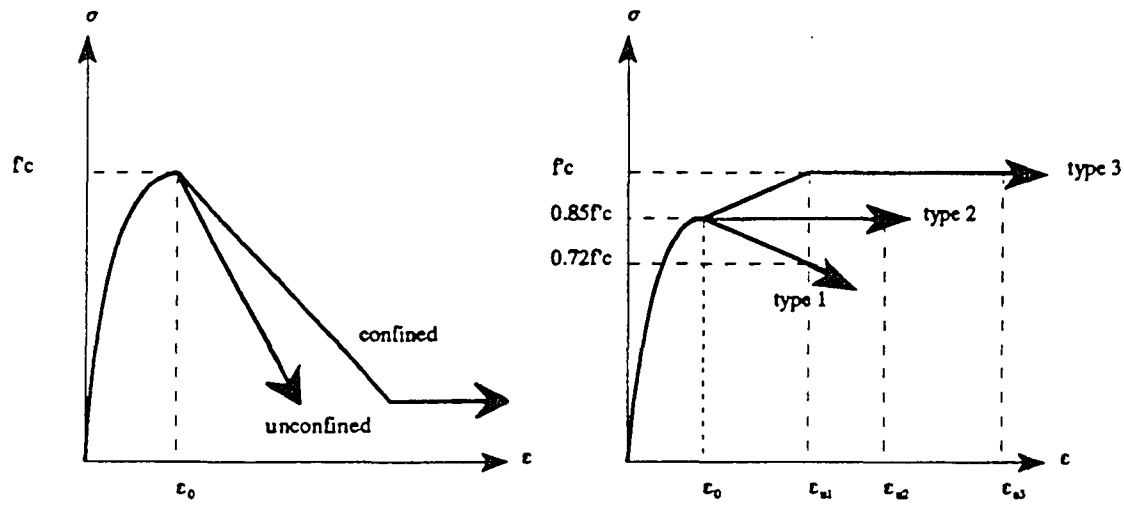

Figure 2-11 : Stress-Strain Relationships of Concrete (a). Kent, and Park, 1971; (b). Chen, and Ausuta, 1976

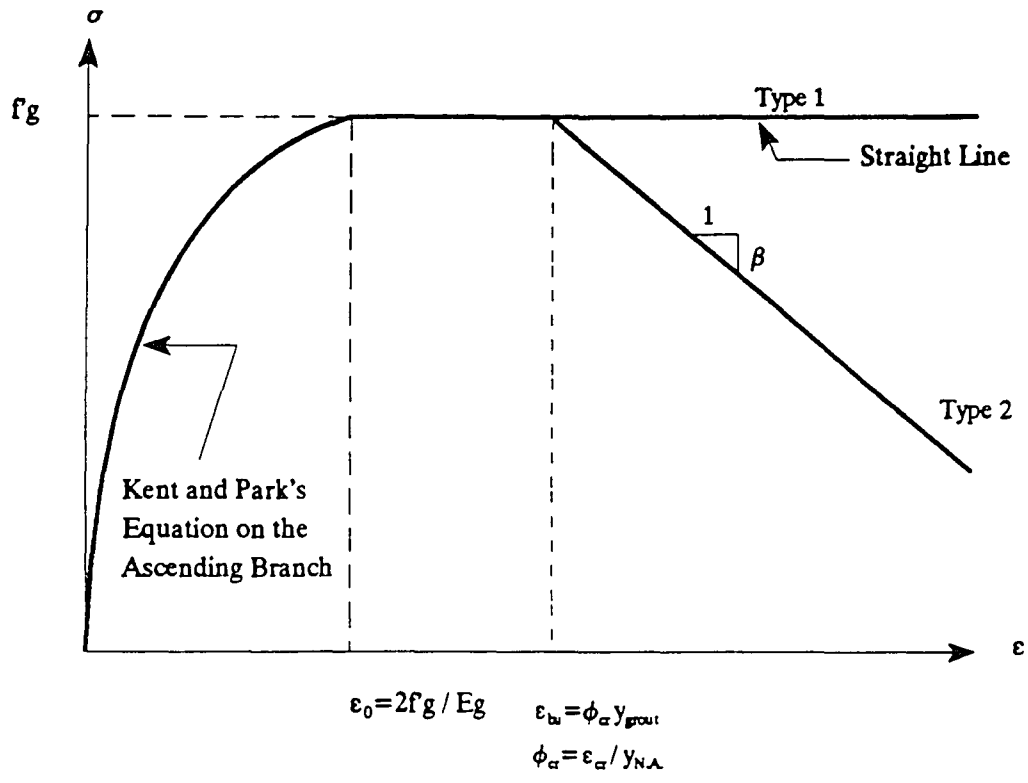

Figure 2-12 : Proposed Stress-Strain Relationahips for the Confined Grout

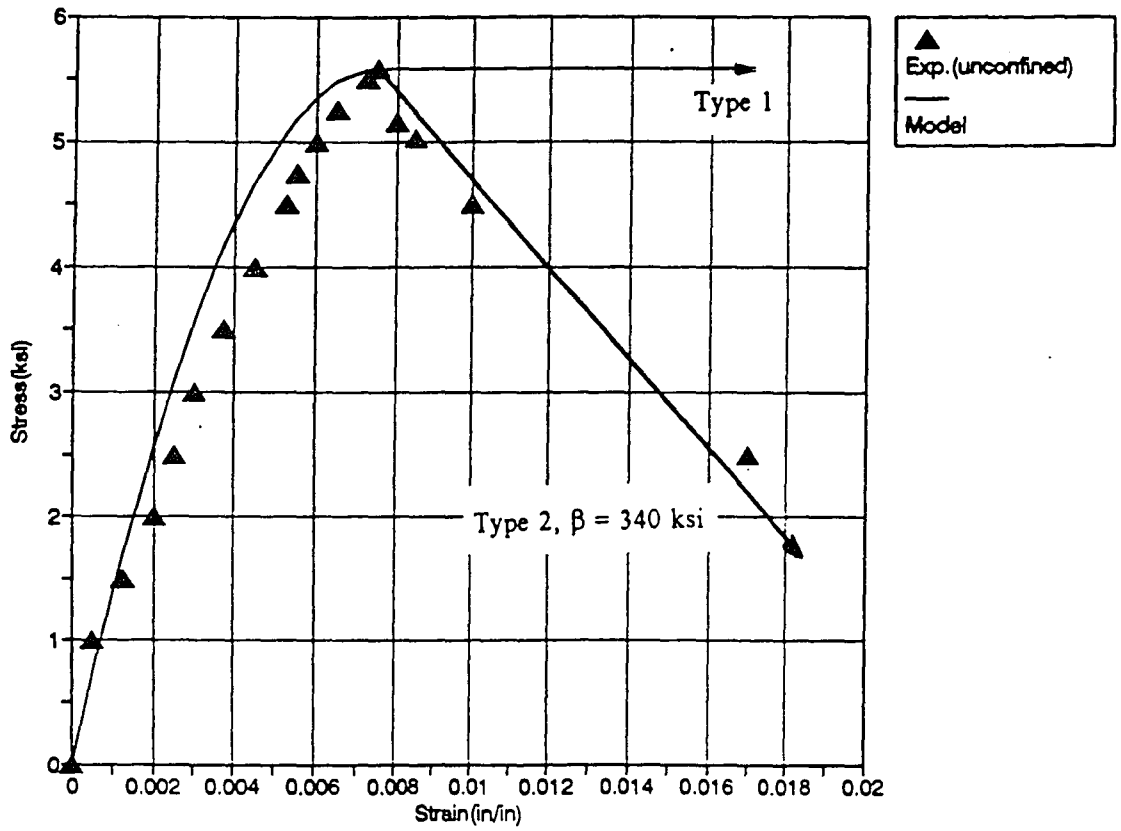

Grout Mix #1 (by weight)
water/cement = 0.60
water/silica = 3.0

Figure 2-13 : Comparion of Stress-Strain Curves between Experimental Result and Proposed Model (Mix #1)

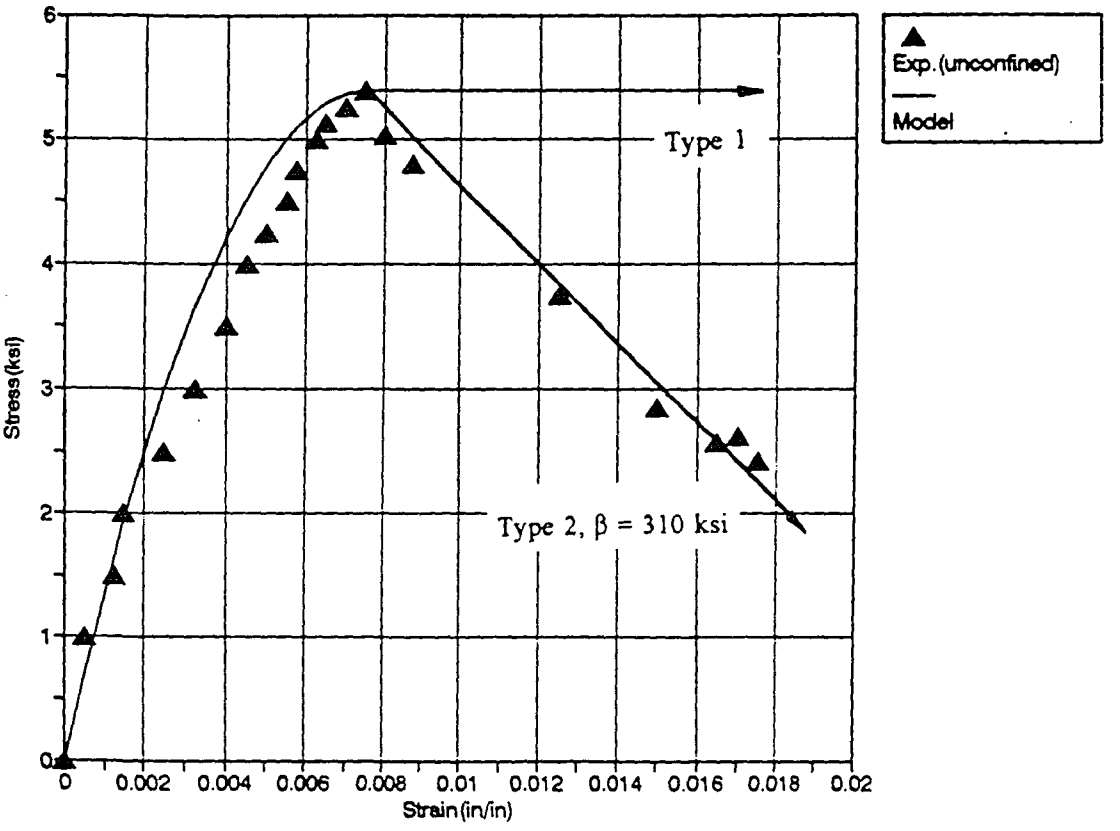

Grout Mix #2 (by weight)
water/cement = 0.65
water/silica = 3.25

Figure 2-14 : Comparion of Stress-Strain Curves between Experimental Result and Proposed Model (Mix #2)

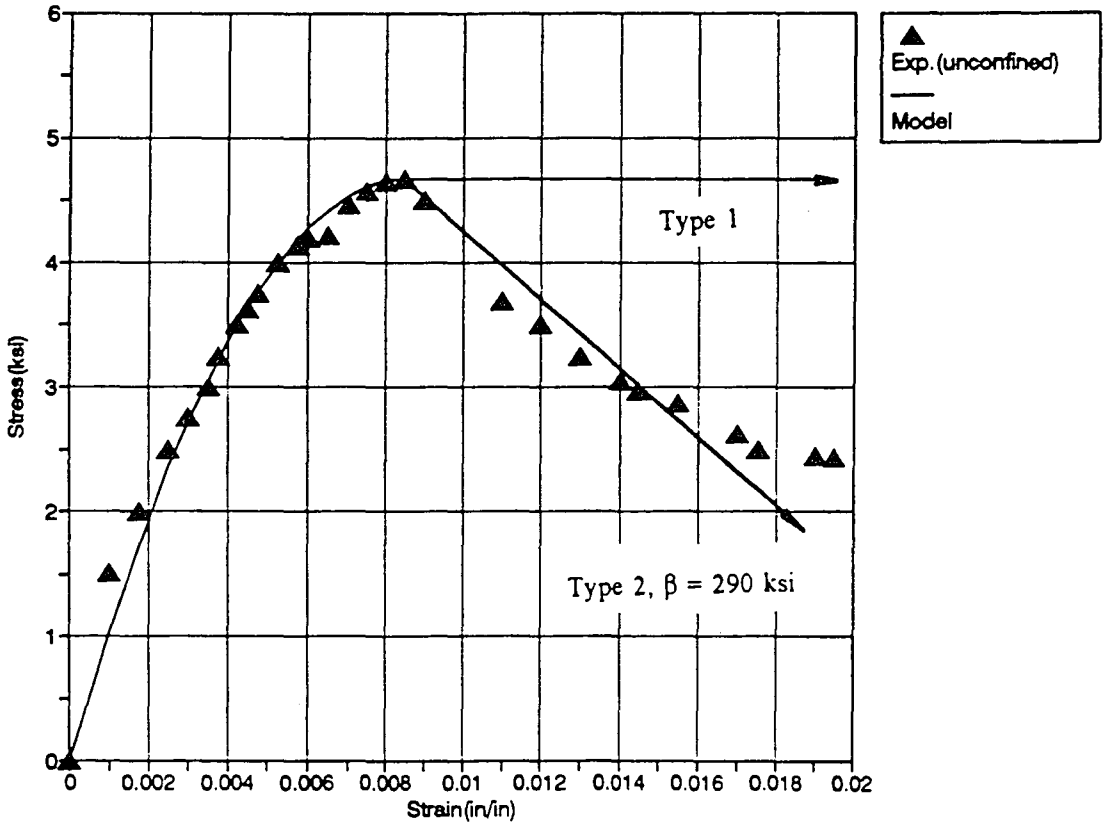

Grout Mix #3 (by weight)
water/cement = 0.70
water/silica = 3.5

Figure 2-15 : Comparion of Stress-Strain Curves between Experimental Result and Proposed Model (Mix #3)

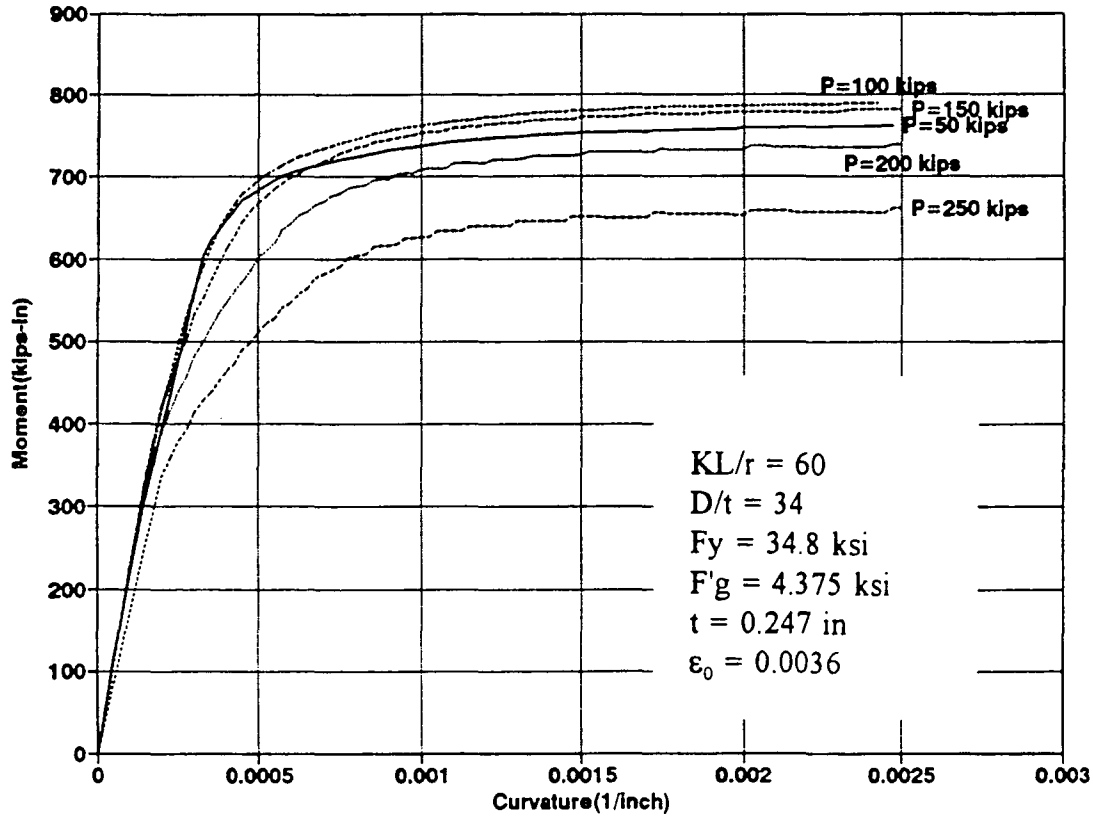

Figure 2-16 : Moment-Thrust-Curvature Curves for Undamaged, Internally Grout Filled Tubular Section, No Local Buckling

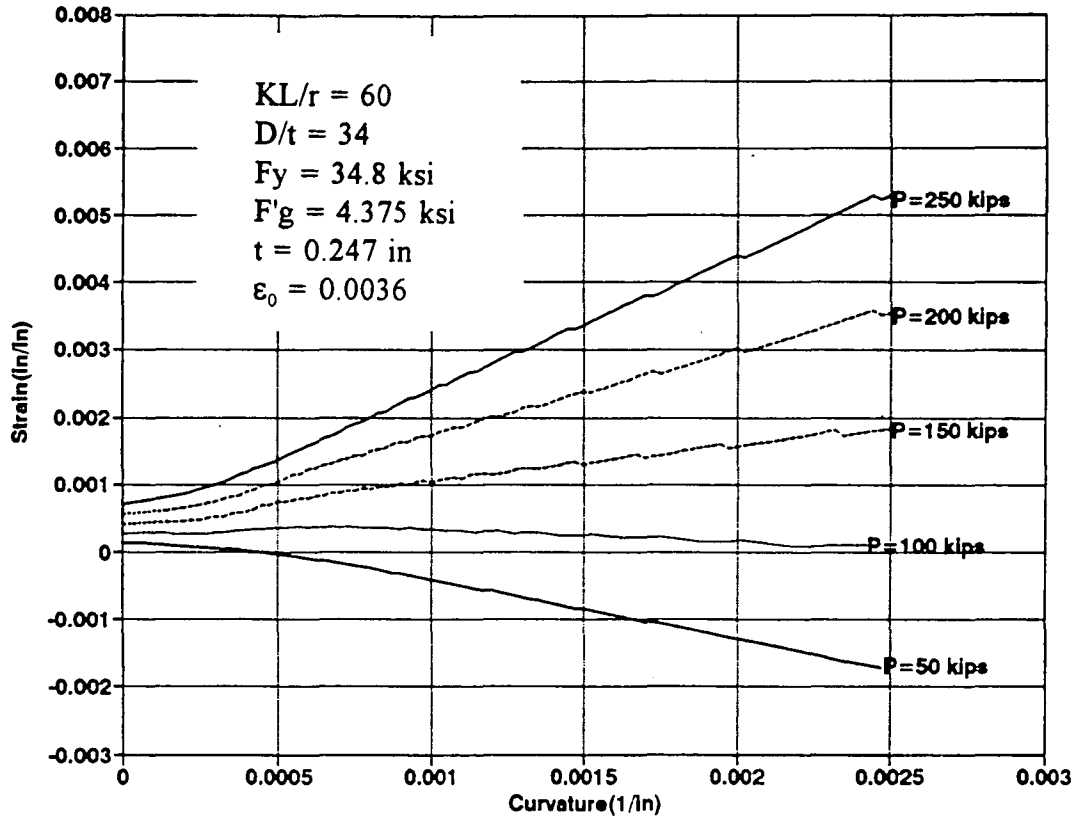

Figure 2-17 : Strain-Thrust-Curvature Curves for Undamaged, Internally Grout Filled Tubular Section, No Local Buckling

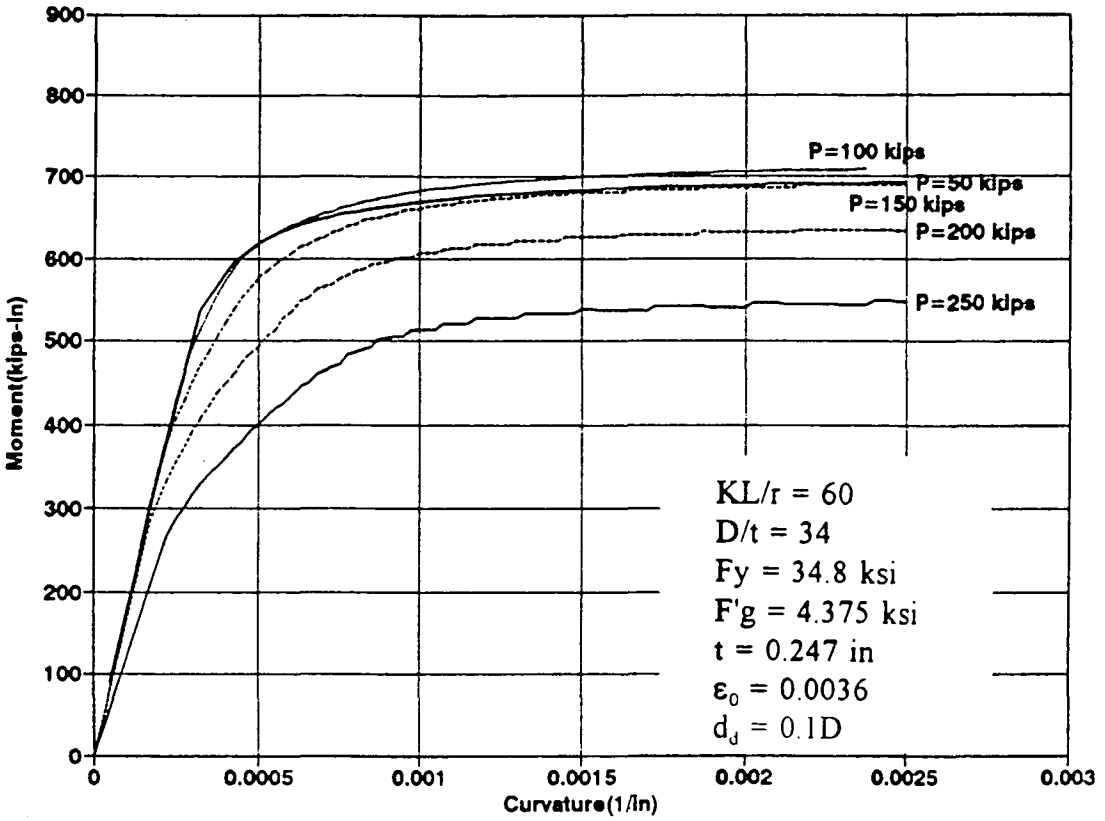

Figure 2-18 : Moment-Thrust-Curvature Curves for Dent-Damaged, Internally Grout Filled Tubular Section, No Local Buckling

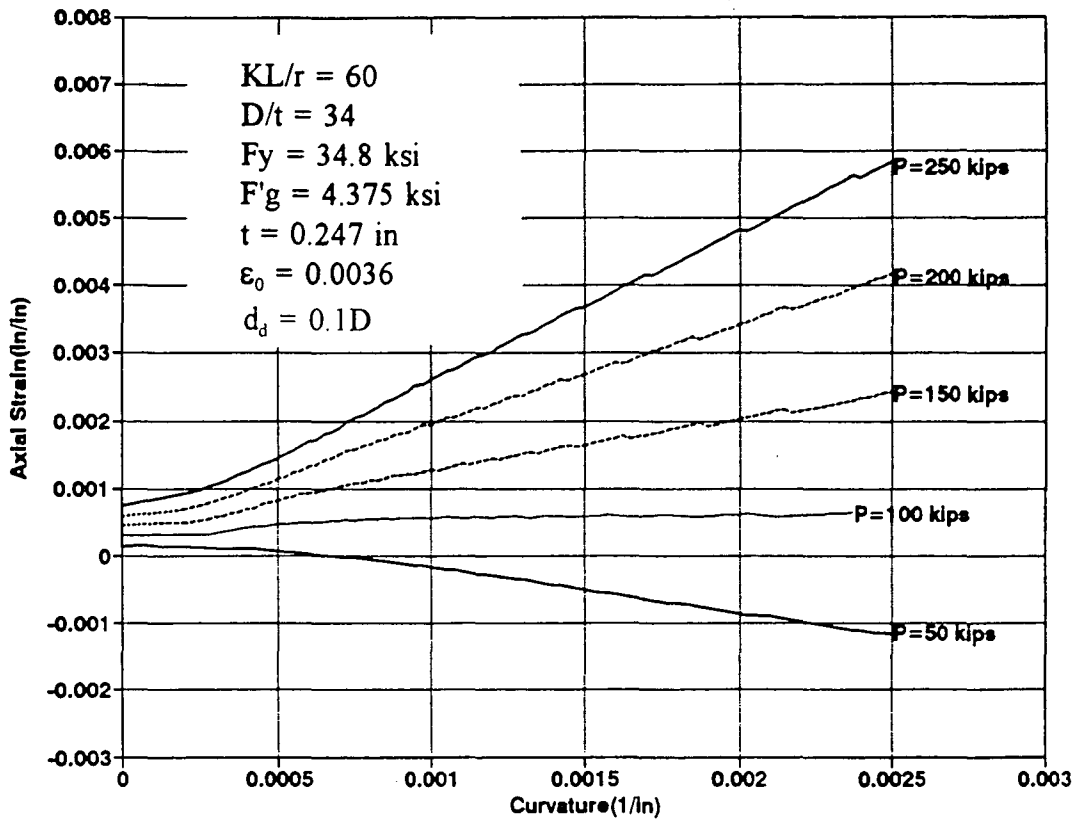

Figure 2-19 : Strain-Thrust-Curvature Curves for Dent-Damaged, Internally Grout Filled Tubular Section, No Local Buckling

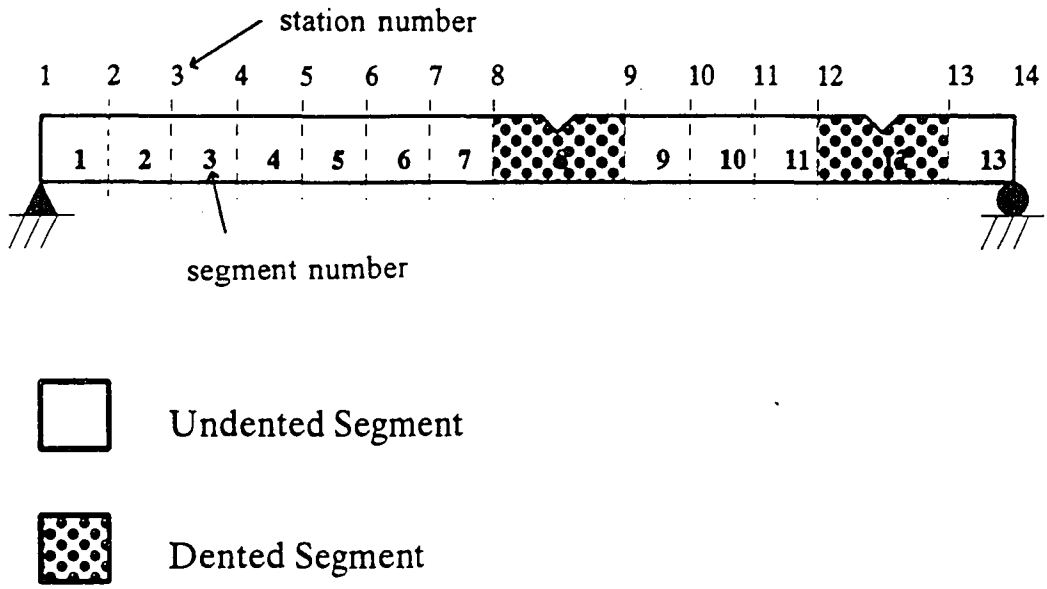

Figure 3-1 : Segments and Stations for Numerical Integration Analysis of Dented Tubular

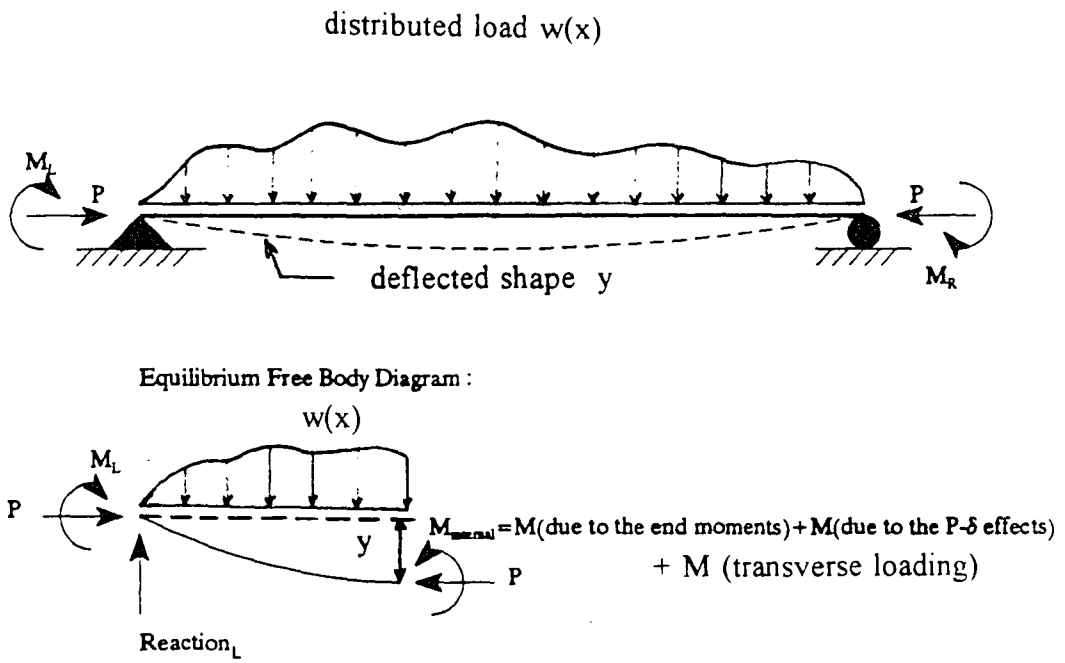

Figure 3-2 : Load Condition and Equilibrium Diagram

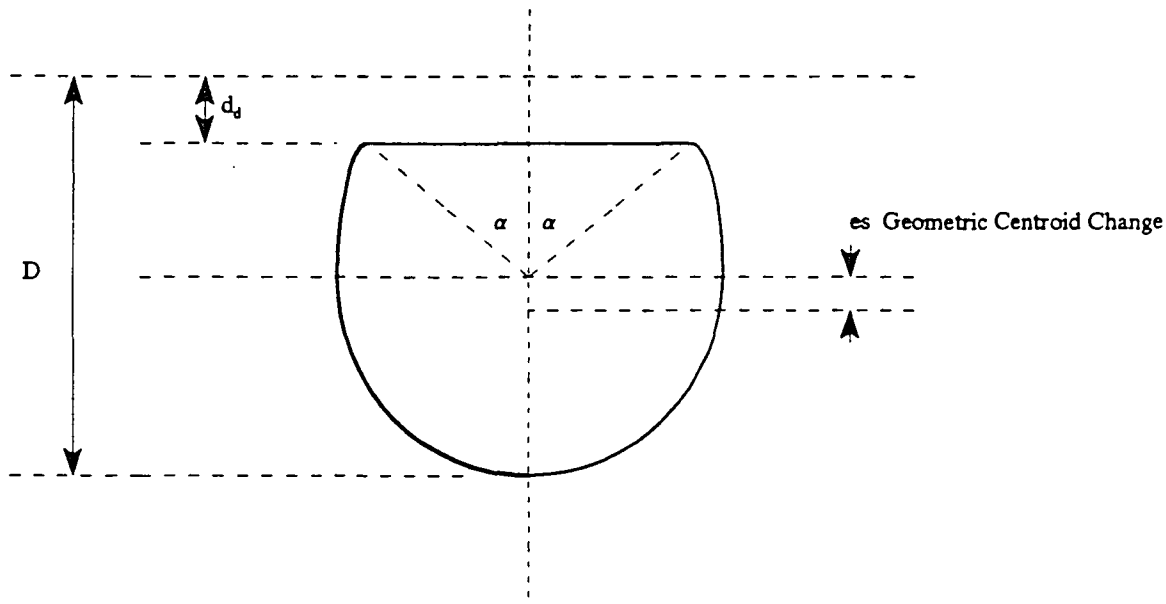

Figure 3-3 : Geometric Centroid Change due to Dent Damage

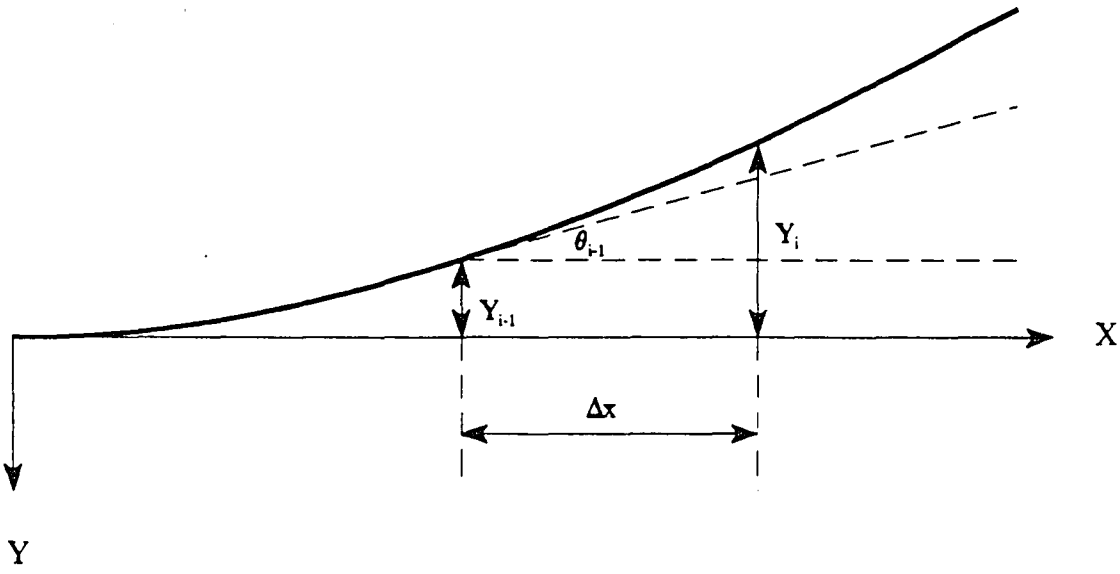

$$Y_i = Y_{i-1} - \theta_{i-1}\,\Delta x - \int x\,\Phi(x)\,dx$$

Figure 3-4 : Numerical Integration Method between Two Successive Stations

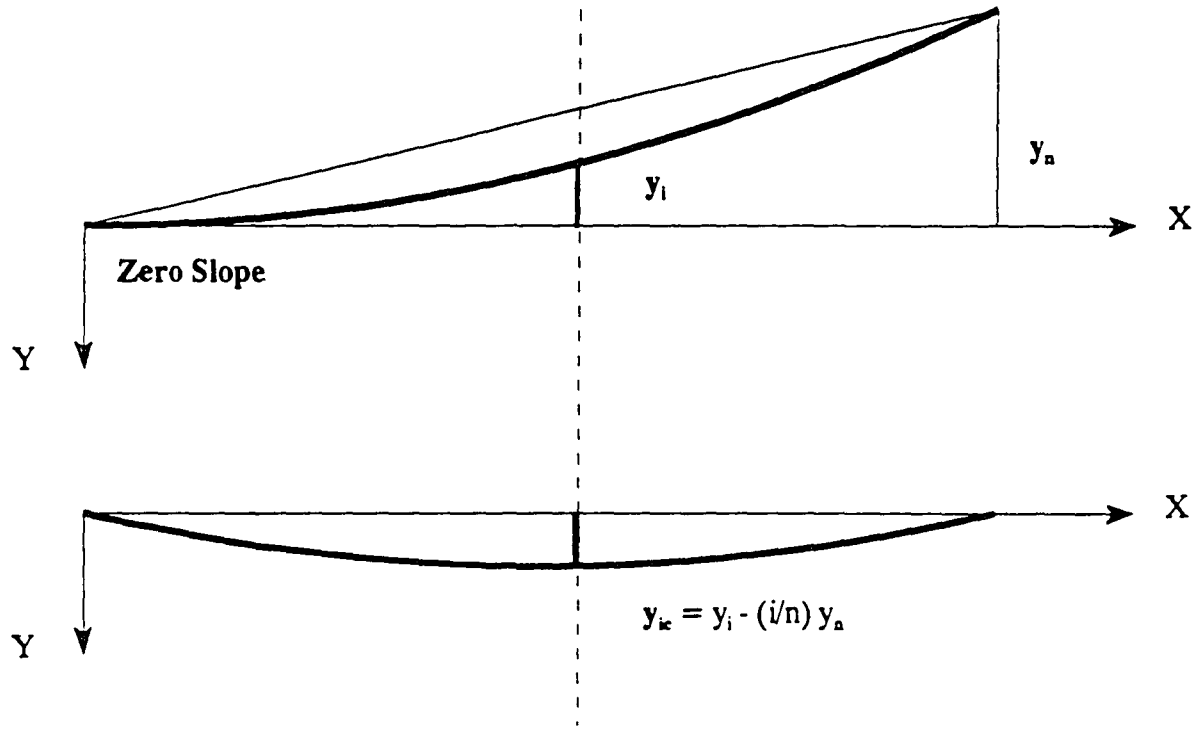

Figure 3-5 : Linear Correction to Deflections

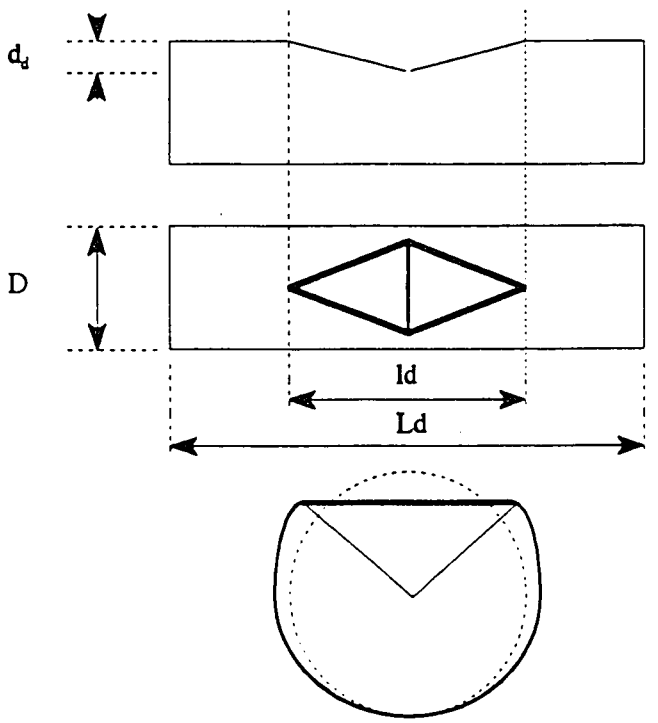

Ld(dent segment length) :
Ld is taken to be 2.0 l_d which is considered as a sufficient limit to preclude cross-sectional distortion at its ends.
where :

$$l_d = D\sqrt{(0.25 \cdot \Pi \cdot d_d/t)}$$

Figure 3-6 : Idealized Dent Geometry

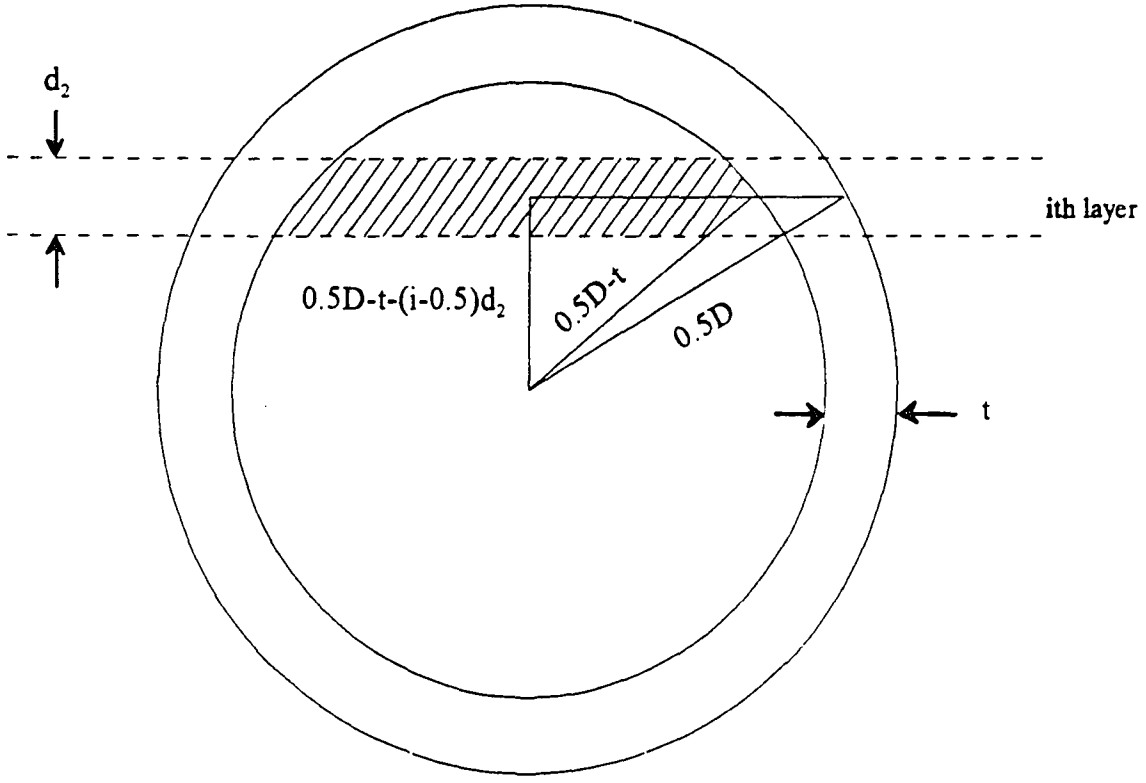

Figure 3-7 : Area Calculation of Each Layer

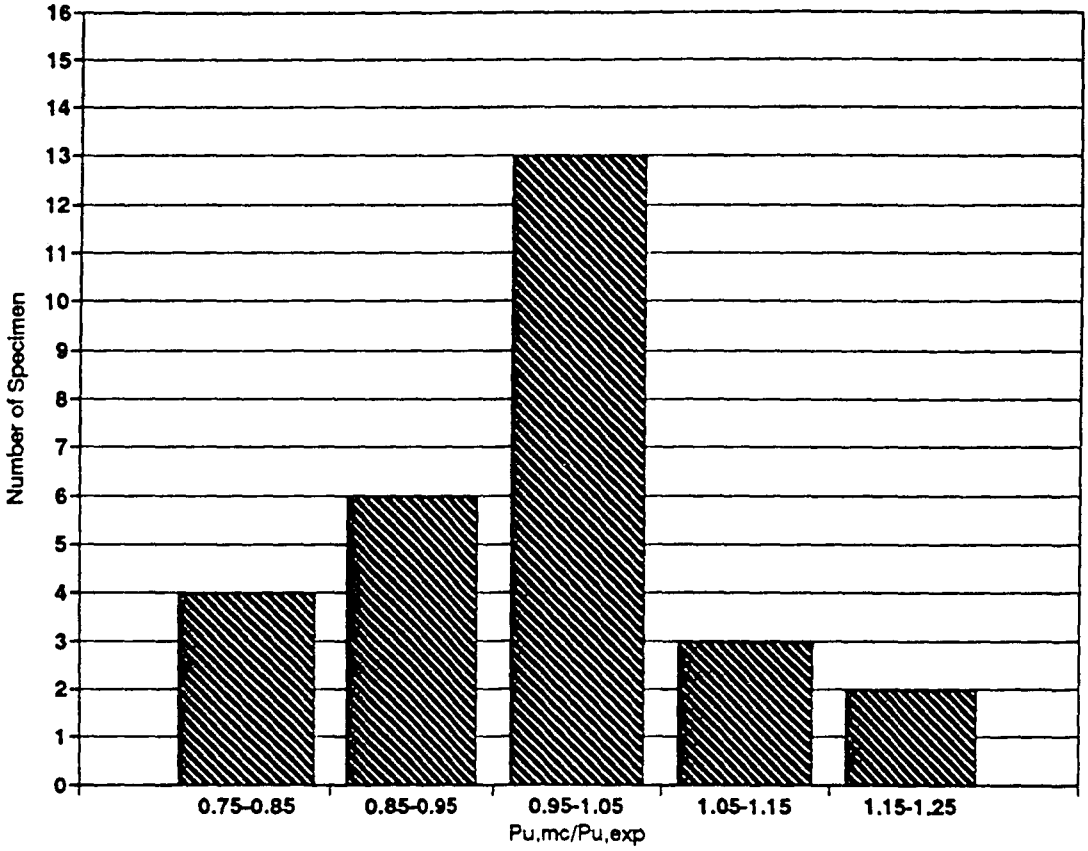

Figure 4-1 : Histogram of Predicted-to-Measured Ultimate Strength Ratio for Unrepaired Specimens (n=28, mean=0.98, C.O.V.=0.096)

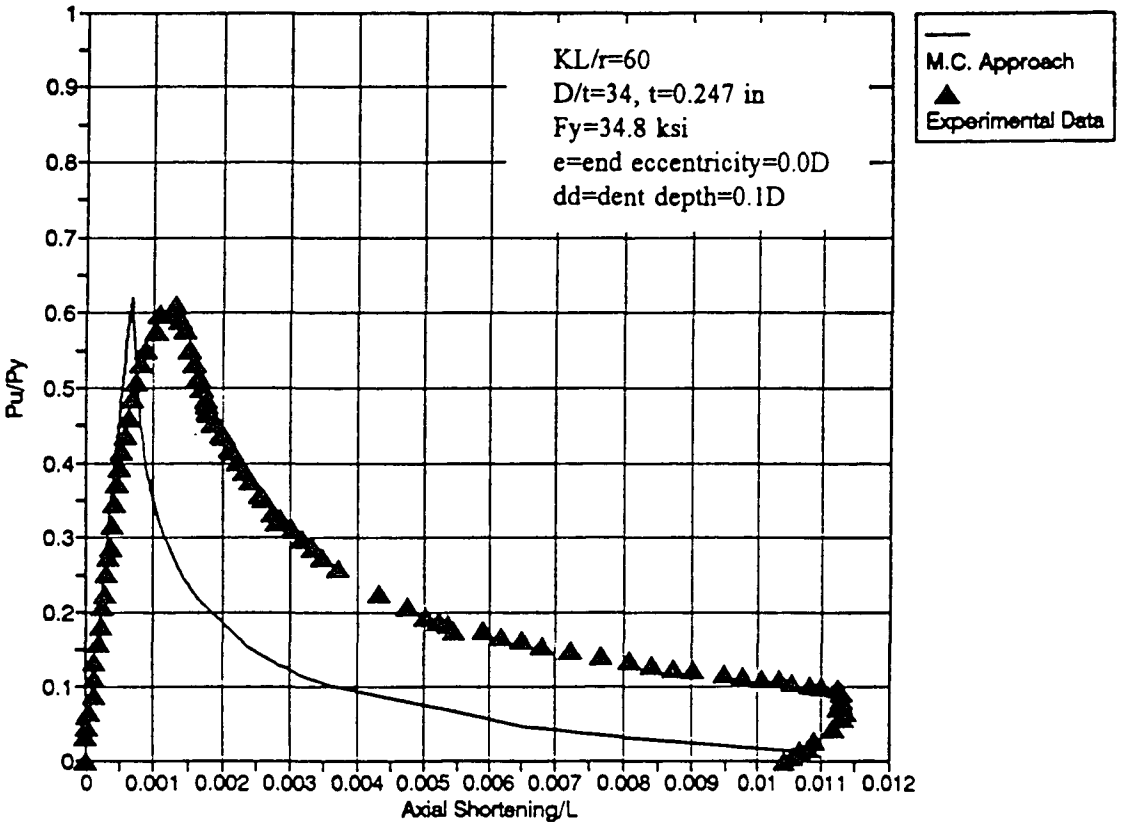

Figure 4-2 : Axial Compression-Shortening Response for Specimen A1 [Ricles and Gillum, 1992]

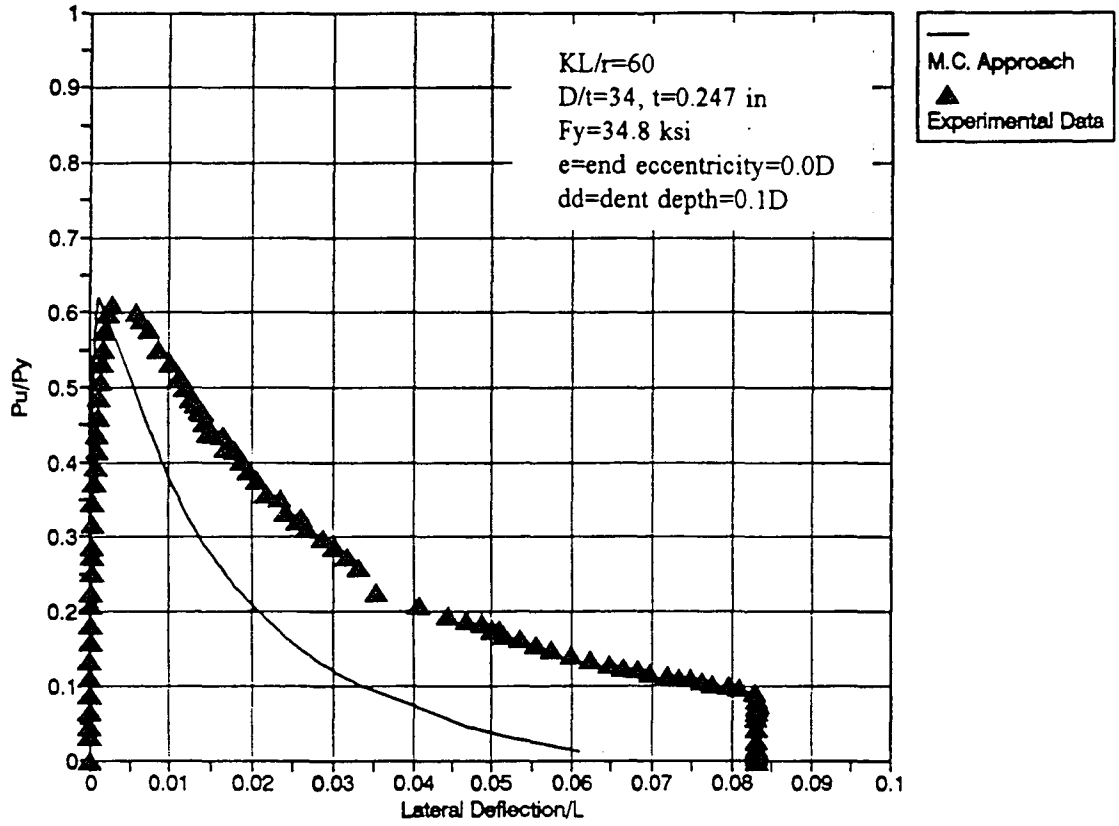

Figure 4-3 : Axial Compression-Lateral Deflection Response for Specimen A1 [Ricles and Gillum, 1992]

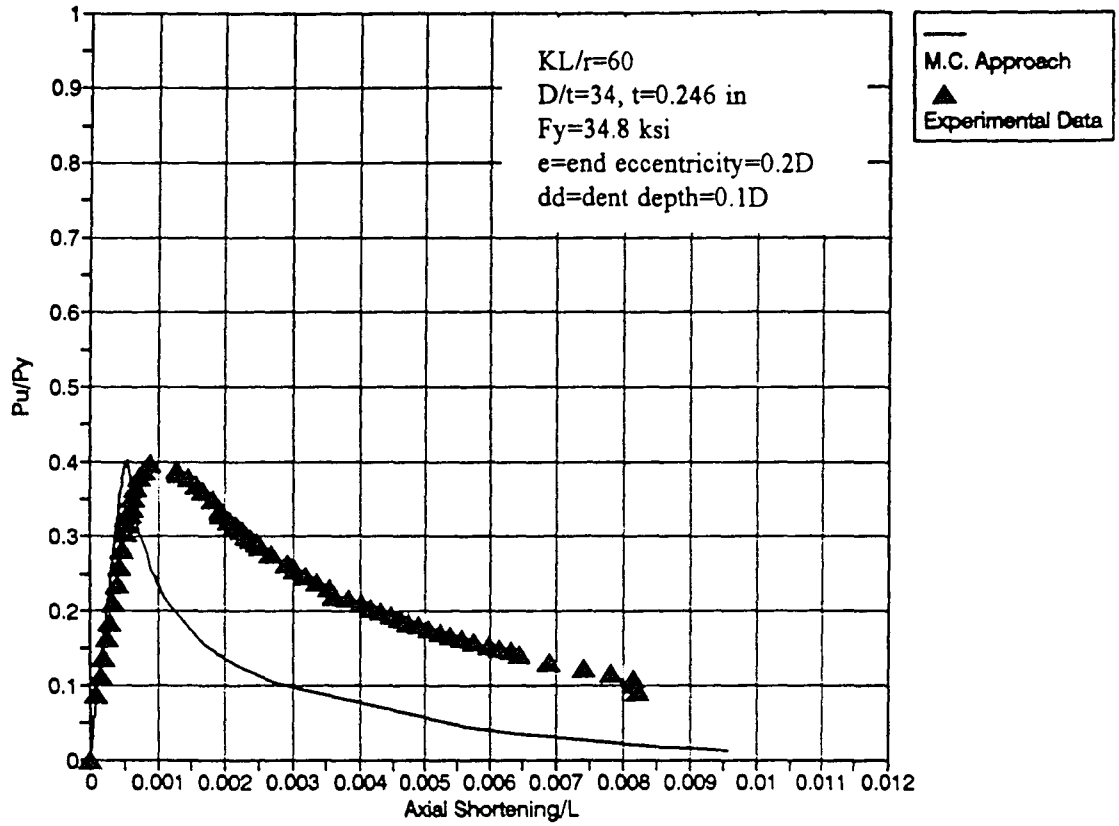

Figure 4-4 : Axial Compression-Shortening Response for Specimen A2 [Ricles and Gillum, 1992]

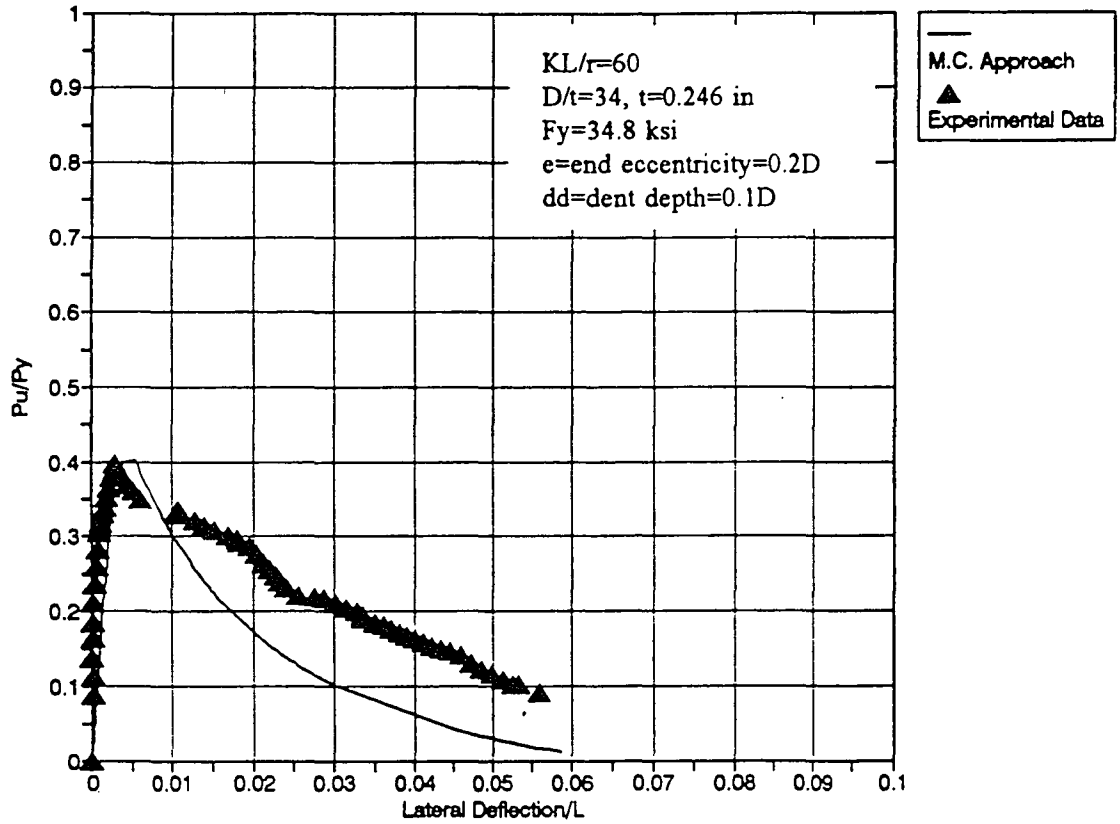

Figure 4-5 : Axial Compression-Lateral Deflection Response for Specimen A2 [Ricles and Gillum, 1992]

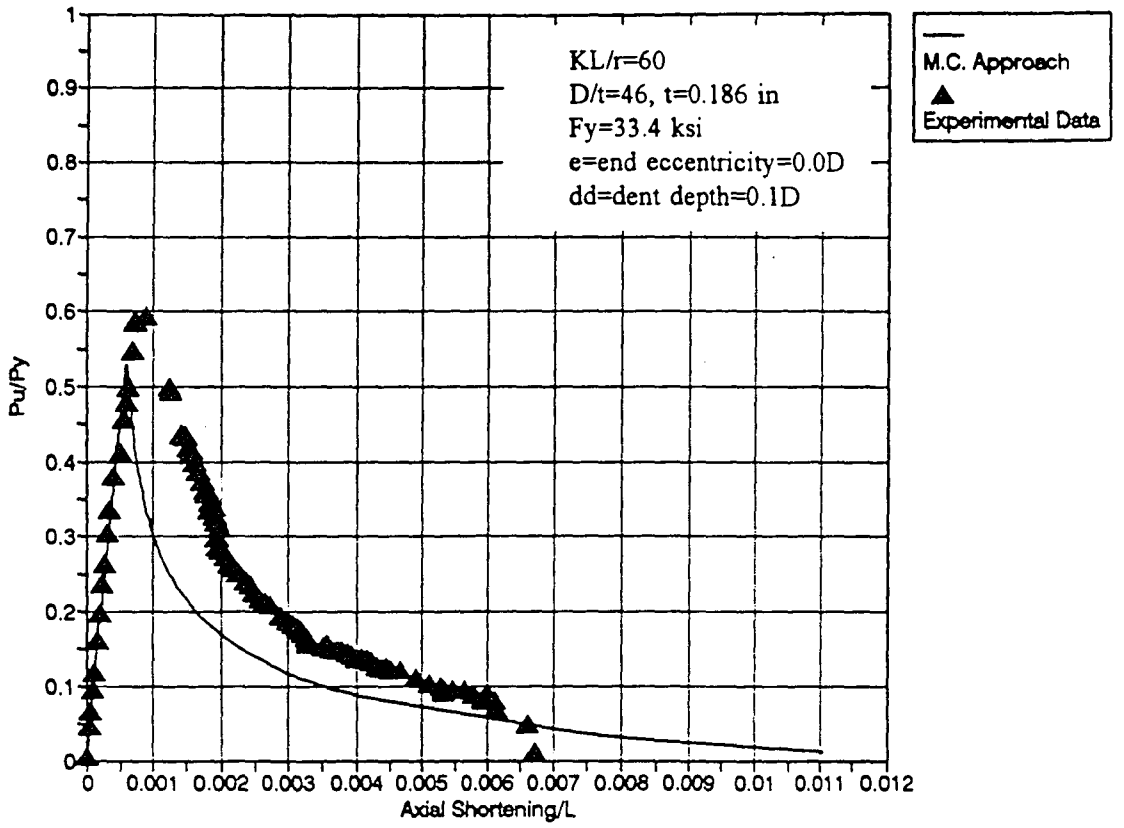

Figure 4-6 : Axial Compression-Shortening Response for Specimen B1 [Ricles and Gillum, 1992]

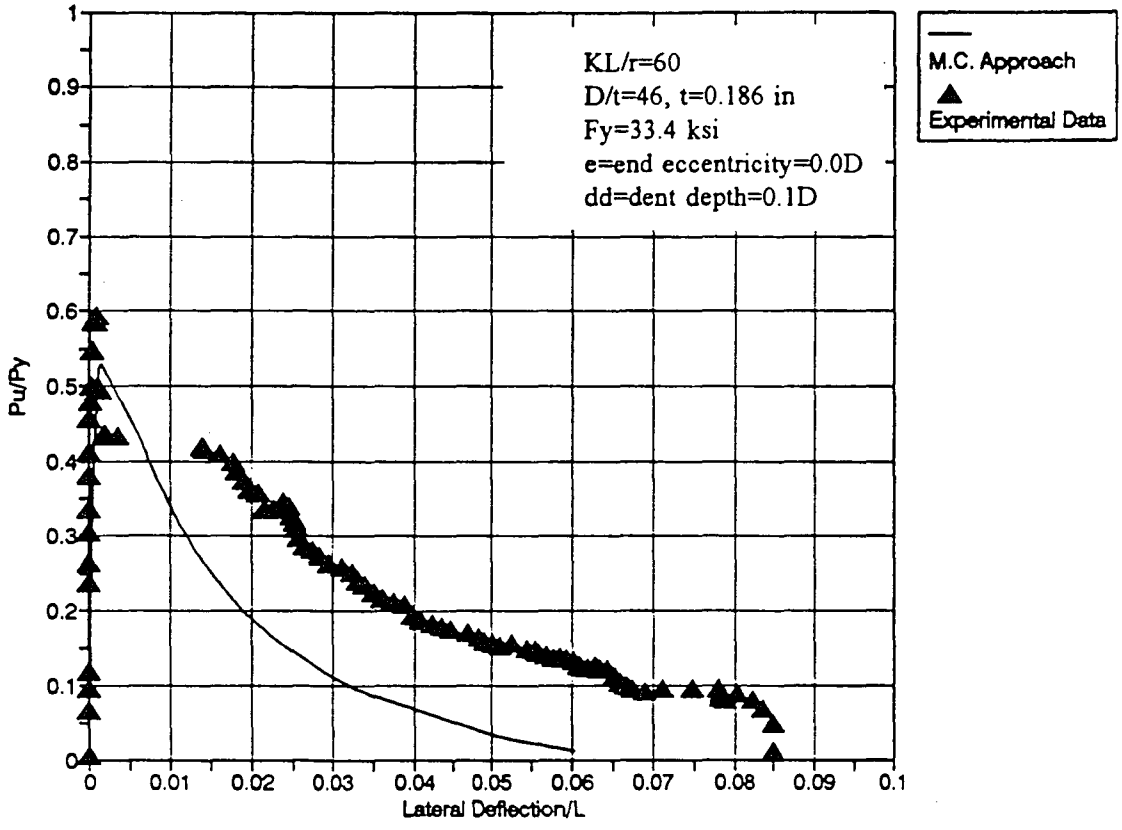

Figure 4-7 : Axial Compression-Lateral Deflection Response for Specimen B1 [Ricles and Gillum, 1992]

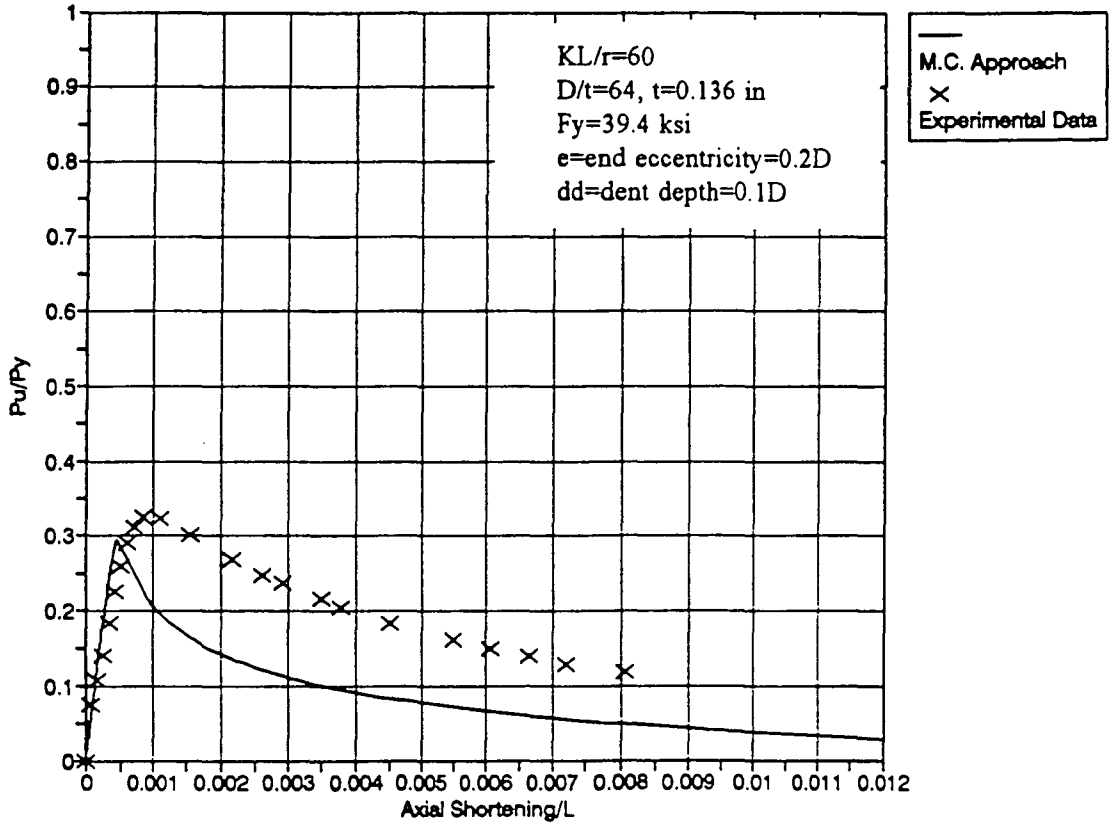

Figure 4-8 : Axial Compression-Shortening Response for Specimen C2

[Ricles and Gillum, 1992]

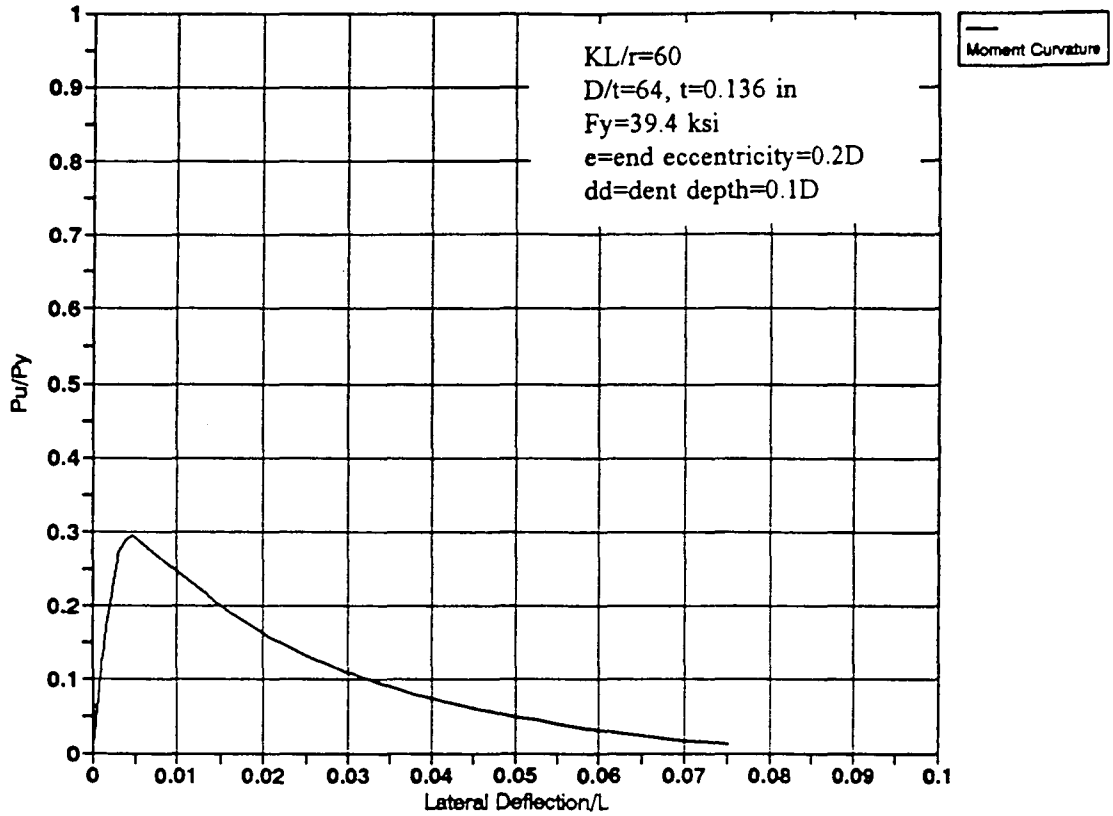

Figure 4-9 : Axial Compression-Lateral Deflection Response for Specimen C2 [Ricles and Gillum, 1992]

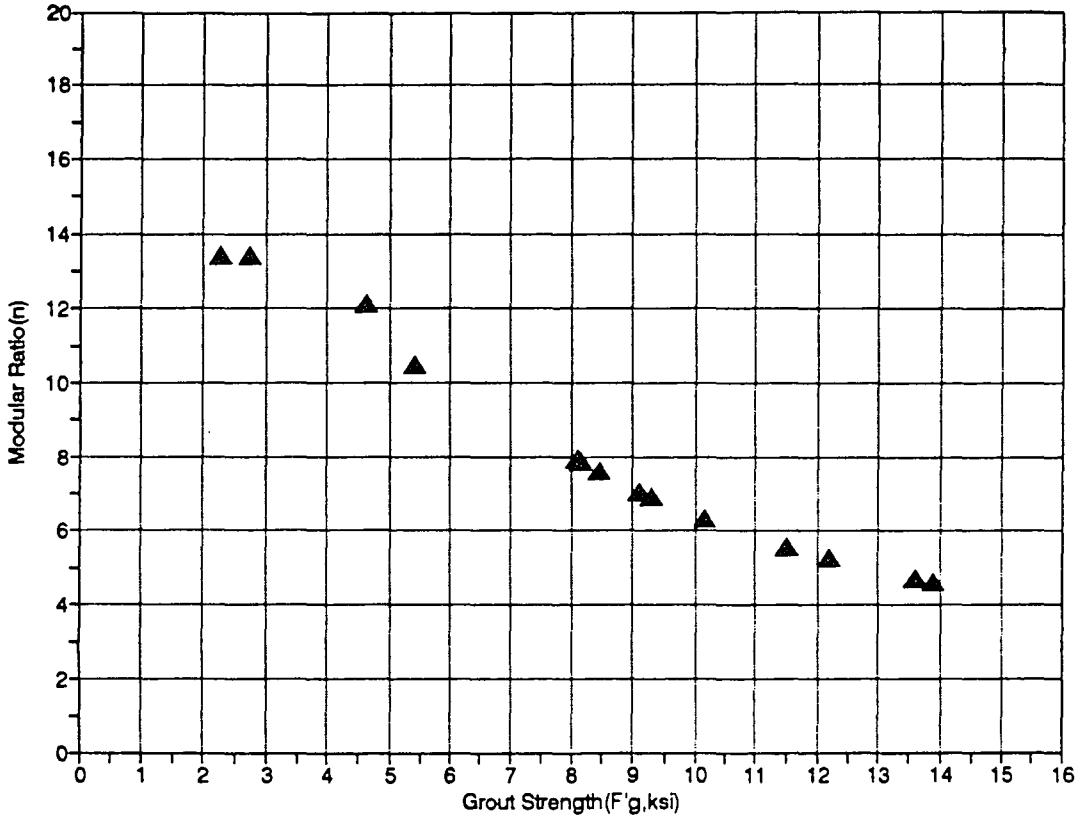

Figure 4-10 : Typical Relationships between Modular Ratio and Grout Strength

(Data points were taken from 27 test results for Es=29000 ksi

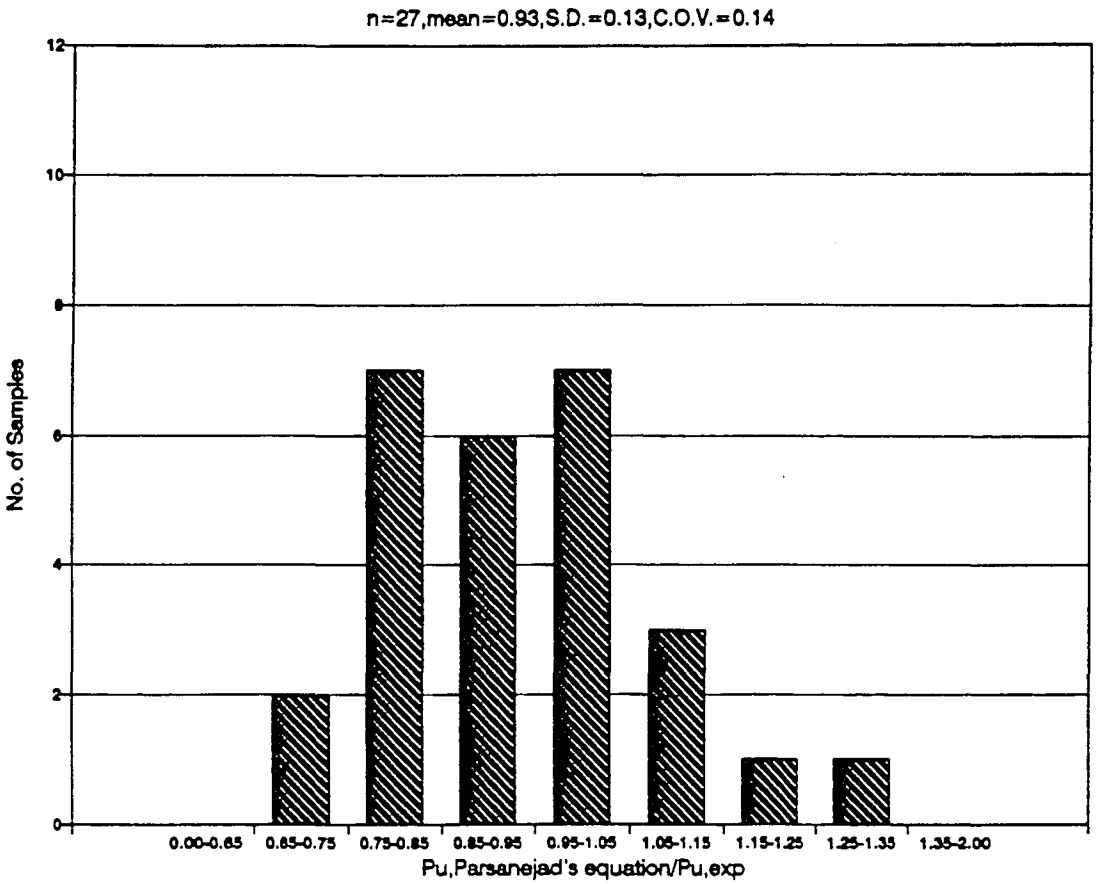

Figure 4-11 : Histogram of Predicted-to-Measured Ultimate Strength Ratio Using Parsanejad's Approach (n=27, mean=0.93, C.O.V.=0.14)

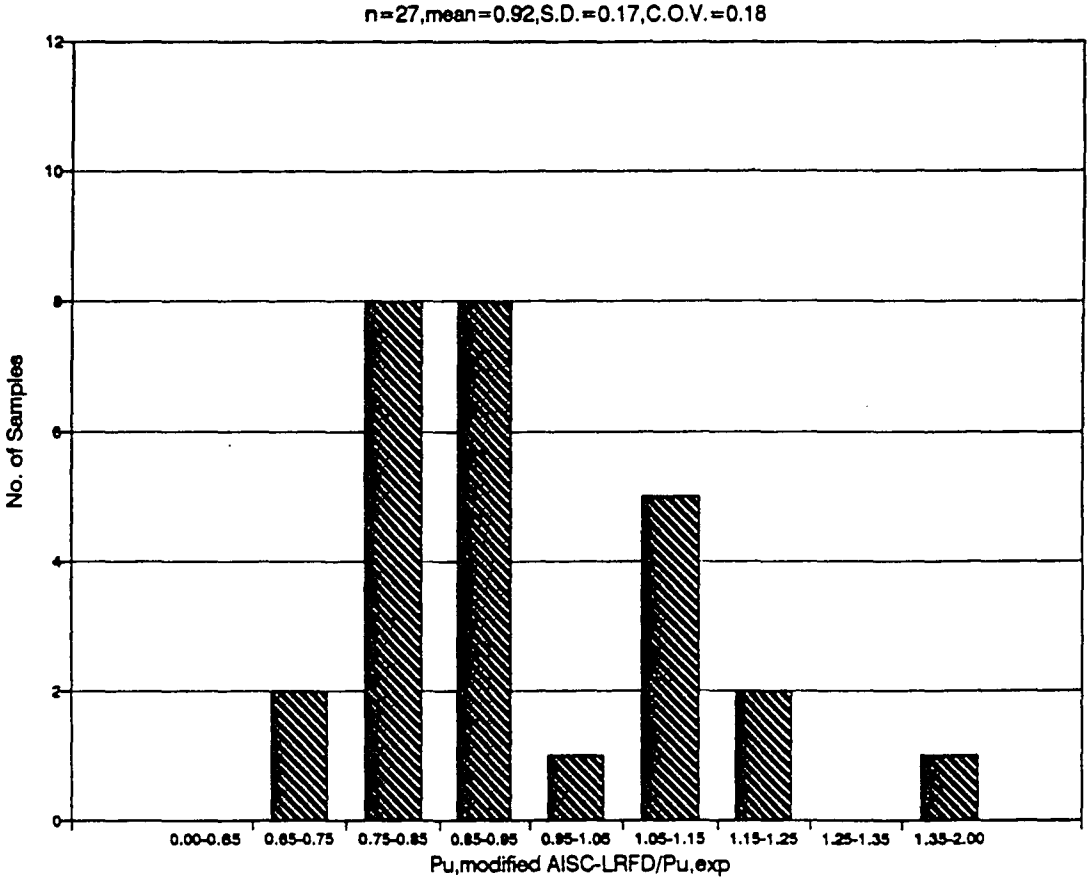

Figure 4-12 : Histogram of Predicted-to-Measured Ultimate Strength Ratio Using Modified AISC-LRFD Approach (n=27, mean=0.92, C.O.V.=0.18)

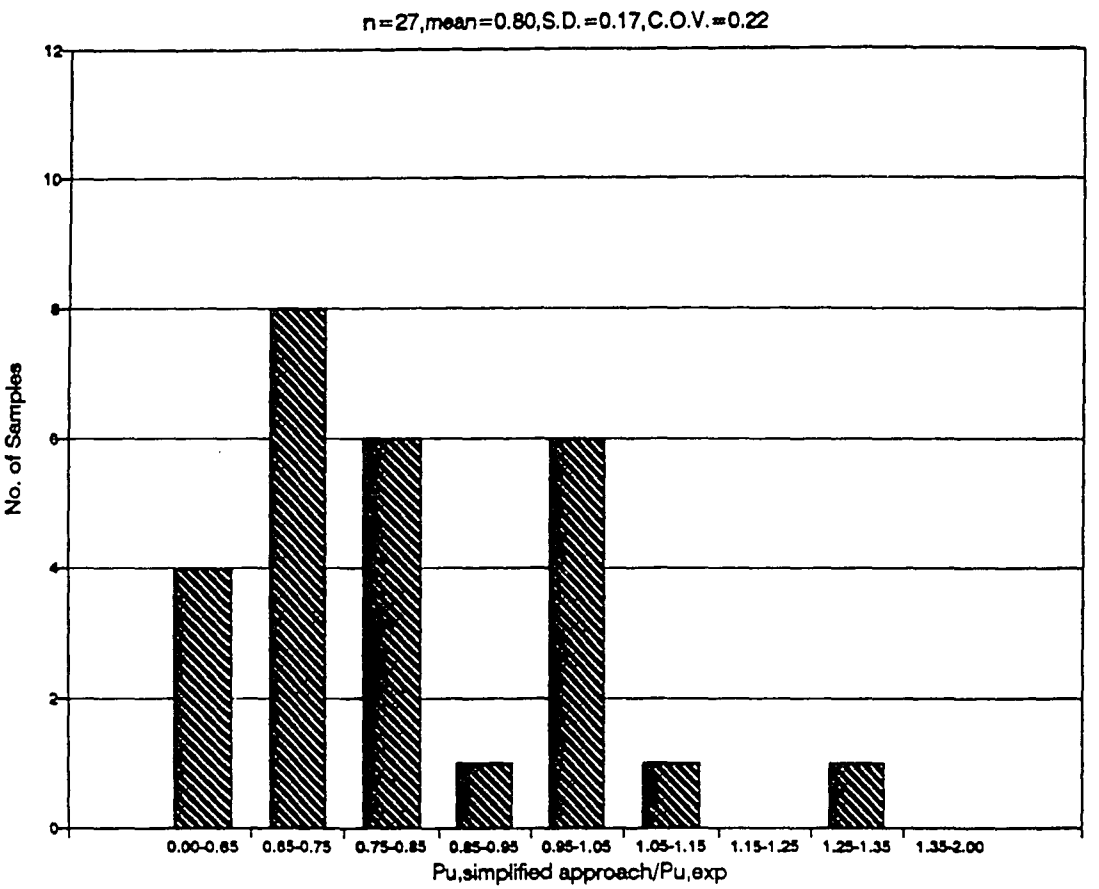

Figure 4-13 : Histogram of Predicted-to-Measured Ultimate Strength Ratio Using Simplified AISC-LRFD Approach (n=27, mean=0.80, CO.V.=0.22)

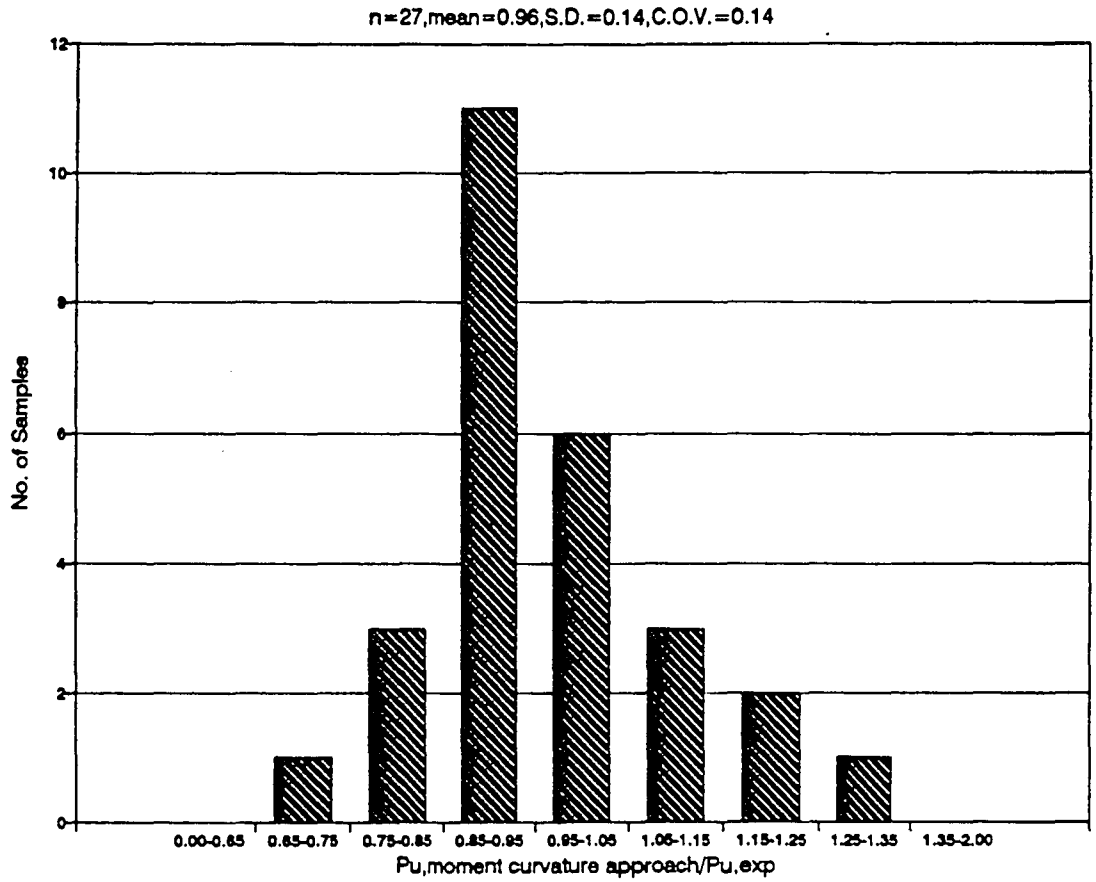

Figure 4-14 : Histogram of Predicted-to-Measured Ultimate Strength Ratio Using Moment Curvature Approach (n=27, mean=0.96, C.O.V.=0.14)

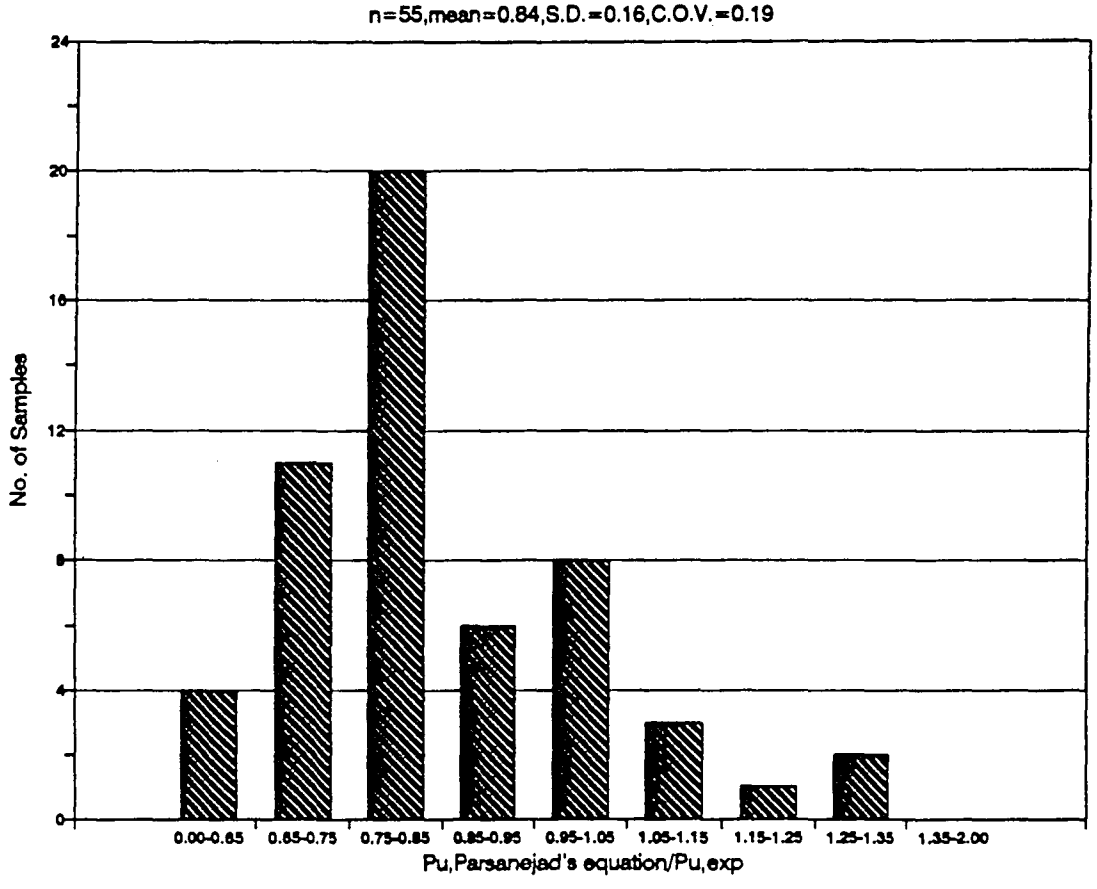

Figure 4-15 : Histogram of Predicted-to-Measured Ultimate Strength Ratio Using Parsanejad's Approach with Boswell and D' Mello's Reported Modular Ratio (n=55, mean=0.84, C.O.V.=0.19)

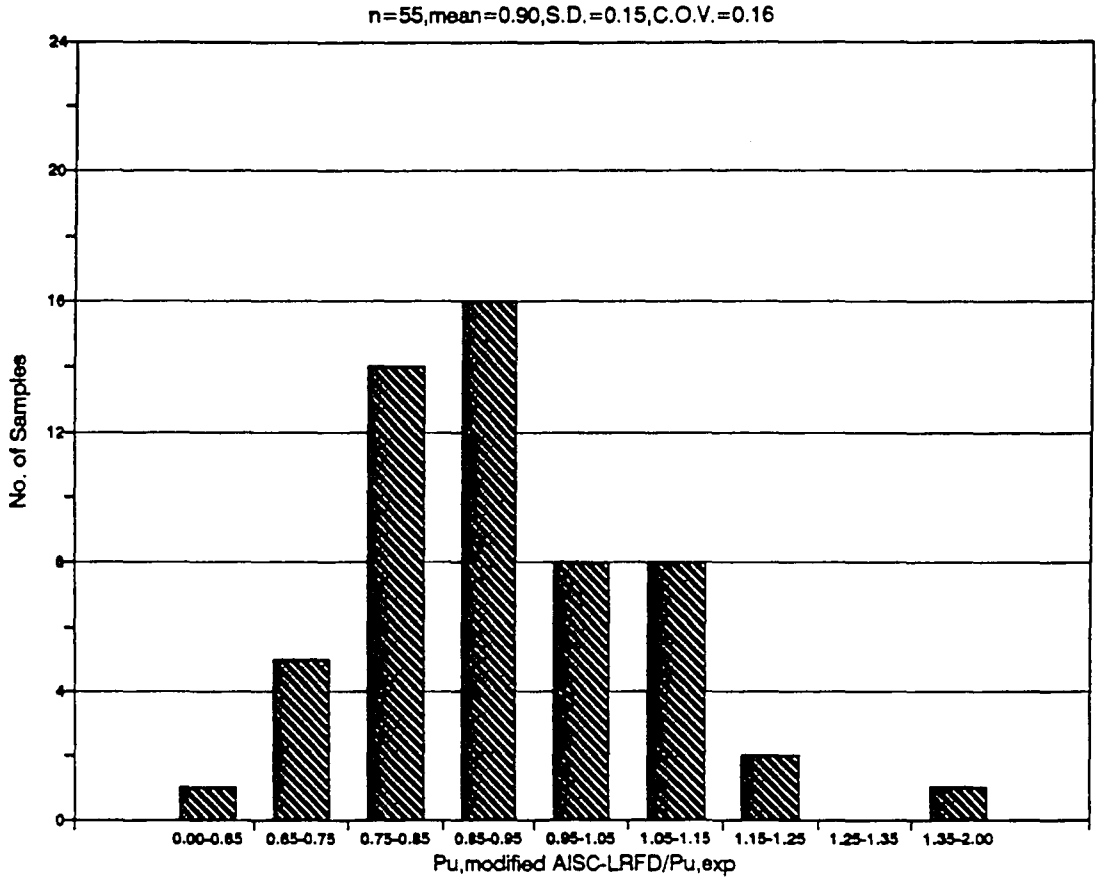

Figure 4-16 : Histogram of Predicted-to-Measured Ultimate Strength Ratio Using Modified AISC-LRFD Approach with Boswell and D' Mello's Reported Modular Ratio (n=55, mean=0.90, C.O.V.=0.16)

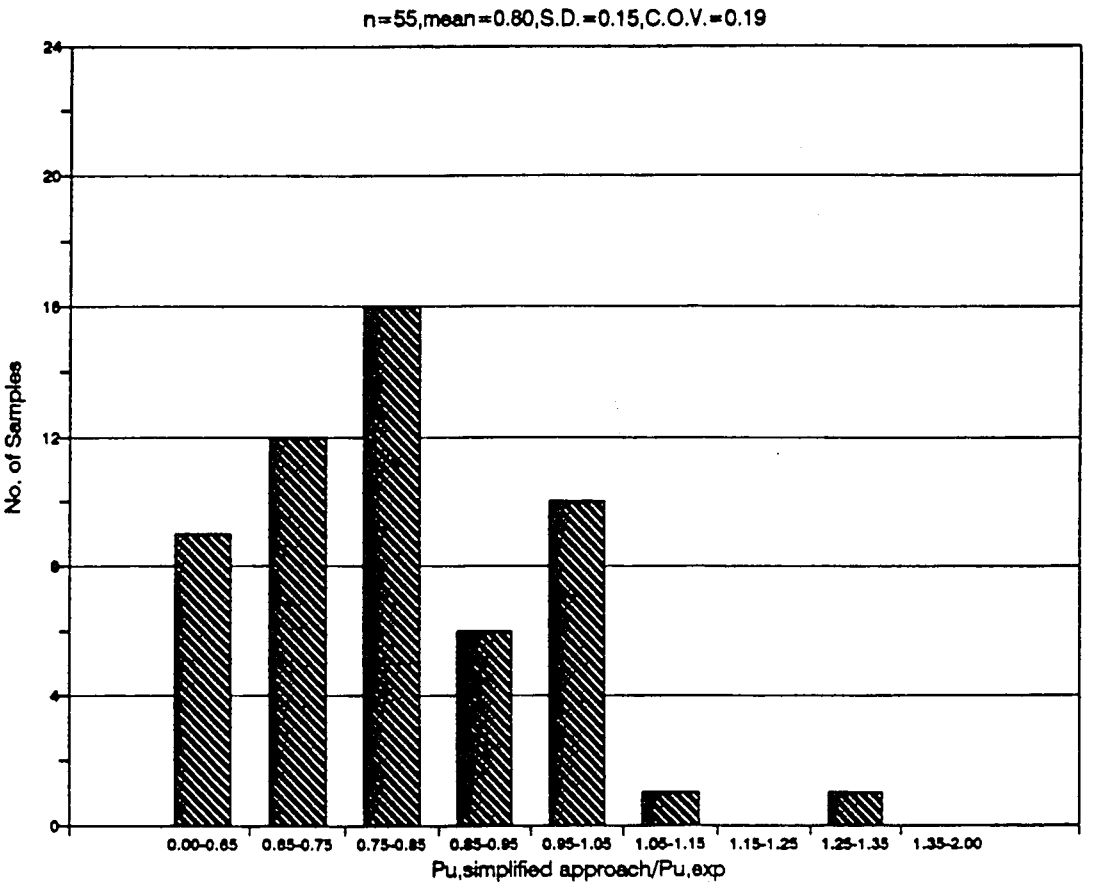

Figure 4-17 : Histogram of Predicted-to-Measured Ultimate Strength Ratio Using Simplified AISC-LRFD Approach with Boswell and D' Mello's Reported Modular Ratio (n=55, mean=0.80, C.O.V.=0.19)

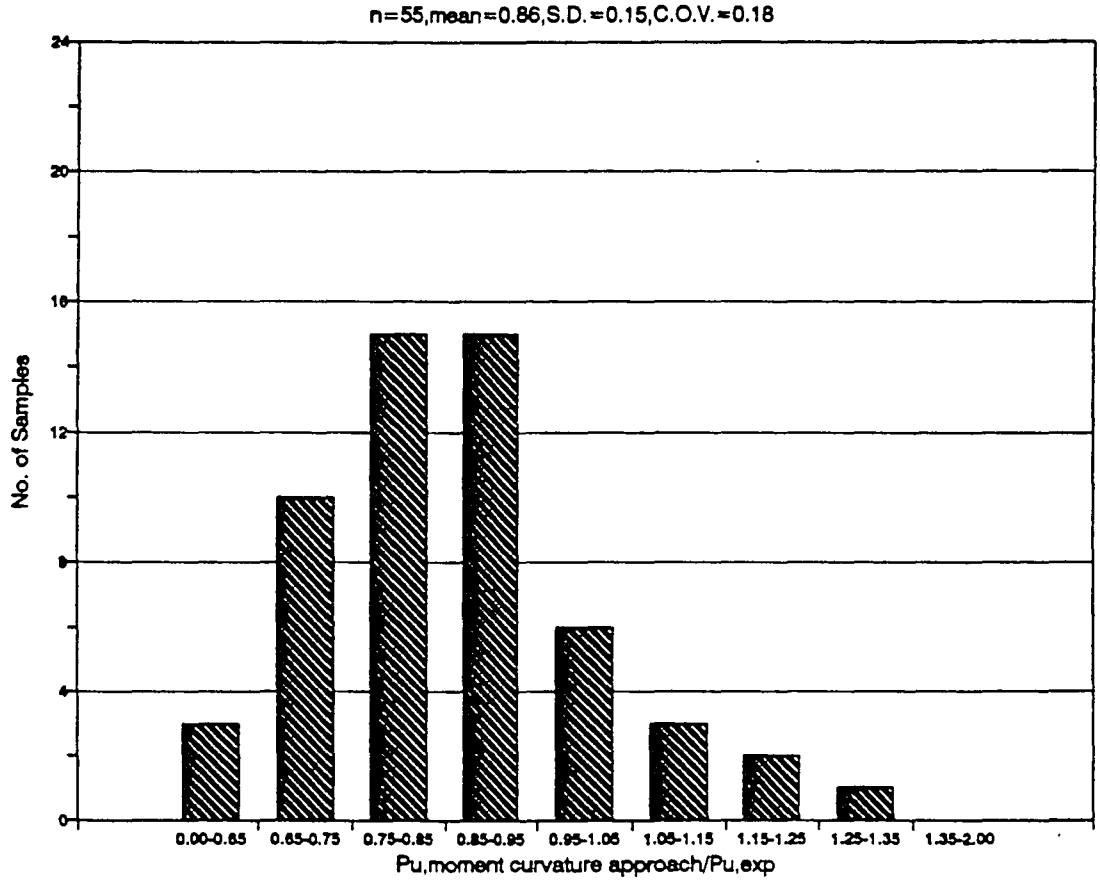

Figure 4-18 : Histogram of Predicted-to-Measured Ultimate Strength Ratio Using Moment Curvature Approach with Boswell and D' Mello's Reported Modular Ratio (n=55, mean=0.86, C.O.V.=0.18)

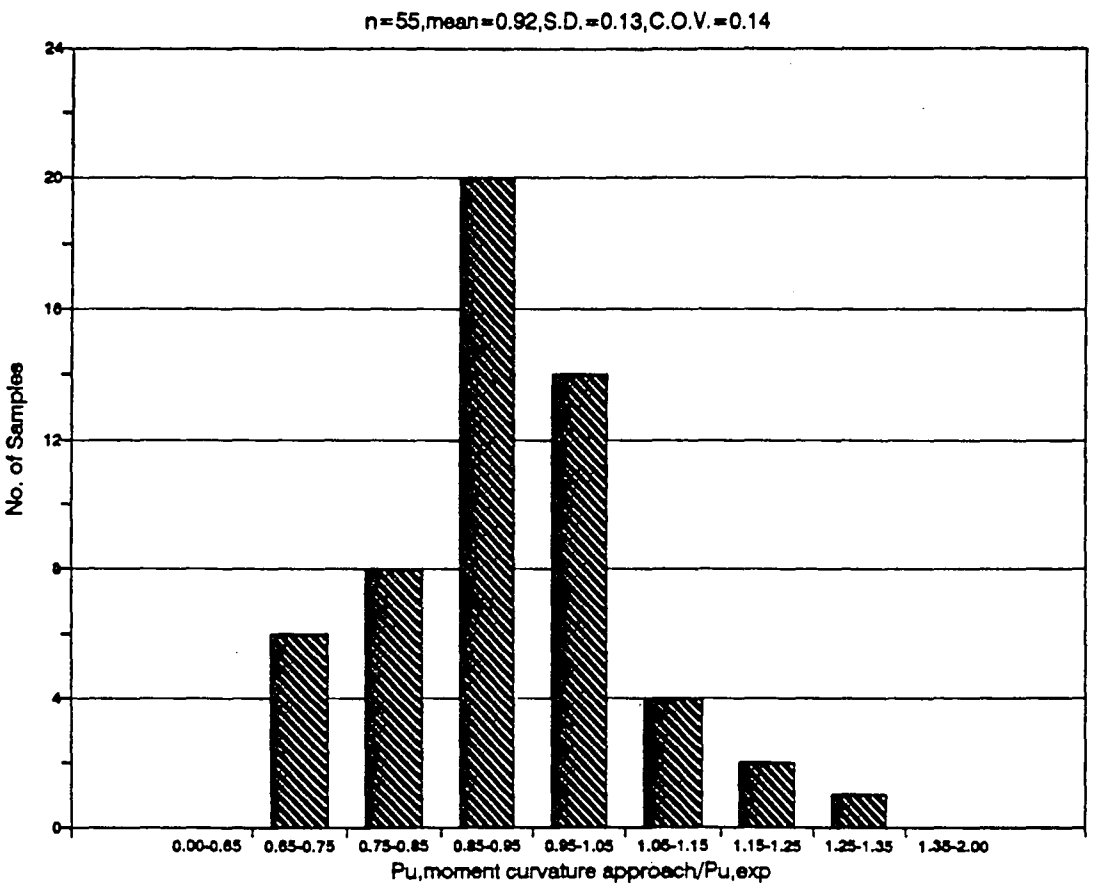

Figure 4-19 : Histogram of Predicted-to-Measured Ultimate Strength Ratio Using Moment Curvature Approach with Modified Modular Ratio, Boswell and D' Mello's Data

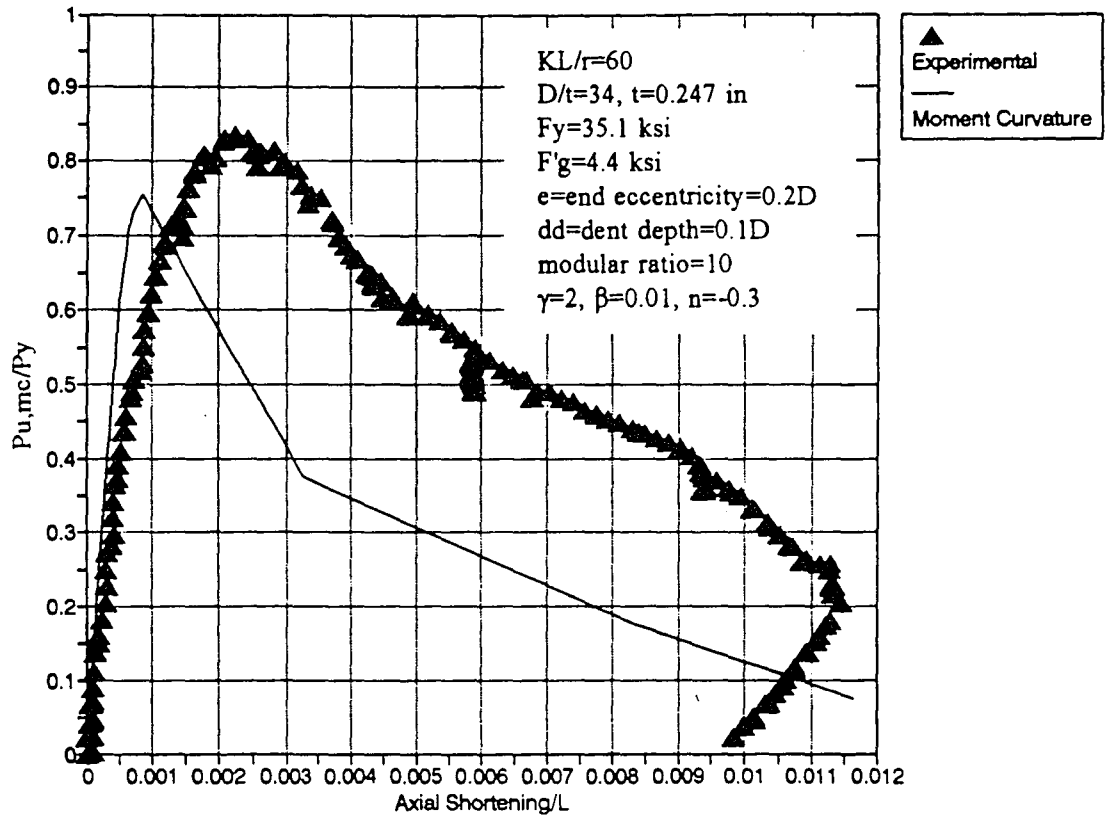

Figure 4-20(a) : Axial Compression-Shortening Response for Specimen A3 [Ricles and Gillum, 1992]

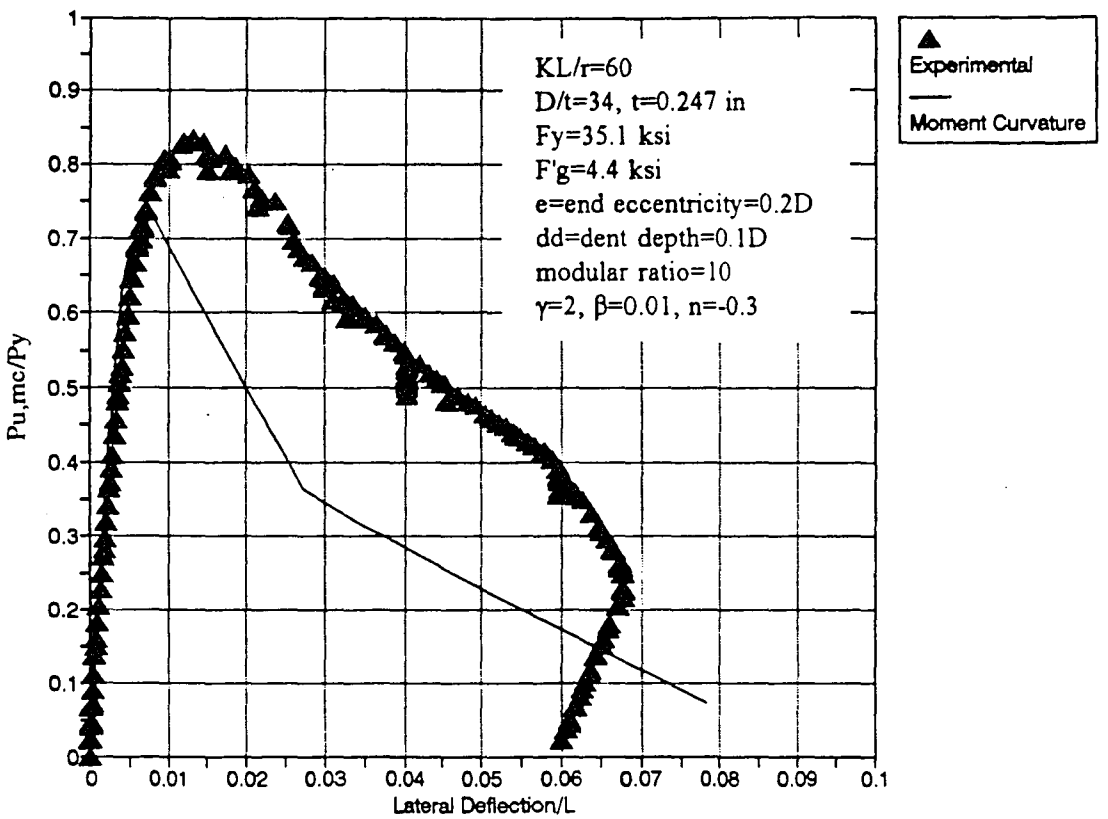

Figure 4-20(b) : Axial Compression-Lateral Deflection Response for Specimen A3 [Ricles and Gillum, 1992]

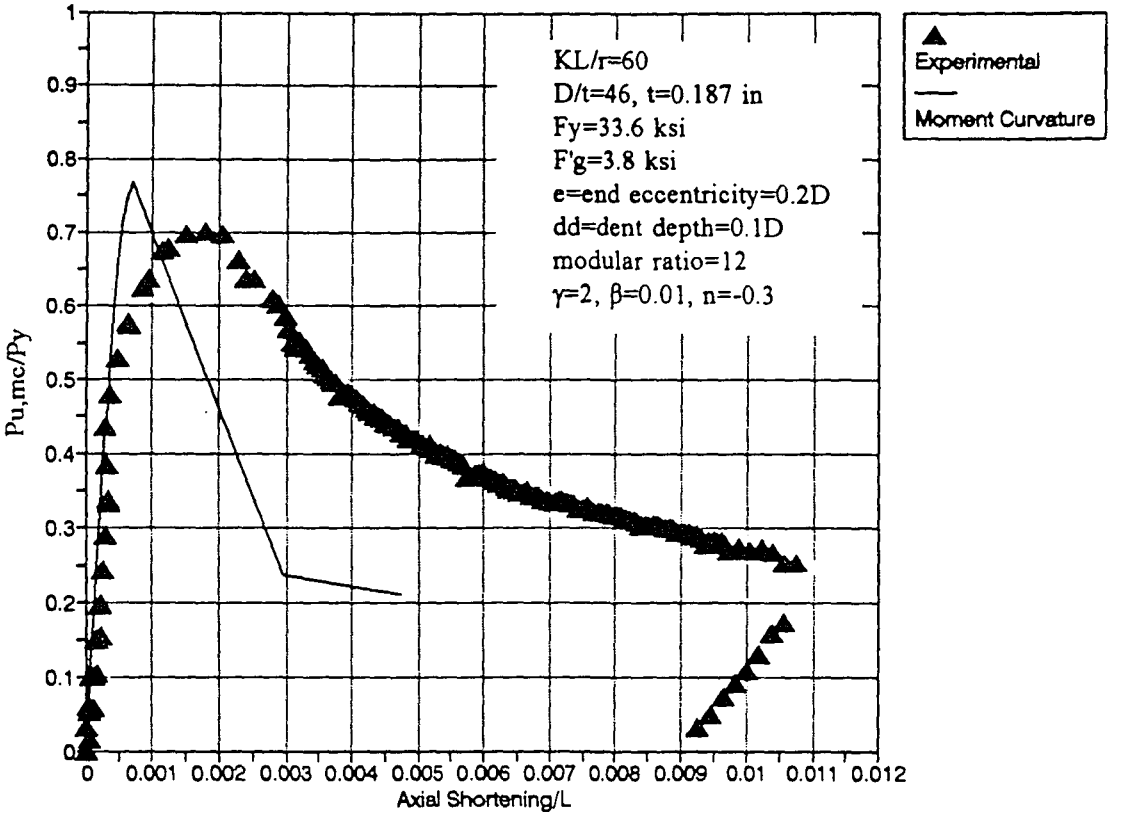

Figure 4-21(a) : Axial Compression-Shortening Response for Specimen B3 [Ricles and Gillum, 1992]

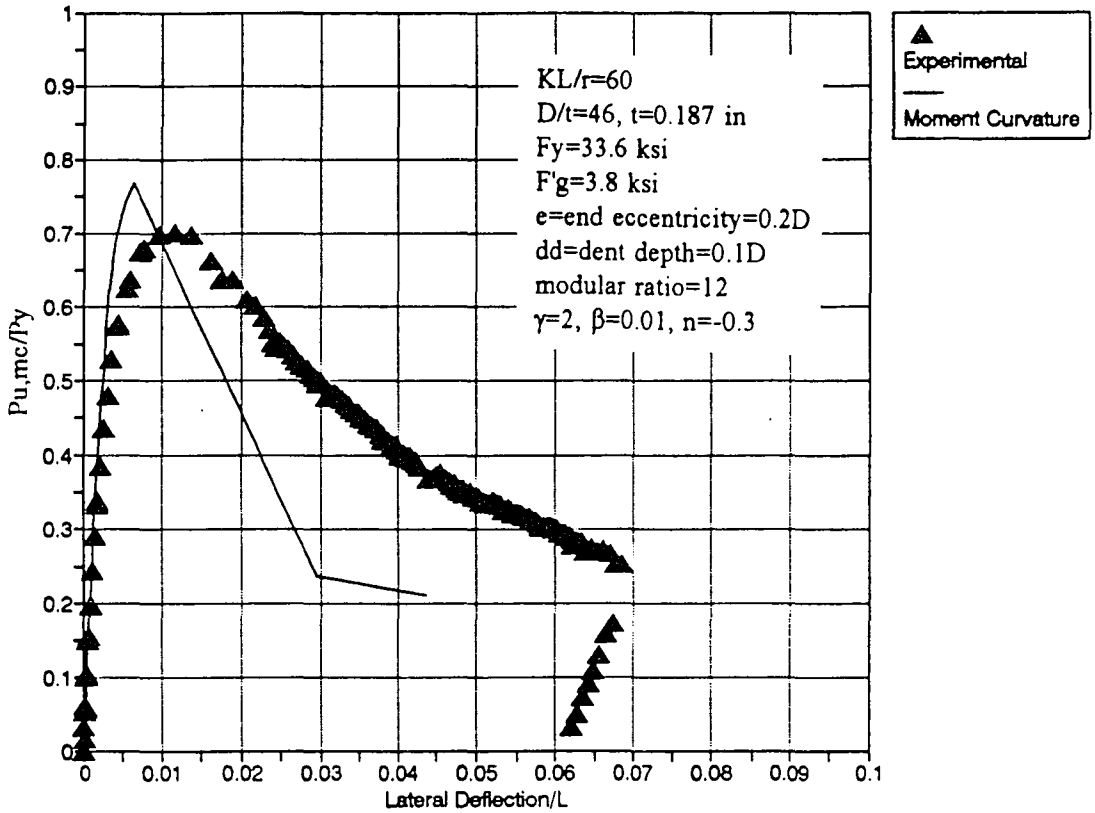

Figure 4-21(b) : Axial Compression-Lateral Deflection Response for Specimen B3 [Ricles and Gillum, 1992]

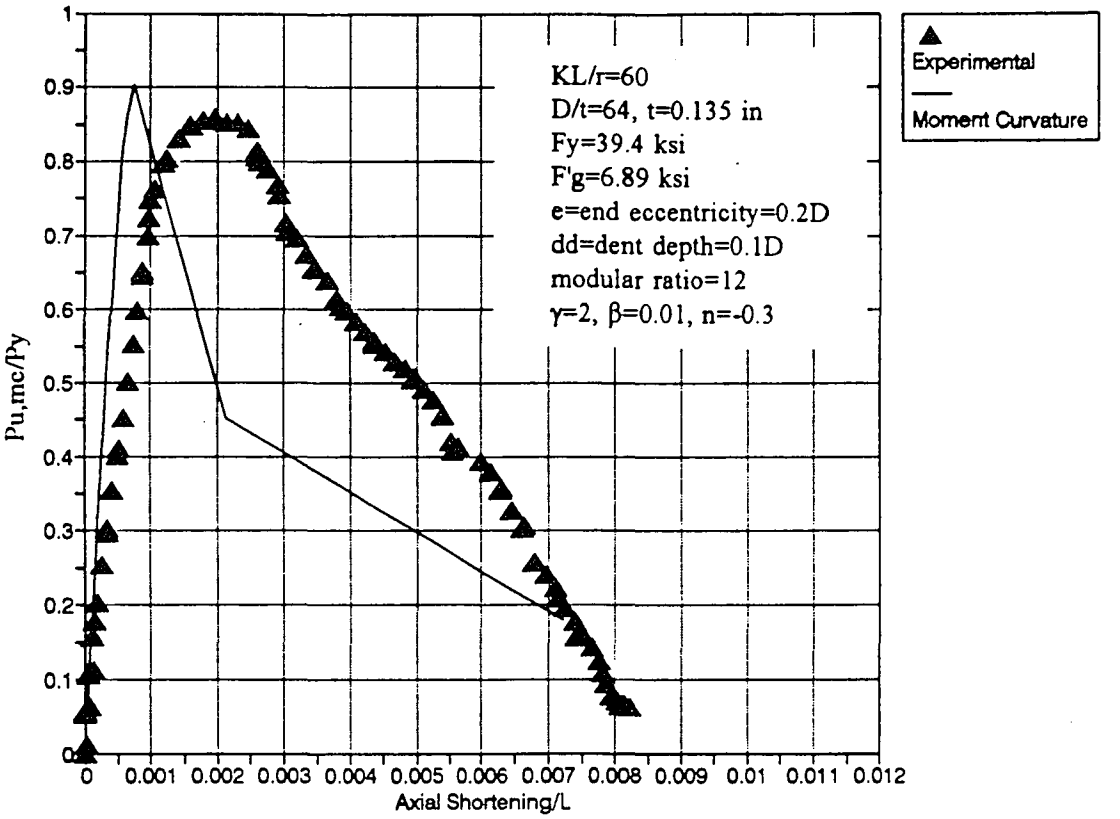

Figure 4-22(a) : Axial Compression-Shortening Response for Specimen C3 [Ricles and Gillum, 1992]

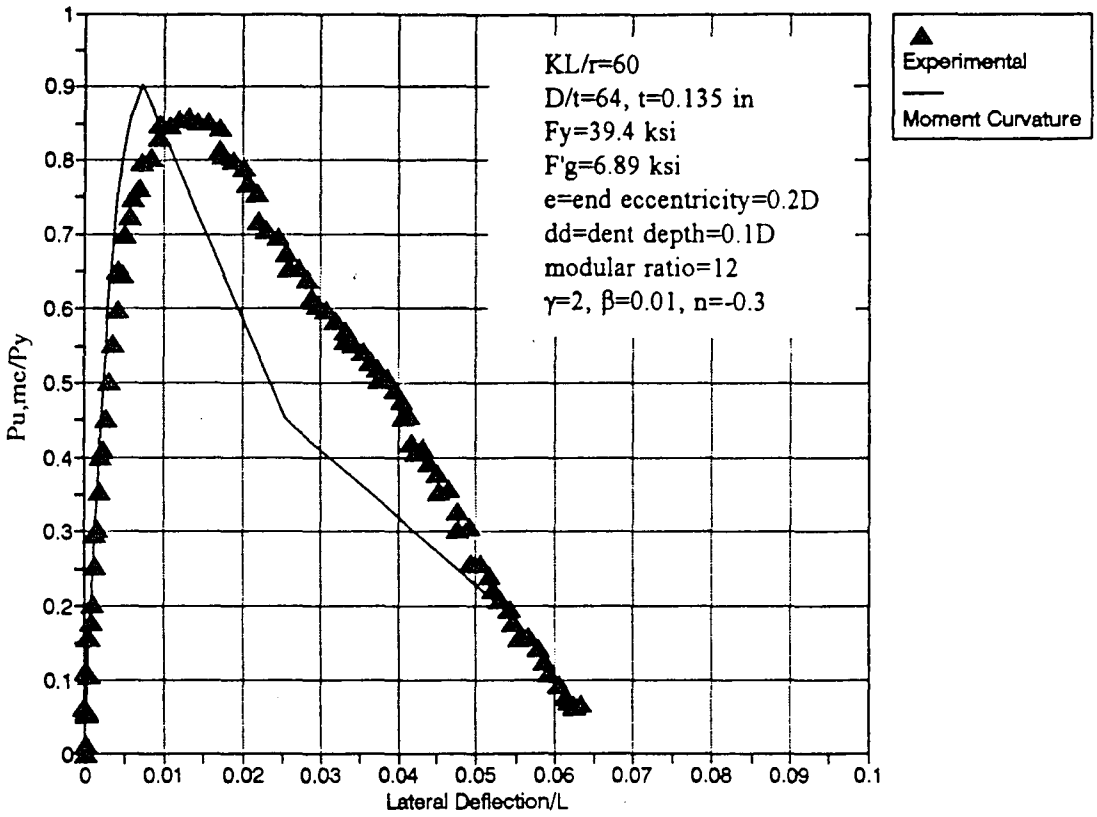

Figure 4-22(b) : Axial Compression-Lateral Deflection Response for Specimen C3 [Ricles and Gillum, 1992]

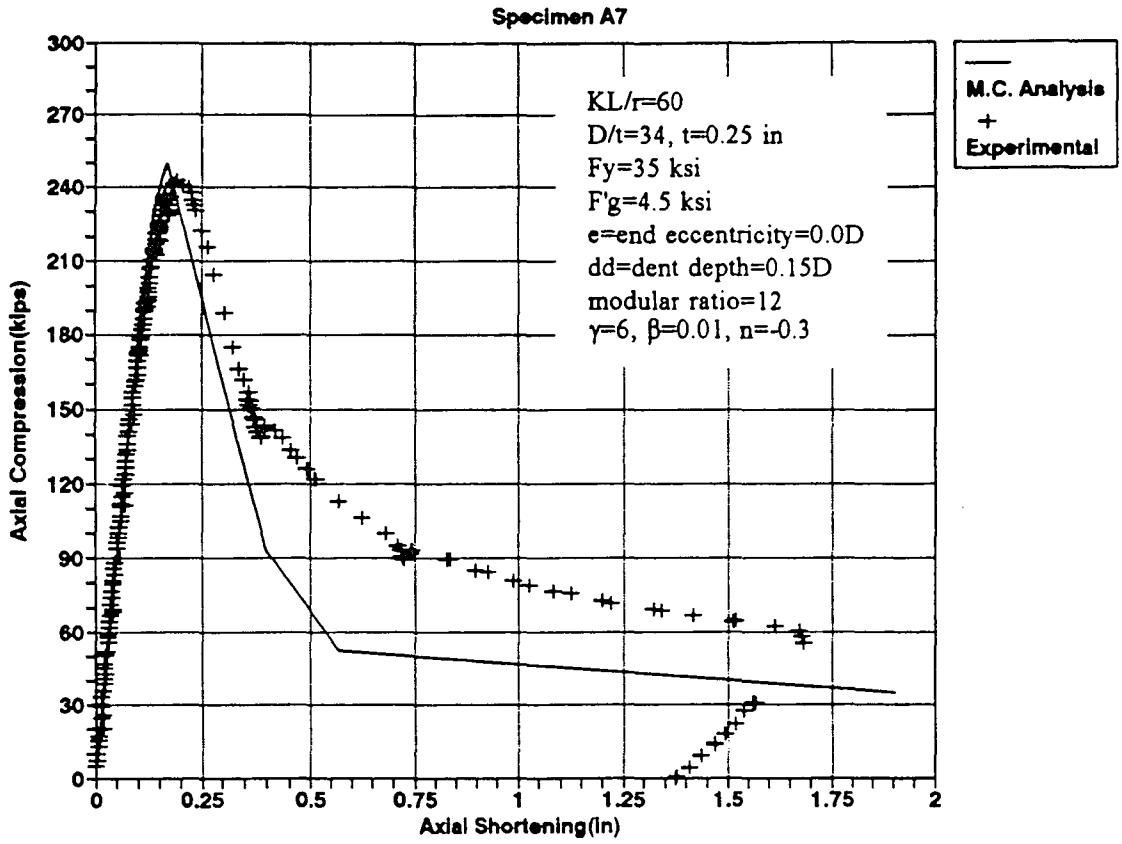

Figure 4-23(a) : Axial Compression-Shortening Response for Specimen A7

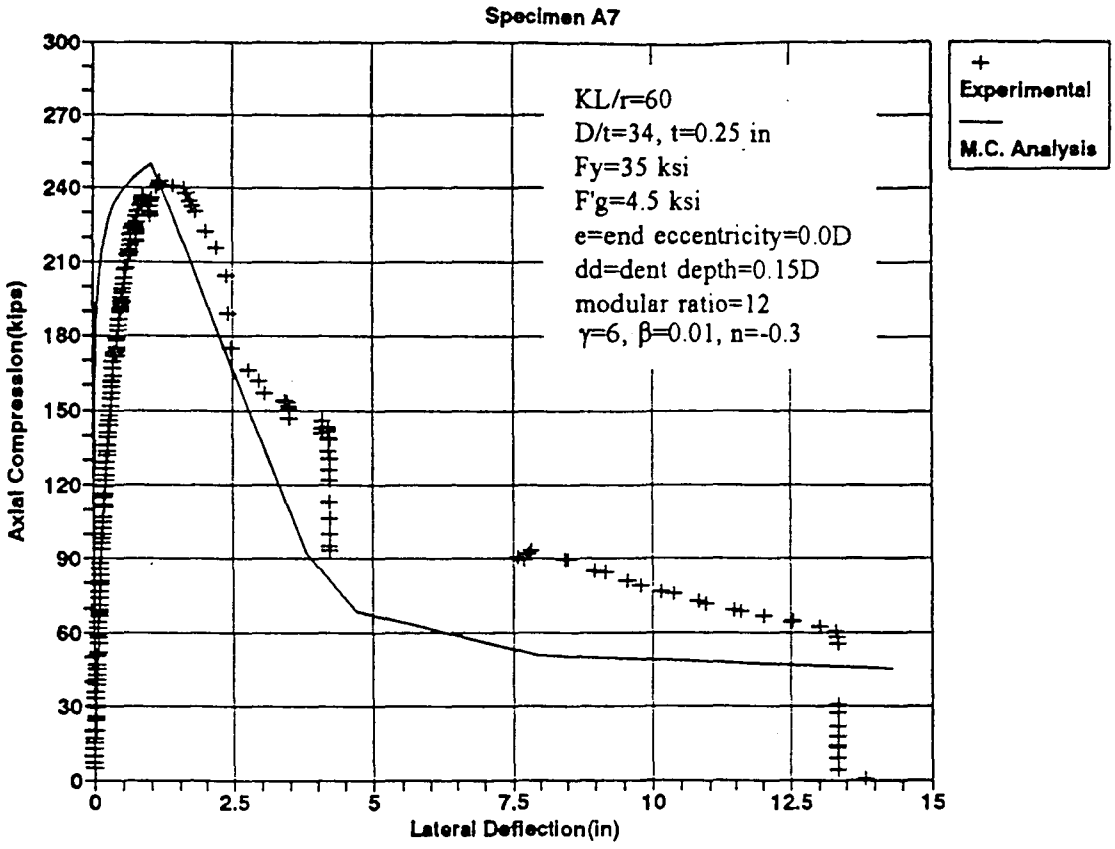

Figure 4-23(b) : Axial Compression-Lateral Deflection Response for Specimen A7

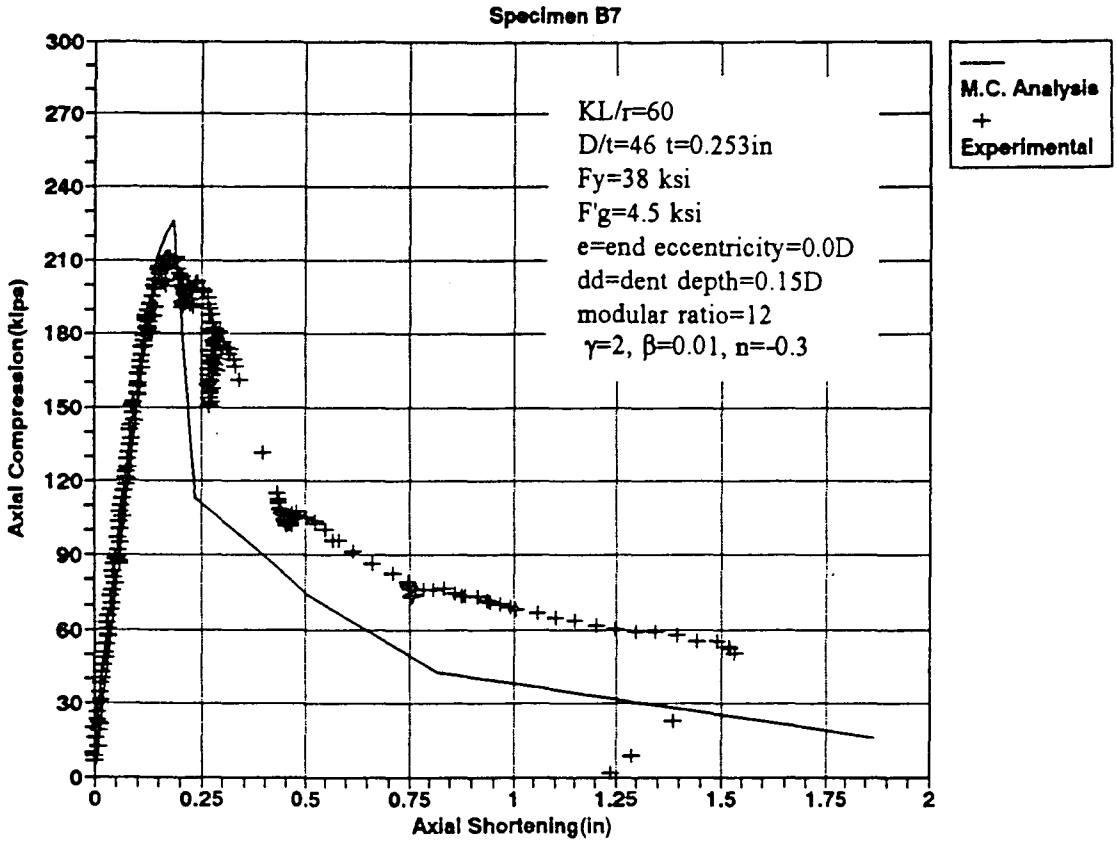

Figure 4-24(a) : Axial Compression-Shortening Response for Specimen B7

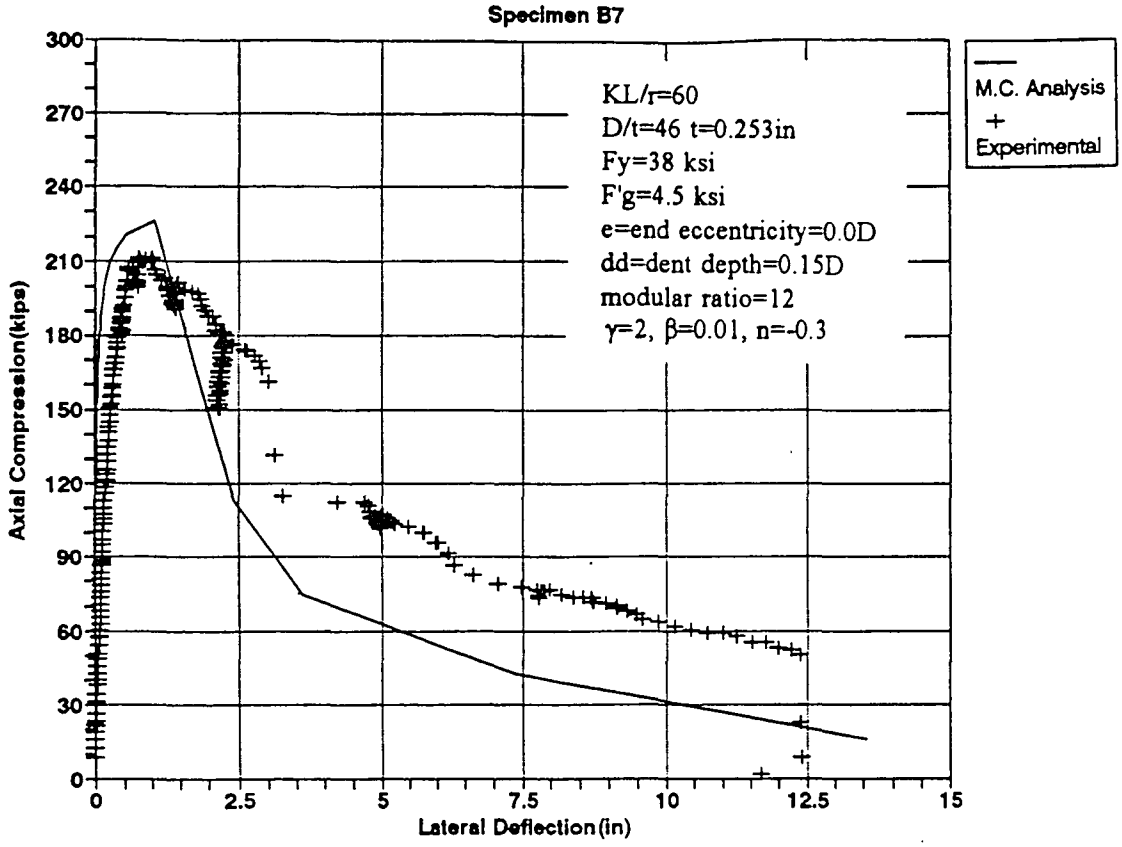

Figure 4-24(b) : Axial Compression-Lateral Deflection Response for Specimen B7

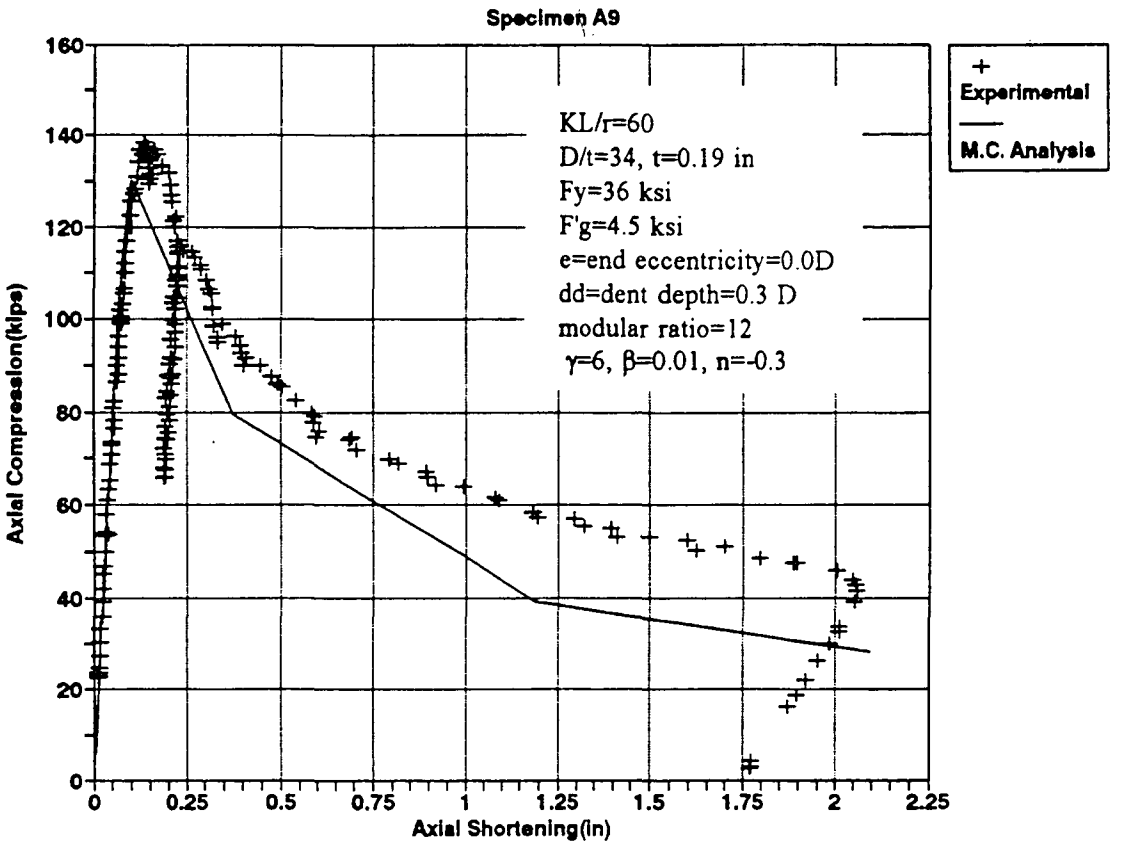

Figure 4-25(a) : Axial Compression-Shortening Response for Specimen A9

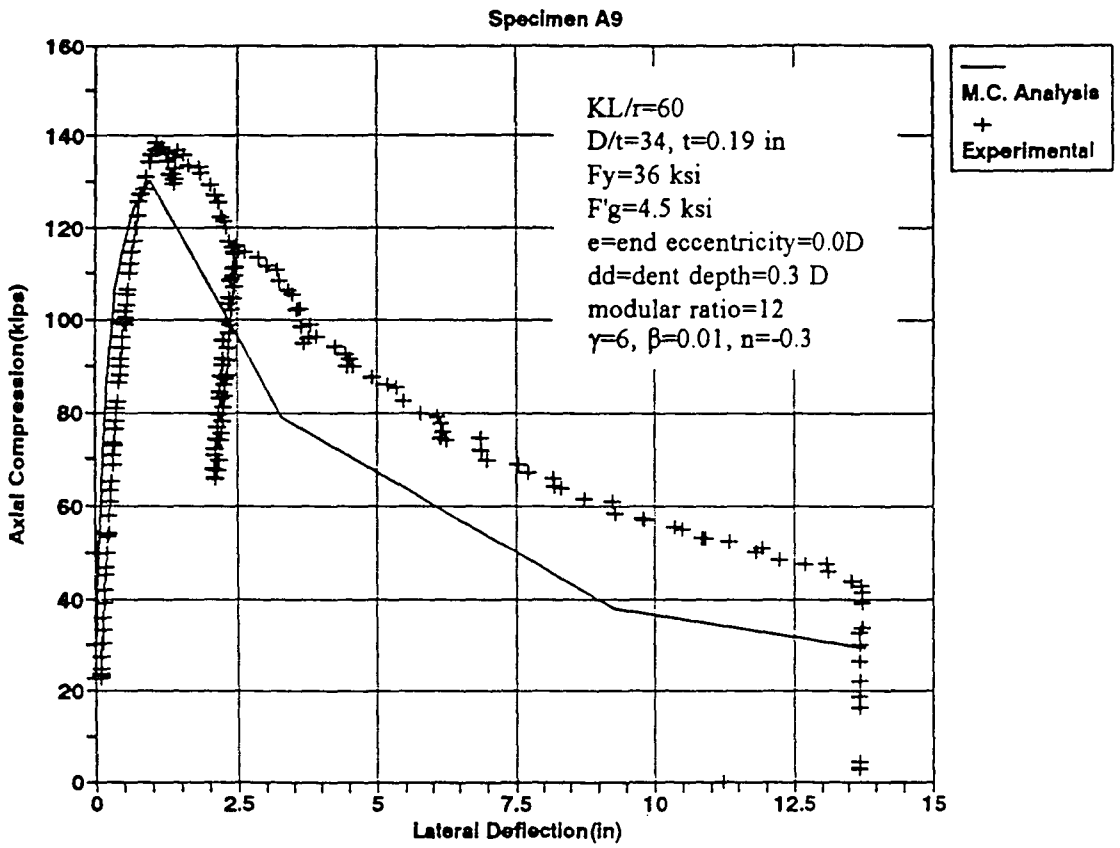

Figure 4-25(b) : Axial Compression-Lateral Deflection Response for Specimen A9

Specimen #1	
Max Compressive Grout Strain	0.00444
Max Tensile Steel Strain	0.00209
KL/r	28.66
D/t	72.07

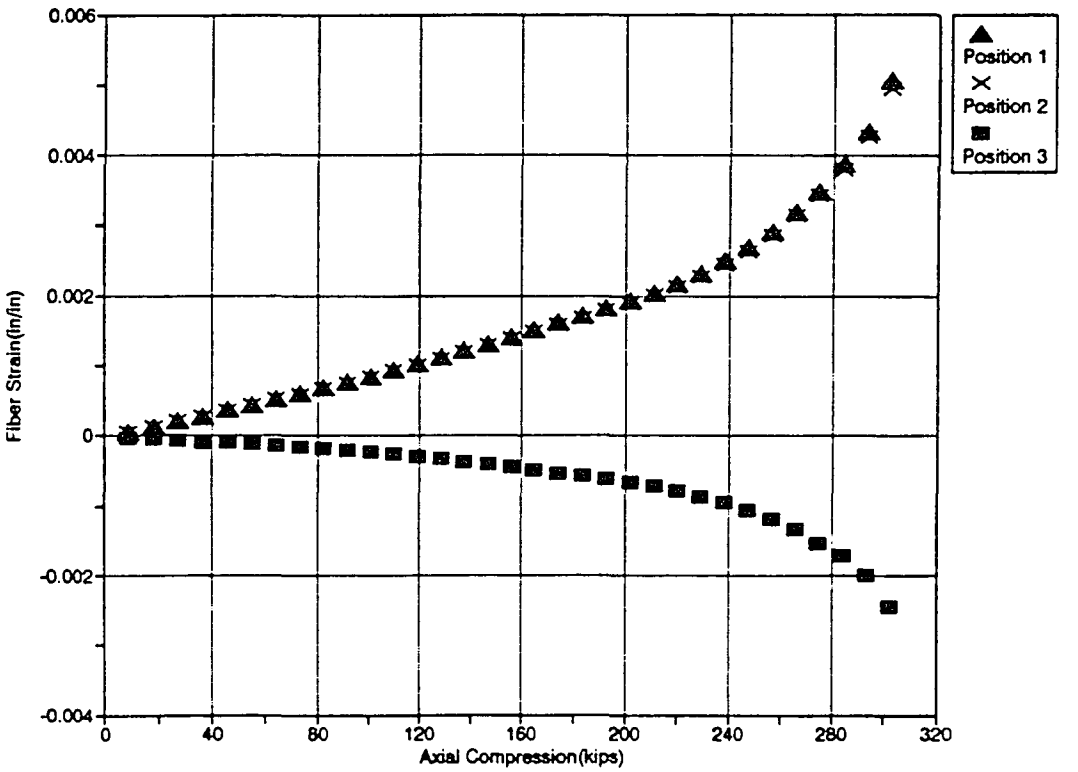

Position 1 = Top Extreme Fiber of Steel

Position 2 = Top Extreme Fiber of Grout

Position 3 = Bottom Extreme Fiber of Steel

Figure 4-26 : Fiber Strains at 3 Locations for Undamaged, Internally Grout Filled Specimen #1 [Tebbett and Forsyth, 1984]

Specimen #3	
Max Compressive Grout Strain	0.00445
Max Tensile Steel Strain	0.00202
KL/r	58.01
D/t	37.44

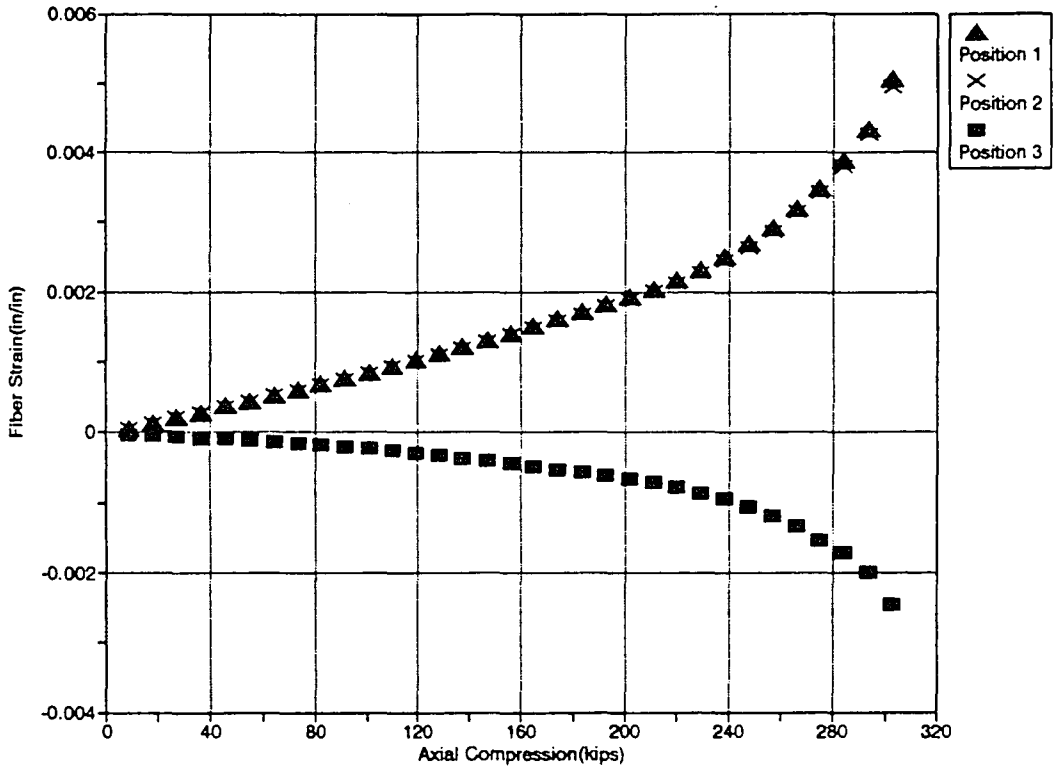

Position 1 = Top Extreme Fiber of Steel

Position 2 = Top Extreme Fiber of Grout

Position 3 = Bottom Extreme Fiber of Steel

Figure 4-27 : Fiber Strains at 3 Locations for Undamaged, Internally Grout Filled Specimen #3 [Tebbett and Forsyth, 1984]

Specimen #5	
Max Compressive Grout Strain	0.00444
Max Tensile Steel Strain	0.00244
KL/r	86.86
D/t	16.29

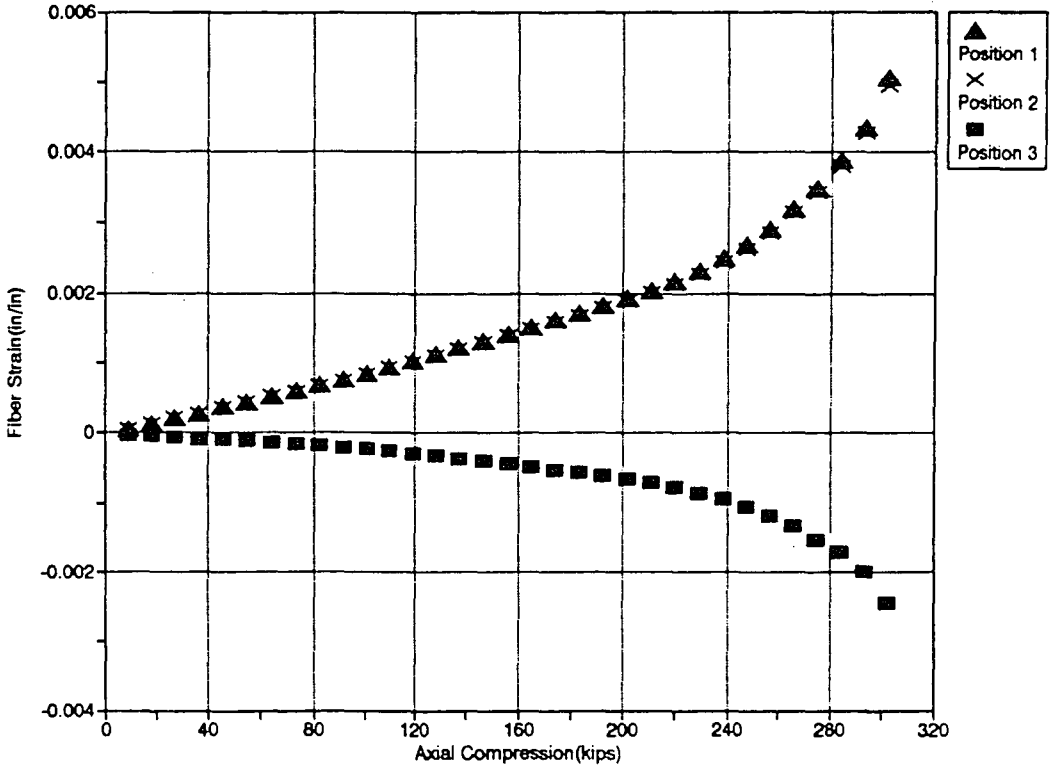

Position 1 = Top Extreme Fiber of Steel

Position 2 = Top Extreme Fiber of Grout

Position 3 = Bottom Extreme Fiber of Steel

Figure 4-28 : Fiber Strains at 3 Locations for Undamaged, Internally Grout Filled Specimen #5 [Tebbett and Forsyth, 1984]

Specimen A3	
Max Compressive Grout Strain	0.00301
Max Tensile Steel Strain	0.00120
KL/r	60
D/t	34

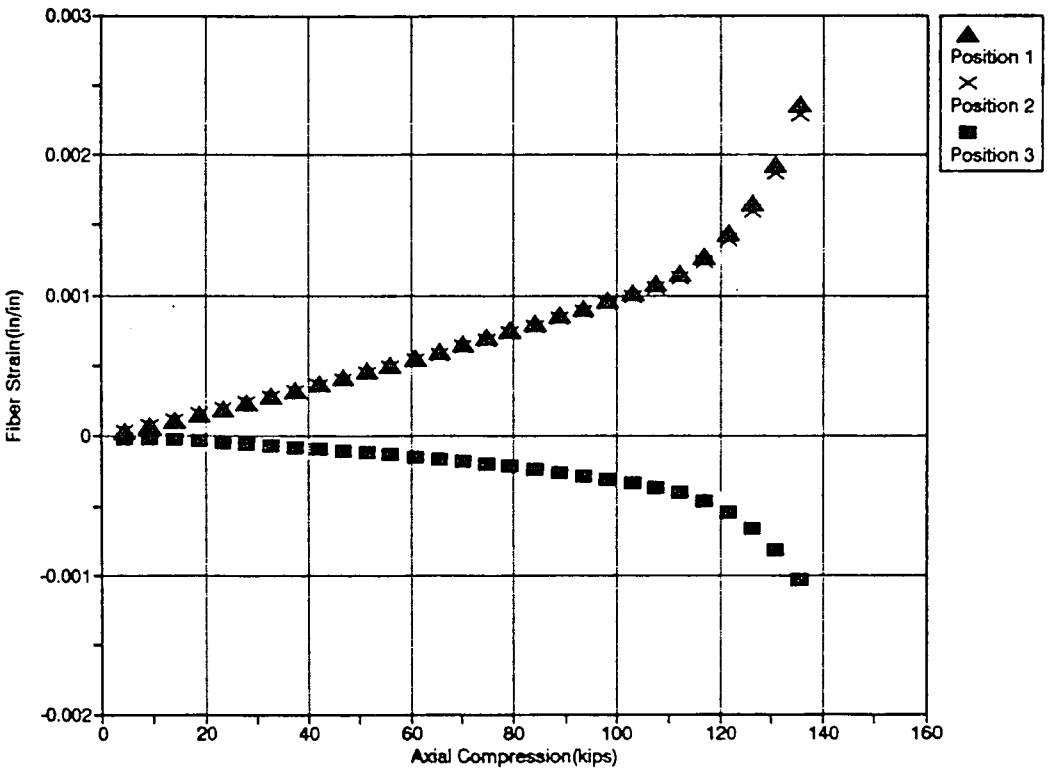

Position 1 = Top Extreme Fiber of Steel

Position 2 = Top Extreme Fiber of Grout

Position 3 = Bottom Extreme Fiber of Steel

Figure 4-29 : Fiber Strains at 3 Locations for Dent-Damaged, Internally Grout Repaired Specimen A3 [Ricles and Gillum, 1992]

Specimen B3	
Max Compressive Grout Strain	0.00303
Max Tensile Steel Strain	0.00115
KL/r	60
D/t	46

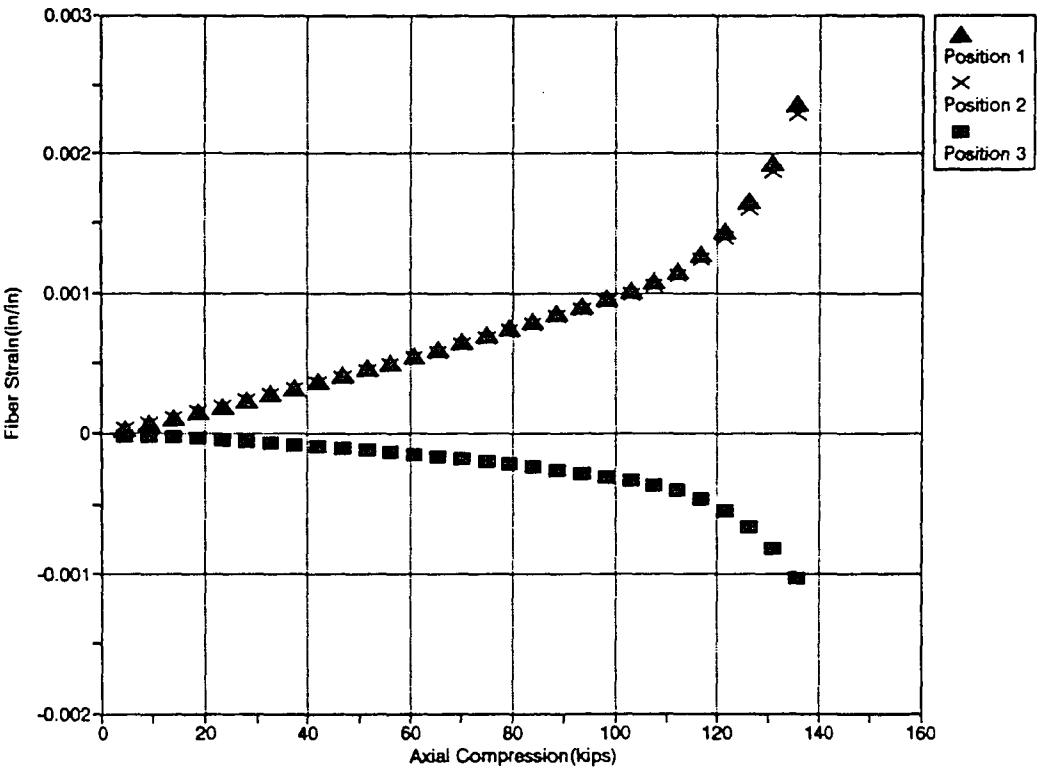

Position 1 = Top Extreme Fiber of Steel

Position 2 = Top Extreme Fiber of Grout

Position 3 = Bottom Extreme Fiber of Steel

Figure 4-30 : Fiber Strains at 3 Locations for Dent-Damaged, Internally Grout Repaired Specimen B3 [Ricles and Gillum, 1992]

Specimen C3	
Max Compressive Grout Strain	0.00540
Max Tensile Steel Strain	0.00136
KL/r	60
D/t	64

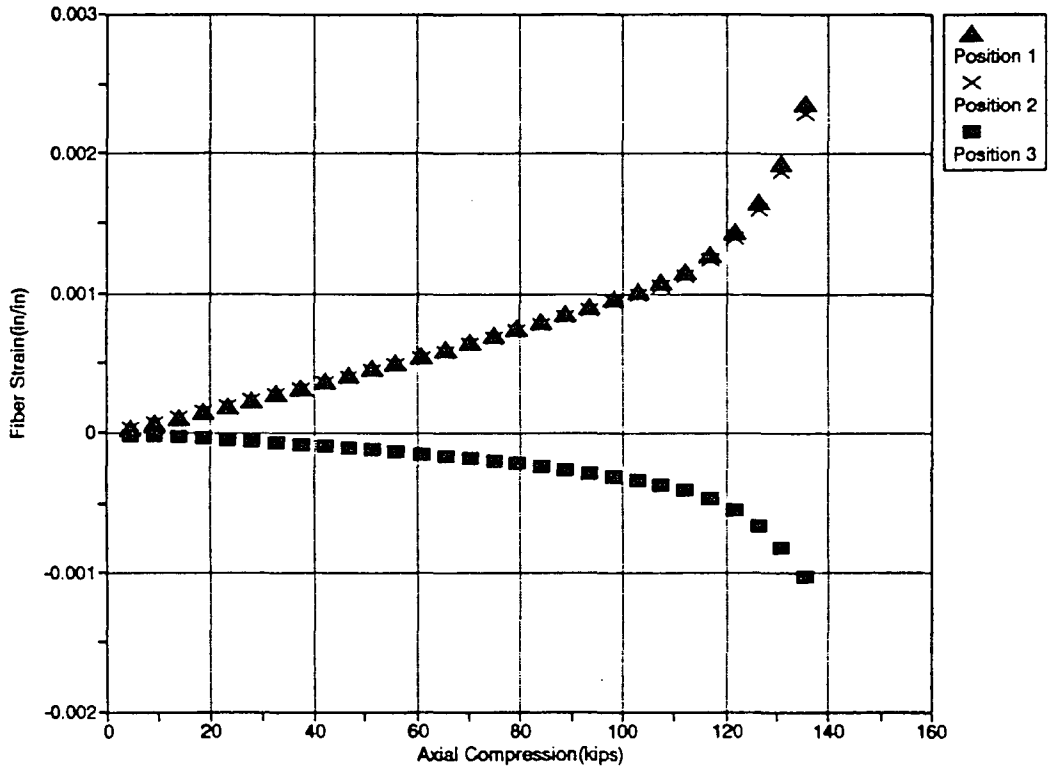

Position 1 = Top Extreme Fiber of Steel

Position 2 = Top Extreme Fiber of Grout

Position 3 = Bottom Extreme Fiber of Steel

Figure 4-31 : Fiber Strains at 3 Locations for Dent-Damaged, Internally Grout Repaired Specimen C3 [Ricles and Gillum, 1992]

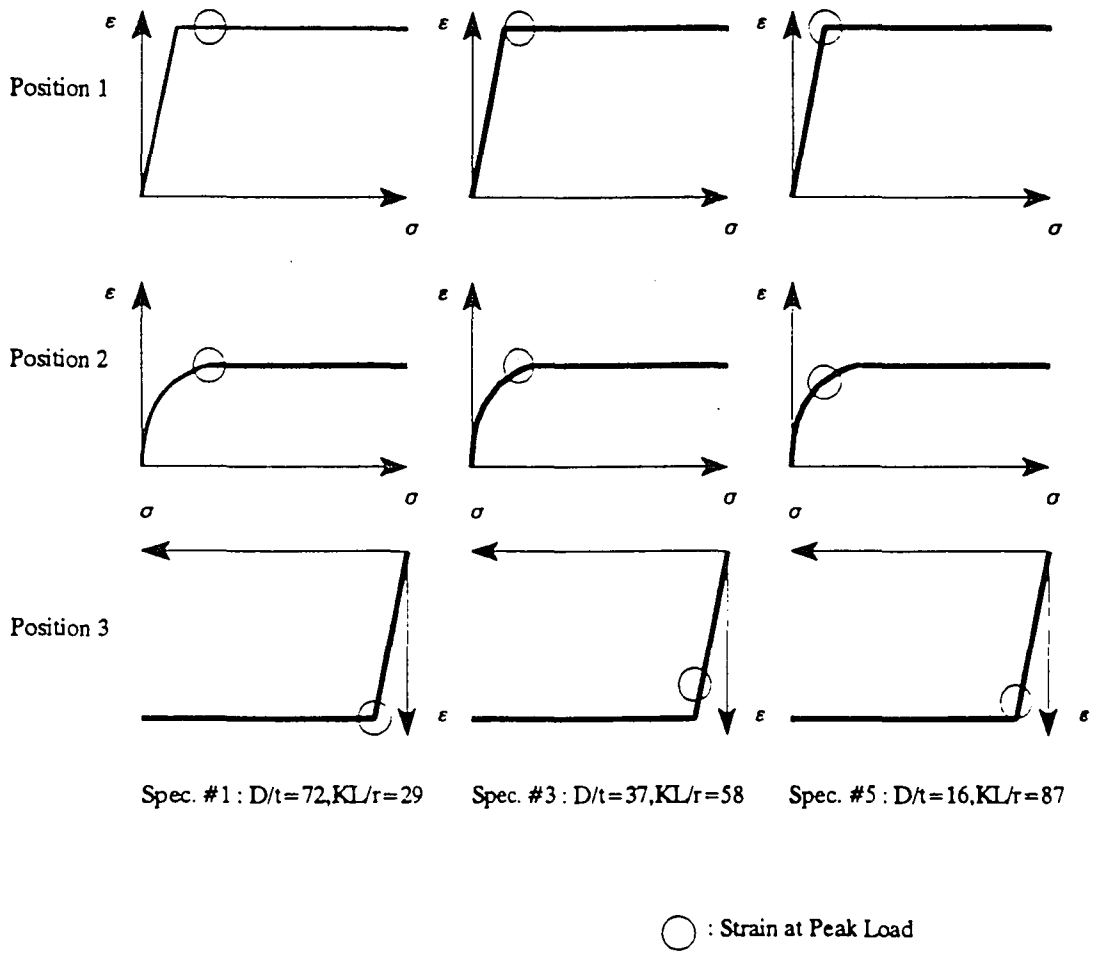

Figure 4-32 : Comparisons of Stress-Strain Histories at Three Locations for Specimen #1, #2, and #3 [Tebbett and Forsyth, 1984]

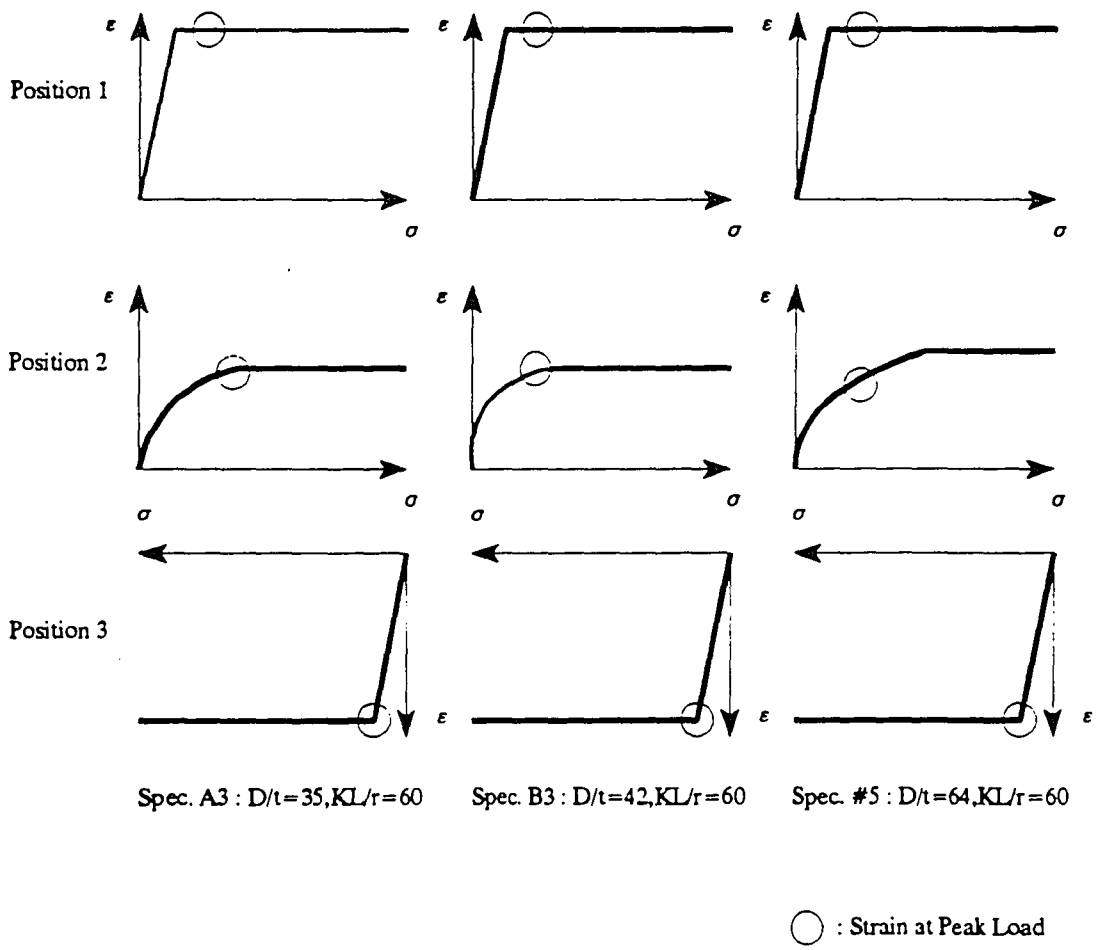

Figure 4-33 : Comparisons of Stress-Strain Histories at Three Locations for Specimen A3, B3, and C3 [Ricles and Gillum, 1992]

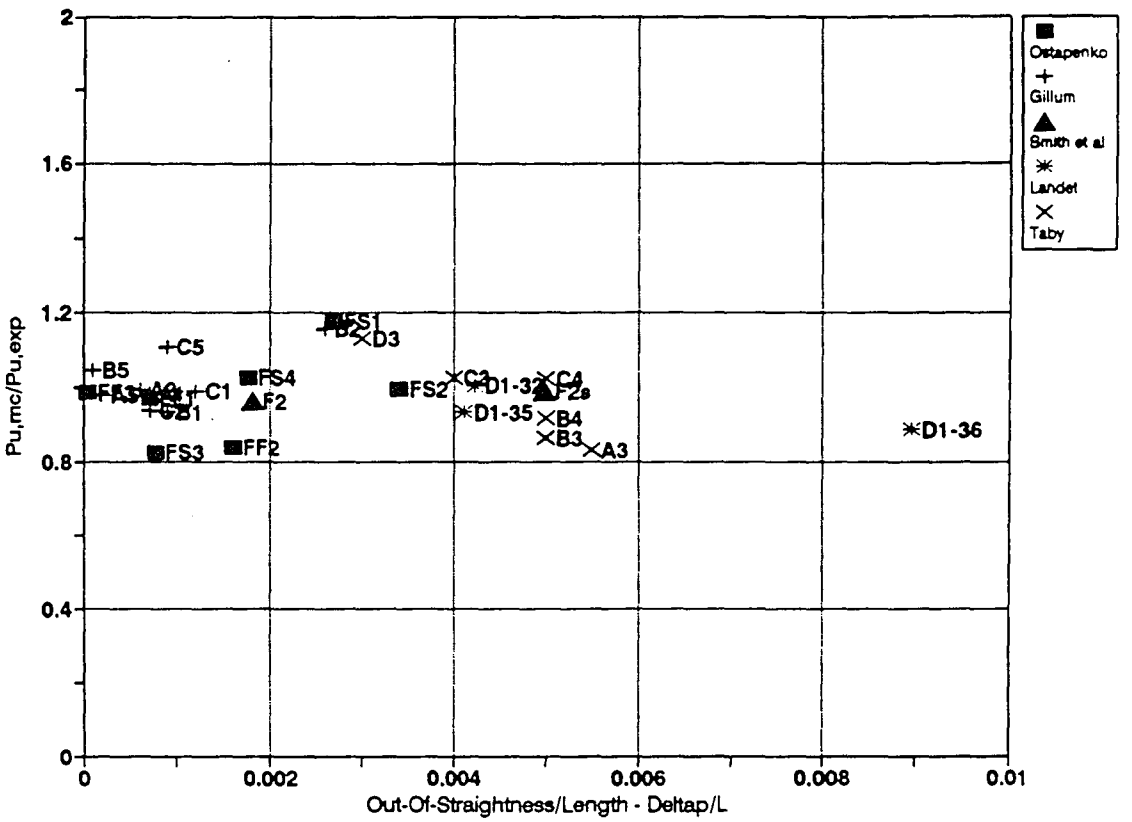

Figure 4-34 : Variations of Predicted-to-Measured Ultimate Strength (Pu,mc/Pu,exp) Ratio with Respect to Out-Of-Straightness-to-Length Ratio Using Moment Curvature Approacch (Unrepaired, Dented Specimens)

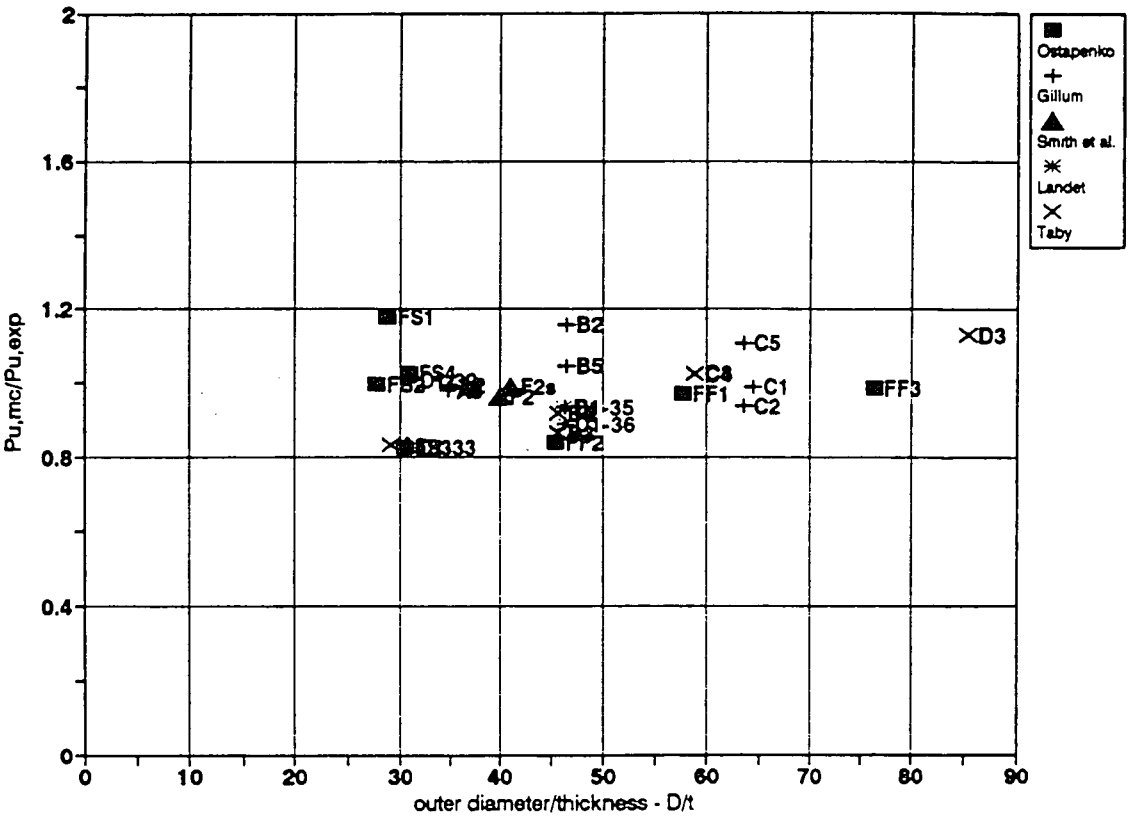

Figure 4-35 : Variations of Predicted-to-Measured Ultimate Strength (Pu,mc/Pu,exp) Ratio with Respect to Diameter-to-Thickness Ratio Using Moment Curvature Approacch (Unrepaired, Dented Specimens)

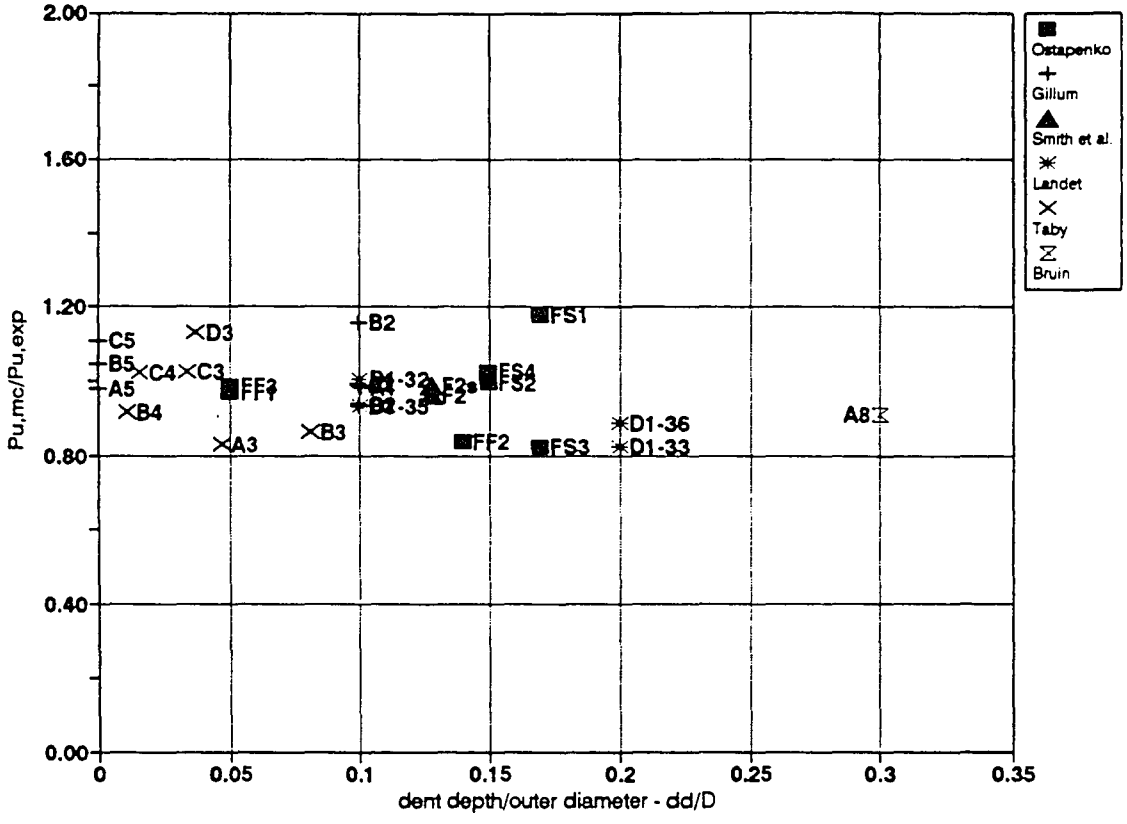

Figure 4-36 : Variations of Predicted-to-Measured Ultimate Strength (Pu,mc/Pu,exp) Ratio with Respect to Dent Depth-to-Diameter Ratio Using Moment Curvature Approacch (Unrepaired, Dented Specimens)

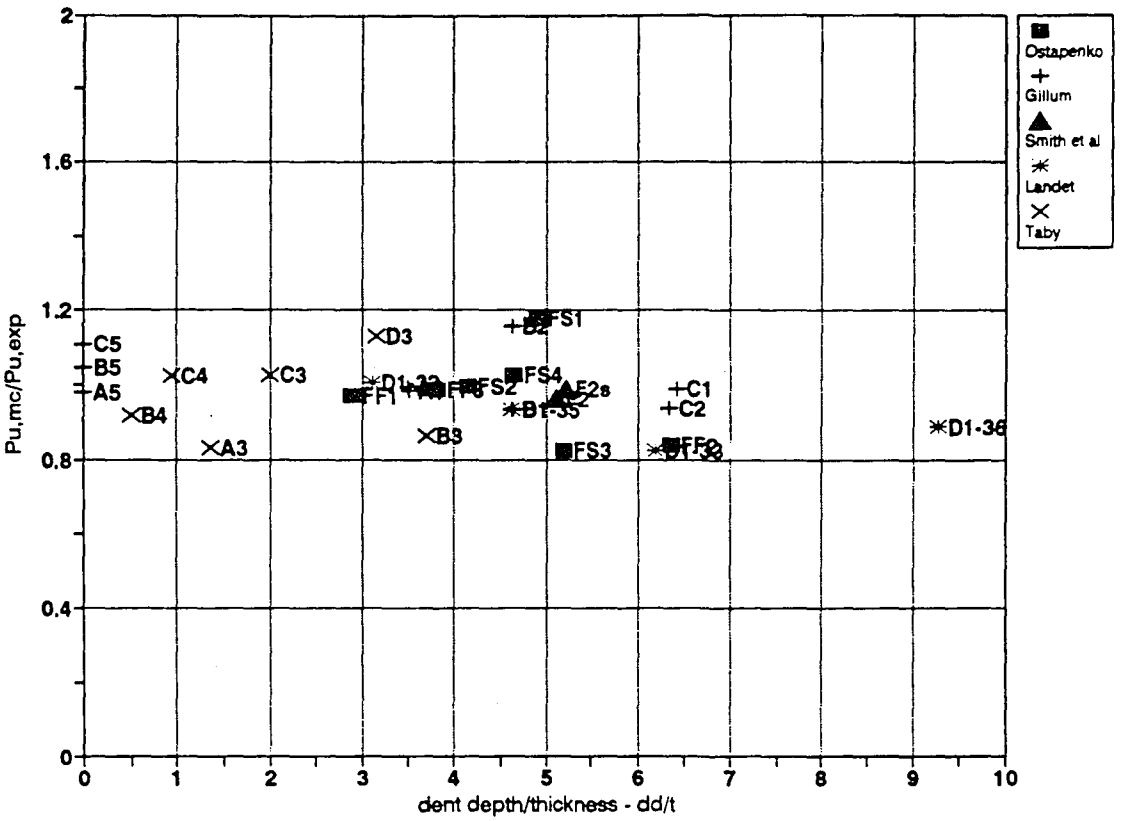

Figure 4-37 : Variations of Predicted-to-Measured Ultimate Strength (Pu,mc/Pu,exp) Ratio with Respect to Dent Depth-to-Thickness Ratio Using Moment Curvature Approacch (Unrepaired, Dented Specimens)

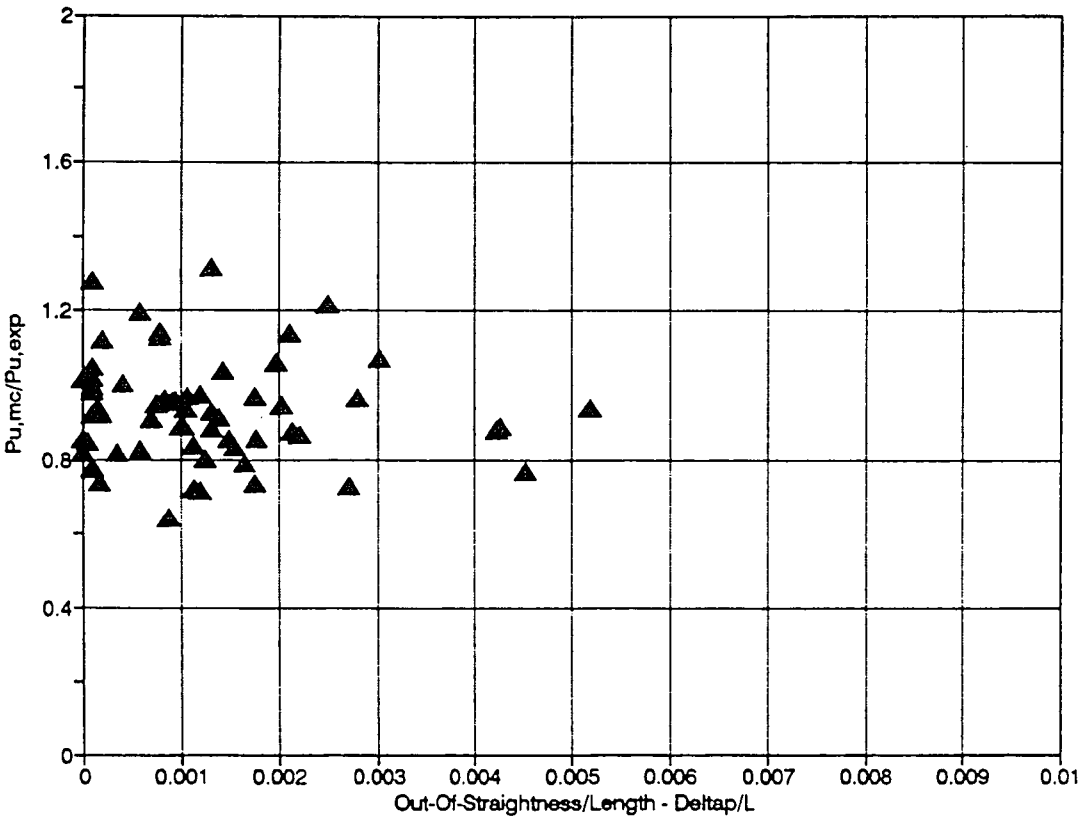

Figure 4-38 : Variations of Predicted-to-Measured Ultimate Strength (Pu,mc/Pu,exp) Ratio with Respect to Out-Of-Straightness-to-Length Ratio Using Moment Curvature Approacch (Internally Grout Repaired Specimens)

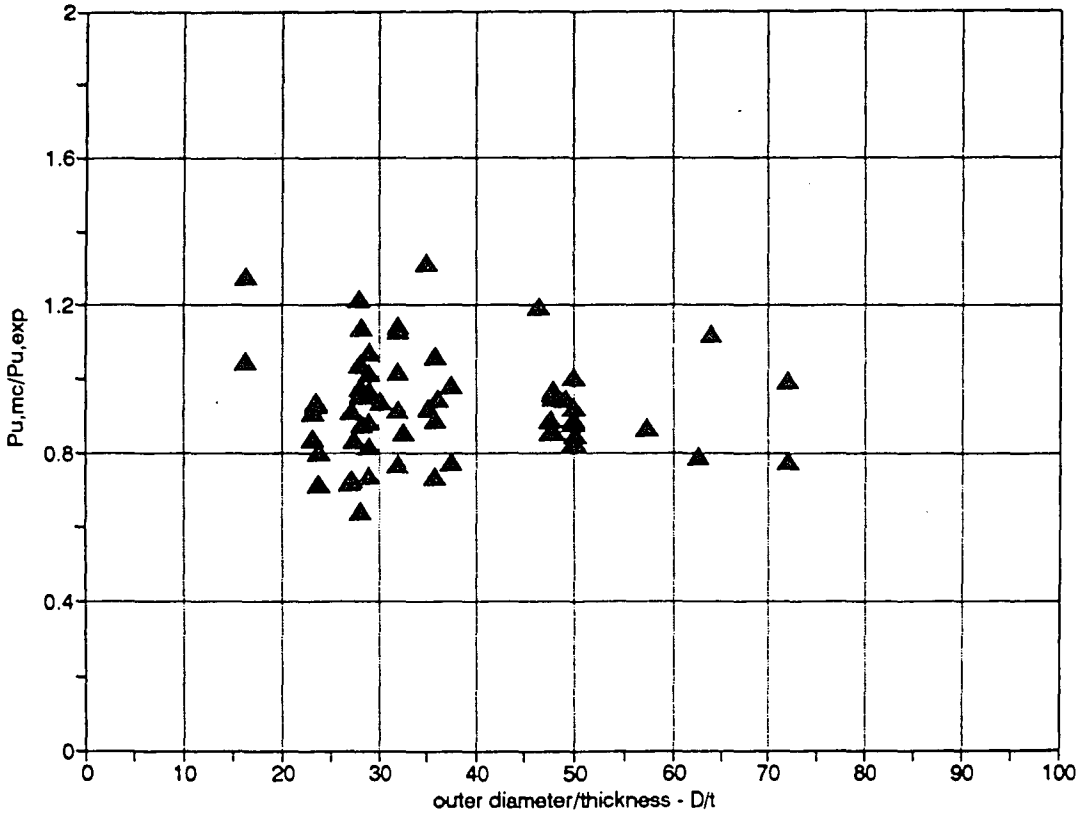

Figure 4-39 : Variations of Predicted-to-Measured Ultimate Strength (Pu,mc/Pu,exp) Ratio with Respect to Diameter-to-Thickness Ratio Using Moment Curvature Approacch (Internally Grout Repaired Specimens)

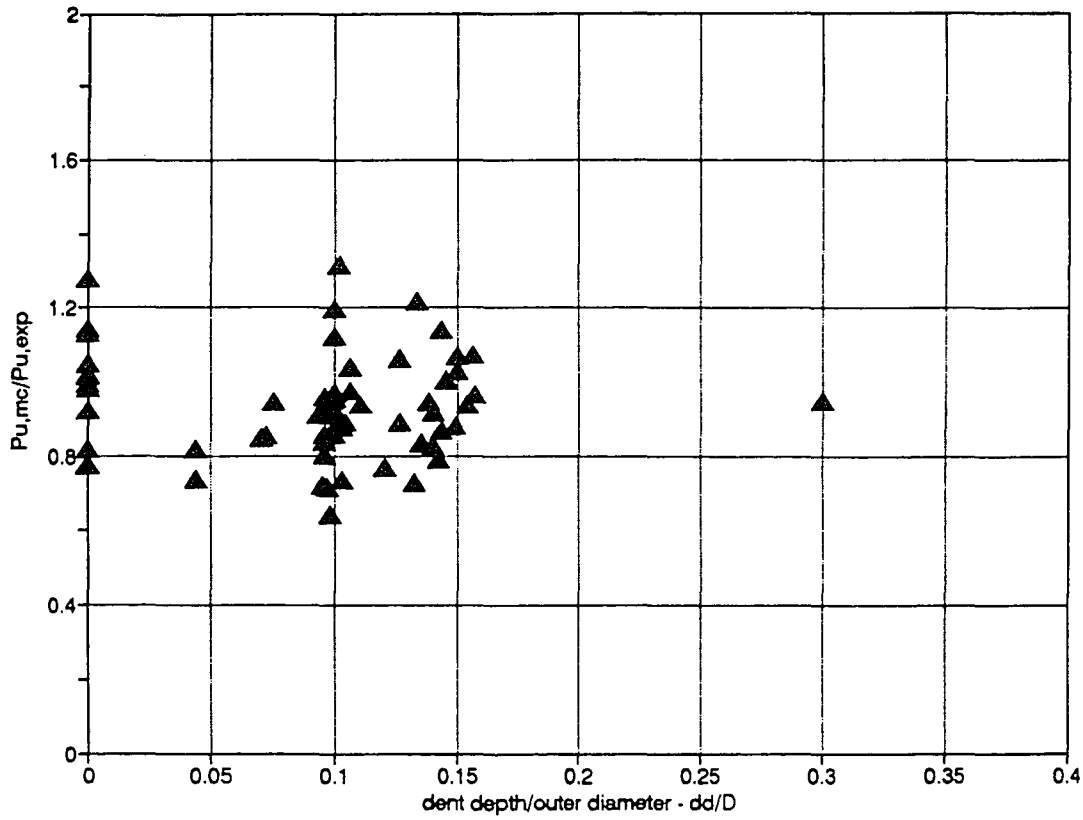

Figure 4-40 : Variations of Predicted-to-Measured Ultimate Strength (Pu,mc/Pu,exp) Ratio with Respect to Dent Depth-to-Diameter Ratio Using Moment Curvature Approacch (Internally Grout Repaired Specimens)

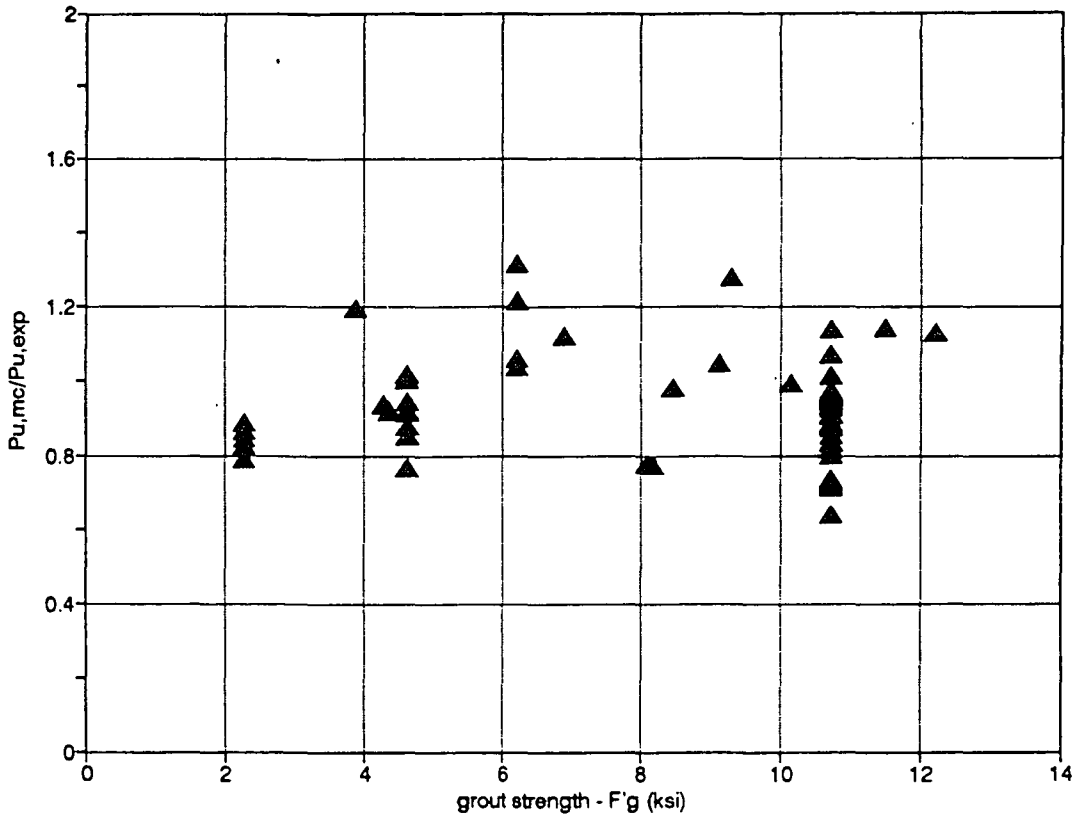

Figure 4-41 : Variations of Predicted-to-Measured Ultimate Strength (Pu,mc/Pu,exp) Ratio with Respect to Grout Strength Using Moment Curvature Approacch (Internally Grout Repaired Specimens)

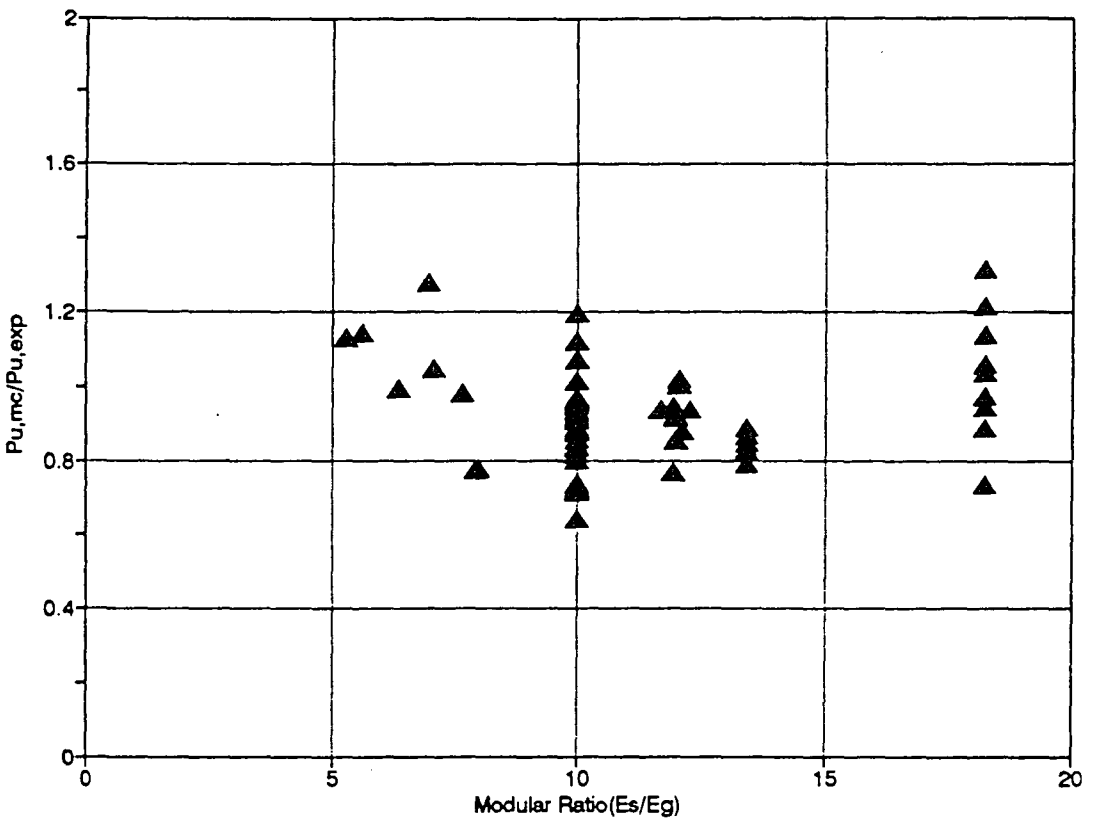

Figure 4-42 : Variations of Predicted-to-Measured Ultimate Strength (Pu,mc/Pu,exp) Ratio with Respect to Modular Ratio Using Moment Curvature Approacch (Internally Grout Repaired Specimens)

Dented Segment Length	Ld=(2D)(0.25*PI*DD/T)	2D	D	0.5D
(in)	28.6	17.248	6.624	4.312
Pu,acp/Py=0.397	Pu,mc/Py=0.400	Pu,mc/Py=0.405	Pu,mc/Py=0.410	Pu,mc/Py=0.415

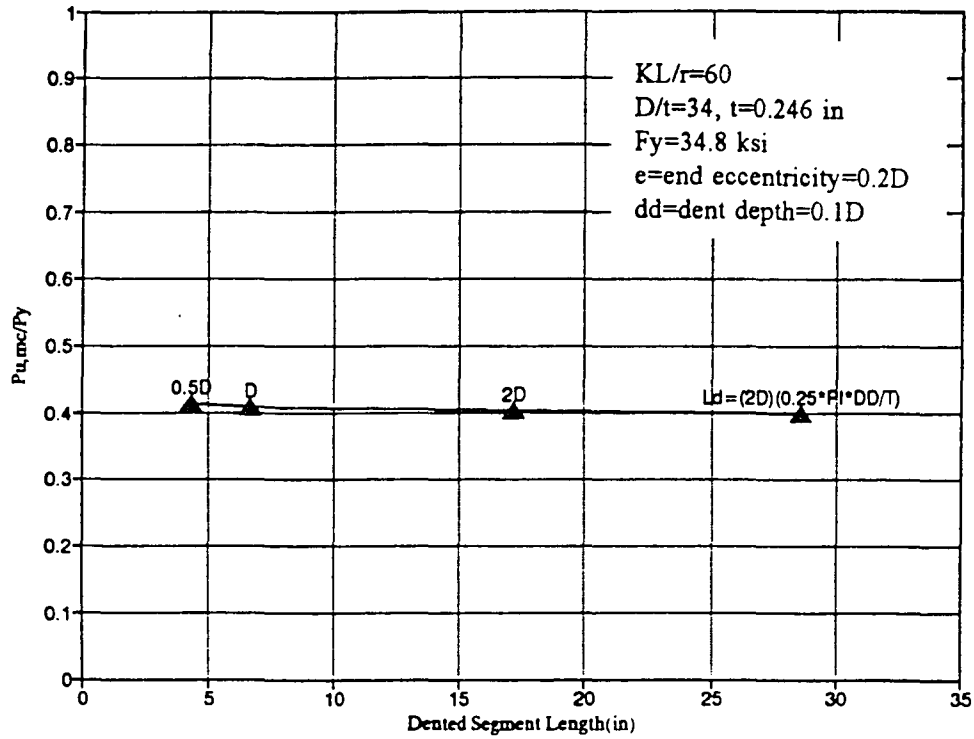

Figure 4-43 : Effects of the Model's Dented Segment Length on the Residual Strength Prediction Using Moment Curvature Approach

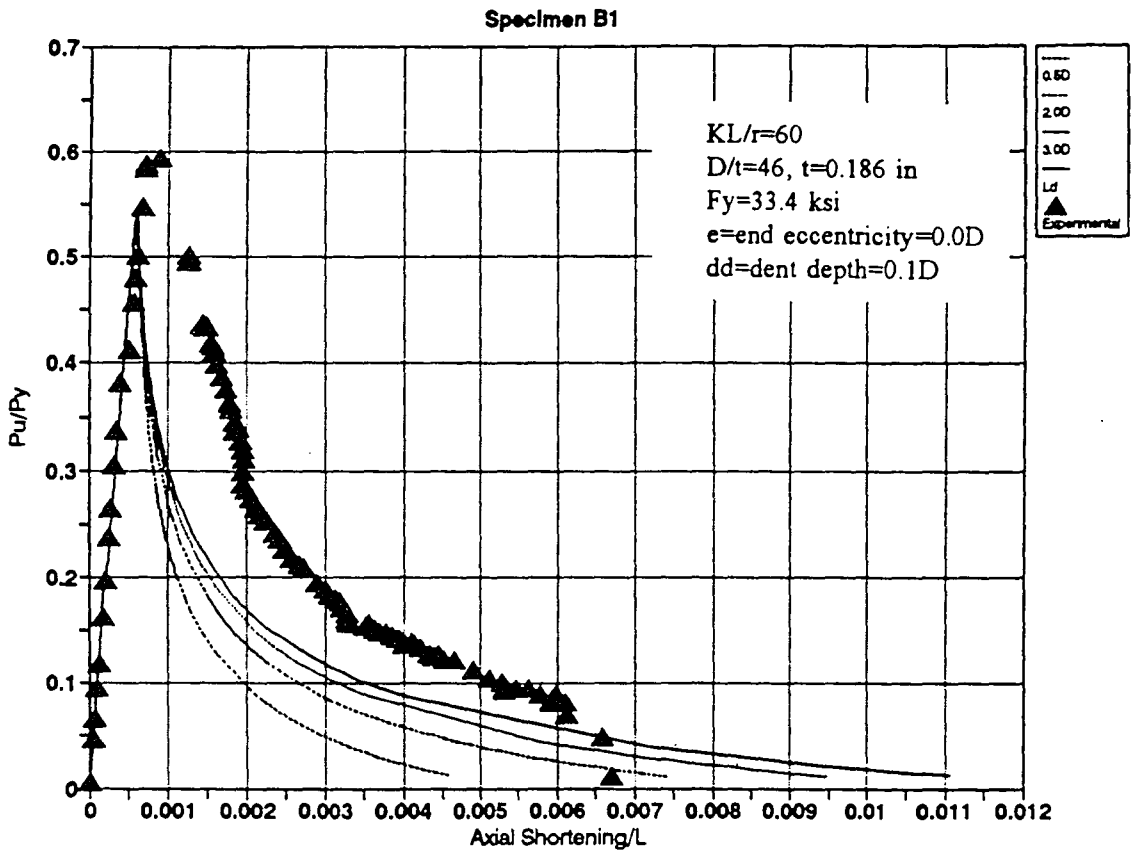

Figure 4-44 : Effects of Dented Segment Length on the Axial Compression-Shortening Response of Non-Repaired Tubulars Using Moment Curvature Approach

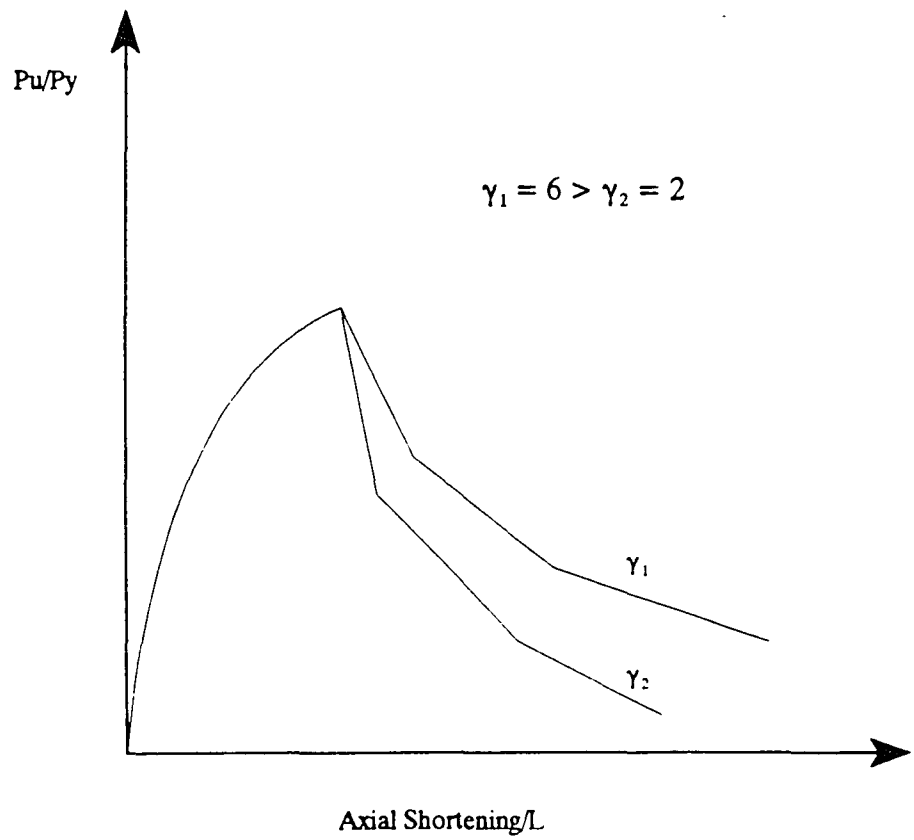

Figure 4-45 : Effect of γ Factor on the Axial Compression-Shortening Response of Internally Grout Repaired Tubulars Using Moment Curvature Approach

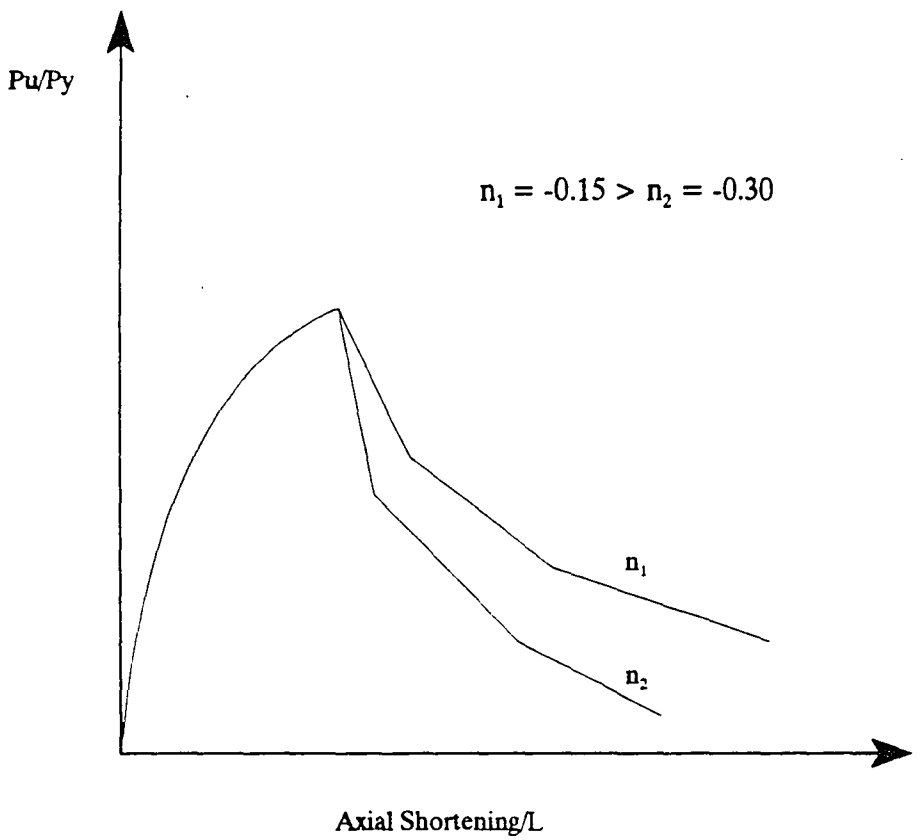

Figure 4-46 : Effect of n Factor on the Axial Compression-Shortening Response of Internally Grout Repaired Tubulars Using Moment Curvature Approach

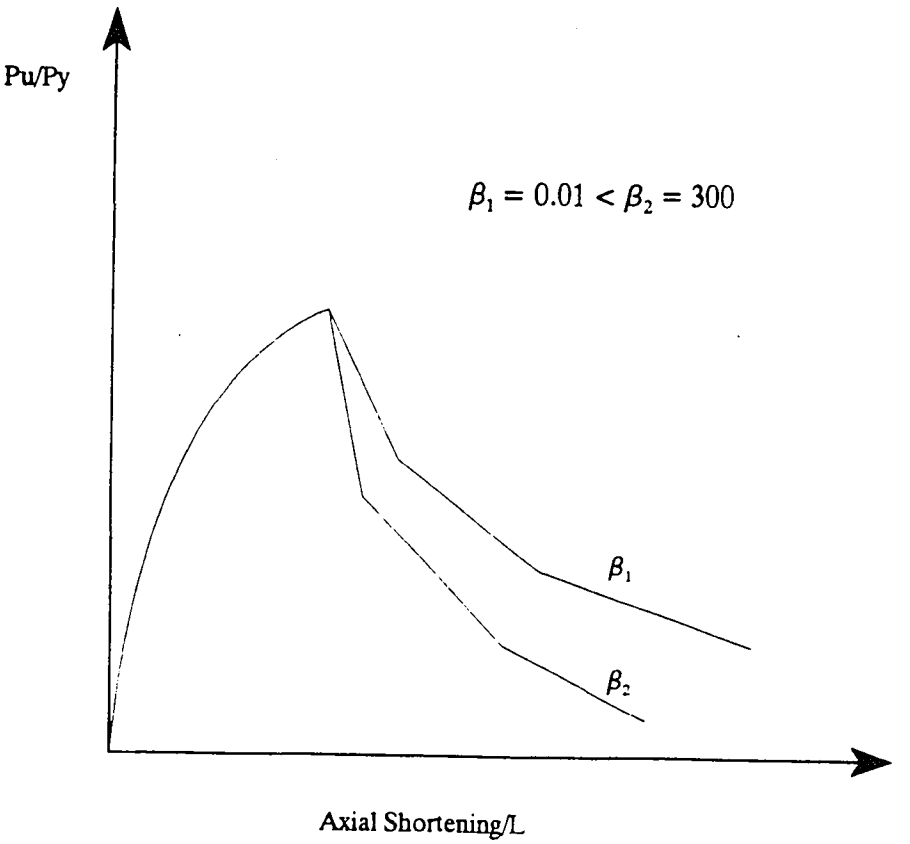

Figure 4-47 : Effect of β Factor on the Axial Compression-Shortening Response of Internally Grout Repaired Tubulars Using Moment Curvature Approach

Initial Out-Of-Straightness/L	= 0.0001
Yield Stress(Fy,ksi)	= 34.8
Young's Modulus(Es,ksi)	= 29071
KL/r	= 60

Dent Depth(1/D)	0.00	0.10	0.15	0.20	0.30	0.40
D/t=34	0.99	0.63	0.50	0.40	0.28	0.20
D/t=46	0.99	0.56	0.42	0.34	0.22	0.15
D/t=64	0.99	0.48	0.35	0.26	0.15	0.09

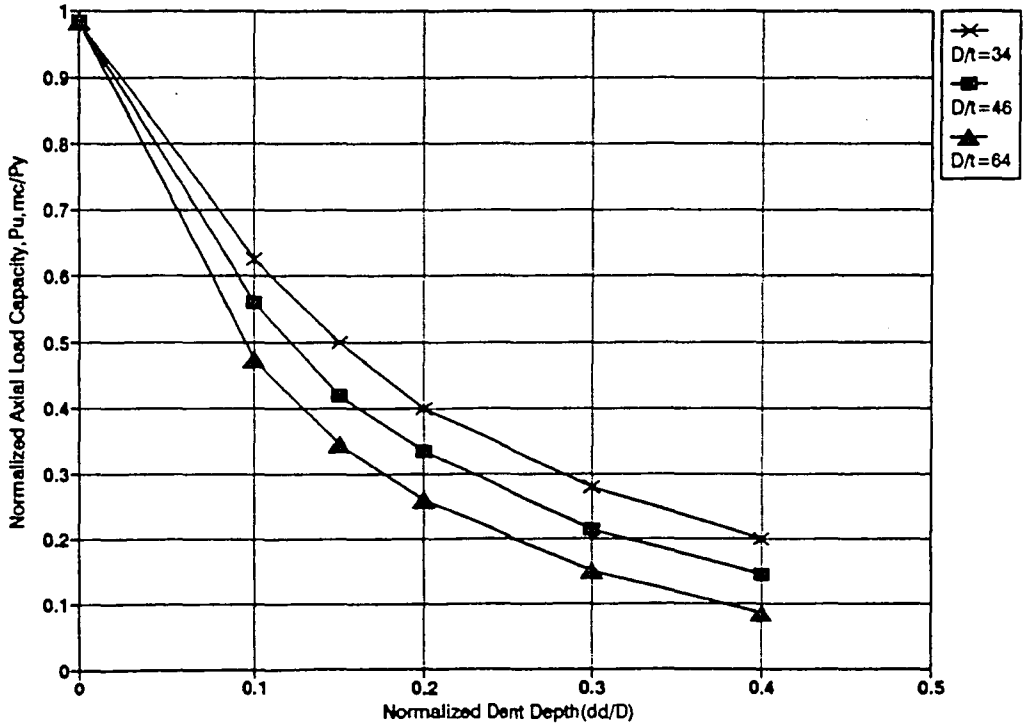

Figure 5-1 : Effects of Dent Depth-to-Diameter Ratio on Residual Strength

(Out-Of-Straightness=0.0001L, Unrepaired Member)

Initial Out-Of-Straightness/L	= 0.0005
Yield Stress(Fy,ksi)	= 34.8
Young's Modulus(Es,ksi)	= 29071
KL/r	= 60

Dent Depth(1/D)	0.00	0.10	0.15	0.20	0.30	0.40
D/t=34	0.93	0.61	0.49	0.40	0.28	0.20
D/t=46	0.93	0.55	0.42	0.33	0.22	0.14
D/t=64	0.93	0.47	0.34	0.26	0.15	0.09

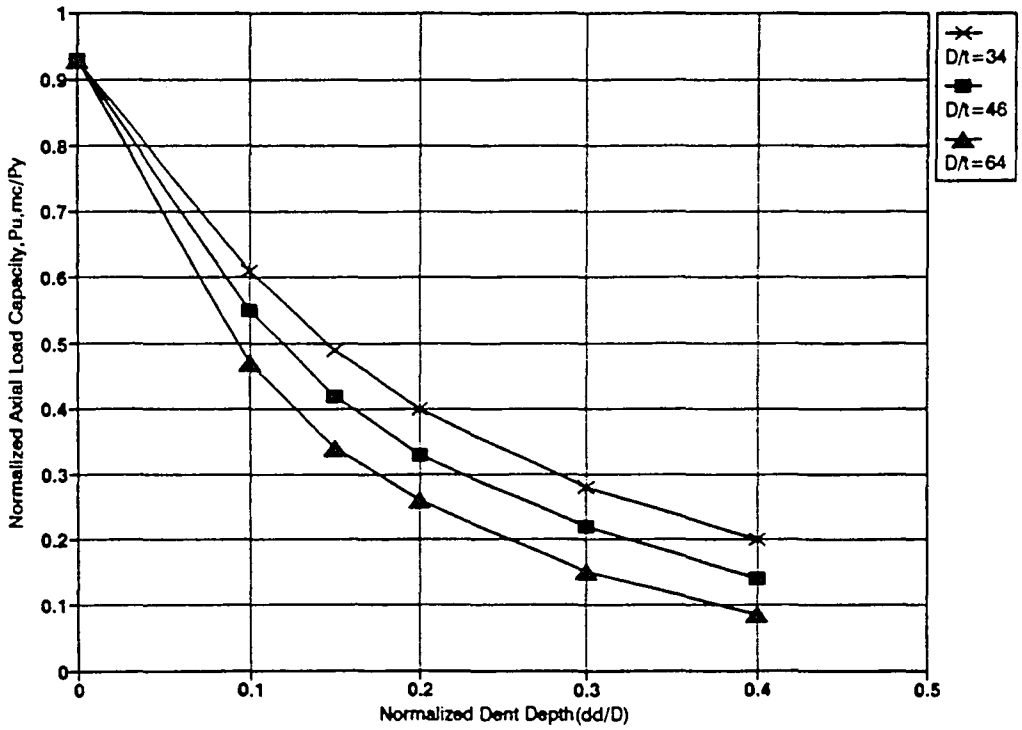

Figure 5-2 : Effects of Dent Depth-to-Diameter Ratio on Residual Strength (Out-Of-Straightness=0.0005L, Unrepaired Member)

Initial Out-Of-Straightness/L	= 0.001
Yield Stress(Fy,ksi)	= 34.8
Young's Modulus(Es,ksi)	= 29071
KL/r	= 60

Dent Depth(1/D)	0.00	0.10	0.15	0.20	0.30	0.40
D/t=34	0.88	0.60	0.48	0.39	0.27	0.20
D/t=46	0.88	0.54	0.41	0.32	0.21	0.14
D/t=64	0.88	0.45	0.33	0.25	0.15	0.09

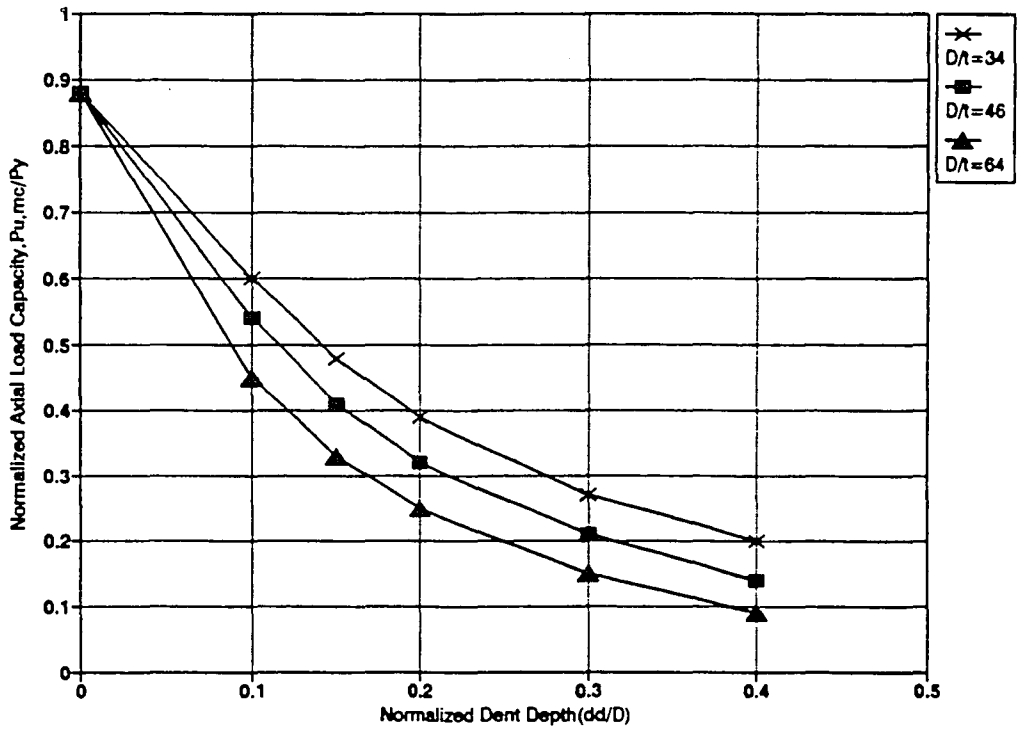

Figure 5-3 : Effects of Dent Depth-to-Diameter Ratio on Residual Strength (Out-Of-Straightness=0.001L, Unrepaired Member)

Initial Out-Of-Straightness/L	= 0.002
Yield Stress(Fy,ksi)	= 34.8
Young's Modulus(Es,ksi)	= 29071
KL/r	= 60

Dent Depth(1/D)	0.00	0.10	0.15	0.20	0.30	0.40
D/t=34	0.83	0.57	0.46	0.37	0.26	0.19
D/t=46	0.80	0.51	0.39	0.31	0.21	0.14
D/t=64	0.80	0.43	0.32	0.24	0.14	0.08

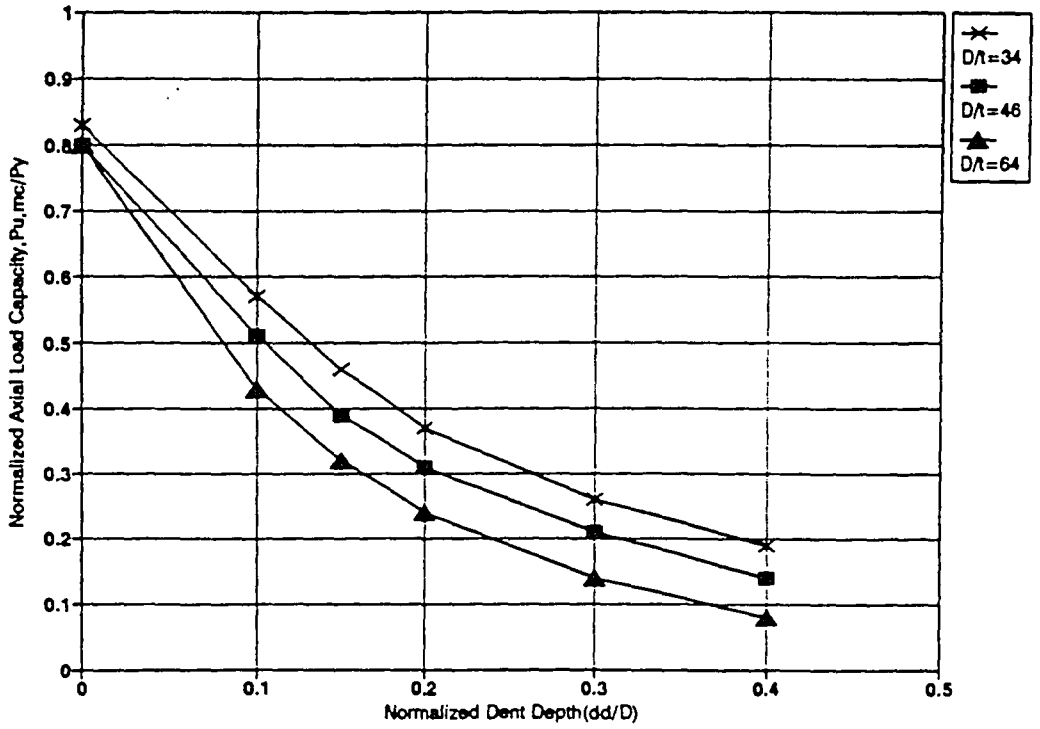

Figure 5-4 : Effects of Dent Depth-to-Diameter Ratio on Residual Strength (Out-Of-Straightness=0.002L, Unrepaired Member)

Initial Out-Of-Straightness/L	= 0.005
Yield Stress(Fy,ksi)	= 34.8
Young's Modulus(Es,ksi)	= 29071
KL/r	= 60

Dent Depth(1/D)	0.00	0.10	0.15	0.20	0.30	0.40
D/t=34	0.69	0.50	0.41	0.33	0.24	0.18
D/t=46	0.65	0.45	0.34	0.28	0.19	0.13
D/t=64	0.65	0.38	0.28	0.22	0.13	0.08

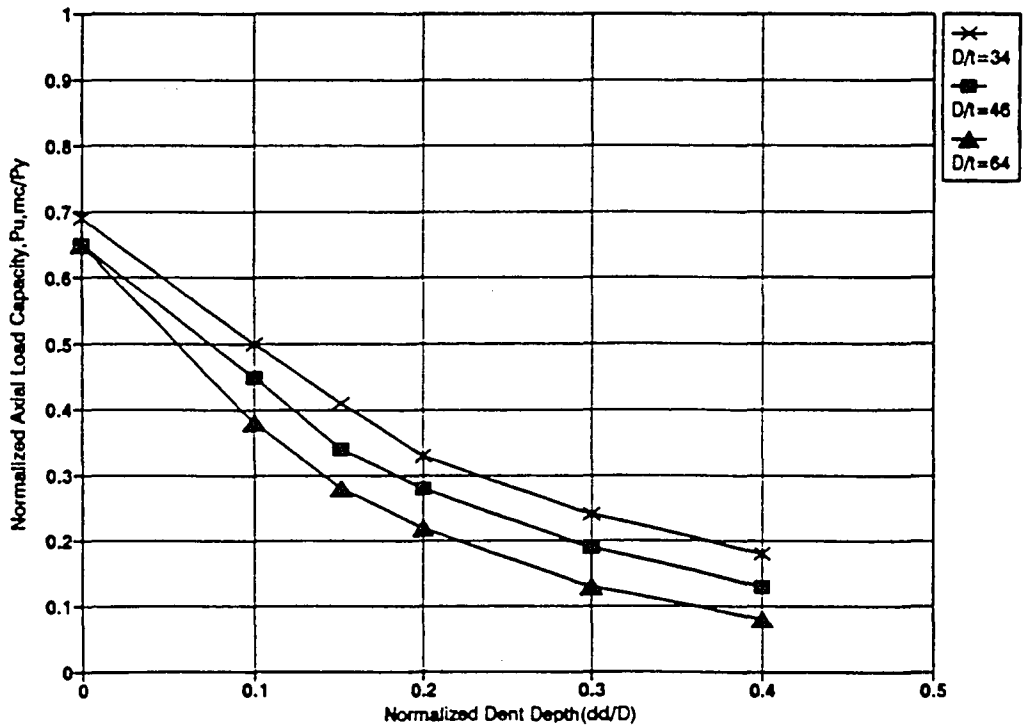

Figure 5-5 : Effects of Dent Depth-to-Diameter Ratio on Residual Strength (Out-Of-Straightness=0.005L, Unrepaired Member)

Initial Out-Of-Straightness/L	= 0.01
Yield Stress(Fy,ksi)	= 34.8
Young's Modulus(Es,ksi)	= 29071
KL/r	= 60

Dent Depth(1/D)	0.00	0.10	0.15	0.20	0.30	0.40
D/t=34	0.55	0.41	0.34	0.28	0.21	0.15
D/t=46	0.52	0.38	0.29	0.24	0.16	0.11
D/t=64	0.52	0.32	0.24	0.19	0.12	0.07

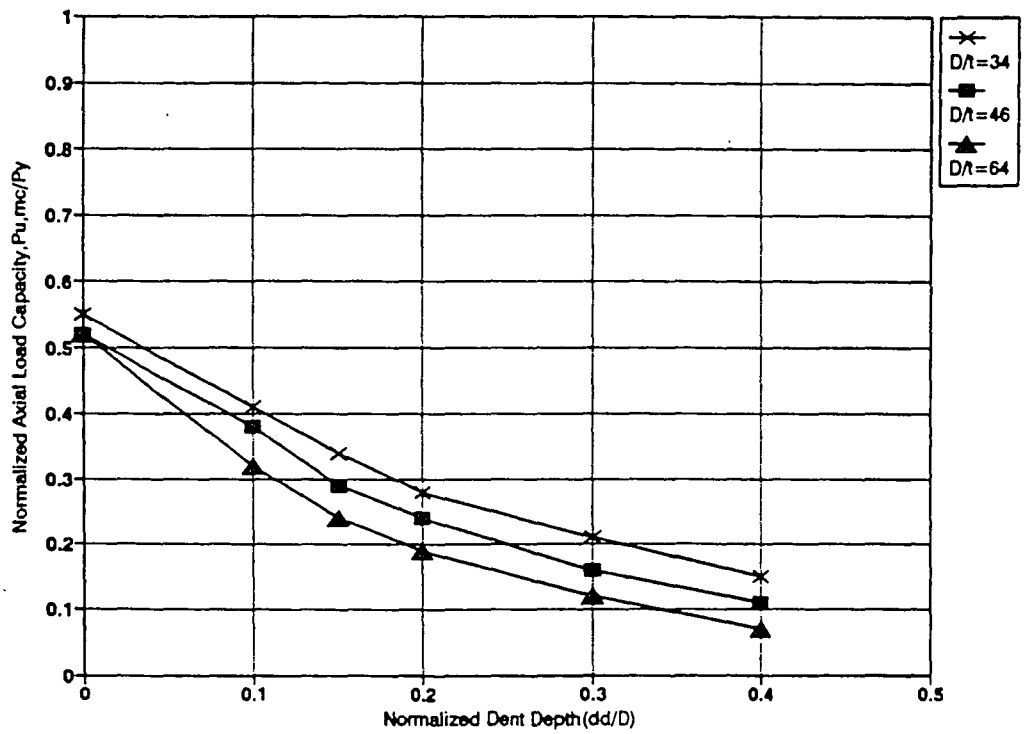

Figure 5-6 : Effects of Dent Depth-to-Diameter Ratio on Residual Strength (Out-Of-Straightness=0.01L, Unrepaired Member)

Initial Out-Of-Straightness/L	= 0.02
Yield Stress(Fy,ksi)	= 34.8
Young's Modulus(Es,ksi)	= 29071
KL/r	= 60

Dent Depth(1/D)	0.00	0.10	0.15	0.20	0.30	0.40
D/t=34	0.39	0.31	0.26	0.22	0.16	0.12
D/t=46	0.39	0.29	0.23	0.19	0.13	0.09
D/t=64	0.39	0.25	0.19	0.15	0.09	0.06

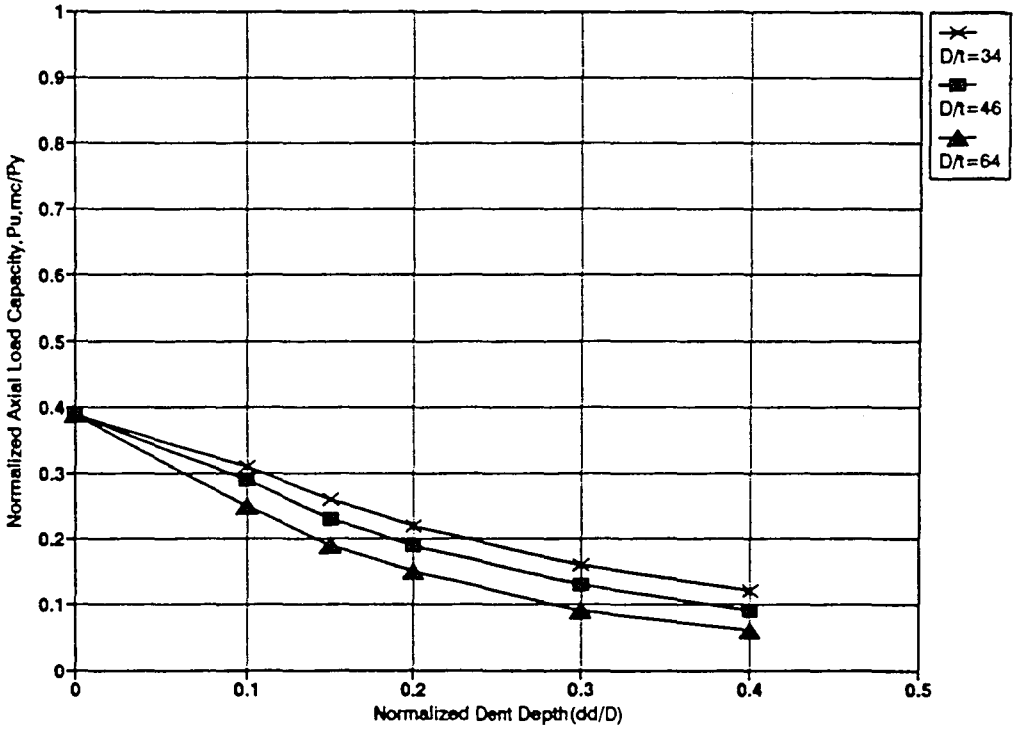

Figure 5-7 : Effects of Dent Depth-to-Diameter Ratio on Residual Strength (Out-Of-Straightness=0.02L, Unrepaired Member)

Initial Out-Of-Straightness/L	= 0.0005
Yield Stress(Fy,ksi)	= 34.8
Young's Modulus(Es,ksi)	= 29071
KL/r	= 60

Dent Depth(1/D)	0.00	0.10	0.15	0.20	0.30	0.40
D/t=34	0.98	0.62	0.48	0.38	0.24	-
D/t=46	-	-	-	-	-	-
D/t=64	0.95	0.57	0.44	0.34	-	-

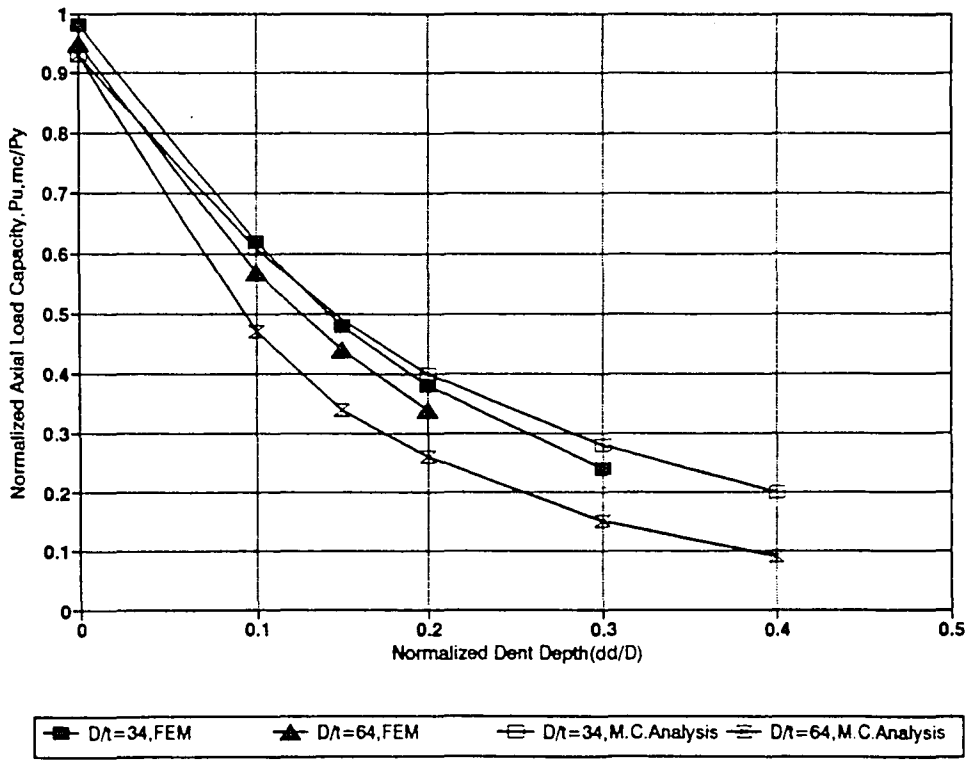

Figure 5-8 : Effects of Dent Depth-to-Diameter Ratio on Residual Strength Using Finite Element Analysis

(Out-Of-Straightness=0.0005L, Unrepaired Member) [Ricles et al., 1994]

Pu,mc/Py (for D/t=34)	Dent Depth(1/D)					
Out-Of-Straightness/L	0.00	0.10	0.15	0.20	0.30	0.40
0.0001	0.99	0.63	0.50	0.40	0.28	0.20
0.0005	0.93	0.61	0.49	0.40	0.28	0.20
0.0010	0.88	0.60	0.48	0.39	0.27	0.20
0.0020	0.83	0.57	0.46	0.37	0.26	0.19
0.0050	0.69	0.50	0.41	0.33	0.24	0.18
0.0100	0.55	0.41	0.34	0.28	0.21	0.15
0.0200	0.39	0.31	0.26	0.22	0.16	0.12

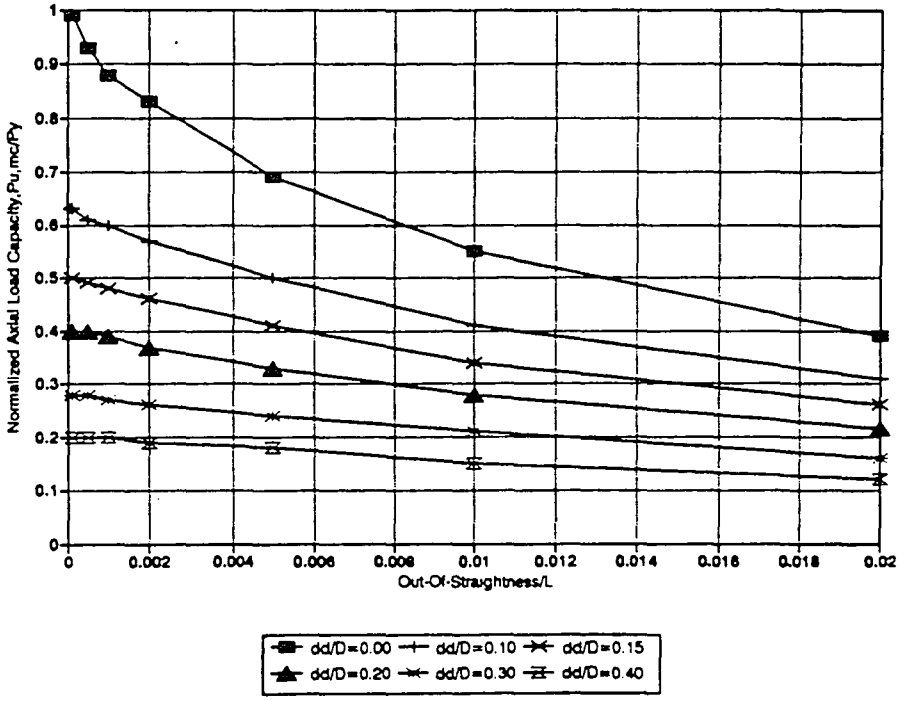

Figure 5-9 : Effects of Out-Of-Straightness-to-Length Ratio on Residual Strength (D/t=34, Unrepaired Member)

Pu,mc/Py (D/t=46)	Dent Depth(1/D)					
Out-Of-Straightness/L	0.00	0.10	0.15	0.20	0.30	0.40
0.0001	0.99	0.56	0.42	0.34	0.22	0.15
0.0005	0.93	0.55	0.42	0.33	0.22	0.14
0.0010	0.88	0.54	0.41	0.32	0.21	0.14
0.0020	0.80	0.51	0.39	0.31	0.21	0.14
0.0050	0.65	0.45	0.34	0.28	0.19	0.13
0.0100	0.52	0.38	0.29	0.24	0.16	0.11
0.0200	0.39	0.29	0.23	0.19	0.13	0.09

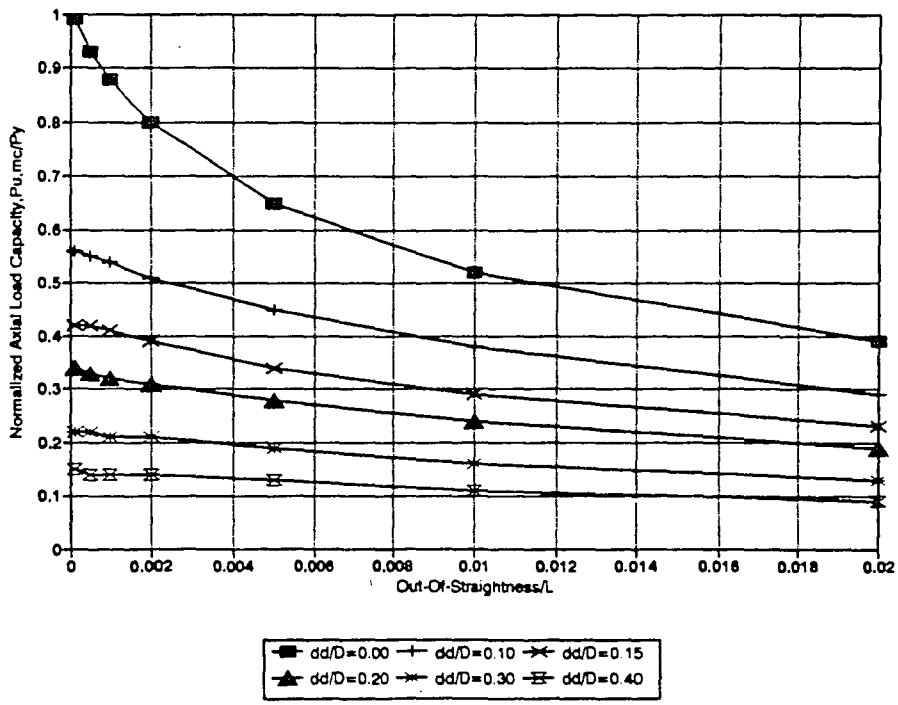

Figure 5-10 : Effects of Out-Of-Straightness-to-Length Ratio on Residual Strength (D/t=46, Unrepaired Member)

Pu,mc/Py (for D/t=64)	Dent Depth(1/D)					
Out-Of-Straightness/L	0.00	0.10	0.15	0.20	0.30	0.40
0.0001	0.99	0.48	0.35	0.26	0.15	0.09
0.0005	0.93	0.47	0.34	0.26	0.15	0.09
0.0010	0.88	0.45	0.33	0.25	0.15	0.09
0.0020	0.80	0.43	0.32	0.24	0.14	0.08
0.0050	0.65	0.38	0.28	0.22	0.13	0.08
0.0100	0.52	0.32	0.24	0.19	0.12	0.07
0.0200	0.39	0.25	0.19	0.15	0.09	0.06

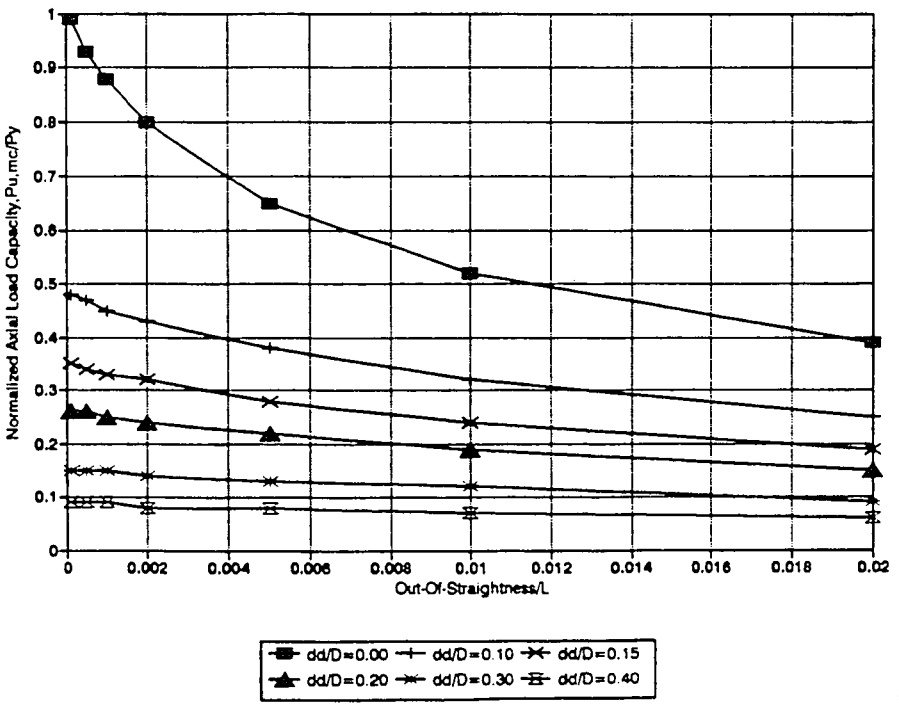

Figure 5-11 : Effects of Out-Of-Straightness-to-Length Ratio on Residual Strength (D/t=64, Unrepaired Member)

Initial Out-Of-Straightness/L	= 0.0001
Yield Stress(Fy,ksi)	= 34.8
Young's Modulus(Es,ksi)	= 29071
Grout Strength(F'g,ksi)	= 5
Elastic Modulus of Grout(Eg,ksi)	= 2907.1
KL/r	= 60

Dent Depth(1/D)	0.00	0.10	0.15	0.20	0.30	0.40
D/t=34	1.38	1.33	1.28	1.20	0.96	0.70
D/t=46	1.59	1.56	1.50	1.37	1.09	0.78
D/t=64	1.96	1.89	1.81	1.65	1.30	0.90

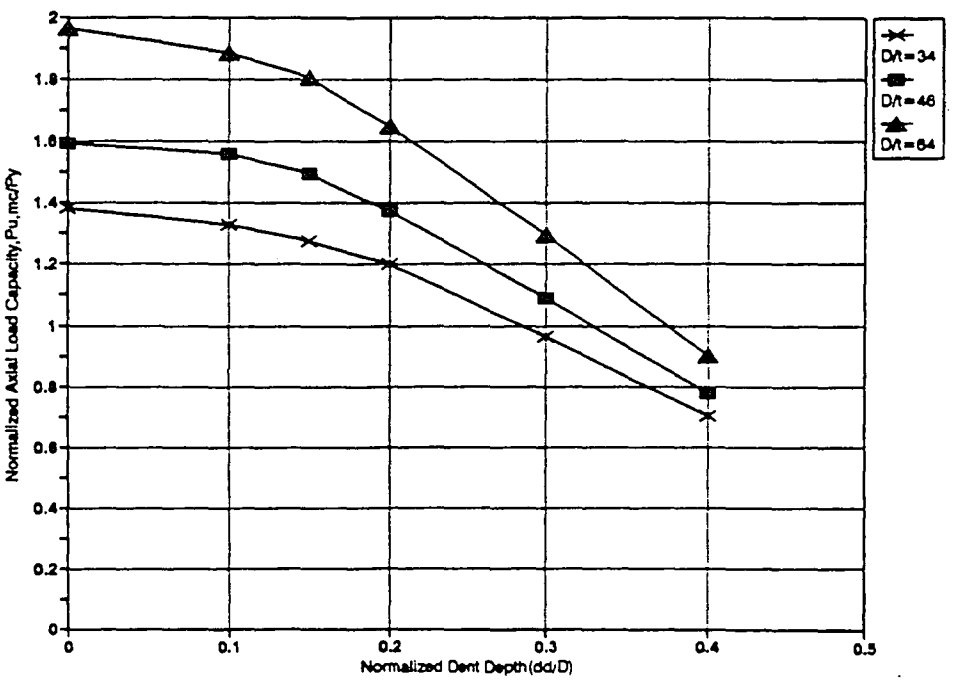

Figure 5-12 : Effects of Dent Depth-to-Diameter Ratio on Repaired Strength

(Out-Of-Straightness=0.0001L, Internally Grout Repaired Member)

Initial Out-Of-Straightness/L	= 0.0005
Yield Stress(Fy,ksi)	= 34.8
Young's Modulus(Es,ksi)	= 29071
Grout Strength(F'g,ksi)	= 5
Elastic Modulus of Grout(Eg,ksi)	= 2907.1
KL/r	= 60

Dent Depth(1/D)	0.00	0.10	0.15	0.20	0.30	0.40
D/t=34	1.33	1.28	1.23	1.15	0.94	0.68
D/t=46	1.56	1.50	1.44	1.34	1.06	0.75
D/t=64	1.89	1.85	1.73	1.61	1.26	0.86

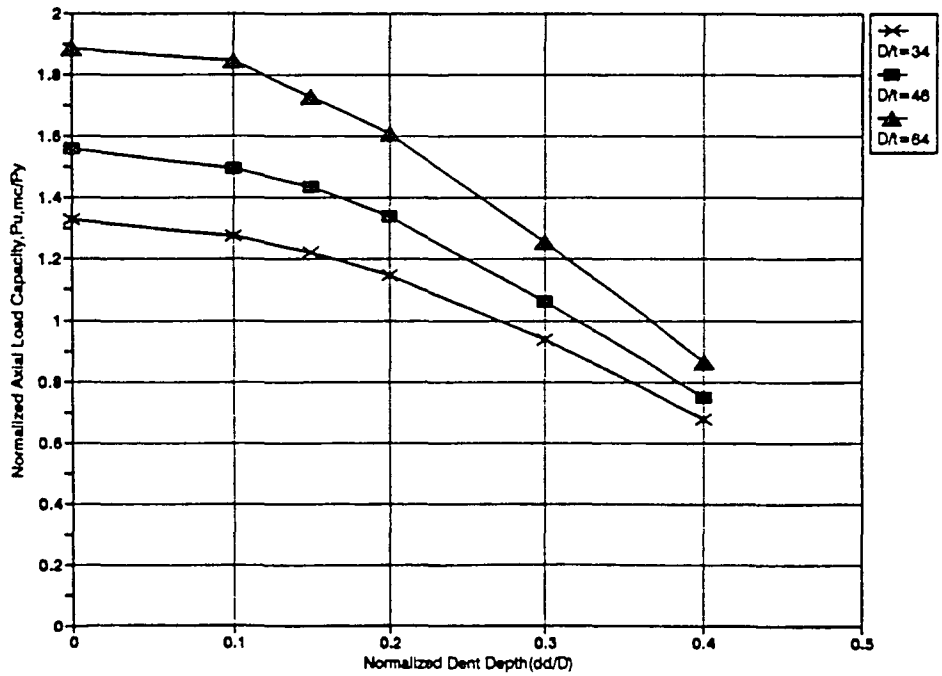

Figure 5-13 : Effects of Dent Depth-to-Diameter Ratio on Repaired Strength (Out-Of-Straightness=0.0005L, Internally Grout Repaired Member)

Initial Out-Of-Straightness/L	= 0.001
Yield Stress(Fy,ksi)	= 34.8
Young's Modulus(Es,ksi)	= 29071
Grout Strength(F'g,ksi)	= 5
Elastic Modulus of Grout(Eg,ksi)	= 2907.1
KL/r	= 60

Dent Depth(1/D)	0.00	0.10	0.15	0.20	0.30	0.40
D/t=34	1.30	1.25	1.20	1.12	0.91	0.65
D/t=46	1.53	1.47	1.40	1.28	1.03	0.72
D/t=64	1.85	1.77	1.69	1.57	1.22	0.82

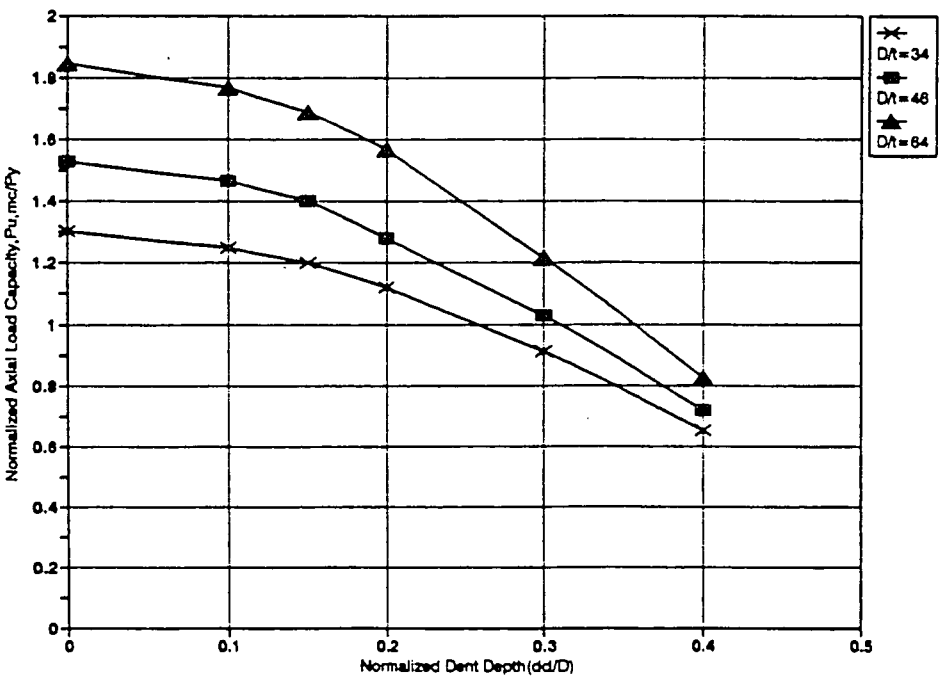

Figure 5-14 : Effects of Dent Depth-to-Diameter Ratio on Repaired Strength (Out-Of-Straightness=0.001L, Internally Grout Repaired Member)

Initial Out-Of-Straightness,L	= 0.002
Yield Stress(Fy,ksi)	= 34.8
Young's Modulus(Es,ksi)	= 29071
Grout Strength(F'g,ksi)	= 5
Elastic Modulus of Grout(Eg,ksi)	= 2907.1
KL/r	= 60

Dent Depth(1/D)	0.00	0.10	0.15	0.20	0.30	0.40
D/t=34	1.23	1.17	1.15	1.07	0.86	0.60
D/t=46	1.44	1.37	1.31	1.22	0.97	0.69
D/t=64	1.73	1.65	1.57	1.45	1.14	0.79

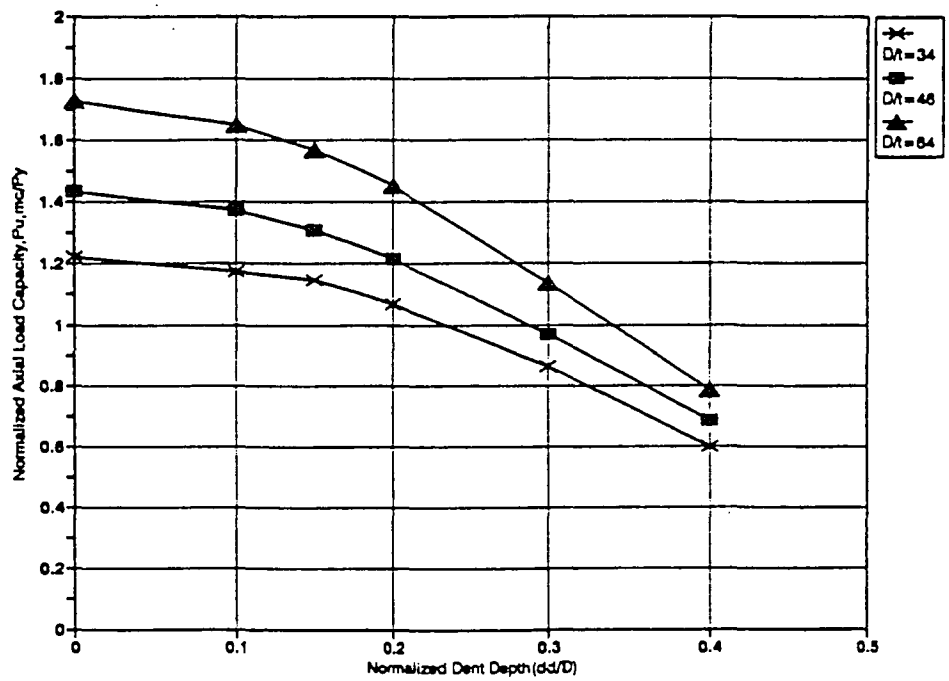

Figure 5-15 : Effects of Dent Depth-to-Diameter Ratio on Repaired Strength

(Out-Of-Straightness=0.002L, Internally Grout Repaired Member)

Initial Out-Of-Straightness/L	= 0.005
Yield Stress(Fy,ksi)	= 34.8
Young's Modulus(Es,ksi)	= 29071
Grout Strength(F'g,ksi)	= 5
Elastic Modulus of Grout(Eg,ksi)	= 2907.1
KL/r	= 60

Dent Depth(1/D)	0.00	0.10	0.15	0.20	0.30	0.40
D/t=34	1.04	1.02	0.96	0.91	0.70	0.52
D/t=46	1.22	1.15	1.12	1.03	0.81	0.56
D/t=64	1.45	1.37	1.34	1.22	0.90	0.63

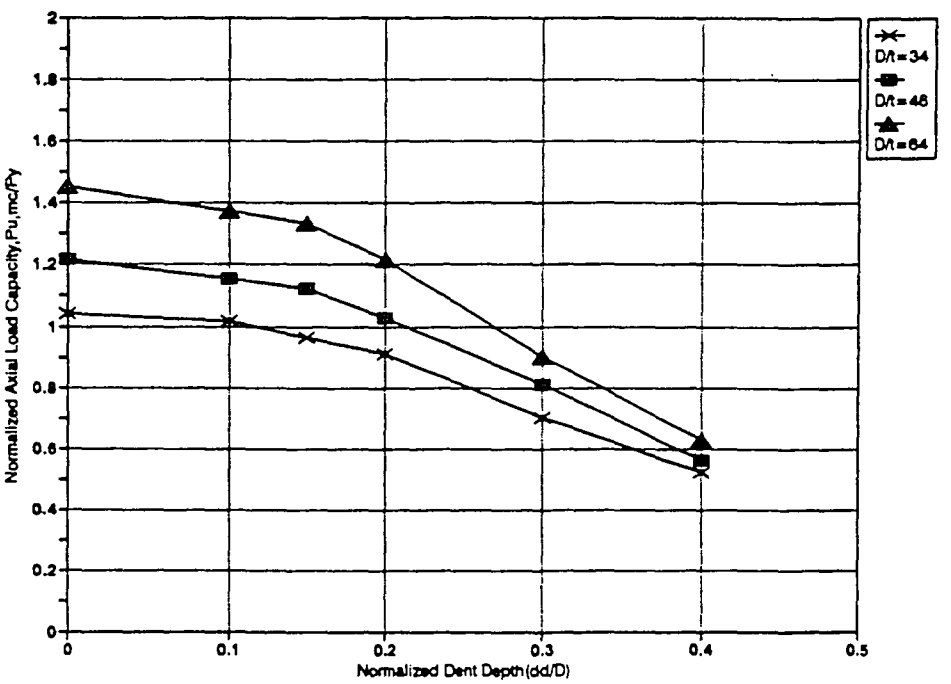

Figure 5-16 : Effects of Dent Depth-to-Diameter Ratio on Repaired Strength (Out-Of-Straightness=0.005L, Internally Grout Repaired Member)

Initial Out-Of-Straightness/L	= 0.01
Yield Stress(Fy,ksi)	= 34.8
Young's Modulus(Es,ksi)	= 29071
Grout Strength(F'g,ksi)	= 5
Elastic Modulus of Grout(Eg,ksi)	= 2907.1
KL/r	= 60

Dent Depth(1/D)	0.00	0.10	0.15	0.20	0.30	0.40
D/t=34	0.86	0.81	0.76	0.70	0.55	0.39
D/t=46	0.97	0.94	0.87	0.78	0.62	0.44
D/t=64	1.14	1.06	0.98	0.90	0.67	0.47

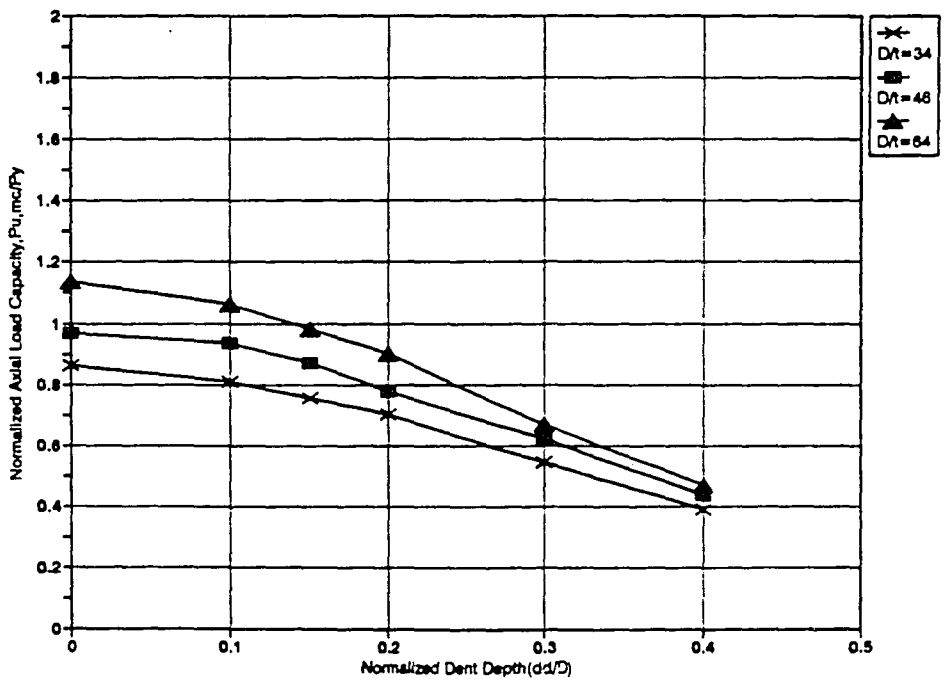

Figure 5-17 : Effects of Dent Depth-to-Diameter Ratio on Repaired Strength

(Out-Of-Straightness=0.01L, Internally Grout Repaired Member)

Initial Out-Of-Straightness/L	= 0.02
Yield Stress(Fy,ksi)	= 34.8
Young's Modulus(Es,ksi)	= 29071
Grout Strength(F'g,ksi)	= 5
Elastic Modulus of Grout(Eg,ksi)	= 2907.1
KL/r	= 60

Dent Depth(1/D)	0.00	0.10	0.15	0.20	0.30	0.40
D/t=34	0.60	0.55	0.52	0.47	0.37	0.26
D/t=46	0.66	0.62	0.56	0.51	0.41	0.28
D/t=64	0.75	0.71	0.63	0.55	0.43	0.31

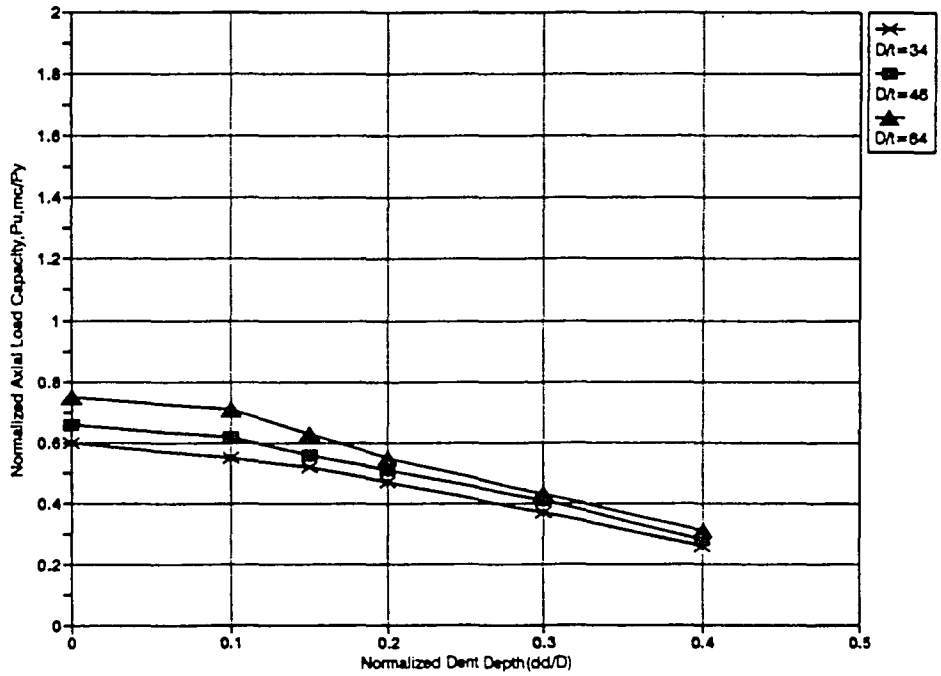

Figure 5-18 : Effects of Dent Depth-to-Diameter Ratio on Repaired Strength (Out-Of-Straightness=0.02L, Internally Grout Repaired Member)

Pu,mc/Py (for D/t=34)	Dent Depth(1/D)					
Out-Of-Straightness/L	0.00	0.10	0.15	0.20	0.30	0.40
0.0001	1.38	1.33	1.28	1.20	0.96	0.70
0.0005	1.33	1.28	1.23	1.15	0.94	0.68
0.0010	1.30	1.25	1.20	1.12	0.91	0.65
0.0020	1.23	1.17	1.15	1.07	0.86	0.60
0.0050	1.04	1.02	0.96	0.91	0.70	0.52
0.0100	0.86	0.81	0.76	0.70	0.55	0.39
0.0200	0.60	0.55	0.52	0.47	0.37	0.26

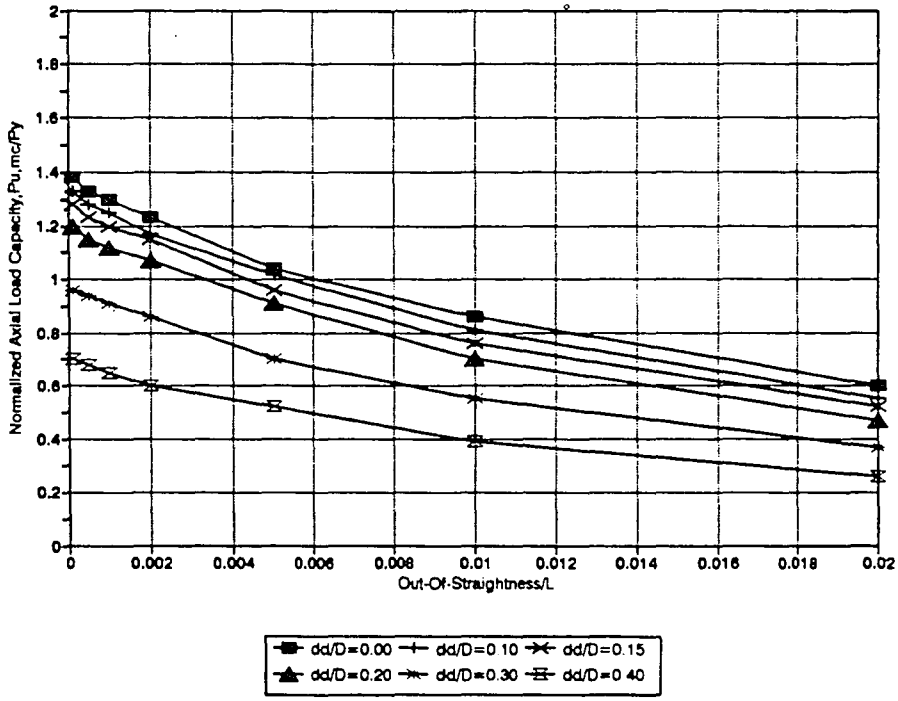

Figure 5-19 : Effects of Out-Of-straightness-to-Length Ratio on Repaired Strength (D/t=34, Internally Grout Repaired Member)

Pu,mc/Py (for D/t=46)	Dent Depth(1/D)					
Out-Of-Straightness/L	0.00	0.10	0.15	0.20	0.30	0.40
0.0001	1.59	1.56	1.50	1.37	1.09	0.78
0.0005	1.56	1.50	1.44	1.34	1.06	0.75
0.0010	1.53	1.47	1.40	1.28	1.03	0.72
0.0020	1.44	1.37	1.31	1.22	0.97	0.69
0.0050	1.22	1.15	1.12	1.03	0.81	0.56
0.0100	0.97	0.94	0.87	0.78	0.62	0.44
0.0200	0.66	0.62	0.56	0.51	0.41	0.28

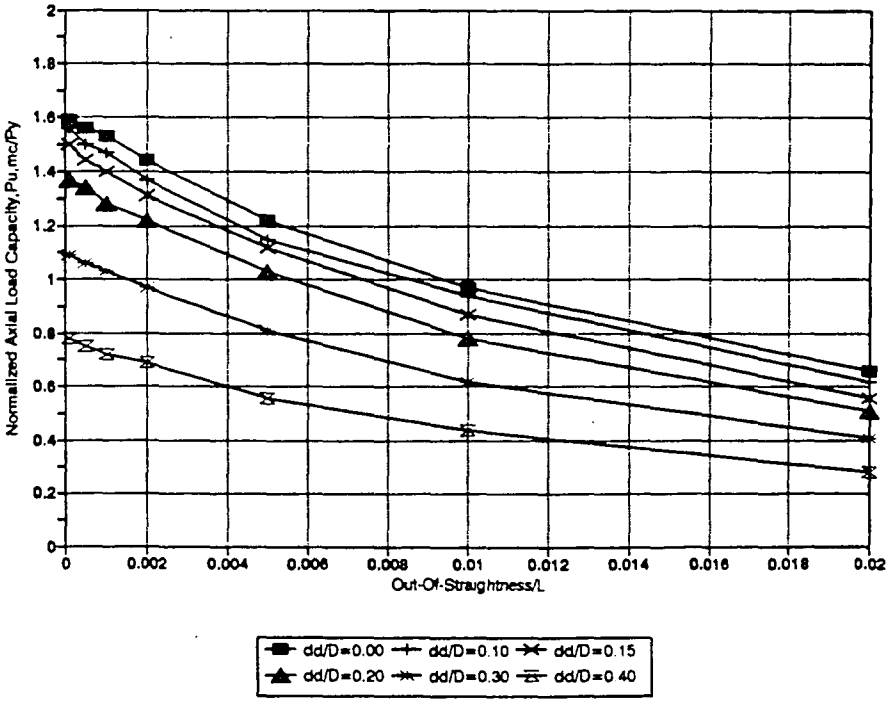

Figure 5-20 : Effects of Out-Of-straightness-to-Length Ratio on Repaired Strength (D/t=46, Internally Grout Repaired Member)

Pu,mc/Py (for D/t=64)	Dent Depth(1/D)					
Out-Of-Straightness/L	0.00	0.10	0.15	0.20	0.30	0.40
0.0001	1.96	1.89	1.81	1.65	1.30	0.90
0.0005	1.89	1.85	1.73	1.61	1.26	0.86
0.0010	1.85	1.77	1.69	1.57	1.22	0.82
0.0020	1.73	1.65	1.57	1.45	1.14	0.79
0.0050	1.45	1.37	1.34	1.22	0.90	0.63
0.0100	1.14	1.06	0.98	0.90	0.67	0.47
0.0200	0.75	0.71	0.63	0.55	0.43	0.31

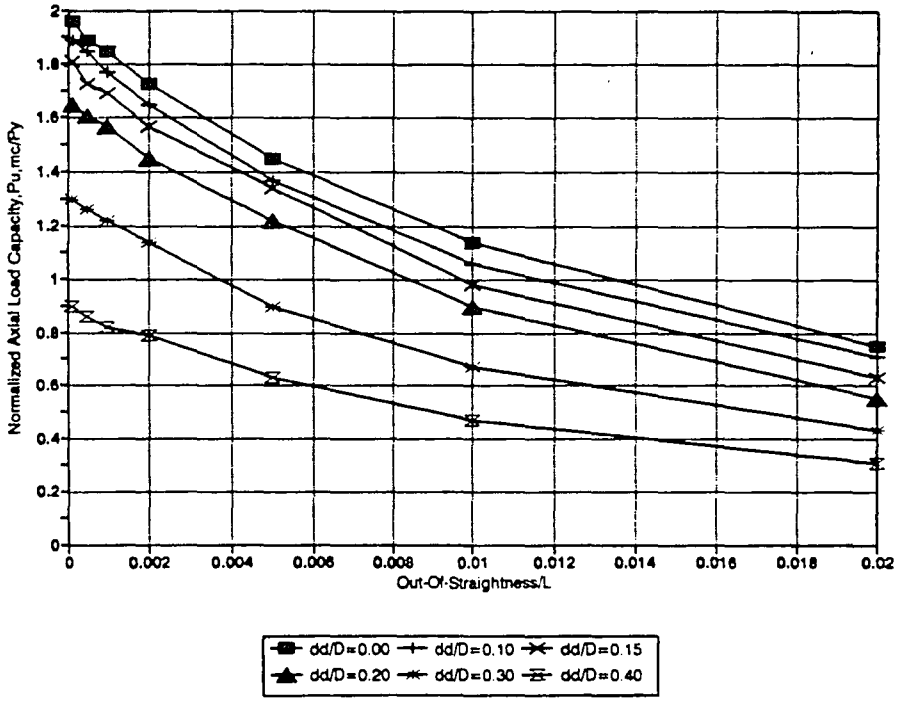

Figure 5-21 : Effects of Out-Of-straightness-to-Length Ratio on Repaired Strength (D/t=64, Internally Grout Repaired Member)

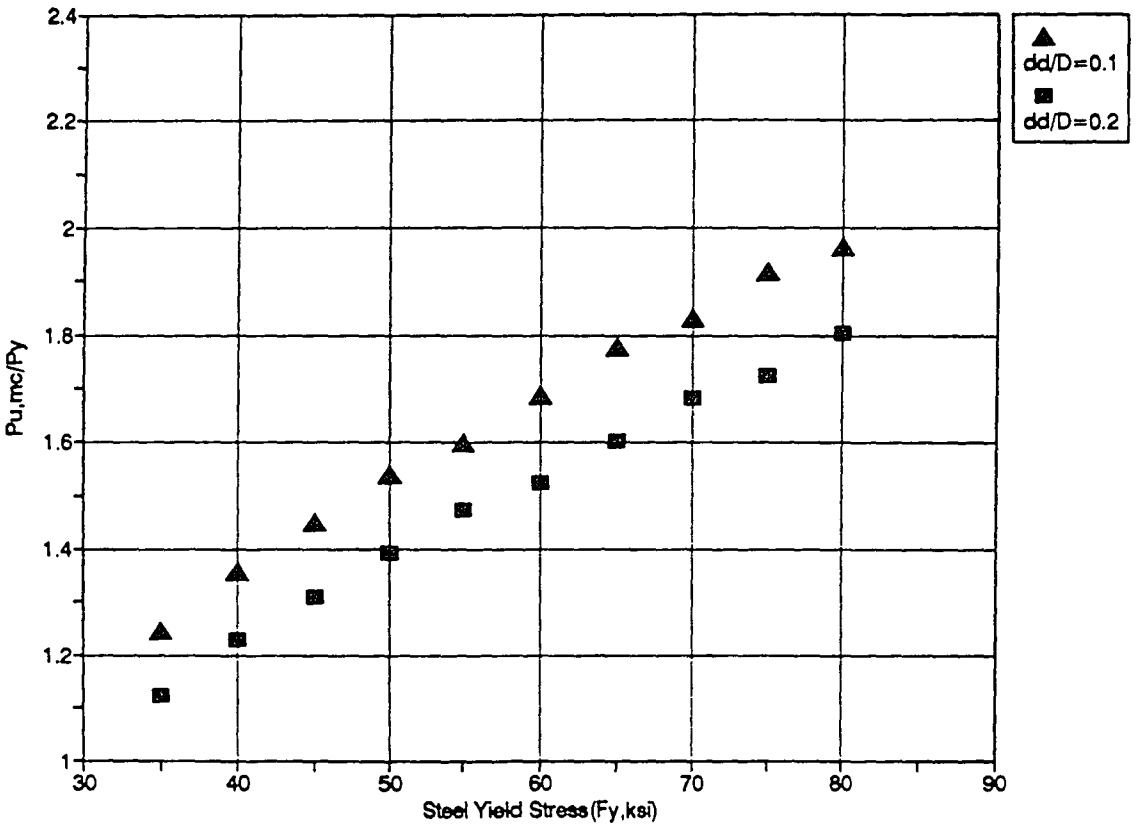

Figure 5-22 : Effects of Fy on the Ultimate Strength of Internally Grout Repaired Specimen (D/t=34, KL/r=60, F'g=6.9 ksi, δ/L=0.0006)

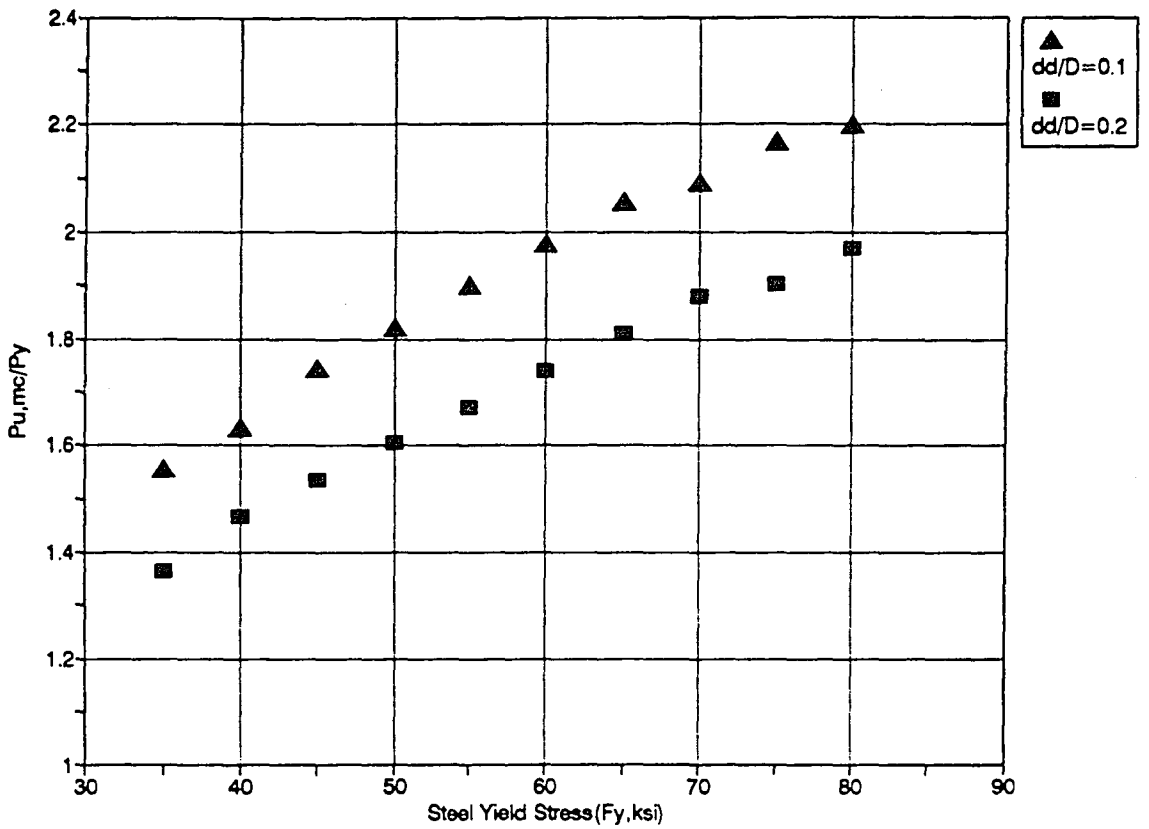

Figure 5-23 : Effects of Fy on the Ultimate Strength of Internally Grout Repaired Specimen (D/t=64, KL/r=60, F'g=6.9 ksi, δ/L=0.0006)

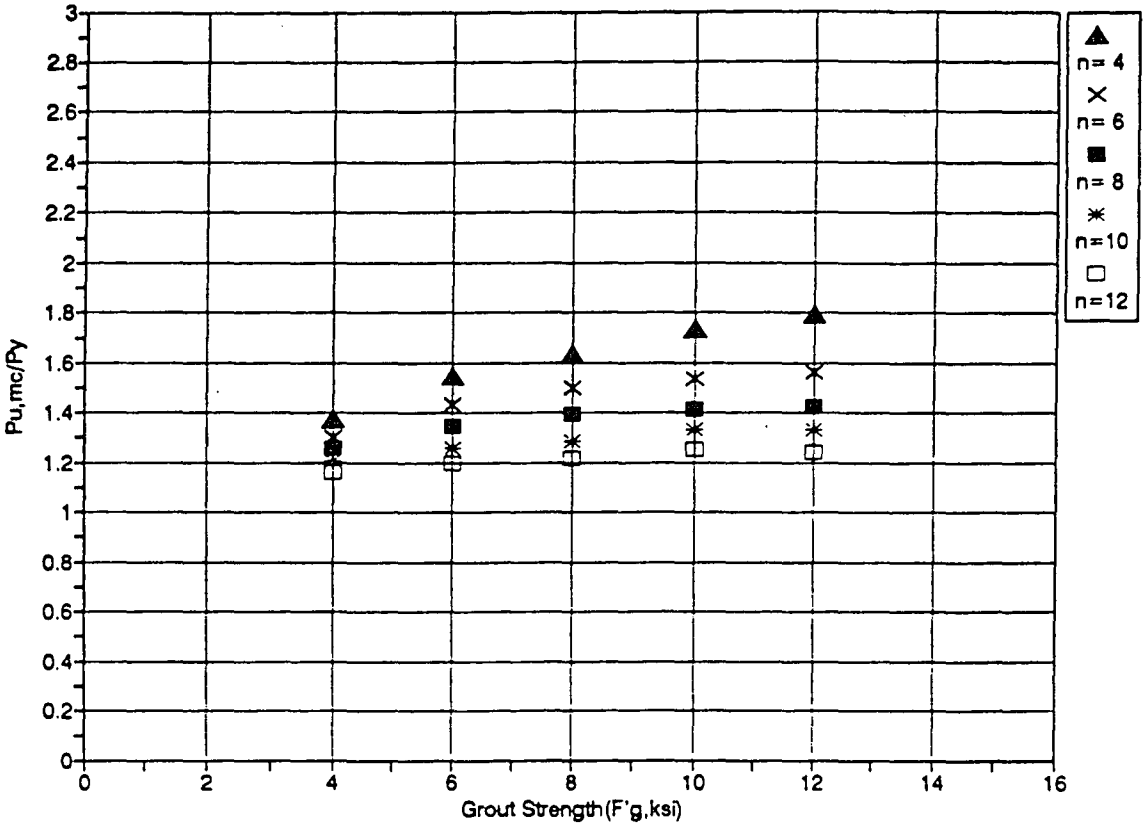

Figure 3-24 : Effects of Grout Strength F'g on the Ultimate Strength of Internally Grout Repaired Specimen (D/t=34, KL/r=60, Fy=39.4 ksi, δ/L=0.0006, dd/D=0.1)

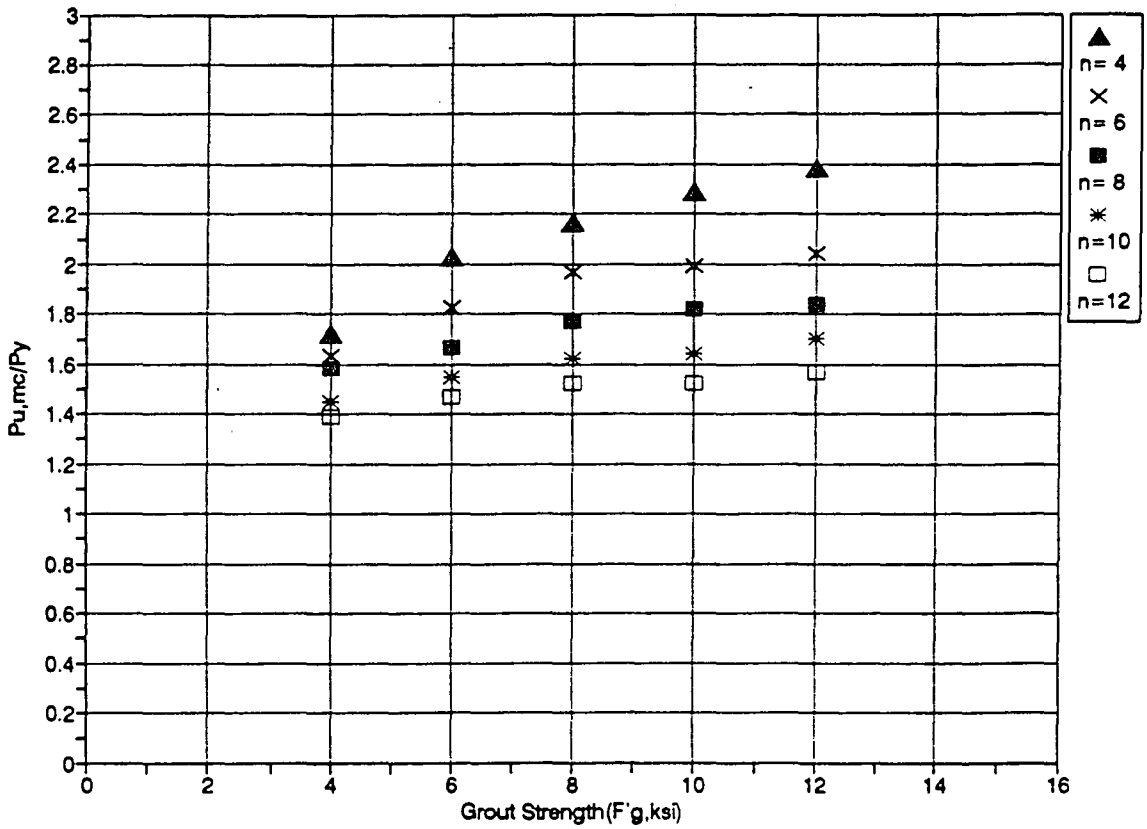

Figure 5-25 : Effects of Grout Strength F'g on the Ultimate Strength of Internally Grout Repaired Specimen (D/t=64, KL/r=60, Fy=39.4 ksi, δ/L=0.0006, dd/D=0.1)

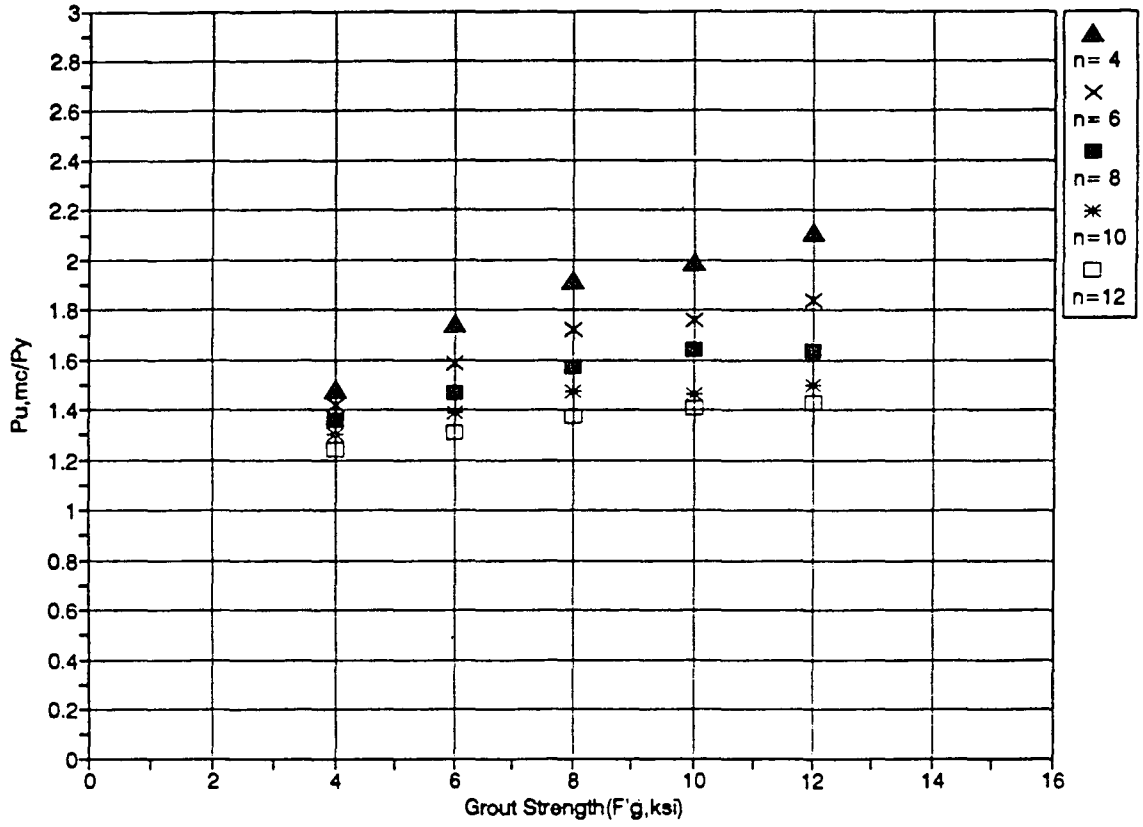

Figure 5-26 : Effects of Grout Strength F'g on the Ultimate Strength of Internally Grout Repaired Specimen (D/t=64, KL/r=60, Fy=39.4 ksi, δ/L=0.0006, dd/D=0.2)

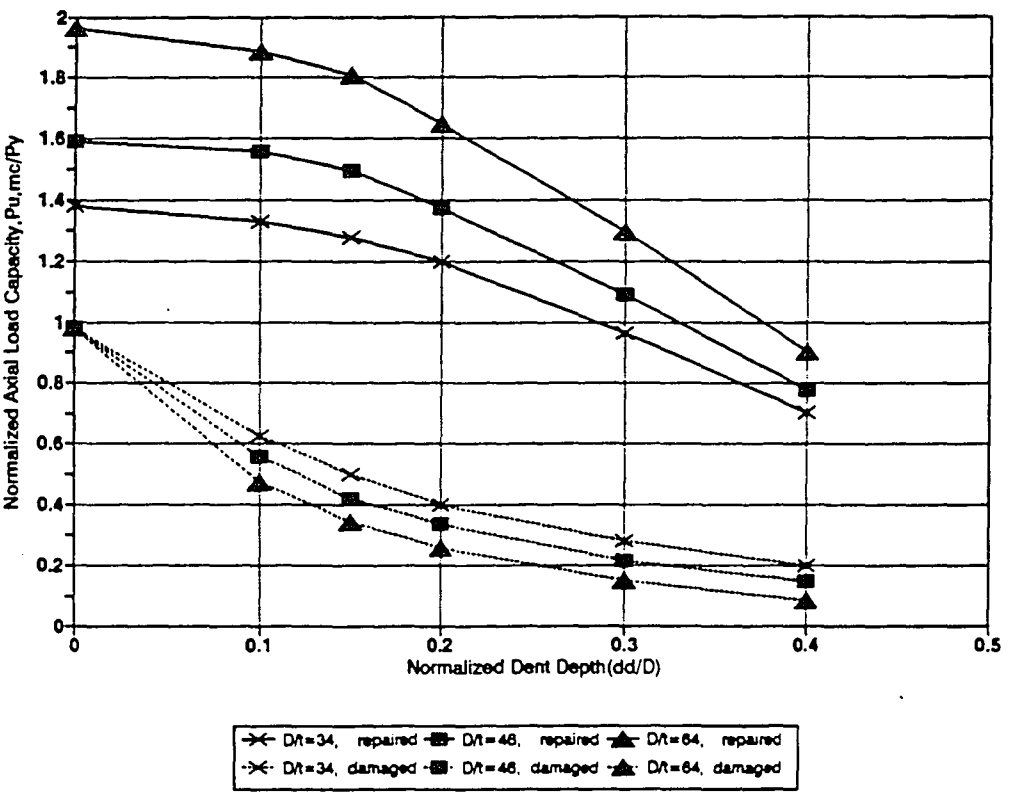

Figure 5-27 : Evaluation of the Effectiveness of the Internal Grout Repair, $\delta/L=0.0001$

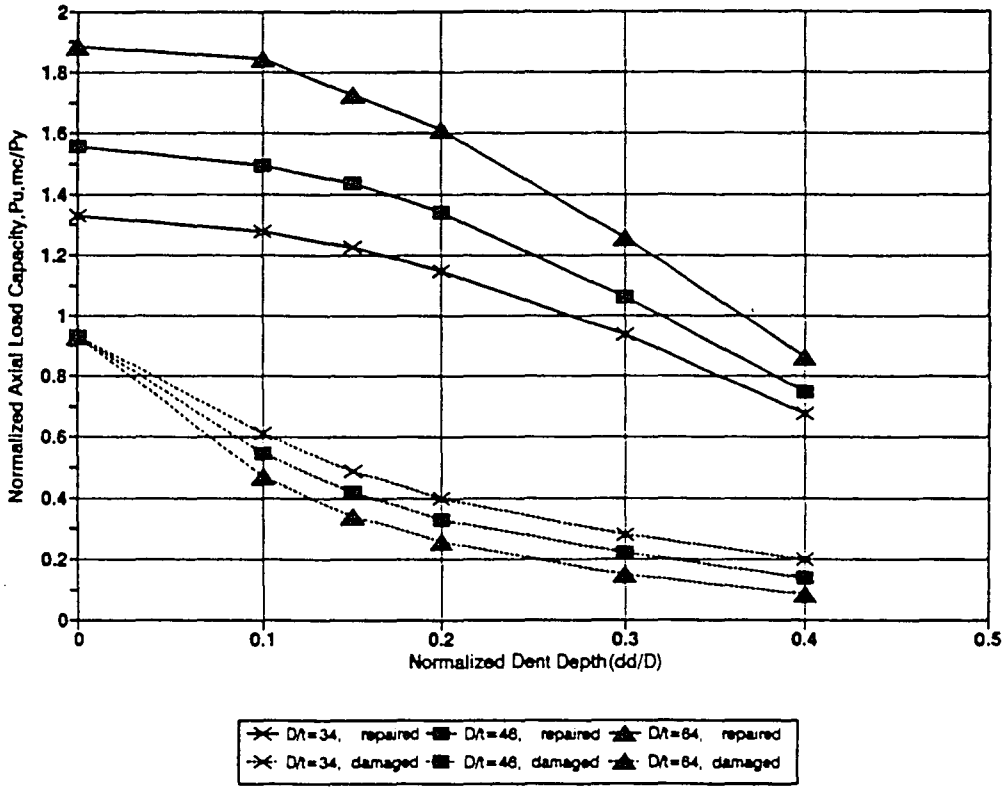

Figure 5-28 : Evaluation of the Effectiveness of the Internal Grout Repair, $\delta/L=0.0005$

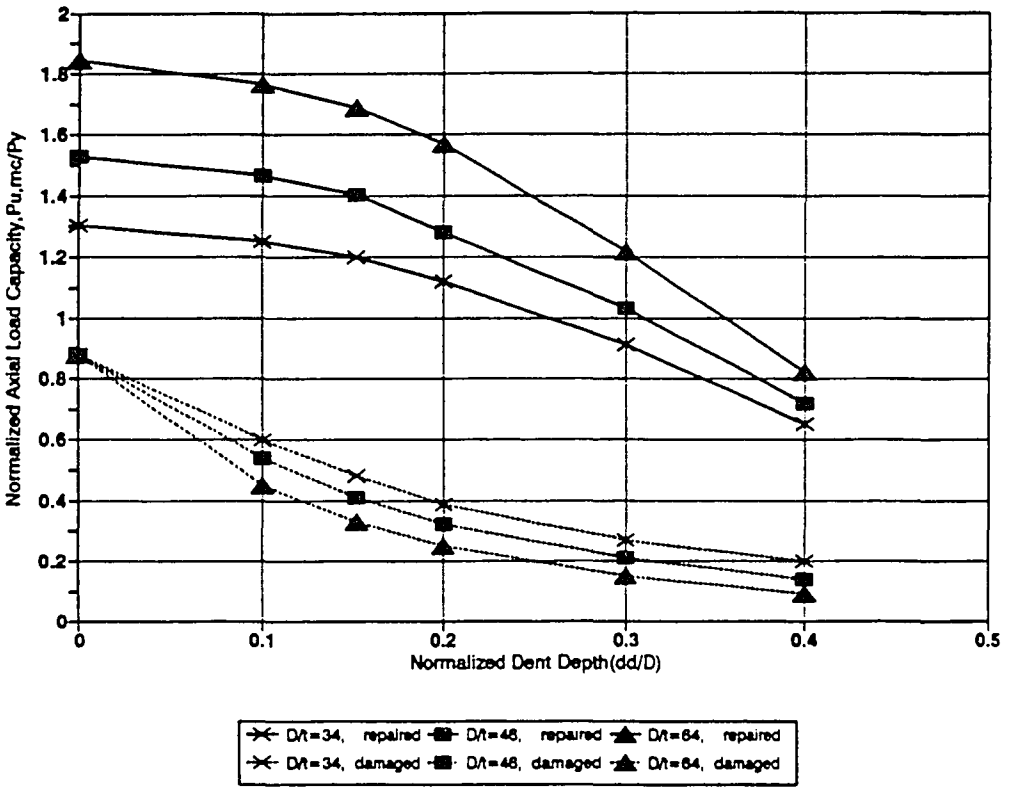

Figure 5-29 : Evaluation of the Effectiveness of the Internal Grout Repair, $\delta/L=0.001$

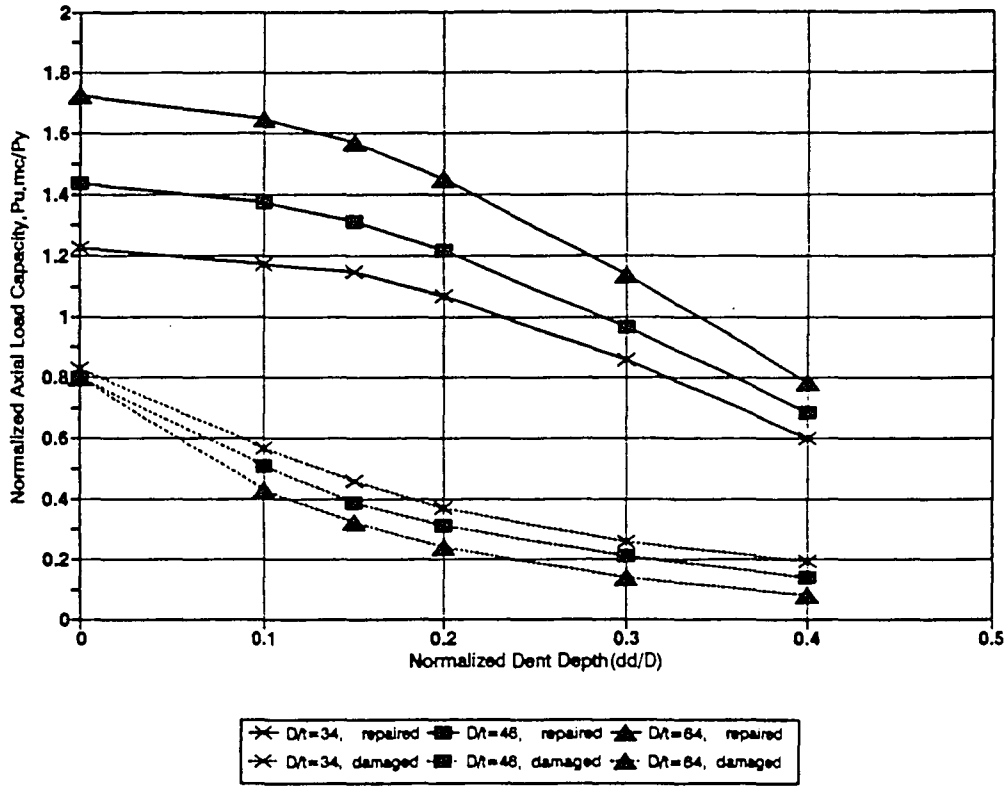

Figure 5-30 : Evaluation of the Effectiveness of the Internal Grout Repair, $\delta/L=0.002$

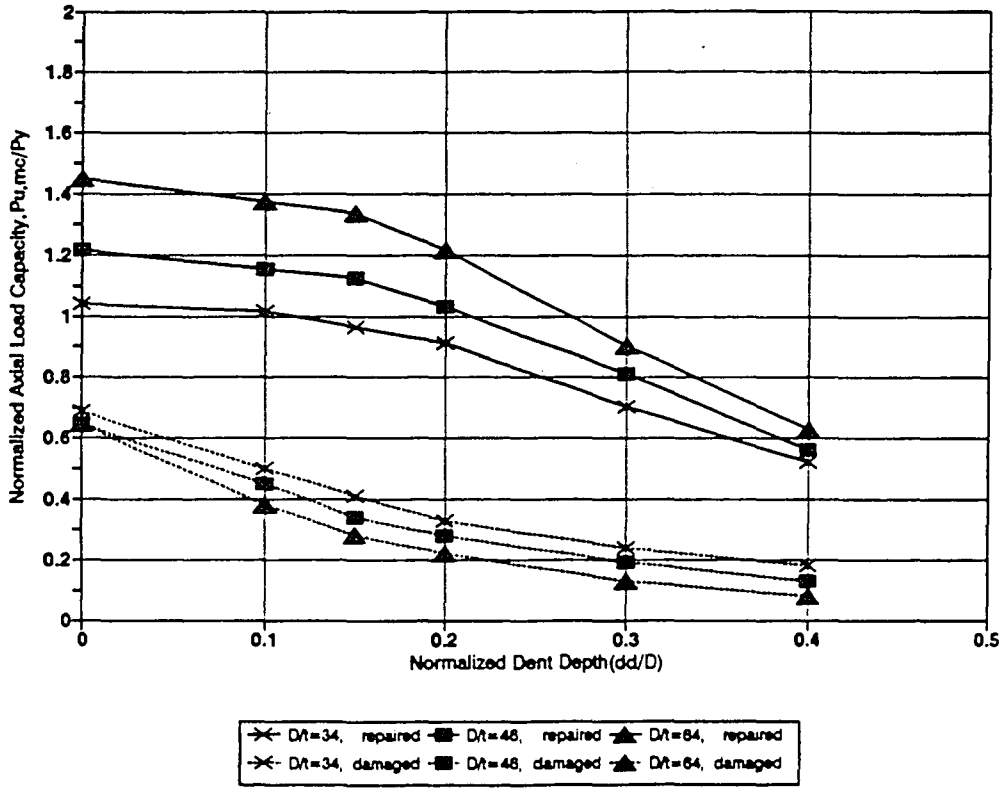

Figure 5-31 : Evaluation of the Effectiveness of the Internal Grout Repair, $\delta/L=0.005$

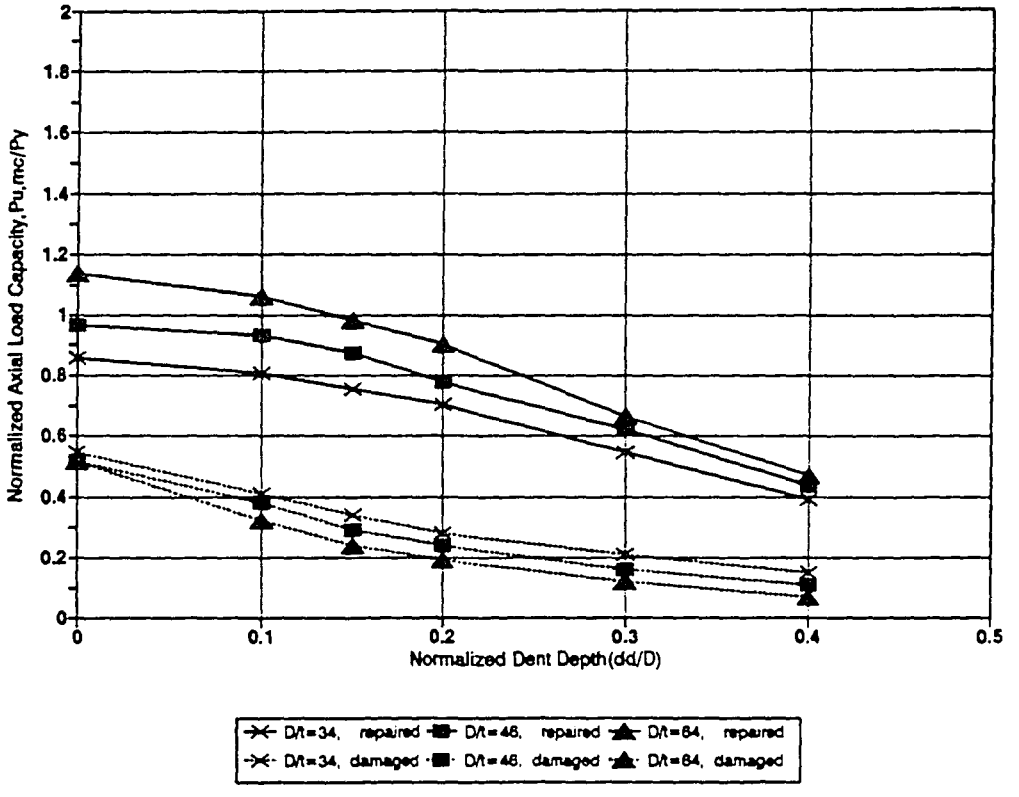

Figure 5-32 : Evaluation of the Effectiveness of the Internal Grout Repair, $\delta/L=0.01$

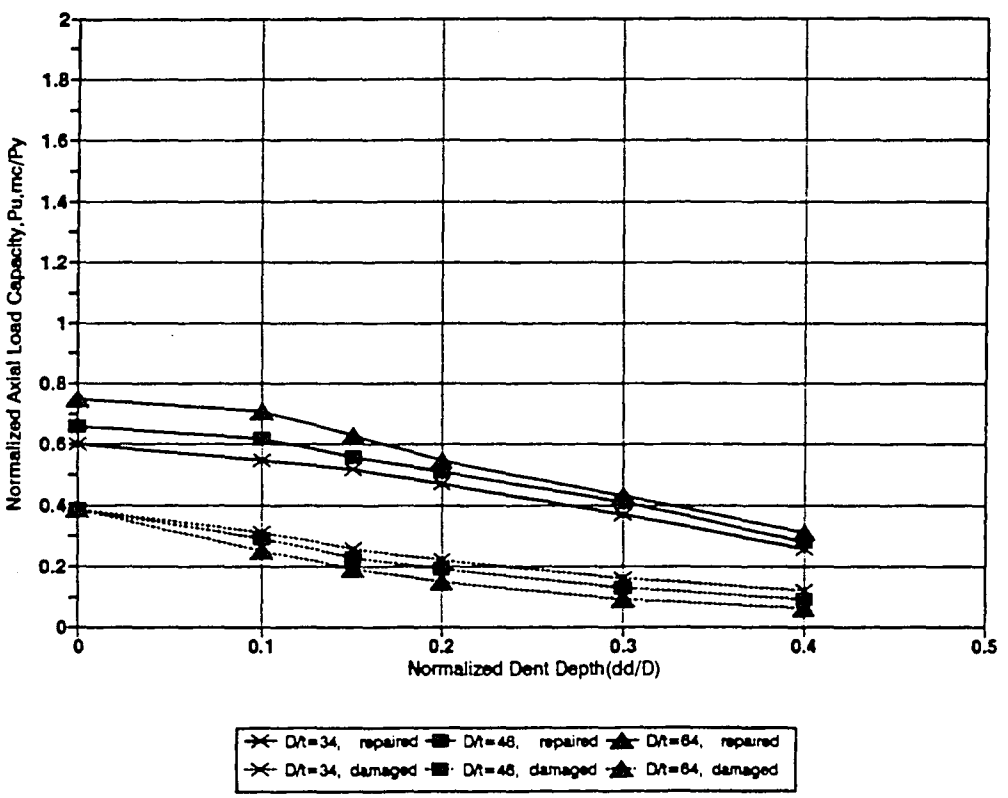

Figure 5-33 : Evaluation of the Effectiveness of the Internal Grout Repair, $\delta/L=0.02$

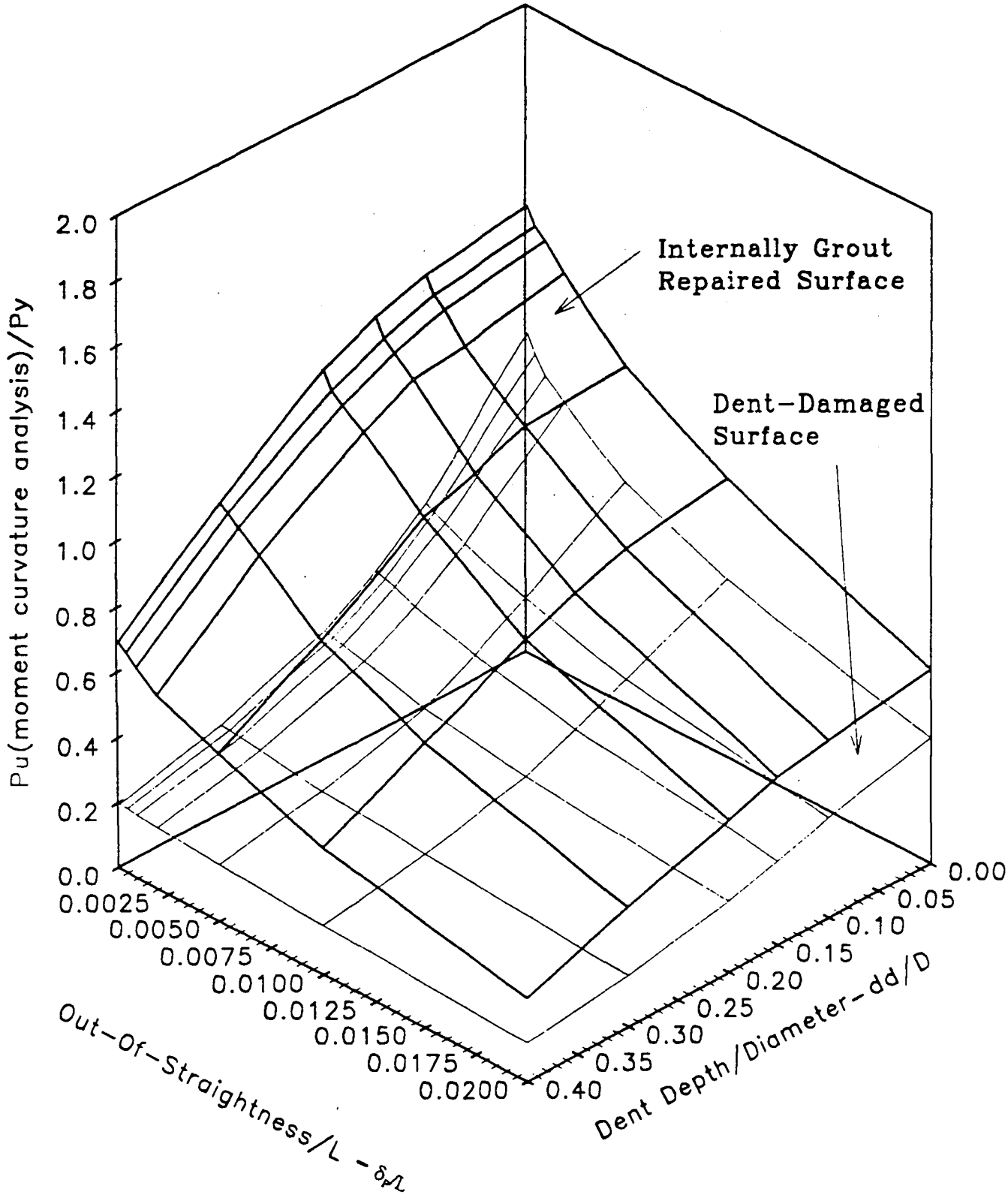

Figure 5-34 : Comparison of Residual Strength with Repaired Strength for KL/r=60 and D/t=34 (F'g=5.0 ksi and Fy=34.8 ksi)

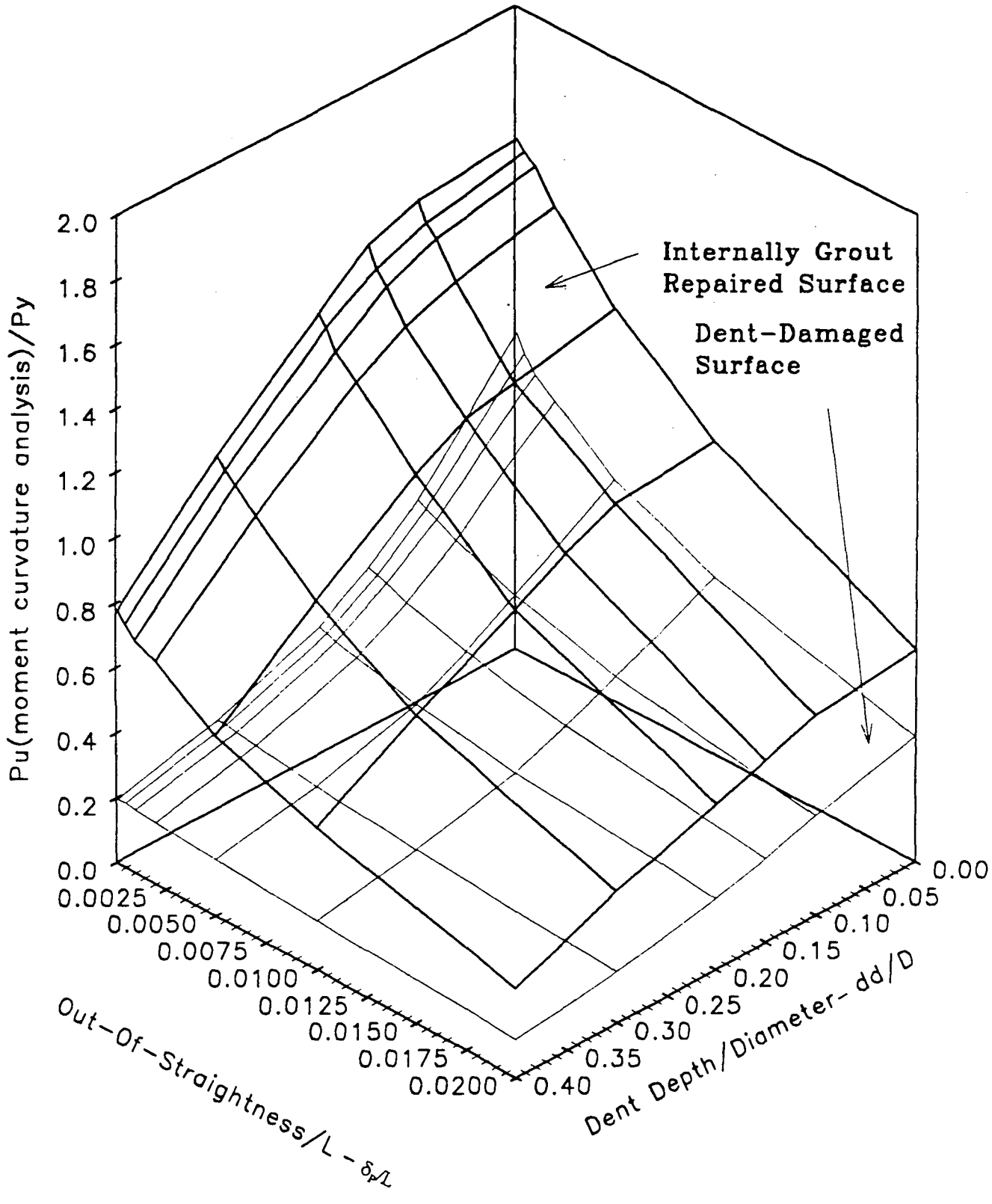

Figure 5-35 : Comparison of Residual Strength with Repaired Strength for KL/r=60 and D/t=46 (F'g=5.0 ksi and Fy=34.8 ksi)

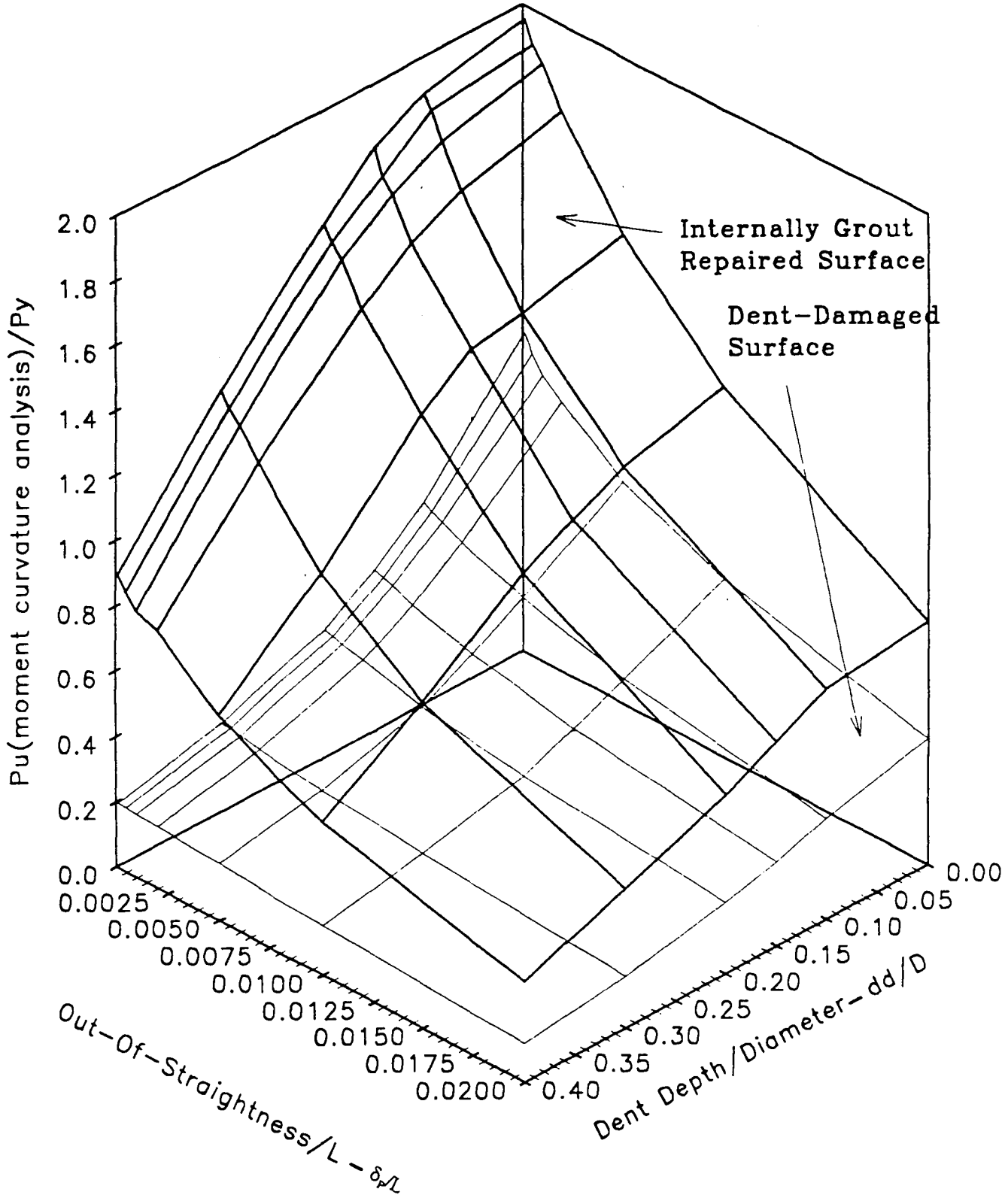

Figure 5-36 : Comparison of Residual Strength with Repaired Strength for KL/r=60 and D/t=64 (F'g=5.0 ksi and Fy=34.8 ksi)

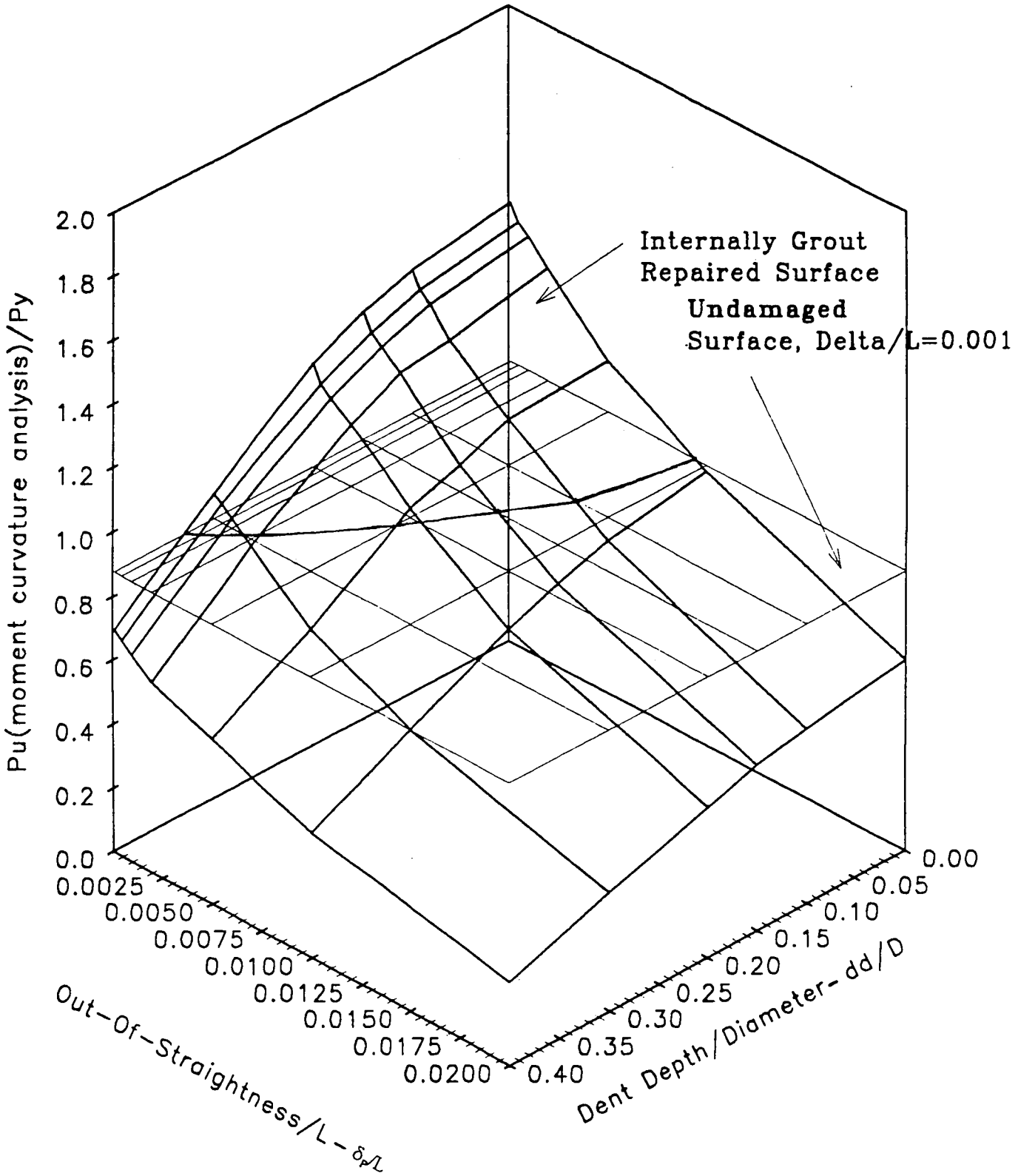

Figure 5-37 : Comparison of Residual Strength with Undamaged Capacity for KL/r=60 and D/t=34 (F'g=5.0 ksi and Fy=34.8 ksi)

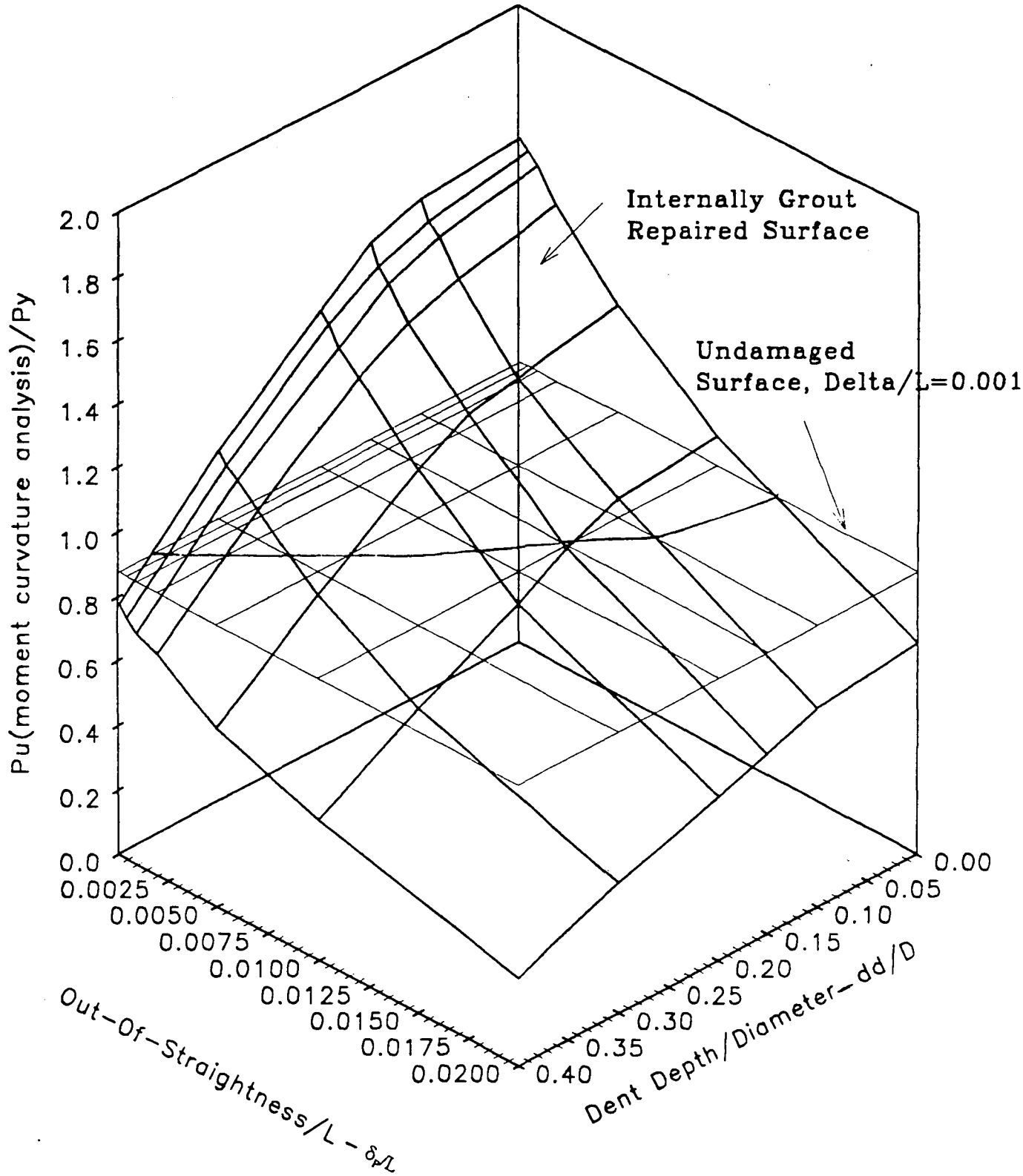

Figure 5-38 : Comparison of Residual Strength with Undamaged Capacity for KL/r=60 and D/t=46 (F'g=5.0 ksi and Fy=34.8 ksi)

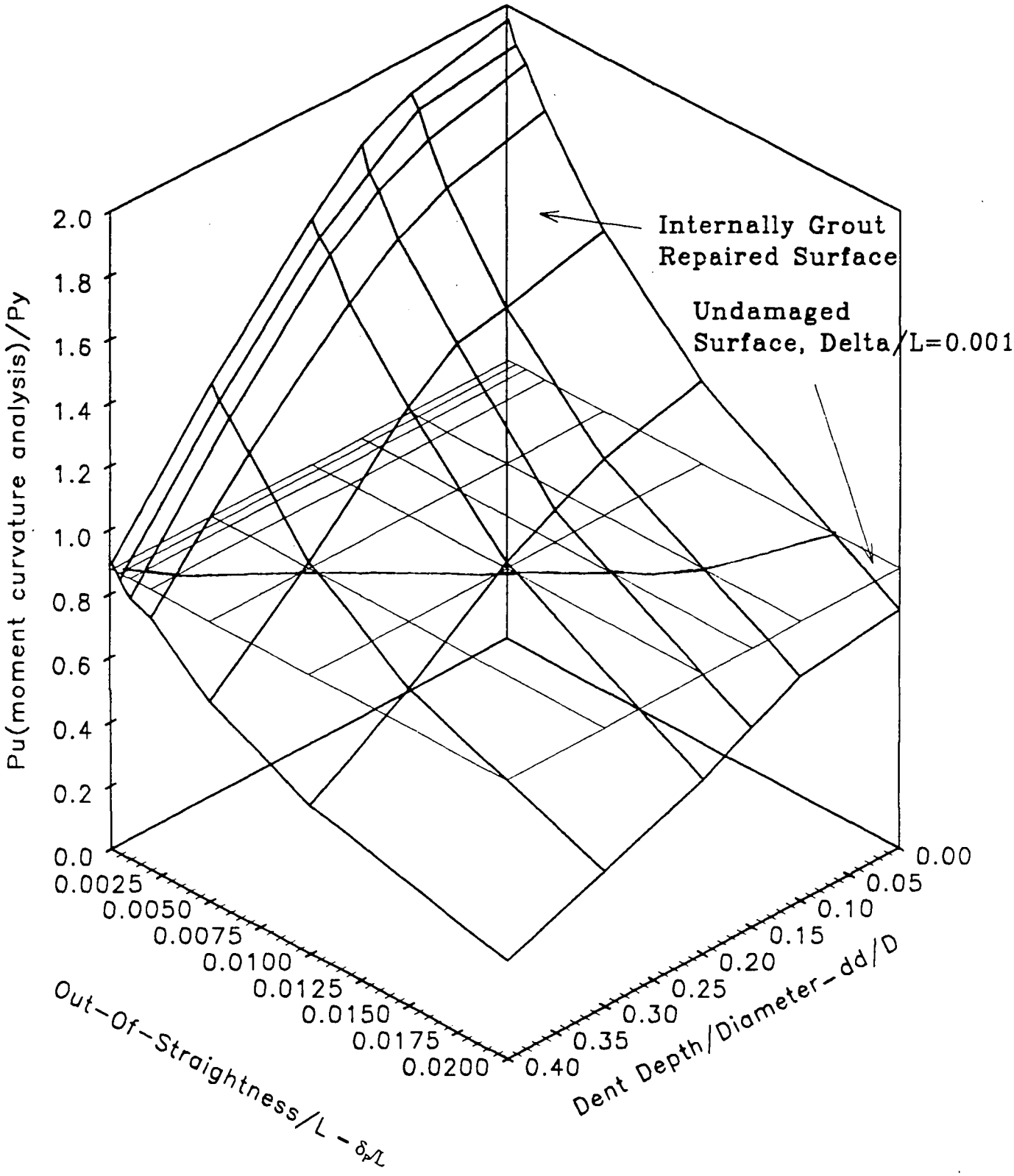

Figure 5-39 : Comparison of Residual Strength with Undamaged Capacity for KL/r=60 and D/t=64 (F'g=5.0 ksi and Fy=34.8 ksi)

$$f\left(\frac{\delta}{L}, \frac{dd}{D}\right) = -\left(\frac{\delta}{L}\right) + 0.0099 - 0.008\left(\frac{dd}{D}\right) - 0.0639\left(\frac{dd}{D}\right)^2$$

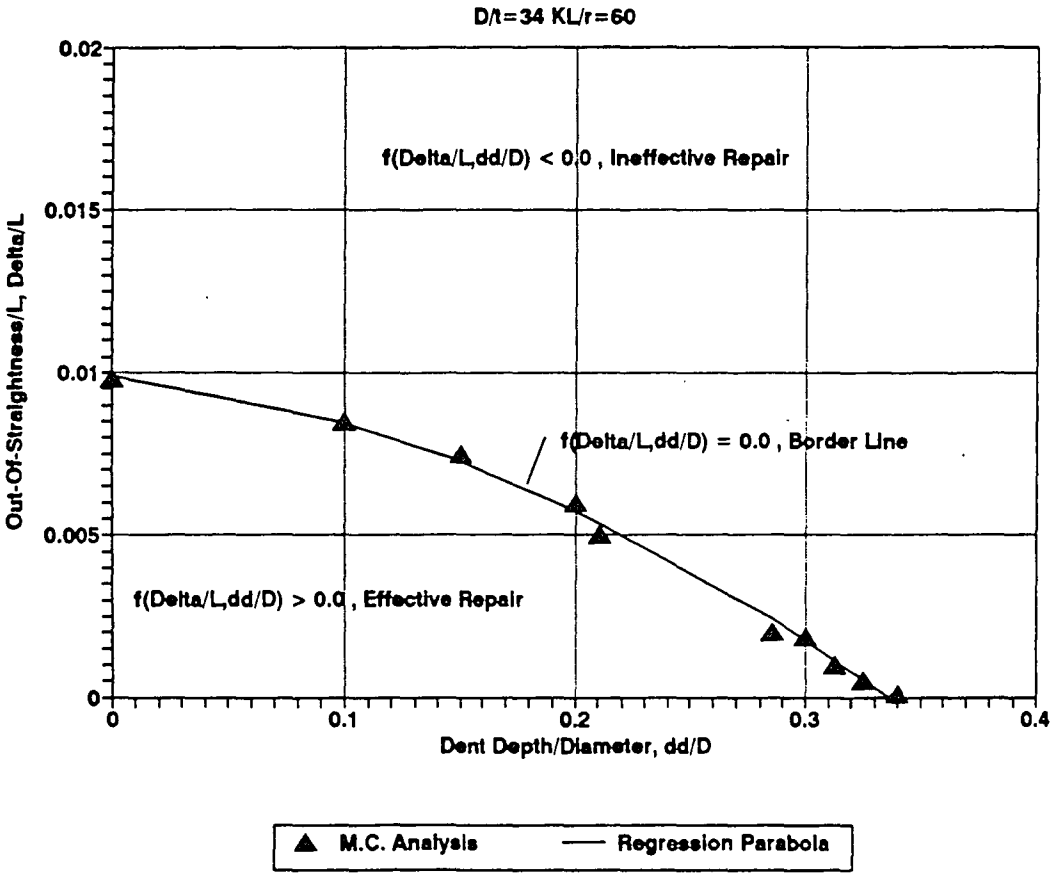

Figure 5-40 : Limit State Equation for KL/r=60 and D/t=34

(F'g=5.0 ksi and Fy=34.8 ksi)

$$f\left(\frac{\delta}{L}, \frac{dd}{D}\right) = -\left(\frac{\delta}{L}\right) + 0.0132 - 0.0128\left(\frac{dd}{D}\right) - 0.0634\left(\frac{dd}{D}\right)^2$$

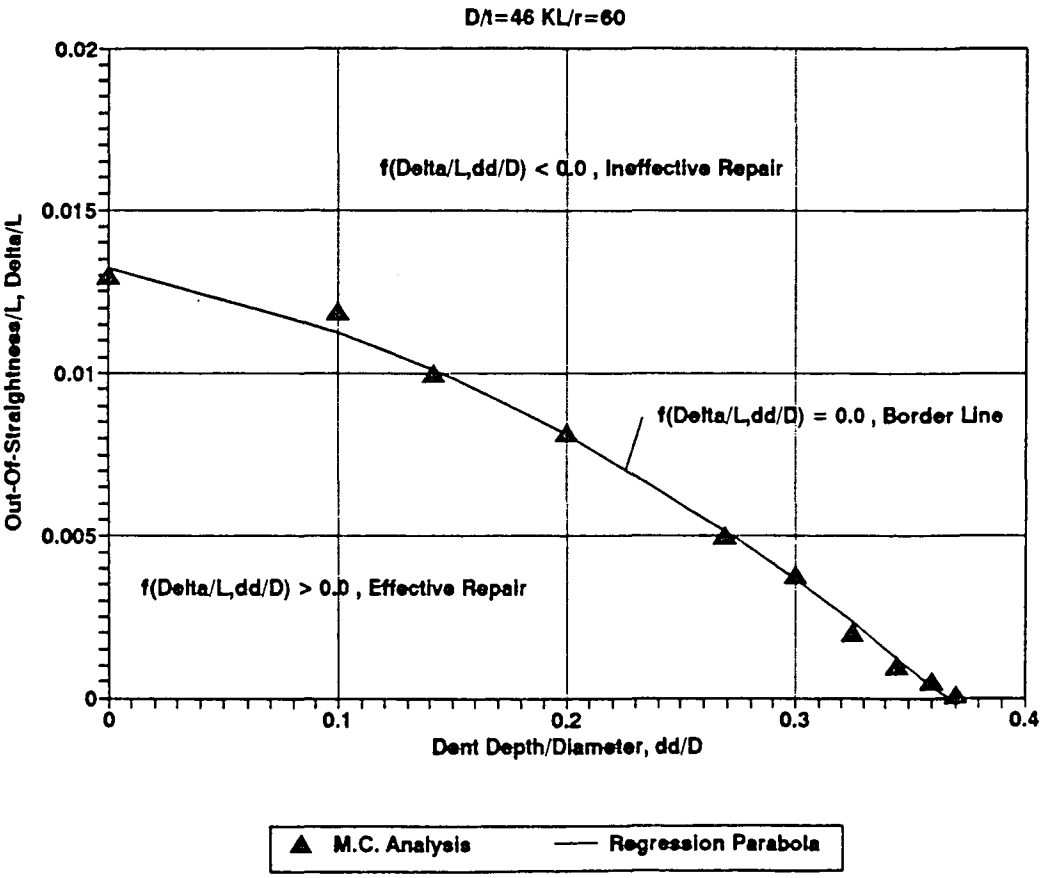

Figure 5-41 : Limit State Equation for KL/r=60 and D/t=46

(F'g=5.0 ksi and Fy=34.8 ksi)

$$f\left(\frac{\delta}{L}, \frac{dd}{D}\right) = -\left(\frac{\delta}{L}\right) + 0.0171 - 0.0225\left(\frac{dd}{D}\right) - 0.0501\left(\frac{dd}{D}\right)^2$$

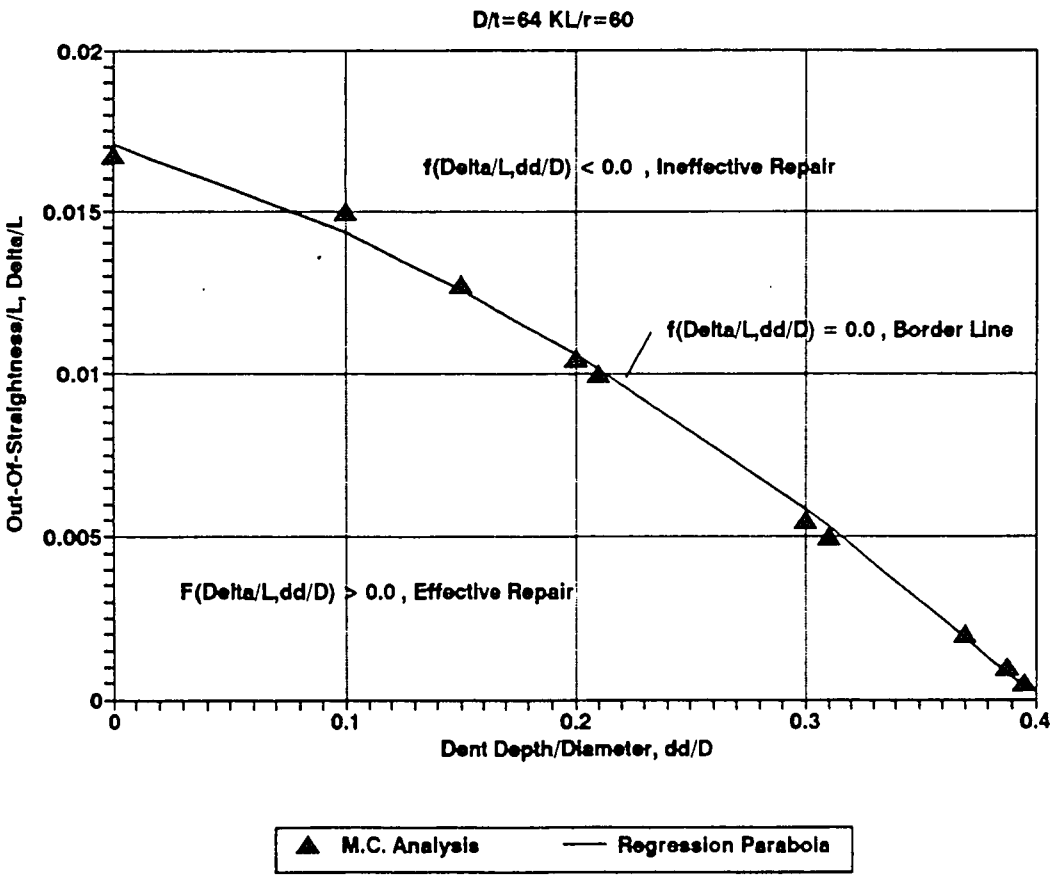

Figure 5-42 : Limit State Equation for KL/r=60 and D/t=64

(F'g=5.0 ksi and Fy=34.8 ksi)

APPENDIX A : Approximate Moment Curvature Relationships

1. Approximate Moment Curvature Expressions for Undented Tubular Sections without Local Buckling

$$p=\frac{P}{P_y}, m=\frac{M}{M_y}, \phi=\frac{\Phi}{\Phi_y}$$

for $\phi \leq \phi_1$

$$m=a\phi$$

for $\phi_1 < \phi \leq \phi_2$

$$m=b-\frac{c}{\sqrt{\phi}}$$

for $\phi_2 < \phi$

$$m=m_{pc}-\frac{f}{\phi^2}$$

where :

$$a=\frac{m_1}{\phi_1}$$

$$b = \frac{m_2\sqrt{\Phi_2} - m_1\sqrt{\Phi_1}}{\sqrt{\Phi_2} - \sqrt{\Phi_1}}$$

$$c = \frac{m_2 - m_1}{\frac{1}{\sqrt{\Phi_1}} - \frac{1}{\sqrt{\Phi_2}}}$$

$$f = (m_{pc} - m_2)\,\Phi_2^2$$

and

$m_1 = f_1\,(R)\,(1\text{-}p)$

$\phi_1 = f_1\,(R)\,(1\text{-}p)$

$m_2 = f_1\,(R)\,(1\text{-}p^2)$

$\phi_2 = f_2\,(R)\,(1+p^2)$

$m_{pc} = 1.273\,(1\text{-}p^{1.75})$

$f_1\,(R) = 1.0$	without residual stress
$f_1\,(R) = 0.9$	with residual stress
$f_2\,(R) = 1.0$	without residual stress
$f_2\,(R) = 0.9+0.2p$	with residual stress

2. Moment Curvature Expressions for Undented Tubular Sections with Local Buckling

$$m = (m_{max} + m_{min}) e^{\frac{(\phi - \phi_{lb})(EI)_{max}}{m_{max} - m_{min}}} + m_{min}$$

where :for $\phi_1 \prec \phi_{lb} \leq \phi_2$

$$m_{max} = b - \frac{c}{\sqrt{\phi_{lb}}}$$

for $\phi_2 \prec \phi_{lb}$

$$m_{max} = m_{pc} - \frac{f}{\phi^2_{lb}}$$

for $0 \leq p \leq 0.4$ and $36 \leq D/t \leq 72$ ($d_t = 0.01\ D/t$)

$$m_{min} = \frac{1}{\frac{1}{0.75 - 0.54 d_t} + (15.86 + 12.89 d_t) p + (104 - 710.8 d_t + 1036 d_t) p^2}$$

$$\phi_{lb} = \frac{1}{(-0.292 + 1.06 d_t - 0.336 d_t^2) + p(0.068 + 0.061 d_t - 1.759 d_t^2)}$$

$$(EI)_{max} = -0.094 - 0.129p + 0.367d_t + 0.77pd_t$$

for $0 \le p \le 0.4$ and $72 \le D/t \le 96$

$$m_{min} = \frac{1}{\frac{1}{0.53 - 0.208d_t} + 25.14p - 129.04p^2}$$

$$\phi_{1b} = 2.0 - 1.25p - 0.625d_t$$

$$(EI)_{max} = 0.17 - 0.43p$$

for $0.4 \le p \le 1.0$ and $36 \le D/t \le 72$

$$m_{min} = (0.617 - 1.343d_t - 0.772d_t)(1 - p)$$

$$\phi_{1b} = \frac{1}{-0.644 + 2.567d_t - 0.486d_t^2} + \frac{p - 0.4}{2.263 - 12.03d_t - 7.71d_t^2}$$

$$(EI)_{max} = -0.146 - 0.675p$$

for $0.4 \leq p \leq 1.0$ and $72 \leq D/t \leq 96$

$$m_{min.} = 0.05(1-p)$$

$$\phi_{ib} = 1.7 - 0.5p - 0.625 d_t$$

$$(EI)_{max} = 0.34$$

for $\phi \leq \phi_1$

$$m = a\phi$$

for $\phi_1 < \phi \leq \phi_{pud}$

$$m = b - \frac{c}{\sqrt{\phi}}$$

for $\phi_{pud} < \phi$

$$m = m_{pud}\left[1 - S_d\left(\frac{\phi}{\phi_{pud}} - 1\right)\right]$$

where :

$$a = \frac{m_1}{\phi_1}$$

$$b = \frac{m_{pud}\sqrt{\phi_{pud}} - m_1\sqrt{\phi_1}}{\sqrt{\phi_{pud}} - \sqrt{\phi_1}}$$

$$C = \frac{m_{pud} - m_1}{\frac{1}{\sqrt{\phi_1}} - \frac{1}{\sqrt{\phi_{pud}}}}$$

and

$m_1 = 0.8\, f_1(R)\, m_{pud}$

$\phi_1 = f_1(R)\,(1-p)\,(1- d_d \sin\beta / D)$

$f_1(R) = 1.0$ without residual stress

$f_1(R) = 0.9$ with residual stress

$\phi_{pud} = (1+2\beta/\pi)\,(\phi_0)$

$\phi_0 = 2.8 - 0.1\, d_d/t - 2.5\, p \geq 1.0$

$S_d = 0.1 + 0.4\, p + 0.6 \sin\beta + 0.8\, p \sin\beta$ (for $\beta \leq \pi/2$)

4. Moment Capacity of Dented Tubular Sections - m_{pud}

$$m_{pud}=\frac{M_{pud}}{M_y}$$

the design interaction equation :

$$M_{pud}=M_{ud}\left[1-\left(\frac{P}{P_{ud}}\right)^{\alpha}\right]$$

$$\alpha=1.75-0.1\frac{d_d}{t}\left(1-2\frac{\beta}{\pi}\right)\geq 1.0$$

where :

$$P_{ud}=P_u e^{\left(-0.08\frac{d_d}{t}\right)}$$

for $D/t \leq 100$

$$P_u=P_y$$

for $D/t > 100$

$$P_u=P_y\left[1.95-0.3\,(D/t)^{0.25}\right]$$

and

$$M_{ud}=M_u e^{(-0.06\frac{d_d}{t}\cos\beta}$$

for $0 < F_yD/t \leq 2500.451$, where F_y is in ksi

$$M_u=M_p$$

for $2500.451 < F_yD/t \leq 6500.592$, where F_y is in ksi

$$M_u=M_p(1.13-1.54\frac{F_yD}{Et})$$

for $6500.592 < F_yD/t \leq 20000.705$, where F_y is in ksi

$$M_u=M_p(0.96-0.77\frac{F_yD}{Et})$$

5. Moment-Thrust-Strain Relationships for both Undented and Dented Tubular Sections

for $p \leq p_1$, $M/M_p < 0.75$

$$\varepsilon = p$$

for $p \leq p_1$, $M/M_p \geq 0.75$

$$\varepsilon = p - k_1 p^2$$

for $p_1 < p \leq p_2$

$$\varepsilon = \frac{c^2}{(b-p)^2}$$

for $p_2 < p$

$$\varepsilon = \sqrt{\frac{f}{p_0 - p}}$$

where :

$$b = \frac{p_2\sqrt{\varepsilon_2} - p_1\sqrt{\varepsilon_1}}{\sqrt{\varepsilon_2} - \sqrt{\varepsilon_1}}$$

$$C = \frac{p_2 - p_1}{\frac{1}{\sqrt{\varepsilon_1}} - \frac{1}{\sqrt{\varepsilon_2}}}$$

and

for $M/M_p < 0.75$

$p_1 = (1-M/M_p)^{1.2}$

$p_2 = (1 - 0.9\ M/M_p)^{0.8}$

$\varepsilon_1 = (1-M/M_p)^{1.2}$

$\varepsilon_2 = 1+(M/M_p)^2$

for $M/M_p \geq 0.75$

$p_1 = (1-M/M_p)^{0.9}$

$p_2 = 1.3 - 1.18\ M/M_p$

$\varepsilon_1 = 1.2 - M/M_p$

$\varepsilon_2 = 1.0$

$p_0 = (1-M/M_p)^{0.57}$

APPENDIX B : BS 5400 Approach for Internally Grout Filled Members

1. Geometric and Material Properties :

Steel Tube :

D = outside diameter

t = tube wall thickness

F_y = yield stress

E_s = elastic modulus

KL = effective length

A_s = cross-section area

I_s = moment of inertia

Internal Grout :

f'_g = grout strength

E_g = elastic modulus

A_g = cross-section area

I_g = moment of inertia

2. Axial Compression Capacity

$$P_{cr}=K_1 P_u$$

where

K_1 = Buckling Coefficient.

$$K_1=\frac{1}{2}\left[1+\frac{1+\eta}{\lambda^2}\right]-\sqrt{\frac{1}{4}\left[1+\frac{1+\eta}{\lambda^2}\right]^2-\frac{1}{\lambda^2}}$$

P_u = Squash Capacity

$$P_u=C_2 F_y A_s+0.67 A_g\left[f'_g+C_1\frac{t}{D}F_y\right]$$

C_1 and C_2 are the coefficients accounting for the confinement and triaxial effects.

$$C_1=0.0, for \frac{KL}{D}\geq 25$$

$$C_1=9.47-0.726\left(\frac{KL}{D}\right)+\frac{1}{72}\left(\frac{KL}{D}\right)^2, for \frac{KL}{D}<25$$

$$C_2 = 1, for \frac{KL}{D} \geq 25$$

$$C_2 = 0.75 + 0.01\left(\frac{KL}{D}\right), for \frac{KL}{D} < 25$$

P_E = Euler Load

$$P_E = \frac{\pi^2}{(KL)^2}\left[E_s I_s + E_g I_g\right]$$

λ = Slenderness Ratio

$$\lambda = \sqrt{\frac{P_u}{P_E}}$$

$\acute{\eta}$ = Member Imperfection Factor

$$\eta = 0.002\pi(\lambda - 0.2)\sqrt{1.1\frac{E_s}{F_y}} \geq 0.0$$

3. Moment Capacity :

$$M_u = M_p(1+0.01m)$$

where

$$M_p = (D-t)^2 t F_y$$

and

$$m = 5.5\left[\left(\frac{0.6f'_g}{F_y}\right)\left(\frac{D}{t}\right)\right]^{0.66}$$

4. Combined Axial Load and Moment :

$$U.C. = \frac{P}{P_{cr}} + \left(1 - \frac{K_2}{K_1} - \frac{4K_3}{K_1}\right)\left(\frac{M}{M_u}\right) + \left(\frac{4K_3}{K_1}\right)\left(\frac{M}{M_u}\right)^2 \leq 1.0$$

where

$$K_2 = (K_{20})\frac{[115 - 30(2\beta - 1)(1.8 - \alpha_c) - 100\lambda]}{50(2.1 - \beta)} \geq 0.0$$

$$K_2 \leq K_{20}$$

$$K_{20}=0.9\alpha^2{}_c+0.2\leq 0.75$$

and

$$K_3=K_{30}+\frac{\lambda\left[(0.5\beta+0.4)\left(\alpha^2{}_c-0.5\right)+0.15\right]}{1+\lambda^3}$$

$$K_{30}=0.04-\frac{\alpha_c}{15}\geq 0.0$$

$$\alpha_c=\frac{0.67A_g\left(f'_g+C_1\frac{t}{D}F_y\right)}{P_u}$$

β = ratio of smaller to larger end moments

5. Modified BS 5400 Approach : (neglecting the confinement and triaxial stress effects)

C_1 = 0.0

C_2 = 1.0

APPENDIX C

1. Input File for the Dent-Damaged, Unrepaired Members

```
(1) TOTAL NUMBER OF SEGMENTS, N<=100
21
(3) DENT DEPTH, (in)
0.868
(4) DENT DIRECTIONAL ANGLE, (radian)
0.
(5) DENT LOCATION, (# of segment)
11
(6) LENGTH OF DENT SEGMENT, (in)
28.
(7) TUBE LENGTH, (in)
178.8
(8) ELASTIC MODULUS OF STEEL TUBE, Es (ksi)
29071
(9) OUTER DIAMETER OF THE TUBE, D (in)
8.626
(10)THICKNESS OF THE TUBE, t (in)
0.247
(11)STEEL YIELD STRENGTH, Fy (ksi)
34.8
(12)THE RATIO OF END ECCENTRICITY LEFT TO RIGHT
(NEGATIVE - SINGLE CURVATURE, POSITIVE - DOUBLE CURVATURE)
-1.
(13)LEFT END ECCENTRICITY
0.0
(14)INITIAL OUT-OF-STRAIGHTNESS AT THE MIDSPAN NORMALIZED BY L
0.0006
(15)INPUT THE CONVERGENCE FACTOR
1000.
(16)CONSIDER LOCAL BUCKLING EFFECT ? (INPUT Y or N)
Y
(17)CONSIDER RESIDUAL STRESS EFFECT ? (INPUT Y or N)
Y
```

2. Output File for the Dent-Damaged, Unrepaired Members

P / Py	AXIAL SHORTENING / L	LATERAL DEFLECTION / L
0.0050	0.000005444407	0.000000000018
0.0100	0.000010888850	0.000000000073
0.0150	0.000016333329	0.000000000164
0.0200	0.000021777845	0.000000000291
0.0250	0.000027222396	0.000000000453
0.0300	0.000032666982	0.000000000652
0.0350	0.000038111605	0.000000000887
0.0400	0.000043556266	0.000000001158
0.0450	0.000049000963	0.000000001465
0.0500	0.000054445697	0.000000001808
0.0550	0.000059890467	0.000000002188
0.0600	0.000065335274	0.000000002604
0.0650	0.000070780118	0.000000003058
0.0700	0.000076224999	0.000000003549
0.0750	0.000081669918	0.000000004078
0.0800	0.000087114871	0.000000004644
0.0850	0.000092559862	0.000000005250
0.0900	0.000098004891	0.000000005894
0.0950	0.000103449961	0.000000006577
0.1000	0.000108895070	0.000000007301
0.1050	0.000114340219	0.000000008065
0.1100	0.000119785410	0.000000008869
0.1150	0.000125230642	0.000000009716
0.1200	0.000130675916	0.000000010604
0.1250	0.000136121233	0.000000011536
0.1300	0.000141566594	0.000000012511
0.1350	0.000147011999	0.000000013530
0.1400	0.000152457449	0.000000014594
0.1450	0.000157902954	0.000000015705
0.1500	0.000163348506	0.000000016862
0.1550	0.000168794106	0.000000018067
0.1600	0.000174239755	0.000000019321
0.1650	0.000179685454	0.000000020625
0.1700	0.000185131203	0.000000021980
0.1750	0.000190577005	0.000000023386
0.1800	0.000196022859	0.000000024846
0.1850	0.000201468768	0.000000026360
0.1900	0.000206914734	0.000000027931

0.1950	0.000212360755	0.000000029557
0.2000	0.000217806835	0.000000031242
0.2050	0.000223252975	0.000000032987
0.2100	0.000228699178	0.000000034795
0.2150	0.000234145441	0.000000036664
0.2200	0.000239591771	0.000000038599
0.2250	0.000245038169	0.000000040602
0.2300	0.000250484635	0.000000042672
0.2350	0.000255931170	0.000000044814
0.2400	0.000261377776	0.000000047025
0.2450	0.000266824460	0.000000049313
0.2500	0.000272271220	0.000000051679
0.2550	0.000277718060	0.000000054124
0.2600	0.000283164983	0.000000056652
0.2650	0.000288611990	0.000000059264
0.2700	0.000294059086	0.000000061965
0.2750	0.000299506272	0.000000064756
0.2800	0.000304953552	0.000000067641
0.2850	0.000310400929	0.000000070623
0.2900	0.000315848388	0.000000073706
0.2950	0.000321295952	0.000000076894
0.3000	0.000326743625	0.000000080190
0.3050	0.000332191410	0.000000083598
0.3100	0.000337639312	0.000000087123
0.3150	0.000343087335	0.000000090770
0.3200	0.000348535484	0.000000094543
0.3250	0.000353983766	0.000000098448
0.3300	0.000359432195	0.000000102501
0.3350	0.000364880760	0.000000106689
0.3400	0.000370329469	0.000000111021
0.3450	0.000375778321	0.000000115497
0.3500	0.000381227368	0.000000120167
0.3550	0.000386676568	0.000000124991
0.3600	0.000392125923	0.000000129970
0.3650	0.000397575486	0.000000135156
0.3700	0.000403025270	0.000000140564
0.3750	0.000408475235	0.000000146152
0.3800	0.000413925384	0.000000151925
0.3850	0.000419375788	0.000000157952
0.3900	0.000424826430	0.000000164218
0.3950	0.000430277363	0.000000170774
0.4000	0.000435728480	0.000000177514
0.4050	0.000441179915	0.000000184573
0.4100	0.000446631644	0.000000191925
0.4150	0.000452083684	0.000000199589
0.4200	0.000457536054	0.000000207582
0.4250	0.000462988772	0.000000215924

0.4300	0.000468441860	0.000000224636
0.4350	0.000473895341	0.000000233740
0.4400	0.000479349240	0.000000243262
0.4450	0.000484803583	0.000000253229
0.4500	0.000490258400	0.000000263669
0.4550	0.000495713812	0.000000274705
0.4600	0.000501169683	0.000000286200
0.4650	0.000506626134	0.000000298274
0.4700	0.000512083206	0.000000310969
0.4750	0.000517540944	0.000000324331
0.4800	0.000522999400	0.000000338410
0.4850	0.000528458627	0.000000353261
0.4900	0.000533918687	0.000000368945
0.4950	0.000539379707	0.000000385588
0.5000	0.000544841583	0.000000403087
0.5050	0.000550304575	0.000000421703
0.5100	0.000555768716	0.000000441467
0.5150	0.000561234180	0.000000462554
0.5200	0.000566700969	0.000000484967
0.5250	0.000572169123	0.000000508745
0.5300	0.000577639155	0.000000534400
0.5350	0.000583110859	0.000000561727
0.5400	0.000588584526	0.000000591018
0.5450	0.000594060478	0.000000622594
0.5500	0.000599538595	0.000000656334
0.5550	0.000605019882	0.000000693245
0.5600	0.000610503668	0.000000732654
0.5650	0.000615991097	0.000000775706
0.5700	0.000621482367	0.000000822563
0.5750	0.000626977927	0.000000873710
0.5800	0.000632478346	0.000000929716
0.5850	0.000637984293	0.000000991250
0.5900	0.000643496561	0.000001059104
0.5950	0.000649016722	0.000001134852
0.6000	0.000654544761	0.000001218478
0.6050	0.000660082574	0.000001311878
0.6100	0.000665631822	0.000001416713
0.6150	0.000671195185	0.000001535662
0.6200	0.000676773245	0.000001669309
0.6250	0.000682782006	0.000002233657
0.5520	0.000718204441	0.000037656090
0.5490	0.000719708238	0.000039159890
0.5460	0.000721242210	0.000040693860
0.5340	0.000727709366	0.000047161020
0.5310	0.000729409312	0.000048860960
0.5250	0.000732936599	0.000052388250
0.5220	0.000734748999	0.000054200650

0.5130	0.000740440810	0.000059892460
0.5100	0.000742412035	0.000061863680
0.4980	0.000750743979	0.000070195630
0.4950	0.000752929840	0.000072381490
0.4920	0.000755161188	0.000074612840
0.4770	0.000767062363	0.000086514020
0.4740	0.000769584009	0.000089035660
0.4710	0.000772157527	0.000091609180
0.4680	0.000774783945	0.000094235600
0.4650	0.000777464292	0.000096915940
0.4530	0.000788746165	0.000108197800
0.4410	0.000801034312	0.000120486000
0.4320	0.000810888235	0.000130339900
0.4290	0.000814260782	0.000133712400
0.4260	0.000817799960	0.000137251600
0.4230	0.000821316993	0.000140768700
0.4170	0.000828713976	0.000148165600
0.4140	0.000832502449	0.000151954100
0.4110	0.000836328867	0.000155780500
0.3990	0.000852673722	0.000172125400
0.3900	0.000865784461	0.000185236100
0.3780	0.000884791450	0.000204243100
0.3750	0.000889764976	0.000209216600
0.3720	0.000894845674	0.000214297300
0.3690	0.000900036260	0.000219487900
0.3660	0.000905339453	0.000224791100
0.3630	0.000910758138	0.000230209800
0.3600	0.000916295213	0.000235746900
0.3570	0.000921953730	0.000241405400
0.3540	0.000927736845	0.000247188500
0.3510	0.000933647750	0.000253099400
0.3480	0.000939689829	0.000259141500
0.3450	0.000945866489	0.000265318100
0.3420	0.000952181343	0.000271633000
0.3390	0.000958638030	0.000278089700
0.3360	0.000965240389	0.000284692000
0.3330	0.000971992383	0.000291444000
0.3300	0.000978898038	0.000298349700
0.3270	0.000985961626	0.000305413300
0.3240	0.000993187450	0.000312639100
0.2850	0.001104101657	0.000423553300
0.2700	0.001157033413	0.000476485100
0.2430	0.001270871770	0.000590323400
0.2400	0.001285262844	0.000604714500
0.2370	0.001300340115	0.000619791700
0.2340	0.001315522995	0.000634974600
0.2310	0.001331134330	0.000650586000

0.2280	0.001347181089	0.000666632700
0.2250	0.001363679106	0.000683130800
0.2220	0.001380644529	0.000700096200
0.2190	0.001398094495	0.000717546200
0.2160	0.001416046669	0.000735498300
0.2130	0.001434519792	0.000753971500
0.2070	0.001473107422	0.000792559100
0.2010	0.001514024695	0.000833476400
0.1980	0.001535413646	0.000854865300
0.1950	0.001557455170	0.000876906800
0.1920	0.001580175249	0.000899626900
0.1890	0.001603600873	0.000923052500
0.1860	0.001627760620	0.000947212300
0.1830	0.001652684513	0.000972136200
0.1800	0.001678403889	0.000997855600
0.1770	0.001704951958	0.001024404000
0.1740	0.001732363752	0.001051815000
0.1710	0.001760675651	0.001080127000
0.1680	0.001789926505	0.001109378000
0.1650	0.001820157097	0.001139609000
0.1620	0.001851410447	0.001170862000
0.1590	0.001883732145	0.001203184000
0.1560	0.001917169749	0.001236621000
0.1530	0.001951774107	0.001271226000
0.1500	0.001987598782	0.001307050000
0.1170	0.002481133982	0.001800586000
0.0990	0.002854537460	0.002173989000
0.0960	0.002926459545	0.002245911000
0.0840	0.003248050101	0.002567502000
0.0630	0.003980352542	0.003299804000
0.0600	0.004107213456	0.003426665000
0.0570	0.004240901745	0.003560353000
0.0540	0.004381915043	0.003701367000
0.0510	0.004530795384	0.003850247000
0.0480	0.004688138256	0.004007590000
0.0450	0.004854596155	0.004174048000
0.0420	0.005030886829	0.004350339000
0.0390	0.005217798140	0.004537250000
0.0360	0.005416201563	0.004735653000
0.0330	0.005627060367	0.004946512000
0.0300	0.005851439206	0.005170891000
0.0270	0.006090522846	0.005409975000
0.0240	0.006345628993	0.005665081000
0.0210	0.006618229137	0.005937681000
0.0180	0.006909966402	0.006229418000
0.0150	0.007222688146	0.006542140000
0.0120	0.007558474274	0.006877926000

APPENDIX D

1. Input File for the Dent-Damaged, Internally Grout Repaied Members

```
(1) LENGTH OF THE TUBE, L (in)
178.8
(2) OUTER DIAMETER OF THE TUBE, D (in)
8.625
(3) THICKNESS OF THE TUBE, t (in)
0.247
(4) DENT DEPTH, dd (in)
0.857
(5) YIELD STRENGTH OF STEEL, Fy (ksi)
34.8
(6) ELASTIC MODULUS OF THE STEEL TUBE, Es (ksi)
29071
(7) GROUT STRENGTH, Fg (ksi)
4.375
(8) ELASTIC MODULUS OF THE INTERNAL GROUT, Eg (ksi)
2416.667
(9) TOTAL NUMBER OF SEGMENTS, N
21
(10)DENT LOCATION, (# of the segment)
11
(11)DIVIDED LAYERS USED IN THE DENTED SECTION
10,60,10
(12)DIVIDED LAYERS USED IN THE UNDENTED SECTION
10,60,10
(13)LEFT END ECCENTRICITY, (in)
1.725
(14)THE RATIO OF LEFT END ECCENTRICITY TO RIGHT
(NEGATIVE - SINGLE CURVATURE, POSITIVE - DOUBLE CURVATURE)
-1.
(15)CONVERGENCE FACTOR
1000.
(16)NUMBER OF UPPER LIMIT CYCLE FOR THE CONVERGENCE
200
(17)OUT-OF-STRAIGHTNESS AT MIDSPAN NORMALIZED BY L
0.01
(18)INPUT THE n, BETA AND GAMMA FACTORS
-0.2,0.01,2.5
(19)STRAIN HISTORY : INPUT 3 FIBER NUMBERS
1,11,60
```

2. Output File for the Dent-Damaged, Internally Grout Repaired Members

P	AXIAL SHORTENING	LATERAL DEFLECTION	STRAIN HISTORY		
			FIBER 1	FIBER 11	FIBER 80
(kips)	(in)	(in)	(in/in)	(in/in)	(in/in)
5.67	0.00323	0.0197	0.000033	0.000030	-0.000061
11.34	0.00650	0.0400	0.000048	0.000045	-0.000046
17.00	0.00983	0.0610	0.000100	0.000096	-0.000036
22.67	0.01309	0.0826	0.000156	0.000150	-0.000033
28.34	0.01649	0.1044	0.000199	0.000191	-0.000040
34.01	0.01983	0.1261	0.000210	0.000201	-0.000074
39.67	0.02312	0.1491	0.000266	0.000255	-0.000073
45.34	0.02673	0.1725	0.000326	0.000313	-0.000070
51.01	0.03009	0.1962	0.000369	0.000355	-0.000082
56.68	0.03375	0.2204	0.000413	0.000397	-0.000094
62.34	0.03709	0.2454	0.000457	0.000439	-0.000107
68.01	0.04055	0.2707	0.000503	0.000483	-0.000120
73.68	0.04434	0.2967	0.000550	0.000528	-0.000134
79.35	0.04815	0.3233	0.000598	0.000575	-0.000147
85.01	0.05149	0.3505	0.000645	0.000619	-0.000166
90.68	0.05551	0.3784	0.000695	0.000667	-0.000182
96.35	0.05923	0.4070	0.000744	0.000714	-0.000200
102.02	0.06270	0.4363	0.000796	0.000764	-0.000219
107.69	0.06656	0.4663	0.000851	0.000816	-0.000239
113.35	0.07061	0.4970	0.000901	0.000865	-0.000260
119.02	0.07429	0.5290	0.000955	0.000916	-0.000283
124.69	0.07862	0.5614	0.001015	0.000973	-0.000305
130.36	0.08264	0.5947	0.001067	0.001022	-0.000334
136.02	0.08640	0.6294	0.001125	0.001078	-0.000359
141.69	0.09080	0.6711	0.001189	0.001139	-0.000384
147.36	0.09601	0.7203	0.001270	0.001216	-0.000431
153.03	0.10211	0.7884	0.001397	0.001337	-0.000490
158.69	0.11055	0.8935	0.001556	0.001488	-0.000574
164.36	0.12365	1.0591	0.001784	0.001705	-0.000701
170.03	0.14829	1.3584	0.002103	0.002009	-0.000865
175.71	0.15323	1.4039	0.002644	0.002523	-0.001147
85.01	0.57931	4.7122	0.007691	0.007569	0.010619
73.68	0.80638	5.2399	0.008371	0.008217	0.011759
39.67	1.49476	10.4685	0.017076	0.016623	0.024739
17.00	2.08302	10.7492	0.011800	0.011192	0.020313

VITA

The author was born on February 5, 1968, the second child of Mr. Tze-Hua Fan and Mrs. Chu-Ying Lin in the city of Taipei, Republic of China.

He completed his Bachelor of Science in Civil Engineering at National Chiao-Tung University in 1990. From 1990 to 1992 he entered the Army for the 2 years' military service.

In the fall of 1992 he came to Lehigh University to pursue a degree of Master of Science in Civil Engineering.

END

OF

TITLE